ZooKeys 1131: 1–30 (2022)
doi: 10.3897/zookeys.1131.86644
https://zookeys.pensoft.net

RESEARCH ARTICLE

A peer-reviewed open-access journal
ZooKeys
Launched to accelerate biodiversity research

Three new species of *Diploderma* Hallowell, 1861 (Squamata, Agamidae) from the Hengduan Mountain Region, south-western China

Shuo Liu[1,2], Mian Hou[3], Dingqi Rao[2], Natalia B. Ananjeva[4]

1 *Kunming Natural History Museum of Zoology, Kunming Institute of Zoology, Chinese Academy of Sciences, Kunming, Yunnan 650223, China* **2** *Kunming Institute of Zoology, Chinese Academy of Sciences, Kunming, Yunnan 650201, China* **3** *College of Continuing (Online) Education, Sichuan Normal University, Chengdu, Sichuan 610066, China* **4** *Zoological Institute, Russian Academy of Sciences, Universitetskaya nab., 1, St. Petersburg 199034, Russia*

Corresponding authors: Natalia B. Ananjeva (Natalia.Ananjeva@zin.ru), Diqngqi Rao (raodq@mail.kiz.ac.cn)

Academic editor: Johannes Penner | Received 18 May 2022 | Accepted 7 September 2022 | Published 22 November 2022

https://zoobank.org/EEC27CDE-E9B7-4D00-ACD9-ADB1806D737F

Citation: Liu S, Hou M, Rao D, Ananjeva NB (2022) Three new species of *Diploderma* Hallowell, 1861 (Squamata, Agamidae) from the Hengduan Mountain Region, south-western China. ZooKeys 1131: 1–30. https://doi.org/10.3897/zookeys.1131.86644

Abstract

Three new species of *Diploderma* are described from the Hengduan Mountain Region in south-western China, based on morphological and genetic data. The first new species from Yulong County, Yunnan Province is morphologically most similar and phylogenetically closely related to *D. brevicauda*, but it can be diagnosed from the latter by having a relatively longer tail; the second new species from Xiangcheng County, Sichuan Province is phylogenetically closely related to *D. bowoense*, but it can be diagnosed from the latter by the absence of a distinct gular spot; and the third new species from Yongsheng County, Yunnan Province is phylogenetically closely related to *D. yulongense*, but it can be diagnosed from the latter by having different colourations of the ventral and ventrolateral surfaces of the body. Taxonomy and diversity survey are the basis of species conservation, our discoveries contributing to better conservation of the species of this genus.

Keywords

Molecular, morphological, ND2, Sichuan, taxonomy, Yunnan

Introduction

Diploderma Hallowell, 1861, is a genus including 36 species recognised currently (Uetz et al. 2022; Wang et al. 2022). Of the total diversity, 34 species are distributed in China, of which 22 species are only distributed in the Hengduan Mountain Region of south-western China (Wang et al. 2021a, 2022).

In the Hengduan Mountain Region, species of *Diploderma* mainly inhabit the hot-dry river valleys and most species are micro-endemic and only found in a specific section of a given river valley (Wang et al. 2022). Amongst the river valleys in the Hengduan Mountain Region, the Jinsha River Valley has the highest diversity of this genus, especially the upper and middle Jinsha River Valley (Wang et al. 2021a, b).

During our field survey in the Hengduan Mountain Region, China, in April 2022, some specimens of *Diploderma* were collected from the middle Jinsha River Valley in Yongsheng County, the area nearby the upper Jinsha River in Yulong County and the valley of a tributary of the upper Jinsha River in Xiangcheng County in Yunnan and Sichuan provinces, respectively (Fig. 1). Morphologically, these specimens could not be assigned to any recognised species of the genus. Phylogenetic analysis indicated that these populations represent three distinct, undescribed lineages. Herein, we describe these populations as three new species of *Diploderma*.

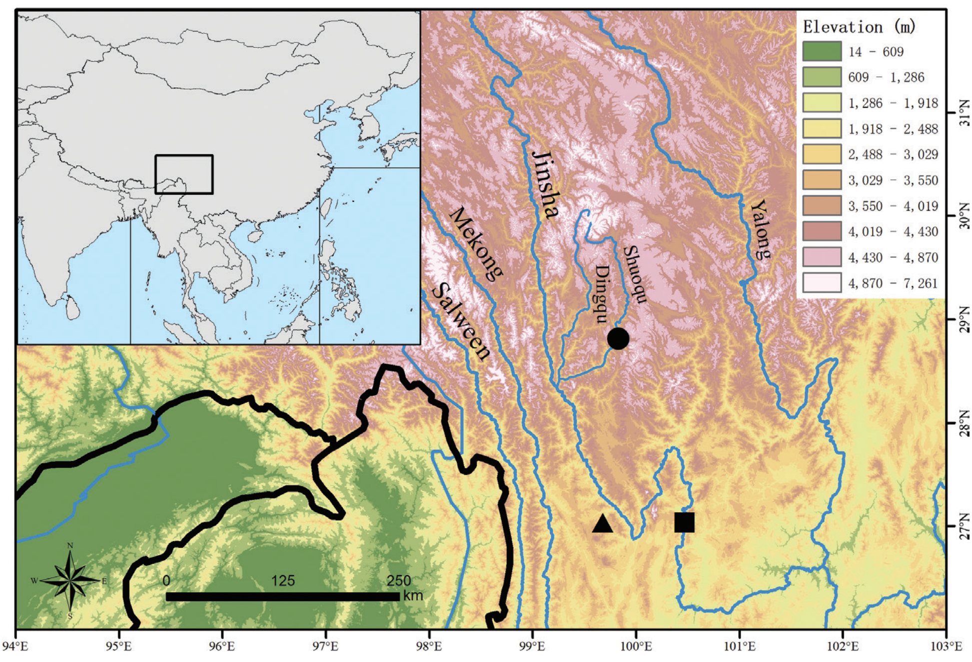

Figure 1. Map showing the type localities of *Diploderma limingense* sp. nov. (black triangle), *Diploderma shuoquense* sp. nov. (black dot) and *Diploderma yongshengense* sp. nov. (black square) in the Hengduan Mountain Region, south-western China. The elevation data were obtained from Geospatial Data Cloud (2022).

Materials and methods

Sampling

Specimens were all collected during the day. Photographs were taken to document the colour pattern in life prior to euthanasia. Liver tissues were stored in 99% ethanol and lizards were preserved in 75% ethanol. Specimens were deposited at Kunming Natural History Museum of Zoology, Kunming Institute of Zoology, Chinese Academy of Sciences (**KIZ**).

Morphology

Specimens were measured using a digital caliper to the nearest 0.1 mm. Measurements were taken on the left side of the specimen and values for paired pholidosis characters were recorded on both sides of the body, with counts provided in left/right order. The following morphometric characters were measured following Wang et al. (2022):

F4S fourth finger subdigital lamellae number, subdigital lamellae scale from the base between third and fourth finger to the tip of fourth finger, excluding the claw;

FLL fore-limb length, measured between the point of insertion at axillary to the tip of fourth finger, excluding the claw, measured as the straightened limb;

HD head depth, measured as the perpendicular distance at the temporal region of head;

HL head length, measured from the tip of snout to the rear border of the angle of jaw;

HLL hind-limb length, measured between the point of insertion at groin to the tip of fourth toe, excluding the claw, measured as the straightened limb;

HW head width, measured between the widest points of the head;

IL infralabial scale number, enlarged, modified labial scales from mental to the corner of mouth;

MD mid-dorsal crest scale number, modified crest scales longitudinally from the first nuchal crest to the scale above cloaca;

NSL nasal-supralabials scale rows, number of horizontal rows of small scales between the first supralabial and the nasal;

SEL snout-eye length, measured between the tip of snout and anterior edge of orbital bone;

SL supralabial scale number, enlarged, modified labial scales from rostral to the corner of mouth;

SOR suborbital scale rows, longitudinal rows of scales between supralabials and inferior-most edge of orbit circle, excluding fine ciliary scales in the orbit;

SVL snout-vent length, measured from the snout tip to anterior edge of the cloaca;

T4L fourth toe length, measured between the tip of fourth toe to the base between third and fourth toe, excluding the claw;

T4S fourth toe subdigital lamellae number, subdigital lamellae scales from the base between third and fourth toe to the tip of fourth toe, excluding the claw;
TAL tail length, measured from the anterior edge of the cloaca to the tip of tail;
TRL trunk length, measured between the limb insertion points between axillary and groin;
VN ventral scale number, ventral body scales counted in a straight line along the medial axis between the transverse gular fold and the anterior edge of cloaca.

We compared morphological characters of the new species with other members of the genus relying on original species descriptions (Hallowell 1861; Günther 1864; Anderson 1878; Boulenger 1906, 1918; Barbour and Dunn 1919; Stejneger 1924; Mertens 1926; Smith 1935; Gressitt 1936; Bourret 1937; Song 1987; Ota 1989; Ota et al. 1998; Li et al. 2001; Gao and Hou 2002; Manthey et al. 2012; Wang et al. 2015, 2016, 2017, 2019b, d, 2021a, b, 2022; Ananjeva et al. 2017; Rao et al. 2017; Liu et al. 2020) and the additional data from Wu et al. (2005), Manthey (2008) and Wang et al. (2017, 2018, 2019b, c, 2021a).

Molecular analysis

Total genomic DNA for the new collected specimens was extracted from liver tissues with the standard extraction method (Sambrook et al. 1989). The mitochondrial gene NADH dehydrogenase subunit 2 (ND2) was amplified and sequenced by using published primers (Wang et al. 2019a). PCR and sequencing methods followed Liu et al. (2020). Sequences were edited and manually managed using SeqMan in Lasergene 7.1 (DNASTAR Inc., Madison, WI, USA) and MEGA 11 (Tamura et al. 2021). Representative species of *Pseudocalotes* Fitzinger were chosen as outgroups according to Wang et al. (2022). Genetic data for 32 species of *Diploderma* and two species of outgroup taxa were obtained from GenBank (Table 1).

Sequences were aligned using MUSCLE (Edgar 2004) integrated in MEGA 11 (Tamura et al. 2021). The best substitution model GTR + Γ was selected using jModelTest 2.1.10 (Darriba et al. 2012). Bayesian Inference (BI) was performed in MrBayes 3.2.7 (Ronquist et al. 2012), based on the selected substitution model. Two runs were performed simultaneously with four Markov chains. The chains were run for 10,000,000 generations and sampled every 1,000 generations. The first 25% of the sampled trees was discarded as burn-in and then the remaining trees were used to estimate Bayesian posterior probabilities (BPP); nodes with BPP values of 0.95 and higher being considered well-supported (Huelsenbeck et al. 2001; Wilcox et al. 2002). Maximum Likelihood (ML) analysis was performed in IQ-TREE 1.6.12 (Nguyen et al. 2015) using the selected substitution model. One thousand bootstrap pseudoreplicates via the ultrafast bootstrap (UFB) approximation algorithm were used to construct a final consensus tree, nodes with UFB values of 95 and above being considered significantly supported (Minh et al. 2013). Uncorrected genetic pairwise distances (p-distances) between species were calculated in MEGA 11 (Tamura et al. 2021) with the pairwise deletion option for handling alignment gaps and missing data.

Table 1. GenBank accession numbers for the sequences used in this study.

Species	Voucher	Locality	Accession Numbers
Diploderma angustelinea	KIZ 029704	Muli, Sichuan, China	MT577930
Diploderma angustelinea	KIZ 029705	Muli, Sichuan, China	MT577924
Diploderma aorun	KIZ 032733	Benzilan, Yunnan, China	MT577938
Diploderma aorun	KIZ 032734	Benzilan, Yunnan, China	MT577939
Diploderma batangense	KIZ 09404	Zhubalong, Tibet, China	MK001412
Diploderma batangense	KIZ 019276	Batang, Sichuan, China	MK001413
Diploderma brevicauda	KIZ 044304	Lijiang, Yunnan, China	MW506023
Diploderma brevicauda	KIZ 044305	Lijiang, Yunnan, China	MW506021
Diploderma brevicauda	KIZ 044306	Lijiang, Yunnan, China	MW506022
Diploderma bowoense	KIZ 044757	Muli, Sichuan, China	MW506020
Diploderma bowoense	KIZ 044758	Muli, Sichuan, China	MW506019
Diploderma brevipes	NMNS 19607	Taiwan, China	MK001429
Diploderma brevipes	NMNS 19608	Taiwan, China	MK001430
Diploderma chapaense	KIZ 034923	Lvchun, Yunnan, China	MG214263
Diploderma chapaense	ZMMU NAP-01911	Chapa, Vietnam	MG214262
Diploderma drukdaypo	KIZ 027627	Jinduo, Tibet, China	MT577950
Diploderma drukdaypo	KIZ 027628	Zhuka, Tibet, China	MT577952
Diploderma dymondi	KIZ 040639	Dongchuan, Yunnan, China	MK001422
Diploderma dymondi	KIZ 040640	Dongchuan, Yunnan, China	MK001423
Diploderma flaviceps	KIZ 01851	Luding, Sichuan, China	MK001416
Diploderma flaviceps	KIZ 01852	Luding, Sichuan, China	MK001417
Diploderma flavilabre	KIZ 032692	Baiyu,Sichuan, China	MT577916
Diploderma flavilabre	KIZ 032694	Baiyu,Sichuan, China	MT577917
Diploderma formosgulae	KIZ 044420	Deqin, Yunnan, China	MW506024
Diploderma formosgulae	KIZ 044421	Deqin, Yunnan, China	MW506025
Diploderma iadinum	KIZ 027697	Yunling, Yunnan, China	MT577956
Diploderma iadinum	KIZ 027702	Yunling, Yunnan, China	MT577957
Diploderma laeviventre	KIZ 014037	Basu, Tibet, China	MK001407
Diploderma laeviventre	KIZ 027691	Basu, Tibet, China	MT577892
Diploderma luei	NMNS 19604	Taiwan, China	MK001433
Diploderma luei	NMNS 19605	Taiwan, China	MK001434
Diploderma makii	NMNS 19609	Taiwan, China	MK001431
Diploderma makii	NMNH 19610	Taiwan, China	MK001432
Diploderma menghaiense	KIZ L0030	Menghai, Yunnan, China	MT598655
Diploderma menghaiense	KIZ L0031	Menghai, Yunnan, China	MT598656
Diploderma micangshanense	KIZ 032801	Shiyan, Hubei, China	MK578665
Diploderma micangshanense	KIZ 023231	Xixia, Henan, China	MK578664
Diploderma panchi	KIZ 032715	Yajiang, Sichuan, China	MT577946
Diploderma panchi	KIZ 032716	Yajiang, Sichuan, China	MT577944
Diploderma panlong	KIZ 040137	Miansha, Sichuan, China	MT577906
Diploderma panlong	KIZ 040138	Miansha, Sichuan, China	MT577907
Diploderma polygonatum	NMNS 19598	Taiwan, China	MK001427
Diploderma polygonatum	NMNS 19599	Taiwan, China	MK001428
Diploderma qilin	KIZ 028332	Balong, Yunnan, China	MT577941
Diploderma qilin	KIZ 028333	Balong, Yunnan, China	MT577942
Diploderma qilin	KIZ 028335	Balong, Yunnan, China	MT577943
Diploderma slowinskii	CAS 214906	Gongshan, Yunnan, China	MK001405
Diploderma slowinskii	CAS 214954	Gongshan, Yunnan, China	MK001406
Diploderma splendidum	KIZ 015973	Yichang, Hubei, China	MK001418
Diploderma splendidum	LSUMZ 81212	Unknown	AF288230

Species	Voucher	Locality	Accession Numbers
Diploderma swild	KIZ 034914	Panzhihua, Sichuan, China	MN266299
Diploderma swild	KIZ 034894	Panzhihua, Sichuan, China	MN266300
Diploderma swinhonis	NMNS 19592	Taiwan, China	MK001419
Diploderma swinhonis	NMNS 19593	Taiwan, China	MK001420
Diploderma varcoae	WK-JK 011	Yuxi, Yunnan, China	MT577903
Diploderma varcoae	KIZ 026132	Mengzi, Yunnan, China	MK001421
Diploderma vela	KIZ 019299	Quzika, Tibet, China	MK001414
Diploderma vela	KIZ 034925	Quzika, Tibet, China	MK001415
Diploderma yangi	SWFU 005410	Chayu, Tibet, China	OL449603
Diploderma yangi	SWFU 005412	Chayu, Tibet, China	OL449604
Diploderma yulongense	KIZ 028291	Hutiaoxia, Yunnan, China	MT577921
Diploderma yulongense	KIZ 028292	Hutiaoxia, Yunnan, China	MT577922
Diploderma yulongense	KIZ 028300	Baishuitai, Yunnan, China	MT577923
Diploderma yulongense	KIZ 09399	Xianggelila, Yunnan, China	MK001410
Diploderma yulongense	KIZ 043196	Xianggelila, Yunnan, China	MK001411
Diploderma yunnanense	CAS 242271	Baoshan, Yunnan, China	MK001408
Diploderma yunnanense	KIZ 040193	Yingjiang, Yunnan, China	MK578658
Diploderma zhaoermii	KIZ 019564	Wenchuan, Sichuan, China	MK001425
Diploderma zhaoermii	KIZ 019565	Wenchuan, Sichuan, China	MK001426
Diploderma limingense sp. nov.	KIZ2022013	Liming, Yunnan, China	OP428781
Diploderma limingense sp. nov.	KIZ2022014	Liming, Yunnan, China	OP428782
Diploderma limingense sp. nov.	KIZ2022015	Liming, Yunnan, China	OP428783
Diploderma limingense sp. nov.	KIZ2022017	Liming, Yunnan, China	OP428784
Diploderma shuoquense sp. nov.	KIZ2022004	Xiangcheng, Sichuan, China	OP428773
Diploderma shuoquense sp. nov.	KIZ2022005	Xiangcheng, Sichuan, China	OP428774
Diploderma shuoquense sp. nov.	KIZ2022006	Xiangcheng, Sichuan, China	OP428775
Diploderma shuoquense sp. nov.	KIZ2022007	Xiangcheng, Sichuan, China	OP428776
Diploderma yongshengense sp. nov.	KIZ2022008	Yongsheng, Yunnan, China	OP428777
Diploderma yongshengense sp. nov.	KIZ2022009	Yongsheng, Yunnan, China	OP428778
Diploderma yongshengense sp. nov.	KIZ2022010	Yongsheng, Yunnan, China	OP428779
Diploderma yongshengense sp. nov.	KIZ2022011	Yongsheng, Yunnan, China	OP428780
Pseudocalotes brevipes	MVZ 224106	Vinh Phuc, Vietnam	AF128502
Pseudocalotes kakhiensis	KIZ 015975	Gongshan, Yunnan, China	MK001435

Results

The obtained sequence alignment is 1031 bp in length. The resulting topologies from BI and ML analyses are consistent (Fig. 2). The specimens from Yulong County formed a clade sister to the clade consisting of *Diploderma qilin* Wang, Ren, Che & Siler, 2020 and *D. brevicauda* (Manthey, Denzer, Hou & Wang, 2012) with strong support by BI, the specimens from Xiangcheng County formed a clade sister to *D. bowoense* Wang, Gao, Wu, Siler & Che, 2021 with strong support by both BI and ML and the specimens from Yongsheng County formed a clade sister to *D. yulongense* (Manthey, Denzer, Hou & Wang, 2012) with strong support by both BI and ML. The minimum average genetic distance between the specimens from Yulong County and other species

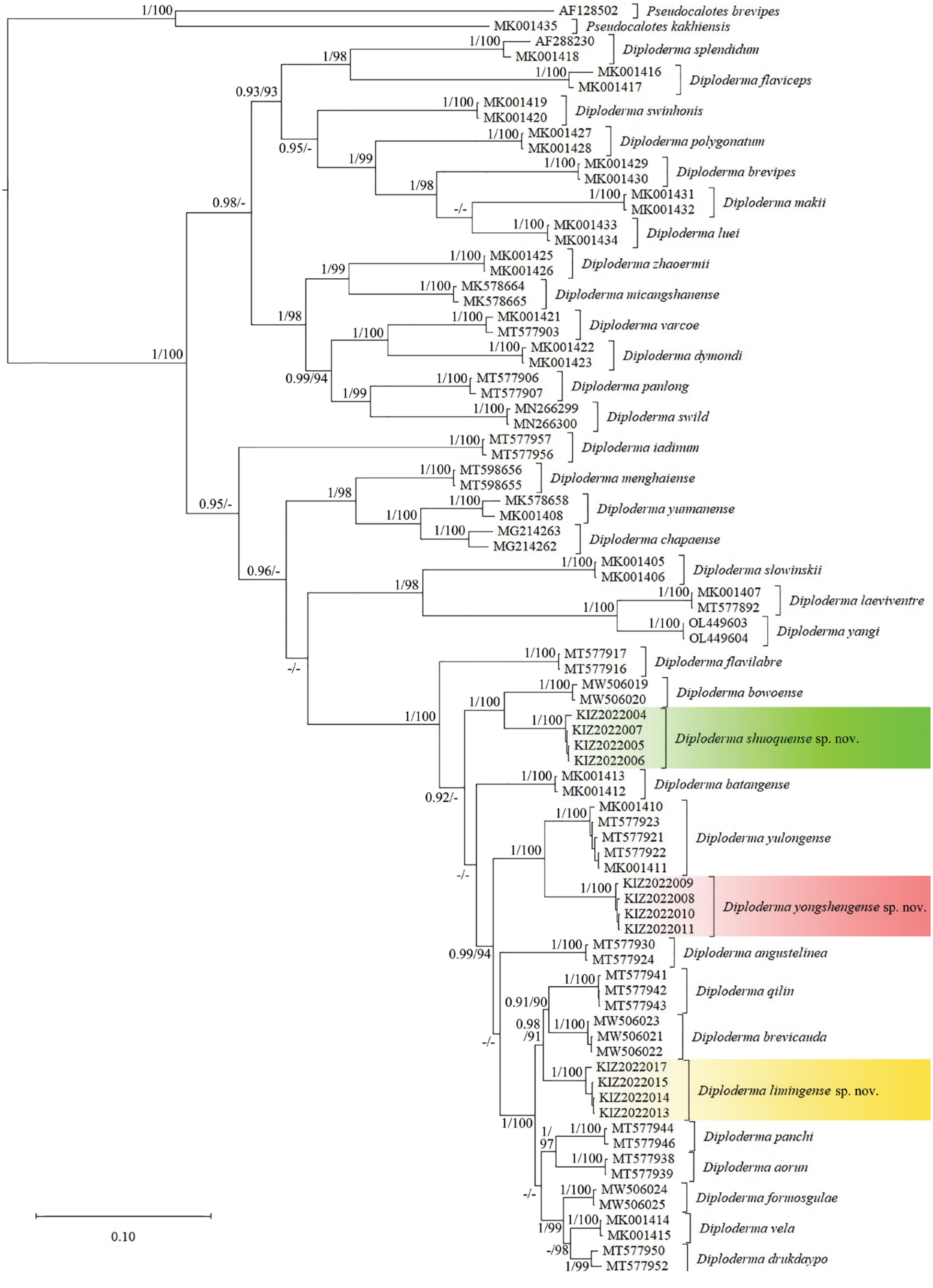

Figure 2. Bayesian phylogram of the genus *Diploderma* inferred from mitochondrial gene ND2 (1031 bp). Numbers before slashes indicate BPP values and numbers after slashes indicate UFB values. The symbol "–" represents the value below 0.90/90.

of *Diploderma* is 4.1% (between *D. brevicauda*), the minimum average genetic distance between the specimens from Xiangcheng County and other species of *Diploderma* is 6.3% (between *D. bowoense*) and the minimum average genetic distance between the specimens from Yongsheng County and other species of *Diploderma* is 5.8% (between *D. yulongense*) (Suppl. material 1).

Taxonomy

***Diploderma limingense* sp. nov.**
https://zoobank.org/3CE0C841-1864-4B05-9D1F-FEB5E193939F
Figs 3–5

Holotype. KIZ2022014, adult male, collected on 21 April 2022 by Shuo Liu from Liming Village, Liming Township, Yulong County, Lijiang City, Yunnan Province, China (27°2'0"N, 99°40'42"E, 2300 m elevation).

Paratypes. KIZ2022013, KIZ2022015, KIZ2022017, three adult males, collecting information the same as the holotype.

Etymology. The specific epithet refers to Liming Township, where the new species was discovered.

Diagnosis. *Diploderma limingense* sp. nov. can be diagnosed from congeners by a combination of the following morphological characteristics: (1) body size medium, SVL 55.6–56.8 mm in males; (2) tail relatively long, TAL/SVL 1.92–2.09 in males; (3) head moderately wide, HW/HL 0.71–0.74 in males; (4) limbs relatively long, FLL/SVL 0.47–0.52 in males, HLL/SVL 0.74–0.82 in males; (5) MD 45–48; (6) F4S 15–16, T4S 21–22; (7) tympanum concealed; (8) nuchal and dorsal crest scales feebly developed, no skin folds under nuchal and dorsal crest scales in males; (9) distinct transverse gular fold present; (10) ventral head and body scales strongly keeled; (11) ventral head scales heterogeneous in size; (12) gular spot present in males, yellowish-white in life; (13) dorsolateral stripes jagged in males, light yellow in life; (14) ventral surfaces of body, limbs and tail light brick red in males in life; (15) five radial stripes around the eye on each side; (16) inner lips bright yellow, tongue light orange, remaining oral cavity mostly light flesh colour in life.

Description of holotype. Adult male, SVL 56.2 mm; tail relatively long, TAL 117.5 mm, TAL/SVL 2.09; limbs relatively long, FLL 26.5 mm on left side, FLL/SVL 0.47, HLL 41.8 mm on left side, HLL/SVL 0.74. Head relatively robust, HW/HL 0.74, HD/HW 0.85; snout moderately long, SEL/HL 0.36. Rostral elongated, bordered by five small postrostral scales; dorsal head scales heterogeneous, all strongly keeled; indistinct Y-shaped ridge on dorsal snout. Nasal oval, separated from first supralabial by single row of scales; loreals small, keeled; suborbital scale rows 4/3, keeled; canthus rostralis elongated, greatly overlapping with each other; enlarged, keeled scales forming single lateral ridge from posteroinferior eye to posterosuperior tympanum on each side; tympanum concealed under scales; SL 8/8, feebly keeled. Mental pentagonal; IL 9/9; enlarged chin shields 4/5, smooth, first one contacting IL on each

Figure 3. Dorsal view (top) and ventral view (bottom) of type series of *Diploderma limingense* sp. nov. in preservative.

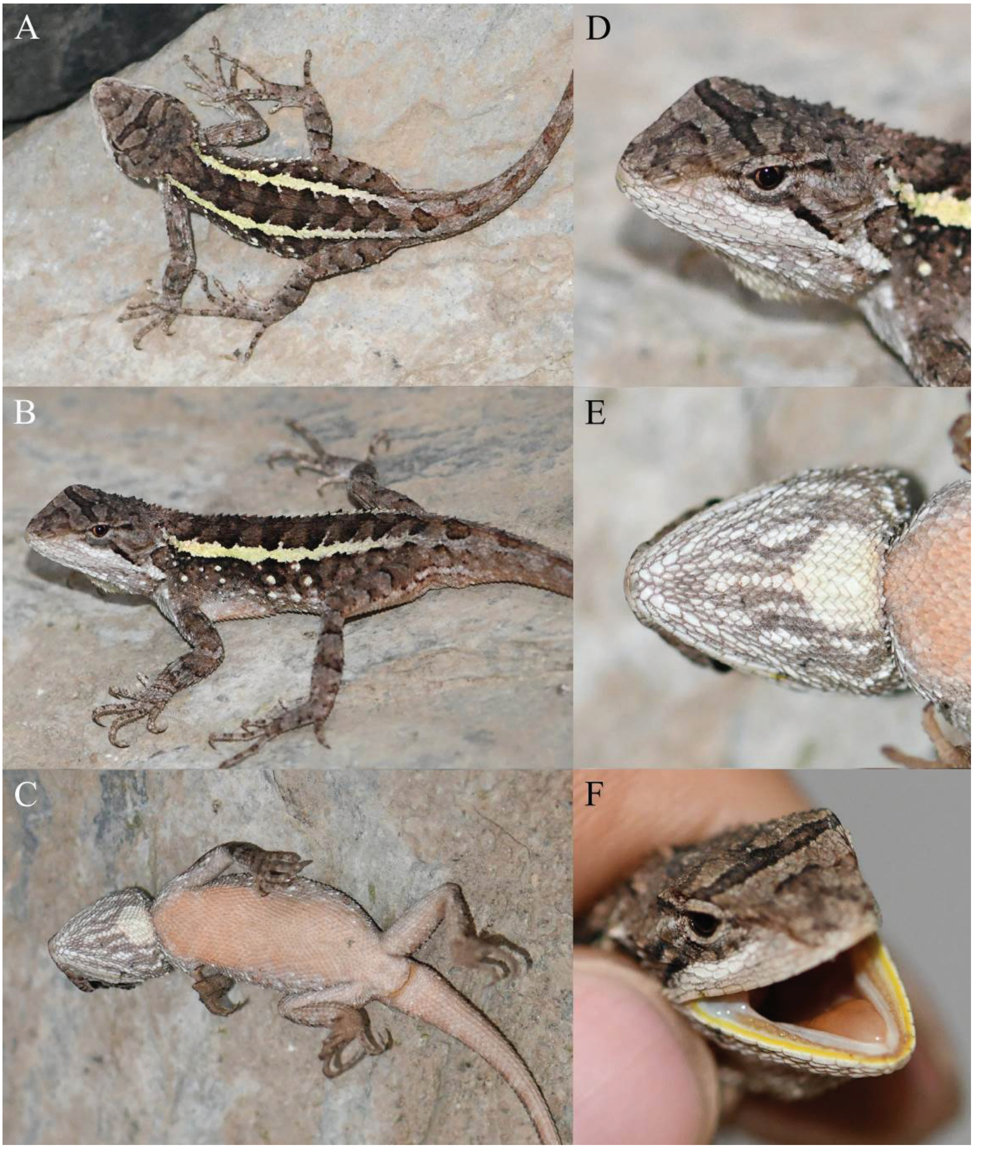

Figure 4. Holotype (KIZ2022014) of *Diploderma limingense* sp. nov. in life **A** dorsal view **B** lateral view **C** ventral view **D** close-up view of the dorsolateral side of the head **E** close-up view of the ventral side of the head **F** close-up view of the oral cavity.

side, remaining ones separated from IL by two rows of small scales; ventral head scales homogeneous in size, smooth or weakly keeled; distinct transverse gular fold present; gular pouch weakly developed.

Distinct shoulder fold present; dorsal body scales heterogeneous in size and shape, all keeled, tip pointing backwards; axillary scales much smaller than remaining dorsals;

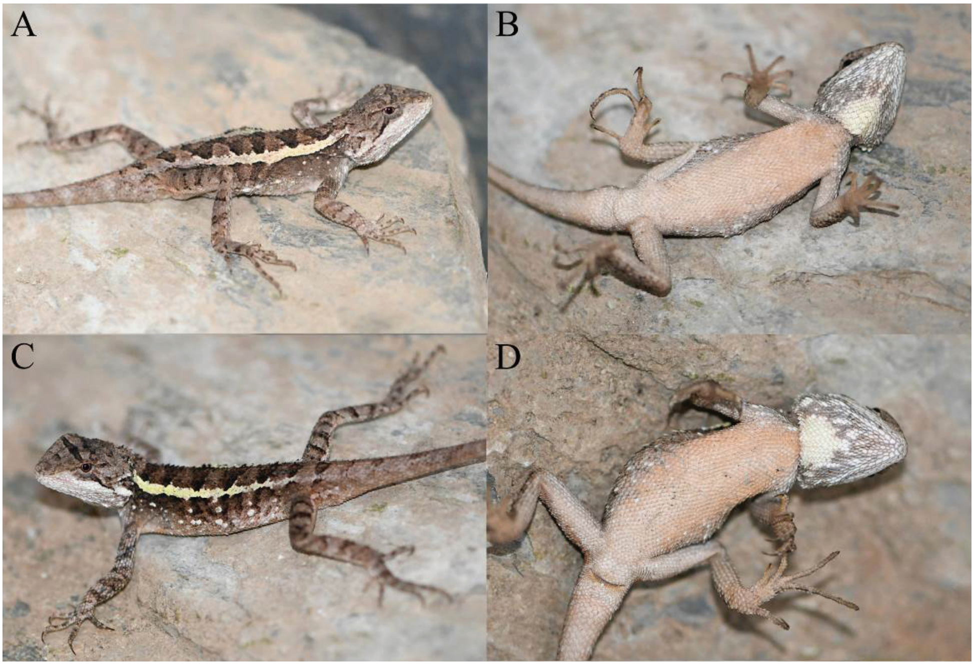

Figure 5. Paratypes of *Diploderma limingense* sp. nov. in life **A** dorsolateral view of the paratype KIZ2022013 **B** ventral view of the paratype KIZ2022013 **C** dorsolateral view of the paratype KIZ2022015 **D** ventral view of the paratype KIZ2022015.

enlarged dorsal scales roughly forming four longitudinal rows from neck to pelvis on each side of body. Nuchal and dorsal crests continuous, scales of nuchal and dorsal crests approximately same in size and shape; no skin fold under nuchal and dorsal crests; MD 45. Dorsal limb scales strongly keeled, homogeneous on fore-limbs and heterogeneous on hind limbs; F4S 15/16, T4S 22/22. Ventral body scales approximately parallel, almost homogeneous, all strongly keeled, VN 63. Ventral limb scales parallel, small on fore-limbs and larger on hind limbs, all strongly keeled. Tail scales all strongly keeled, ventral tail scales larger than dorsal tail scales.

Colouration of holotype in life. Dorsal surface of head brownish-grey. A distinct black transverse band anteriorly and an indistinct black transverse band posteriorly present between orbits on dorsal surface of head. Lateral surfaces of head brownish-grey. Five brownish-black radial stripes around eye on each side. Upper lips greyish-white. Inner lips bright yellow, tongue light orange, remaining oral cavity mostly light flesh colour.

Dorsal surface of body brown. A light yellow jagged dorsolateral stripe present from neck to pelvis on each side of body. Some brownish-black triangular patches distributed along vertebral line between dorsolateral stripes from neck to base of tail, all of which pointing posteriorly. Some yellowish-white spots scattered below dorsolateral stripe on each side of body. Dorsal surfaces of limbs greyish-brown with indistinct dark transverse bands. Dorsal surface of tail brownish-grey with some indistinct dark transverse bands.

Ventral surface of head greyish-white. A roughly triangular, yellowish-white gular spot present on posterior central part, many grey stripes forming reticulated pattern present on other region of ventral head. Ventral surfaces of body, limbs and tail light brick red with no patterns.

Variations. The variations of morphological character of the type series are provided in Table 2. The variations of colouration in life are very small: the paratype KIZ2022013 has few yellowish-white spots below dorsolateral stripe on each side of body, except for this, all other paratypes closely resemble the holotype.

Comparisons. From species of *Diploderma* which are only distributed on East Asian islands, *Diploderma limingense* sp. nov. differs from *D. brevipes* (Gressitt, 1936), *D. luei* (Ota, Chen & Shang, 1998), *D. makii* (Ota, 1989), *D. polygonatum* Hallowell, 1861 and *D. swinhonis* (Günther, 1864) by the presence of a transverse gular fold (vs. absence).

From species of *Diploderma* which are distributed on mainland, but relatively distant from that of *Diploderma limingense* sp. nov., *Diploderma limingense*

Table 2. Morphological data of the type series of *Diploderma limingense* sp. nov. Morphometric measurements are in mm. For measurement methods and abbreviations, see the Materials and methods section.

	KIZ2022014 Holotype ♂	KIZ2022013 Paratype ♂	KIZ2022015 Paratype ♂	KIZ2022017 Paratype ♂
SVL	56.2	56.8	55.6	56.1
TAL	117.5	110.1	113.5	107.7
HL	18.0	18.5	18.0	18.0
HW	13.3	13.2	13.2	13.1
HD	11.3	11.2	11.0	11.4
SEL	6.5	6.7	6.3	6.9
FLL	26.5	27.5	28.7	27.6
HLL	41.8	44.9	45.6	43.4
T4L	10.7	10.9	11.2	9.9
TRL	25.1	24.2	23.6	24.9
TAL/SVL	2.09	1.94	2.04	1.92
SEL/HL	0.36	0.36	0.35	0.38
HW/HL	0.74	0.71	0.73	0.73
HD/HW	0.85	0.85	0.83	0.87
FLL/SVL	0.47	0.48	0.52	0.49
HLL/SVL	0.74	0.79	0.82	0.77
TRL/SVL	0.45	0.43	0.42	0.44
SL	8/8	8/8	8/9	9/9
IL	9/9	8/9	10/8	9/9
NSL	2/1	1/1	1/1	1/1
MD	45	45	47	48
F4S	15/16	16/16	15/16	16/16
T4S	22/22	22/22	22/21	21/21
SOR	4/3	3/4	3/3	3/3
VN	63	58	59	63

sp. nov. differs from *D. chapaense* (Bourret, 1937), *D. fasciatum* (Mertens, 1926), *D. hamptoni* (Smith, 1935), *D. menghaiense* Liu, Hou, Wang, Ananjeva & Rao, 2020, *D. micangshanense* (Song, 1987), *D. ngoclinense* (Ananjeva, Orlov & Nguyen, 2017) and *D. yunnanense* (Anderson, 1878) by the presence of a transverse gular fold (vs. absence); from *D. dymondi* (Boulenger, 1906), *D. varcoae* (Boulenger, 1918), by having concealed tympana (vs. exposed); from *D. grahami* (Stejneger, 1924) by having a much longer tail (TAL/SVL 1.92–2.09 vs. 1.64) and a distinct transverse gular fold (vs. feeble); and from *D. splendidum* (Barbour & Dunn, 1919) by having jagged dorsolateral stripes in males (vs. smooth).

From species of *Diploderma* which occupy distributions relatively close to that of *Diploderma limingense* sp. nov. in the Hengduan Mountain Region, *Diploderma limingense* sp. nov. differs from *D. panlong* Wang, Che & Siler, 2020, *D. slowinskii*, (Rao, Vindum, Ma, Fu & Wilkinson, 2017) and *D. swild* Wang, Wu, Jiang, Chen, Miao, Siler & Che, 2019 by having concealed tympana (vs. exposed); from *D. angustelinea* Wang, Ren, Wu, Che & Siler, 2020, *D. aorun* Wang, Jiang, Zheng, Xie, Che & Siler, 2020, *D. bowoense*, *D. batangense* (Li, Deng, Wu & Wang, 2001), *D. flavilabre* Wang, Che & Siler, 2020, *D. formosgulae* Wang, Gao, Wu, Dong, Shi, Qi, Siler & Che, 2021, *D. iadinum* (Wang, Jiang, Siler & Che, 2016), *D. laeviventre* (Wang, Jiang, Siler & Che, 2016), *D. yangi* Wang, Zhang & Li, 2022, *D. yulongense* and *D. zhaoermii* (Gao & Hou, 2002) by having a yellowish-white gular spot in males in life (vs. chartreuse, blue, green, lilac, orange or yellow); from *D. drukdaypo* (Wang, Ren, Jiang, Zou, Wu, Che & Siler, 2019) by having strongly keeled ventral scales of body (vs. smooth or weakly keeled); from *D. flaviceps* (Barbour & Dunn, 1919) by the presence of a colourful gular spot in males in life (vs. absence) and no skin fold under dorsal and nuchal crests in males (vs. strongly developed and erected); from *D. panchi* Wang, Zheng, Xie, Che & Siler, 2020 by having bright yellow inner lips in life (vs. inner lips flesh colour); and from *D. vela* (Wang, Jiang & Che, 2015) by having feebly developed crests without strongly erected crest scales or skin fold in males in life (vs. distinctively erected crest scales on continuous, well-developed skin fold).

Diploderma limingense sp. nov. is phylogenetically sister to *D. qilin* and *D. brevicauda*, but *Diploderma limingense* sp. nov. can be differentiated from *D. qilin* by having bright yellow inner lips and light orange tongue in life (vs. both inner lips and tongue light flesh colour) and from *D. brevicauda* by having a relatively longer tail in males (TAL/SVL 1.92–2.09 vs. 1.40–1.84) and more mid-dorsal crest scales (MD 45–48 vs. 34–43).

Distribution. This species is known only from the type locality, Liming Township, Yulong County, Lijiang City, Yunnan Province, China (Fig. 1).

Natural history. All specimens were collected between 9 and 11 a.m. on the ground in coniferous and broad-leaved mixed forest and there was no water body nearby (Fig. 12A, B). No female or juvenile was found. The population density of this species was moderate and as the habitats of this species not being threatened. According to IUCN Criteria, we recommend listing this new species as Least Concern (LC).

***Diploderma shuoquense* sp. nov.**
https://zoobank.org/53A4844E-ADBF-4BE0-A924-355D1534019E
Figs 6–8

Holotype. KIZ2022004, adult male, collected on 23 April 2022 by Shuo Liu from the Shuoqu River Valley, Qingde Town, Xiangcheng County, Ganzi Prefecture, Sichuan Province, China (28°48'50"N, 99°49'47"E, 2700 m elevation).

Paratypes. KIZ2022005–KIZ2022007, three adult males, collecting information the same as the holotype.

Etymology. The specific epithet refers to the Shuoqu River, by which the new species was discovered.

Diagnosis. *Diploderma shuoquense* sp. nov. can be diagnosed from congeners by a combination of the following morphological characteristics: (1) body size small, SVL 48.2–52.3 mm in males; (2) tail moderately long, TAL/SVL 1.87–1.97 in males; (3) limbs moderately long, FLL/SVL 0.45–0.49 in males, HLL/SVL 0.69–0.74 in males; (4) head moderately wide, HW/HL 0.72–0.74 in males; (5) MD 34–40; (6) F4S 13–16, T4S 19–21; (7) tympanum concealed; (8) nuchal and dorsal crest scales feebly developed, not distinctively erected or raised on skin folds in males; (9) distinct transverse gular fold present; (10) ventral head scales smooth or weakly keeled and ventral body scales strongly keeled; (11) ventral head scales homogeneous in size; (12) no distinct gular spot in males; (13) dorsolateral stripes jagged in males, yellowish-white or greyish-white in life; (14) 8–10 radial stripes around the eye on each side; (15) oral cavity, inner lips and tongue pink in life.

Description of holotype. Adult male, SVL 52.3 mm; tail moderately long, TAL 98.3 mm, TAL/SVL 1.88; limbs moderately long, FLL 23.4 mm on left side, FLL/SVL 0.45, HLL 36.6 mm on left side, HLL/SVL 0.70. Head relatively robust, HW/HL 0.74, HD/HW 0.82; snout relatively short, SEL/HL 0.34. Rostral rectangular, bordered by six small postrostral scales; dorsal head scales heterogeneous, all strongly keeled; indistinct Y-shaped ridge on dorsal snout. Nasal oval, separated from first supralabial by single row of scales; loreals small, keeled; suborbital scale rows 3/4, keeled; canthus rostralis elongated, greatly overlapping with each other; enlarged, keeled scales forming single lateral ridge from posteroinferior eye to posterosuperior tympanum on each side; tympanum concealed under scales; SL 10/10, feebly keeled. Mental pentagonal; IL 9/9; enlarged chin shields 6/5, smooth, first one contacting IL on left side and first two contacting IL on right side, remaining ones separated from IL by one or two rows of small scales; ventral head scales homogeneous in size, smooth or weakly keeled; distinct transverse gular fold present; gular pouch weakly developed.

Distinct shoulder fold present; dorsal body scales heterogeneous in size and shape, all keeled, tip pointing backwards; axillary scales much smaller than remaining dorsals; enlarged dorsal scales roughly forming four or five longitudinal rows from neck to pelvis on each side of body. Nuchal and dorsal crests feebly developed, slightly raised compared to dorsals, not erect; no skin fold under nuchal and dorsal crests; MD 40. Dorsal limb scales strongly keeled, homogeneous; F4S 15/16, T4S 21/20. Ventral body scales approximately

Figure 6. Dorsal view (top) and ventral view (bottom) of type series of *Diploderma shuoquense* sp. nov. in preservative.

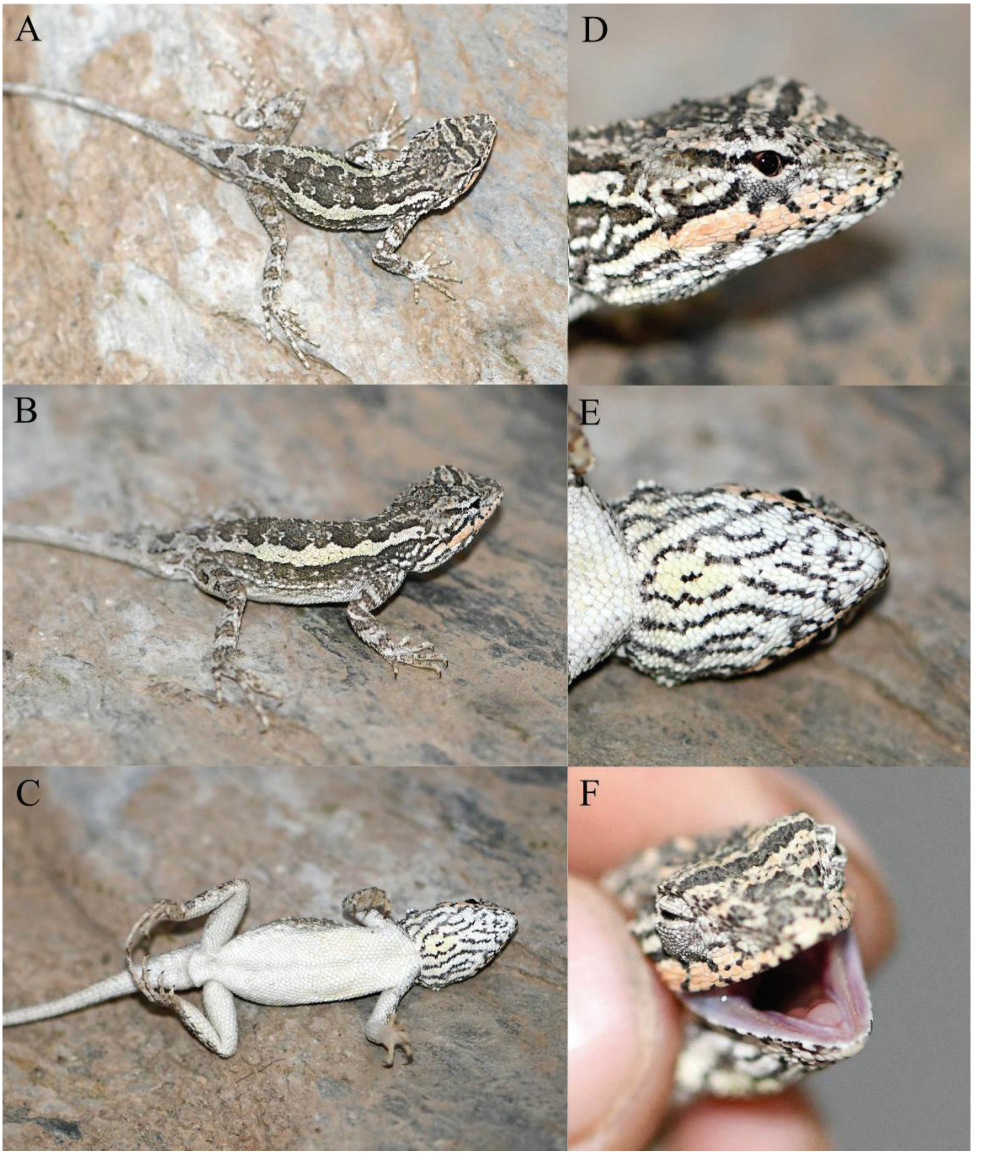

Figure 7. Holotype (KIZ2022004) of *Diploderma shuoquense* sp. nov. in life **A** dorsal view **B** lateral view **C** ventral view **D** close-up view of the lateral side of the head **E** close-up view of the ventral side of the head **F** close-up view of the oral cavity.

parallel, almost homogeneous, all strongly keeled, VN 61. Ventral limb scales parallel, almost homogeneous, approximately equal in size to ventrals, all strongly keeled. Tail scales all strongly keeled, ventral tail scales slightly larger than dorsal tail scales.

Colouration of holotype in life. Dorsal surface of head grey. Two distinct black transverse bands present between orbits on dorsal surface of head and two indistinct

Table 3. Morphological data of the type series of *Diploderma shuoquense* sp. nov. Morphometric measurements are in mm. For measurement methods and abbreviations, see the Materials and methods section.

	KIZ2022004 Holotype ♂	KIZ2022005 Paratype ♂	KIZ2022006 Paratype ♂	KIZ2022007 Paratype ♂
SVL	52.3	48.2	48.4	50.5
TAL	98.3	90.3	95.4	96.3
HL	16.7	14.3	15.4	15.7
HW	12.4	10.5	11.1	11.3
HD	10.2	8.7	9.2	9.8
SEL	5.7	5.4	5.4	5.6
FLL	23.4	22.6	23.5	23.7
HLL	36.6	33.4	36.0	36.4
T4L	8.6	7.8	8.7	8.6
TRL	23.6	22.1	22.5	21.3
TAL/SVL	1.88	1.87	1.97	1.91
SEL/HL	0.34	0.38	0.35	0.36
HW/HL	0.74	0.73	0.72	0.72
HD/HW	0.82	0.83	0.83	0.87
FLL/SVL	0.45	0.47	0.49	0.47
HLL/SVL	0.70	0.69	0.74	0.72
TRL/SVL	0.45	0.46	0.46	0.42
SL	10/10	10/10	9/9	9/8
IL	9/9	11/11	10/10	10/11
NSL	1/1	1/1	1/1	1/1
MD	40	34	39	34
F4S	15/16	14/13	15/15	15/14
T4S	21/20	20/19	20/20	20/19
SOR	3/4	4/4	3/4	4/4
VN	61	59	57	56

greyish-black transverse bands present on dorsal surface of snout. Lateral surfaces of head greyish-white. Ten black radial stripes around eye on each side. Upper lips light orange. Oral cavity, inner lips and tongue pink.

Dorsal surface of body greyish-black. A light yellowish-white dorsolateral longitudinal stripe with strongly jagged upper edge and relatively straight lower edge present on each side of body from occipital region to pelvis. Some indistinct dark and light transverse bands present between two dorsolateral stripes. Some white spots scattered below dorsolateral stripe on each side of body. Dorsal surfaces of limbs dark grey. Some irregular, greyish-white transverse bands present on dorsal surfaces of limbs. Dorsal surface of tail grey with some very indistinct dark transverse bands.

Ventral surface of head white with distinct black vermiculate stripes. A little yellowish colouration present on centre of gular pouch. Ventral surfaces of body, limbs and tail white with no patterns.

Variations. The variations of morphological character of the type series are provided in Table 3. The variations of colouration in life are as follows: the paratypes re-

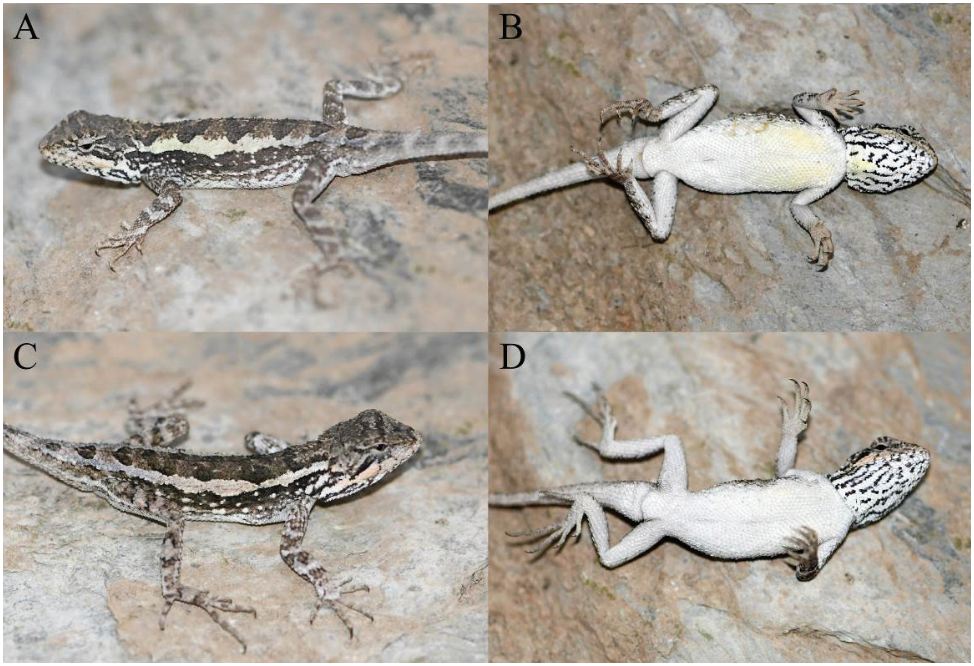

Figure 8. Paratypes of *Diploderma shuoquense* sp. nov. in life **A** dorsolateral view of the paratype KIZ2022005 **B** ventral view of the paratype KIZ2022005 **C** dorsolateral view of the paratype KIZ2022007 **D** ventral view of the paratype KIZ2022007.

semble the holotype in most aspects, except that the dorsal colouration is darker in the paratype KIZ2022007, the light orange colouration on upper lips is more indistinct in the paratypes KIZ2022005 and KIZ2022006, there is no yellowish colouration on the centre of the gular pouch in the paratypes KIZ2022006 and KIZ2022007 and there is some yellowish colouration on the chest in the paratype KIZ2022005.

Comparisons. From species of *Diploderma* which are only distributed on East Asian Islands, *Diploderma shuoquense* sp. nov. differs from *D. brevipes*, *D. luei*, *D. makii*, *D. polygonatum* and *D. swinhonis* by the presence of a transverse gular fold (vs. absence).

From species of *Diploderma* which are distributed on mainland, but relatively distant from that of *Diploderma shuoquense* sp. nov., *Diploderma shuoquense* sp. nov. differs from *D. chapaense*, *D. fasciatum*, *D. hamptoni*, *D. menghaiense*, *D. micangshanense*, *D. ngoclinense* and *D. yunnanense* by the presence of a transverse gular fold (vs. absence); from *D. dymondi*, *D. varcoae*, by having concealed tympana (vs. exposed); from *D. grahami* by having a much longer tail (TAL/SVL 1.87–1.97 vs. 1.64) and a distinct transverse gular fold (vs. feeble); and from *D. splendidum* by having jagged dorsolateral stripes in males (vs. smooth).

From species of *Diploderma* which occupy distributions relatively close to that of *Diploderma shuoquense* sp. nov. in the Hengduan Mountain Region, *Diploderma shuoquense* sp. nov. differs from *D. panlong*, *D. slowinskii* and *D. swild* by having concealed tympana (vs. exposed); from *D. angustelinea*, *D. aorun*, *D. batangense*, *D. flavilabre*, *D. formosgulae*, *D. iadinum*, *D. laeviventre*, *D. yangi*, *D. yulongense* and *D. zhaoermii* by the absence of a distinct gular spot in males in life (vs. presence of a distinct colourful gular spot); from *D. brevicauda* by having a relatively longer tail in males (TAL/SVL 1.87–1.97 vs. 1.40–1.84) and pink inner lips and tongue in life (vs. inner lips light yellow and tongue light orange); from *D. drukdaypo* by having strongly keeled ventral scales of body (vs. smooth or weakly keeled); from *D. flaviceps* by the presence of distinct radial stripes around the eyes (vs. absence) and the absence of a skin fold under dorsal crest in males in life (vs. presence); from *D. panchi* by having less mid-dorsal crest scales (MD 34–40 vs. 42–46) and smooth or weakly keeled ventral scales of head (vs. distinctively keeled); from *D. qilin* by having a relatively shorter tail in males (TAL/SVL 1.87–1.97 vs. 2.01–2.18); and from *D. vela* by having feebly developed crests without strongly erected crest scales or skin fold in males in life (vs. distinctively erected crest scales on continuous, well-developed skin fold).

Diploderma shuoquense sp. nov. is phylogenetically sister to *D. bowoense*, but *Diploderma shuoquense* sp. nov. can be differentiated from the latter by the absence of a light chrome orange gular spot in males in life (vs. presence) and having a wider head (HW/HL 0.72–0.74 vs. 0.65–0.71) and smooth or weakly keeled ventral scales of head (vs. distinctively keeled).

Diploderma shuoquense sp. nov. differs from *Diploderma limingense* sp. nov. by having a smaller body size in males (SVL 48.2–52.3 mm vs. 55.6–56.8 mm), vermiculate stripes covering the whole ventral head (vs. stripes not reaching the centre of gular pouch), white ventral surfaces of body, limbs and tail in males in life (vs. light brick red), pink inner lips and tongue in life (vs. inner lips bright yellow, tongue light orange) and more radial stripes around the eyes (8–10 vs. five on each side).

Distribution. This species is known only from the type locality, Qingde Town, Xiangcheng County, Ganzi Prefecture, Sichuan Province, China (Fig. 1).

Natural history. This species is terrestrial, inhabiting the hot-dry valley. There are many thorny shrubs and some rock piles at the type locality (Fig. 12C, D). All specimens were collected between 1 and 3 p.m. when they were basking on rock piles, no female or juvenile being found. We found many locusts at the type locality, which may be the main prey of this species; however, the population density of this species was very low and the habitats at the type locality being threatened by human activities. According to IUCN Criteria, we recommend listing this new species as Vulnerable (VU).

***Diploderma yongshengense* sp. nov.**

https://zoobank.org/855A40FC-484D-430F-A50E-077512BA9BE8
Figs 9–11

Holotype. KIZ2022009, adult male, collected on 24 April 2022 by Shuo Liu from the Jinsha River Valley, Songping Township, Yongsheng County, Lijiang City, Yunnan Province, China (27°2'2"N, 100°28'16"E, 1700 m elevation).

Figure 9. Dorsal view (top) and ventral view (bottom) of type series of *Diploderma yongshengense* sp. nov. in preservative.

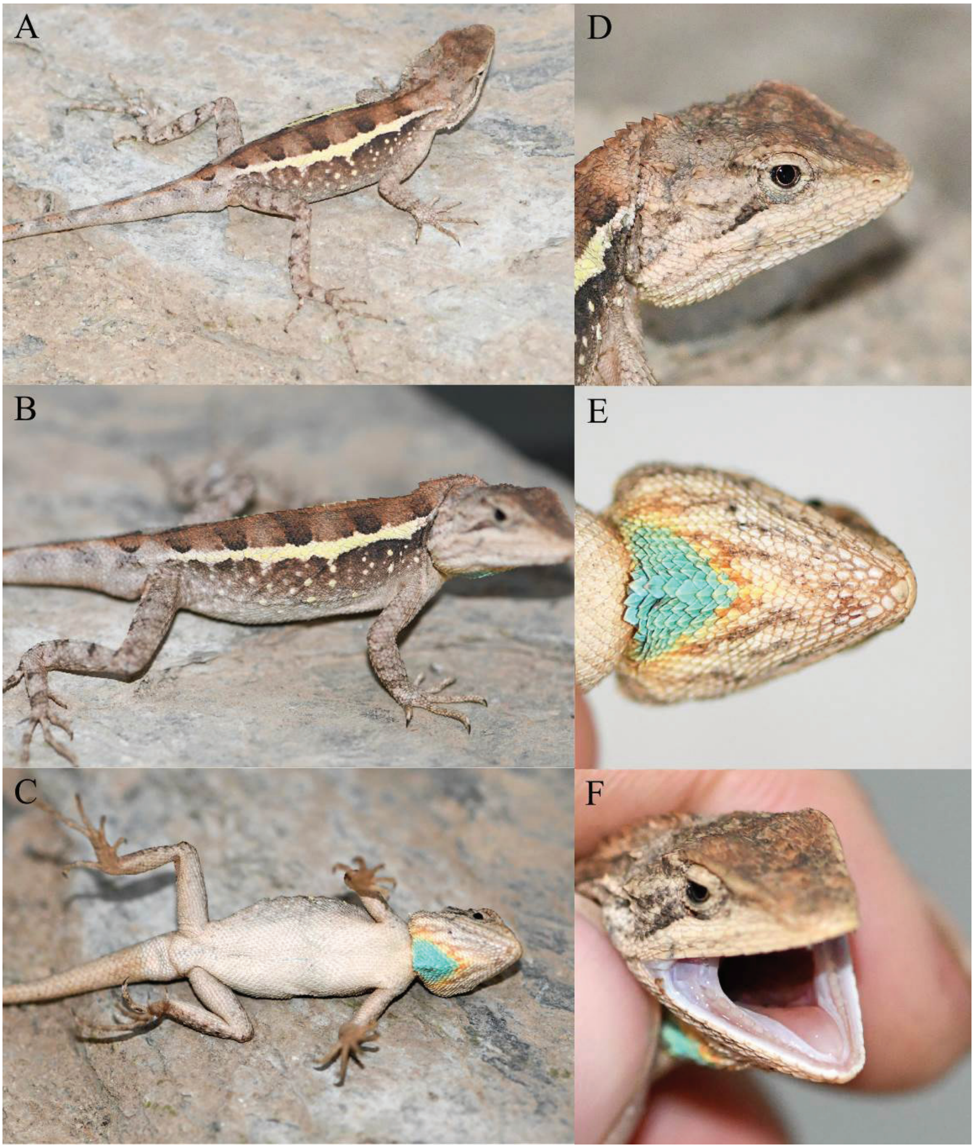

Figure 10. Holotype (KIZ2022009) of *Diploderma yongshengense* sp. nov. in life **A** dorsolateral view **B** lateral view **C** ventral view **D** close up-view of the lateral side of the head **E** close-up view of the ventral side of the head **F** close-up view of the oral cavity.

Paratypes. KIZ2022008, KIZ2022010–KIZ2022011, three adult males, collecting information the same as the holotype.

Etymology. The specific epithet refers to Yongsheng County, where the new species was discovered.

Diagnosis. *Diploderma yongshengense* sp. nov. can be diagnosed from congeners by a combination of the following morphological characteristics: (1) body size moderate,

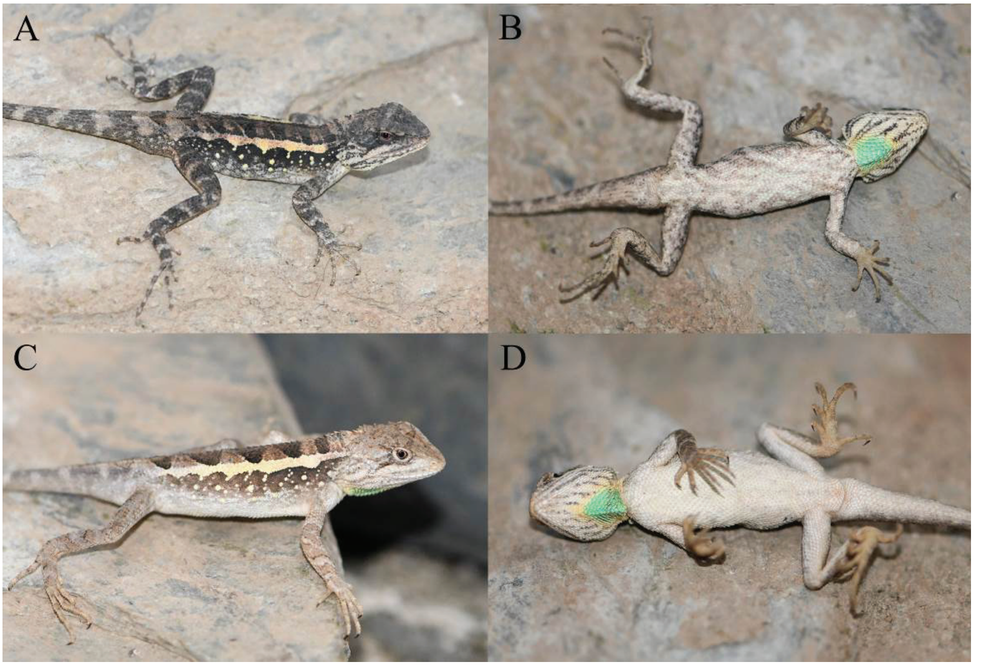

Figure 11. Paratypes of *Diploderma yongshengense* sp. nov. in life **A** dorsolateral view of the paratype KIZ2022008 **B** ventral view of the paratype KIZ2022008 **C** lateral view of the paratype KIZ2022010 **D** ventral view of the paratype KIZ2022010.

SVL 56.5–58.5 mm in males; (2) tail long, TAL/SVL 2.02–2.20 in males; (3) limbs relatively long, FLL/SVL 0.48–0.51 in males, HLL/SVL 0.79–0.87 in males; (4) head moderately wide, HW/HL 0.66–0.75 in males; (5) MD 38–41; (6) F4S 16–19, T4S 22–25; (7) tympanum concealed; (8) nuchal and dorsal crests moderately developed on weak skin folds in males; (9) distinct transverse gular fold present; (10) ventral scales of head and body strongly keeled; (11) ventral head scales heterogeneous in size; (12) gular spot present in males, blue or green in life; (13) dorsolateral stripes jagged in males, light yellow in life; (14) radial stripes around the eyes indistinct; (15) oral cavity, inner lips and tongue light flesh colour in life.

Description of holotype. Adult male, SVL 58.5 mm; tail long, TAL 128.7 mm, TAL/SVL 2.20; limbs relatively long, FLL 27.9 mm on left side, FLL/SVL 0.48, HLL 46.5 mm on left, HLL/SVL 0.79. Head relatively robust, HW/HL 0.75, HD/HW 0.87; snout moderately long, SEL/HL 0.37. Rostral elongated, bordered by five small postrostral scales; dorsal head scales heterogeneous, all strongly keeled; distinct Y-shaped ridge on dorsal snout. Nasal oval, separated from first supralabial by single row of scales; loreals small, keeled; suborbital scale rows 4/4, keeled; canthus rostralis elongated, greatly overlapping with each other; enlarged, keeled scales forming single lateral ridge from posteroinferior eye to posterosuperior tympanum on each side; tympanum concealed under scales; SL 9/9, feebly keeled. Mental pentagonal; IL 11/10; enlarged chin shields 5/5, smooth, first one contacting IL on each side, remaining ones separated from IL by two rows of small scales; ventral head scales heterogeneous in size with the ones on the centre of gular pouch largest, all strongly keeled; distinct transverse gular fold present; gular pouch well developed.

Distinct shoulder fold present; dorsal body scales heterogeneous in size and shape, all keeled, tip pointing backwards; axillary scales much smaller than remaining dorsals; enlarged dorsal scales irregularly scattered on lateral surface of body. Nuchal crest scales approximately same in size and shape as dorsal crest scales; moderately developed skin fold under nuchal crest and feeble skin fold under dorsal crest; MD 38. Dorsal limb scales strongly keeled, mostly homogeneous, except a few enlarged, conical scales on postaxial thighs; F4S 17/16, T4S 23/23. Ventral body scales approximately parallel, almost homogeneous, all strongly keeled, VN 59. Ventral limb scales parallel, almost homogeneous, approximately equal in size to ventrals, all strongly keeled. Tail scales all strongly keeled, ventral tail scales larger than dorsal tail scales.

Colouration of holotype in life. Dorsal surface of head brown with no transverse bands. Lateral surfaces of head brownish-white. No radial stripes present around eyes, only two brownish-black stripes present behind eye on each side. Oral cavity, inner lips and tongue light flesh colour.

Table 4. Morphological data of the type series of *Diploderma yongshengense* sp. nov. Morphometric measurements are in mm. For measurement methods and abbreviations, see the Materials and methods section.

	KIZ2022008 Paratype ♂	KIZ2022009 Holotype ♂	KIZ2022010 Paratype ♂	KIZ2022011 Paratype ♂
SVL	56.5	58.5	56.7	57.6
TAL	117.2	128.7	114.5	123.0
HL	17.9	18.7	17.0	18.8
HW	12.8	14.1	12.1	12.5
HD	11.1	11.0	10.6	11.3
SEL	6.6	6.9	6.3	6.9
FLL	28.6	27.9	27.8	27.4
HLL	49.1	46.5	45.5	47.9
T4L	12.6	11.8	11.3	13.1
TRL	24.3	27.0	24.9	26.1
TAL/SVL	2.07	2.20	2.02	2.14
SEL/HL	0.37	0.37	0.37	0.37
HW/HL	0.72	0.75	0.71	0.66
HD/HW	0.87	0.78	0.88	0.90
FLL/SVL	0.51	0.48	0.49	0.48
HLL/SVL	0.87	0.79	0.80	0.83
TRL/SVL	0.43	0.46	0.44	0.45
SL	10/10	9/9	8/8	9/9
IL	11/10	11/10	10/12	10/10
NSL	1/1	1/1	1/1	1/1
MD	41	38	41	39
F4S	17/18	17/16	19/18	16/17
T4S	22/23	23/23	25/24	24/24
SOR	4/4	4/4	4/4	4/4
VN	55	59	58	54

Dorsal surface of body brown. A light yellow dorsolateral longitudinal stripe with relatively straight upper edge and strongly jagged lower edge present on each side of body from occipital region to pelvis. Some brownish-black transverse bands present between two dorsolateral stripes. Some light yellow spots scattered below dorsolateral stripe on each side of body. Dorsal surfaces of limbs greyish-brown. Some indistinct dark transverse bands present on dorsal surfaces of limbs. Dorsal surface of tail brownish-grey with some indistinct dark transverse bands.

Ventral surface of head yellowish-white. A triangular, light yellow edged light blue gular spot present on posterior central part, indistinct brown stripes present on other region of ventral head. Ventral surfaces of body, limbs and tail white with no patterns.

Variations. The variations of morphological character of the type series are provided in Table 4. The variations of colouration in life are as follows: the paratypes resemble the holotype in most aspects, except that there are indistinct transverse bands on the dorsal surface of the head in all paratypes; the gular spot is light green in the paratypes KIZ2022008 and KIZ2022010; the dorsal colouration is darker, the stripes on the ventral surface of head are more distinct in the paratypes KIZ2022008 and KIZ2022011; and there are some brown speckles on the ventral surfaces of body, limbs and tail in the paratype KIZ2022008.

Comparisons. From species of *Diploderma* which are only distributed on East Asian Islands, *Diploderma yongshengense* sp. nov. differs from *D. brevipes*, *D. luei*, *D. makii*, *D. polygonatum* and *D. swinhonis* by the presence of a transverse gular fold (vs. absence).

From species of *Diploderma* which are distributed on mainland, but relatively distant from that of *Diploderma yongshengense* sp. nov., *Diploderma yongshengense* sp. nov. differs from *D. chapaense*, *D. fasciatum*, *D. hamptoni*, *D. menghaiense*, *D. micangshanense*, *D. ngoclinense* and *D. yunnanense* by the presence of a transverse gular fold (vs. absence); from *D. dymondi*, *D. varcoae*, by having concealed tympana (vs. exposed); from *D. grahami* by having a much longer tail (TAL/SVL 2.02–2.20 vs. 1.64) and a distinct transverse gular fold (vs. feeble); and from *D. splendidum* by having jagged dorsolateral stripes in males (vs. smooth).

From species of *Diploderma* which occupy distributions relatively close to that of *Diploderma yongshengense* sp. nov. in the Hengduan Mountain Region, *Diploderma yongshengense* sp. nov. differs from *D. panlong*, *D. slowinskii* and *D. swild* by having concealed tympana (vs. exposed); from *D. drukdaypo* and *D. vela* by the presence of a colourful gular spot in males in life (vs. absence); from *D. angustelinea*, *D. bowoense*, *D. brevicauda*, *D. formosgulae*, *D. laeviventre*, *D. qilin* and *D. zhaoermii* by having a blue or green gular spot in males in life (vs. chartreuse, lilac, orange or yellow); from *D. aorun* by having less distinct radial stripes around the eyes (vs. more distinct), less distinct stripes on the ventral surface of head (vs. more distinct speckles or vermiculated patterns) and heterogeneous ventral head scales (vs. homogeneous); from *D. batangense* by having white ventral surface of body in males in life (vs. yellow); from *D. flaviceps* by the presence of a colourful gular spot in males in life (vs. absence); from *D. flavilabre* by having light flesh coloured inner lips in life (vs. yellow); from *D. iadinum* by having brown dorsal ground colouration in males in life (vs. emerald green); from *D. panchi* by having less mid-dorsal crest scales (MD 38–41 vs. 42–46)

Figure 12. Habitats of the new species **A** distant view of the type locality of *Diploderma limingense* sp. nov. **B** close view of the type locality of *Diploderma limingense* sp. nov. **C** distant view of the type locality of *Diploderma shuoquense* sp. nov. **D** close view of the type locality of *Diploderma shuoquense* sp. nov. **E** distant view of the type locality of *Diploderma yongshengense* sp. nov. **F** close view of the type locality of *Diploderma yongshengense* sp. nov.

and heterogeneous ventral head scales (vs. homogeneous); and from *D. yangi* by having jagged dorsolateral stripes in males (vs. smooth).

Diploderma yongshengense sp. nov. is phylogenetically sister to *D. yulongense*, but *Diploderma yongshengense* sp. nov. can be differentiated from the latter by having a blue or green gular spot in males in life (vs. chartreuse or opaline green), more distinct stripes on the ventral surface of head (vs. less distinct), white ventral and ventrolateral surface of body in males in life (vs. green) and light yellow dorsolateral stripes and enlarged scales on each side of body in males in life (vs. greenish-yellow).

Diploderma yongshengense sp. nov. differs from *Diploderma limingense* sp. nov. by having less mid-dorsal crest scales (MD 38–41 vs. 45–48), a blue or green gular spot in males in life (vs. yellowish-white), white ventral surfaces of body, limbs and tail in males in life (vs. light brick red) and light flesh coloured inner lips and tongue in life (vs. inner lips bright yellow, tongue light orange).

Diploderma yongshengense sp. nov. differs from *Diploderma shuoquense* sp. nov. by having a larger body size in males (SVL 56.5–58.5 vs. 48.2–52.3), a relatively longer tail in males (TAL/SVL 2.02–2.20 vs. 1.87–1.97), relatively longer hind limbs in males (HLL/SVL 0.79–0.87 vs. 0.69–0.74), more subdigital lamellae of fourth toe (22–25 vs. 19–21) and strongly keeled ventral scales of head (vs. smooth or weakly keeled) and the presence of a distinct colourful gular spot in males in life (vs. absence).

Distribution. This species is presently known from Yongsheng and Ninglang counties, Lijiang City, Yunnan Province, China, it probably occurs in adjacent Muli County, Sichuan Province, China (Fig. 1).

Natural history. This species is terrestrial, inhabiting the hot-dry valley. There are a few trees and many rocks at the type locality (Fig. 12E, F). All specimens were collected between 2 and 4 p.m. when they were basking on large rocks, no female or juvenile being found. The population density of this species was relatively high, however, the habitats of this species being seriously threatened by human activities. According to IUCN Criteria, we recommend listing this new species as Near Threatened (NT).

Discussion

Species of *Diploderma* can be roughly divided into two ecotypes, one inhabiting mountain forests (i.e. *D. brevicauda*, *D. chapaense*, *D. dymondi*, *D. fasciatum*, *D. menghaiense*, *D. swild*, *D. varcoae*, *D. yunnanense* and *Diploderma limingense* sp. nov., etc) and the other inhabiting hot-dry river valleys (i.e. *D. aorun*, *D. bowoense*, *D. drukdaypo*, *D. formosgulae*, *D. laeviventre*, *D. vela*, *D. yangi*, *Diploderma shuoquense* sp. nov. and *Diploderma yongshengense* sp. nov. etc). Mountain forest is often distributed in large areas. Unless there are very high mountains or very large rivers through the forest, different populations living in the forest will not be completely separated and there can be gene exchange between them. Therefore, the species inhabiting forests are usually widely distributed and their diversity is usually low. However, in the Hengduan Mountain Region, there are high mountains between the numerous river valleys, in addition, the altitude drop in different sections of the same river is usually large. Different populations living in the valleys are usually separated from each other and it is difficult for them to make gene exchange. Therefore, in contrast to the species inhabiting forests, the species inhabiting river valleys usually have very small distribution ranges and their diversity is usually very high.

Large areas of forest are not easy to be destroyed completely. Even if some parts are destroyed, there will still be many spaces for species to survive. Therefore, the species inhabiting forests are relatively less threatened by humans. On the contrary, if a section of a river valley is destroyed, such as by expansion of townships and agricultural lands, construction of tourist sites, development of highways and construction of hydroelectric plants (Wang et al. 2016, 2019b, 2021a), the endemic species there may become extinct. Therefore, the species inhabiting river valleys are more vulnerable to human threats. We should focus the conservation efforts on the species that inhabit river valleys and strengthen the protection of the ecological environment of the river valleys in the Hengduan Mountain Region. In addition, we should strengthen the survey of this region to clarify the species diversity of this region, so as to better protect the endemic species in this region.

Acknowledgements

Thanks to the curator of Kunming Natural History Museum of Zoology, Kunming Institute of Zoology, Chinese Academy of Sciences, for his support of the field survey and this study. We also thank the editors and reviewers for their comments on the manuscript. This work was supported by Science-Technology Basic Condition Platform from the Ministry of Science and Technology of the People's Republic of China (2005DKA21402); state theme of Zoological Institute, Russian Academy of Sciences (122031100264-8); the funds from National Science Foundation of China (NSFC) to DQ Rao (NSFC-39570090 and NSFC-31970404); the project of Ministry of Ecology and Environment of China: Investigation and evaluation of amphibian and reptile diversity in Yunling Mountains (2019HB2096001006); and national important research and development project: Biodiversity Conservation and Restoration Technology in High Mountain and Valley Regions of south-western China (2017YFC0505202).

References

Ananjeva NB, Orlov NL, Nguyen TT (2017) A new species of *Japalura* (Agamidae: Lacertilia: Reptilia) from central highland, Vietnam. Asian Herpetological Research 8(1): 14–21. https://doi.org/10.16373/j.cnki.ahr.160031

Anderson J (1878) Anatomical and Zoological Researches: Comprising an Account of the Zoological results of two expeditions to Western Yunnan in 1868 and 1875; and a Monograph of the Two Cetacean Genera *Platanista* and *Orcella*. Bernard Quaritch, London, 985 pp. https://doi.org/10.5962/bhl.title.50434

Barbour T, Dunn ER (1919) Two new Chinese Japaluras. Proceedings of the New England Zoölogical Club 7: 15–19. https://doi.org/10.5962/bhl.part.12089

Boulenger GA (1906) Descriptions of new reptiles from Yunnan. Annals & Magazine of Natural History 17(102): 56–568. https://doi.org/10.1080/00222930608678911

Boulenger GA (1918) Description of a new lizard of the genus *Acanthosaura* from Yunnan. Annals & Magazine of Natural History 9(2): 162. https://doi.org/10.1080/00222931808562358

Bourret R (1937) Notes herpétologiques sur l'indochine française. XV. Lézards et serpents reçu au laboratoire des Sciences Naturelles de l'Université au cours de l'année 1937. Descriptions de deux espèces et de deux varieties nouvelles. Bulletin Générale de l'Instruction Publique 5. Gouvernement Généneral de l'Indochine 1937: 57–82.

Darriba D, Taboada GL, Doallo R, Posada D (2012) jModelTest 2: More models, new heuristics and parallel computing. Nature Methods 9(8): 772. https://doi.org/10.1038/nmeth.2109

Edgar RC (2004) MUSCLE: Multiple sequence alignment with high accuracy and high throughput. Nucleic Acids Research 32(5): 1792–1797. https://doi.org/10.1093/nar/gkh340

Gao ZF, Hou M (2002) Description of a new *Japalura* species from western Sichuan Province, China. Sichuan Journal of Zoology 21(2): 3–5.

Geospatial Data Cloud (2022) SRTMDEMUTM 90m resolution digital elevation data. http://www.gscloud.cn/ [Accessed on 13.05.2022]

Gressitt JL (1936) New reptiles from Formosa and Hainan. Proceedings of the Biological Society of Washington 49: 117–121.

Günther ACLG (1864) The Reptiles of British India. Taylor and Francis, London, 452 pp. https://doi.org/10.5962/bhl.title.5012

Hallowell E (1861) Report upon the Reptilia of the North Pacific Exploring Expedition, under command of Capt. John Rogers. Proceedings. Academy of Natural Sciences of Philadelphia 12: 480–510.

Huelsenbeck JP, Ronquist F, Nielsen R, Bollback JP (2001) Bayesian inference of phylogeny and its impact on evolutionary biology. Science 294(5550): 2310–2314. https://doi.org/10.1126/science.1065889

Li C, Deng QX, Wu Y, Wang Y (2001) A New Species of *Japalura* from Sichuan (Agamidae Gray. *Japalura*). Journal of Sichuan Teachers College 22(4): 329–331.

Liu S, Hou M, Wang J, Ananjeva NB, Rao DQ (2020) A new species of *Diploderma* (Squamata: Sauria: Agamidae) from Yunnan Province, China. Russian Journal of Herpetology 27(3): 127–148. https://doi.org/10.30906/1026-2296-2020-27-3-127-148

Manthey U (2008) Agamid Lizards of Southern Asia – Agamen des südlichen Asien - Draconinae 1. Terralog, Vol. 7a. Edn. Chimaira, Frankfürt am Main, 160 pp.

Manthey U, Denzer W, Hou M, Wang XH (2012) Discovered in historical collections: two new *Japalura* species (Squamata: Sauria: Agamidae) from Yulong Snow Mountains, Lijiang Prefecture, Yunnan, PR China. Zootaxa 3200(1): 27–48. https://doi.org/10.11646/zootaxa.3200.1.2

Mertens R (1926) Herpetologische Mitteilungen – X. Eine neue *Japalura* – Art. Senckenbergiana 8: 146–149.

Minh Q, Nguyen MAT, von Haeseler A (2013) Ultrafast approximation for phylogenetic bootstrap. Molecular Biology and Evolution 30(5): 1188–1195. https://doi.org/10.1093/molbev/mst024

Nguyen L, Schmidt HA, von Haeseler A, Minh BQ (2015) IQ-TREE: A fast and effective stochastic algorithm for estimating maximum-likelihood phylogenies. Molecular Biology and Evolution 32(1): 268–274. https://doi.org/10.1093/molbev/msu300

Ota H (1989) A new species of *Japalura* (Agamidae: Lacertilia: Reptilia) from Taiwan. Copeia 77(3): 569–576. https://doi.org/10.2307/1445482

Ota H, Chen SL, Shang GS (1998) *Japalura leui*: a new agamid lizard from Taiwan (Reptilia: Squamata). Copeia 86(3): 649–659. https://doi.org/10.2307/1447794

Rao DQ, Vindum JV, Ma XH, Fu MX, Wilkinson JA (2017) A new species of *Japalura* (Squamata, Agamidae) from the Nu River valley in southern Hengduan Mountains, Yunnan, China. Asian Herpetological Research 8(2): 86–95. https://doi.org/10.16373/j.cnki.ahr.160053

Ronquist F, Teslenko M, van der Mark P, Ayres DL, Darling A, Hçhna S, Larget B, Liu L, Suchard MA, Huelsenbeck JP (2012) MrBayes 3.2: Efficient Bayesian phylogenetic inference and model choice across a large model space. Systematic Biology 61(3): 539–542. https://doi.org/10.1093/sysbio/sys029

Sambrook J, Fritsch EF, Maniatis T (1989) Molecular Cloning: a Laboratory Manual. Cold Spring Harbor Laboratory Press, New York, 145 pp.

Smith MA (1935) The fauna of British India, including Ceylon and Burma. Reptiles and Amphibia. Vol. II. Sauria. Taylor and Francis, London, 185 pp.

Song MT (1987) Survey of the reptiles of southern Shaanxi. Acta Herpetologica Sinica 6(1): 59–64.

Stejneger LH (1924) Herpetological novelties from China. Occasional papers of the Boston Society of Natural History 5: 119–121.

Tamura K, Stecher G, Kumar S (2021) MEGA11: Molecular Evolutionary Genetics Analysis Version 11. Molecular Biology and Evolution 38(7): 3022–3027. https://doi.org/10.1093/molbev/msab120

Uetz P, Freed P, Aguilar R, Hošek J (2022) The Reptile Database. http://www.reptile-database.org [Accessed on 13.05.2022]

Wang K, Jiang K, Pan G, Hou M, Siler CD, Che J (2015) A new species of *Japalura* (Squamata: Agamidae) from upper Lancang (Mekong) valley of eastern Tibet, China. Asian Herpetological Research 6(3): 159–168. https://doi.org/10.16373/j.cnki.ahr.140042

Wang K, Jiang K, Zou DH, Yan F, Siler CD, Che J (2016) Two new species of *Japalura* (Squamata: Agamidae) from the Hengduan Mountain Range, China. Zoological Research 37(1): 41–56. https://doi.org/10.13918/j.issn.2095-8137.2016.1.41

Wang K, Ren JL, Jiang K, Yuan ZY, Che J, Siler CD (2017) Rediscovery of the enigmatic Mountain Dragon, *Japalura yulongensis* (Reptilia: Sauria: Agamidae), with notes on its natural history and conservation. Zootaxa 4318(2): 351–363. https://doi.org/10.11646/zootaxa.4318.2.8

Wang K, Jiang K, Wang YF, Poyarkov Jr NA, Che J, Siler CD (2018) Discovery of *Japalura chapaensis* Bourret, 1937 (Reptilia: Squamata: Agamidae) from southeast Yunnan Province, China. Zoological Research 39(2): 105–113. https://doi.org/10.24272/j.issn.2095-8137.2017.064

Wang K, Che J, Lin SM, Deepak V, Aniruddha D, Jiang K, Jin JQ, Chen HM, Siler CD (2019a) Multilocus phylogeny and revised classification for mountain dragons of the genus *Japalura s.l.* (Reptilia: Agamidae: Draconinae) from Asia. Zoological Journal of the Linnean Society 185(1): 246–267. https://doi.org/10.1093/zoolinnean/zly034

Wang K, Jiang K, Ren JL, Zou DH, Wu JW, Che J, Siler CD (2019b) A new species of dwarf *Japalura* sensu lato (Reptilia: Squamata: Agamidae) from the upper Mekong River in eastern Tibet, China, with notes on morphological variation, distribution, and conservation of two congeners along the same river. Zootaxa 4544(4): 505–522. https://doi.org/10.11646/zootaxa.4544.4.3

Wang K, Ren JL, Jiang K, Wu JW, Yang CH, Xu HM, Messanger K, Lei KM, Yu HL, Yang JY, Siler CD, Li JT, Che J (2019c) Revised distributions of some species in the genus *Diploderma* (Reptilia: Agamidae) in China. Sichuan Journal of Zoology 38(5): 481–495. https://doi.org/10.11984/j.issn.1000-7083.20180405

Wang K, Wu JW, Jiang K, Chen JM, Miao BF, Siler CD, Che J (2019d) A new species of Mountain Dragon (Reptilia: Agamidae: *Diploderma*) from the *D. dymondi* complex in southern Sichuan Province, China. Zoological Research 40(5): 456–465. https://doi.org/10.24272/j.issn.2095-8137.2019.034

Wang K, Gao W, Wu JW, Dong WJ, Feng XG, Shen WJ, Jin JQ, Shi XD, Qi Y, Siler CD, Che J (2021a) Two New Species of *Diploderma* Hallowell, 1861 (Reptilia: Squamata: Agamidae) from the Hengduan Mountain Region in China and Rediscovery of *D. brevicaudum* (Manthey, Wolfgang, Hou, Wang, 2012). Zootaxa 4941(1): 1–32. https://doi.org/10.11646/zootaxa.4941.1.1

Wang K, Ren JL, Wu JW, Jiang K, Jin JQ, Hou SB, Zheng PY, Xie F, Siler CD, Che J (2021b) Systematic revision of Mountain Dragons (Reptilia: Agamidae: *Diploderma*) in China, with descriptions of six new species and discussion on their conservation. Journal of Zoological Systematics and Evolutionary Research 59(1): 222–263. https://doi.org/10.1111/jzs.12414

Wang K, Zhang YP, Li XQ (2022) A New Species of *Diploderma* (Reptilia: Squamata: Agamidae) from the upper Salween River in Eastern Tibet, China. Zootaxa 5099(2): 201–220. https://doi.org/10.11646/zootaxa.5099.2.3

Wilcox TP, Zwickl DJ, Heath TA, Hillis DM (2002) Phylogenetic relationships of the Dwarf Boas and a comparison of Bayesian and bootstrap measures of phylogenetic support. Molecular Phylogenetics and Evolution 25(2): 361–371. https://doi.org/10.1016/S1055-7903(02)00244-0

Wu JW, Gao ZF, Qin AM (2005) A re-description of *Japalura batangensis*. Sichuan Journal of Zoology 24(3): 344–345.

Supplementary material 1

Uncorrected genetic pairwise distances (*p*-distances) (%) between species based on the mitochondrial ND2 gene sequences

Authors: Shuo Liu, Mian Hou, Dingqi Rao, Natalia B. Ananjeva

Data type: Xls file.

Link: https://doi.org/10.3897/zookeys.1131.86644.suppl1

ZooKeys 1131: 31–58 (2022)
doi: 10.3897/zookeys.1131.94205
https://zookeys.pensoft.net

RESEARCH ARTICLE

A peer-reviewed open-access journal
ZooKeys
Launched to accelerate biodiversity research

A species-group key and notes on phylogeny and character evolution in New Guinean *Exocelina* Broun, 1886 diving beetles (Coleoptera, Dytiscidae, Copelatinae)

Helena Shaverdo[1], Michael Balke[2,3]

1 *Naturhistorisches Museum, Burgring 7, A-1010 Vienna, Austria* **2** *SNSB-Zoologische Staatssammlung München, Münchhausenstraße 21, D-81247 Munich, Germany* **3** *GeoBioCenter, Ludwig-Maximilians-University, Munich, Germany*

Corresponding author: Helena Shaverdo (shaverdo@mail.ru, helena.shaverdo@nhm-wien.ac.at)

Academic editor: Mariano Michat | Received 29 August 2022 | Accepted 27 October 2022 | Published 22 November 2022

https://zoobank.org/E03D8816-8B5A-4A3E-AE3D-763998870CB2

Citation: Shaverdo H, Balke M (2022) A species-group key and notes on phylogeny and character evolution in New Guinean *Exocelina* Broun, 1886 diving beetles (Coleoptera, Dytiscidae, Copelatinae). ZooKeys 1131: 31–58. https://doi.org/10.3897/zookeys.1131.94205

Abstract
Detailed information about the known species groups of *Exocelina* Broun, 1886 from New Guinea is presented, including species numbers, distribution, and references of species-group diagnoses, keys to the species, and species descriptions. An identification key to all species groups is provided. Phylogeny and morphological character evolution are discussed.

Keywords
Morphology, New Guinea, phylogeny, water beetles

Introduction

Exocelina Broun, 1886 is a highly diverse genus of diving beetles. Most species occur in running-water habitats, especially low-order streams and habitats associated with wider mountain streams, throughout the Australian, Pacific and Oriental regions. Mainly lentic lifestyles also occur in four independent and not particularly species rich clades (Toussaint et al. 2015).

The genus was proposed by Broun (1886) for his new, most likely epigean species, *Exocelina advena*, described from Mokohinau Islands, New Zealand. Later, Broun (1893) recognised it as *Copelatus* and renamed it *C. sharpi* due to homonymy with the Neotropical *C. advena* Sharp, 1882. However, this name also turned to be a junior homonym of another Neotropical species (Branden 1884) and was synonymised with *C. australis* (Clark, 1863) by Zimmermann (1920).

Exocelina was infused with new taxonomic life under the name *Copelatus* (*Papuadytes*) Balke, 1998. *Papuadytes* was erected based on morphological characters for 31 New Guinean species, with subsequent addition of a Chinese species (Balke and Bergsten 2003) and seven additional New Guinean species (Balke 1999; Shaverdo et al. 2005). The monophyly and generic status of the group were supported following analyses of copelatine phylogeny based on DNA sequence data (Balke et al. 2004, 2007; Bilton et al. 2015). Transferring more and more Australian *Copelatus* species to *Papuadytes* (Nilsson & Fery, 2006) led to the inclusion of *C. australis* (= *Exocelina advena*) in *Papuadytes*, and the latter name was recognised as being a synonym of *Exocelina* (see Nilsson 2007). Further investigation showed that the genus has a wide distribution in Australasia: 37 species (including 27 new ones) were recorded from New Caledonia (Wewalka et al. 2010; Balke et al. 2014); one species, *E. cheesmanae* (J. Balfour-Browne, 1939), from Vanuatu (Bilton et al. 2015); one species, *E. parvula* (Boisduval, 1835), from Hawaii (Nilsson 2007); two new interstitial species from Australia (Watts and Humphreys 2009; Watts et al. 2016); one new subterranean species, *E. sugayai*, from Malaysia (Balke and Ribera 2020).

However, New Guinea is the core of species diversity of the genus and, therefore, was the focus of our taxonomic project started in 2012. Since the publication of Shaverdo et al. (2005) on *Exocelina* of the island, 116 new species have been described (Table 1), increasing the number of *Exocelina* in New Guinea to 152 species and the number of *Exocelina* worldwide to 209 species (Nilsson and Hájek 2022). We believe that further extensive fieldwork in New Guinea and careful taxonomic investigation of the group might reveal the existence of more new species.

This paper aims to unite and discuss all known information on systematics of the New Guinean *Exocelina* provided in our previous studies (Table 1), focusing on the infrageneric structure of the group. Since all species groups were treated in numerous separate publications, we believe that this paper will provide better orientation in this species-rich genus, and easier species identification. Additionally, since the proposed species-group structure is based not only on morphological characters but also supported by molecular analyses, we believe that it is a good tool for understanding New Guinean *Exocelina* phylogeny and character evolution.

Materials and methods

Our study is based on published articles on the taxonomy of New Guinean *Exocelina*. In cases where specimen study was necessary, we followed the methods described in detail in our previous articles (Shaverdo et al. 2012, 2014; Shaverdo and Balke 2014).

The results are presented as a species-group table and a key to species groups. The table includes all known species groups of New Guinean *Exocelina* with their numbers of species and subspecies, species-group distribution, and references for each group: species-group diagnoses, keys to species identification and species descriptions. The key provides identification to the species-group level and is meant to be a start point in the determination of New Guinean *Exocelina*. To illustrate the key, figures from our published articles are used, as indicated for each figure in the captions.

Results

Species-group structure

We recognise 26 species groups of New Guinean *Exocelina*. The groups were proposed based on our study of morphological characters of the species and data from molecular phylogenetic analyses, where the main diagnostic criteria were structure of the genitalia and relative position of the species in the phylogenetic trees.

Most of the species in New Guinea are lotic, that is, associated with running water habitats. All of these species form one monophyletic group and are, thus, endemic to the island. The only exception is the stagnophilous species *E. baliem* Shaverdo, Hendrich & Balke, 2013, which belongs to the *E. ferruginea* group. This group has two other representatives: the Australian *E. ferruginea* (Sharp, 1882) and the New Caledonian *E. inexpectata* Wewalka, Balke & Hendrich, 2010 (Shaverdo et al. 2013).

Table 1. Checklist of the species groups of New Guinea *Exocelina*.

N	Species group	Number of spp./subspp.	Species distribution IN (Indonesia): Province: Regency PNG (Papua New Guinea): Region: Province	Reference with species-group diagnosis, key, species descriptions
1	*aipo*	4	**IN**: Papua: Pegunungan Bintang, Yahukimo	Balke (1998); Balke et al. 2007 (as *me*-group); Shaverdo et al. (2017a)
2	*aipomek*	1	**IN**: Papua: Pegunungan Bintang **PNG**: Momase: Sandaun	Balke (1998); Shaverdo et al. (2019)
3	*ascendens*	2	**IN**: Papua: Puncak Jaya, Puncak, Pegunungan Bintang	Balke (1998); Shaverdo et al. (2017b)
4	*bacchusi*	5 / 1	**IN**: Papua: Pegunungan Bintang **PNG**: Highlands: Eastern Highlands, Simbu; Momase: Madang, Morobe; Papua: Central, Gulf	Balke (1998); Shaverdo et al. (2019, 2021)
5	*bagus*	1	**IN**: Papua: Nabire	Balke (1998, 2001); Shaverdo et al. (2017b)
6	*broschii*	5	**PNG**: Highlands: Enga, Eastern and Western Highlands, Hela, Simbu; Momase: Madang, Sandaun; Papua: Gulf	Balke (1998); Shaverdo et al. (2005, 2016c)
7	*casuarina*	24	**IN**: West Papua: Nabire; Papua: Puncak, Jayapura, Pegunungan Bintang **PNG**: Highlands: Eastern, Southern and Western Highlands, Enga, Simbu; Momase: East Sepik, Madang, Morobe, Sandaun	Balke (1998, 1999); Shaverdo et al. (2018)

N	Species group	Number of spp./subspp.	Species distribution IN (Indonesia): Province: Regency PNG (Papua New Guinea): Region: Province	Reference with species-group diagnosis, key, species descriptions
8	*danae*	15	**IN**: West Papua: Teluk Wondama; Papua: Paniai, Intan Jaya, Puncak Jaya, Puncak, Pegunungan Bintang **PNG**: Highlands: Eastern and Western Highlands, Enga, Simbu; Momase: Madang, Morobe, Sandaun, Papua: Central, Gulf, National Capital District, Oro (Northern), Fly (Western)	Balke (1998); Shaverdo et al. (2016d)
9	*ekari*	62 / 3	**IN**: West Papua: Fak-Fak, Manokwari, Raja Ampat, Sorong, Teluk Wondama; Papua: Jayapura, Mamberamo Raya, Mimika, Nabire, Paniai, Pegunungan Bintang, Sarmi, Yahukimo, Yapen Islands **PNG**: Highlands: Eastern, Southern and Western Highlands, Enga, Hela, Simbu; Momase: East Sepik, Madang, Morobe, Sandaun; Papua: Gulf, Fly (Western)	Balke (1998); Shaverdo and Balke (2019); Shaverdo et al. (2005, 2012, 2014, 2016a, 2020a, b, 2021)
10	*ferruginea* (*E. baliem*)	1	**IN**: Papua: Jayawijaya	Shaverdo et al. (2013)
11	*iratoi*	1	**IN**: Papua: Puncak	Shaverdo et al. (2017b)
12	*jaseminae*	4	**PNG**: Highlands: Eastern Highlands; Momase: Morobe; Papua: Central	Balke (1998); Shaverdo et al. (2019)
13	*koroba*	1	**PNG**: Highlands: Hela	Shaverdo et al. (2019)
14	*larsoni*	3	**PNG**: Highlands: Eastern Highlands, Simbu; Momase: Madang; Papua: Central, National Capital	Balke (1998); Shaverdo et al. (2019)
15	*likui*	1	**IN**: Papua: Puncak Jaya	Shaverdo et al. (2017b)
16	*mekilensis*	1	**PNG**: Momase: Sandaun	Shaverdo et al. (2019)
17	*monae*	1	**PNG**: Momase: Morobe	Balke (1998)
18	*morobensis*	1	**PNG**: Momase: Morobe	Shaverdo et al. (2019)
19	*okbapensis*	4 / 1	**IN**: Papua: Jayawijaya, Pegunungan Bintang, Yahukimo **PNG**: Momase: Sandaun	Shaverdo et al. (2017a)
20	*pui*	1	**IN**: Papua: Puncak	Shaverdo et al. (2017b)
21	*ransikiensis*	1	**IN**: West Papua: Manokwari; Papua: Nabire	Shaverdo et al. (2016b, 2017b)
22	*skalei*	2	**IN**: West Papua: Kaimana; Papua: Mimika	Shaverdo et al. (2020b)
23	*takime*	2	**IN**: Papua: Pegunungan Bintang **PNG**: Momase: Sandaun	Balke (1998); Shaverdo et al. (2019)
24	*ullrichi*	3	**PNG**: Highlands: Eastern Highlands; Momase: Morobe	Balke (1998); Shaverdo and Balke (2014)
25	*warasera*	4	**PNG**: Highlands: Eastern Highlands, Simbu; Momase: Morobe; Papua: Central	Shaverdo et al. (2019)
26	*wigodukensis*	2	**IN**: Papua: Puncak Jaya	Shaverdo et al. (2017b)

Key to New Guinean species groups of *Exocelina*

The key is proposed for identification of the species groups and species in the case of monotypic groups. The keys to species of individual groups can be found in the publications listed in Table 1.

The key is mostly based on male characters, but organised in a way to get one as far as possible with female identification. In many cases, females cannot be assigned to species due to the similarity of their external and internal structures (for female genitalia see figs 17a, b in Shaverdo et al. (2005) and fig. 7 in Shaverdo et al. (2013)). Some species are rather similar in external morphology and, therefore, in most cases, the male genitalia need to be studied for reliable species identification. However, for some groups, identification of the females is possible to the species group and even to species. The important point here is not to separate females from males from the same locality. Their identification should follow identification of the males of all species from the chosen locality. If co-occurring species are not numerous (2–4 species), successful identifications of females are highly possible.

1 Elytron covered with short longitudinal strioles (Fig. 1) .... ***ferruginea* group (*E. baliem*)**
– Elytron without strioles.. **2**
2 Pronotum with lateral bead, rarely narrow but distinct **3**
– Pronotum without lateral bead, sometimes (especially in females) with bead traces or even narrow bead, in this case several specimens of population should be checked **22**
3 Male protarsomere 5 strongly modified: concave ventrally, sometimes with anteroproximal setae enlarged. Male protarsomere 4 with anterolateral hook-like seta small, not developed (Fig. 2). Male antennomeres modified .... ***aipo* group**
– Male protarsomere 5 not modified. Male protarsomere 4 with anterolateral hook-like seta small to large (Fig. 3). Male antennomeres modified or not...... **4**
4 Median lobe of aedeagus with discontinuous outline in ventral and often in lateral views (Fig. 4) .... ***ekari* group (in part)**
– Median lobe of aedeagus with continuous or slightly discontinuous apically outline in ventral view... **5**
5 Paramere with most of setae very short, inconspicuous, some distal setae stronger. Median lobe without setae, with continuous or slightly discontinuous apically outline in ventral view (Fig. 5A, B) .... ***skalei* group**
– Paramere with strong and long distal setae, rarely with all setae very short, inconspicuous. Median lobe with or without setae, with continuous outline...... **6**
6 Median lobe with fork-like apex of ventral sclerite (Fig. 6A, B)...... ***broschii* group**
– Median lobe with apex of ventral sclerite more or less deeply separated in two (rarely three) lobes (Fig. 6C, D) 7
7 Male antennomere 2 distinctly larger than other antennomeres (Fig. 7) **8**
– Male antennomeres simple or differently modified.. **9**
8 Paramere with very short, inconspicuous setae. Median lobe with minuscule tip of apex curved upwards in lateral view (Fig. 8A) .... ***ullrichi* group**
– Paramere with long, distinct setae. Median lobe with broadly pointed apex in lateral view (Fig. 8B) .... ***danae* group (*miriae* subgroup)**
9 Median lobe in ventral view with distinctly concave apex forming two apical lobes **10**
– Median lobe in ventral view pointed, truncate, or rounded, without two apical lobes **11**
10 Median lobe long and slender, with fine apical setae; its apical lobes narrow and concave in lateral view (Fig. 9A).. ***monae* group**
– Median lobe shorter and more robust, without setae; its apical lobes broader, usually rounded in lateral view (Fig. 9B) ....***jaseminae* group**
11 Median lobe very broad, robust, almost parallel-sided, with weak median constriction in ventral view; lateral sides strongly thickened; apexes of ventral sclerites very unequal: right one much longer than left one (Fig. 10) .... ***larsoni* group**
– Median lobe slender and of different shape; lateral sides not or only slightly thickened; apexes of ventral sclerites equal or slightly unequal in length........ **12**

12 Median lobe with setae **13**
– Median lobe without setae **14**
13 Beetle larger, TL–H 5.3–5.8 mm ...... ***ascendens* group (in part: *E. ascendens*)**
– Beetle smaller, TL–H 3.4–4.75 mm ....***danae* group (in part)**
14 Paramere with distinct dorsal notch and subdistal part well developed (Fig. 11A) **15**
– Paramere without dorsal notch, slightly concave, subdistal part not evidently separated (Fig. 11B) **18**
15 Subdistal part of paramere large, long, with numerous strong setae **16**
– Subdistal part of paramere small, with a tuft of setae.................................... **17**
16 Pronotum with distinct lateral bead. Median lobe longer and slender; lateral sides not thickened; in ventral view, narrow, slightly tapering to narrowly rounded apex; in lateral view, apex thin and elongate (Fig. 12A) .... ***aipomek* group (*E. aipomek*)**
– Pronotum with narrow lateral bead. Median lobe shorter and more robust, lateral sides slightly thickened; in ventral view, broadened medially or subdistally, apex broadly pointed or slightly concave; in lateral view, apex thicker, not elongate (Fig. 12B) .... ***takime* group**
17 Median lobe robust, apex with strong, short prolongation, curved downwards in lateral view (Fig. 13A). Subdistal part of paramere larger .... ***koroba* group (*E. koroba*)**
– Median lobe slender, evenly curved, apex without apical prolongation, very slightly curved downwards in lateral view (Fig. 13B). Subdistal part of paramere smaller ....***okbapensis* group**
18 Paramere with dorsal setae divided into distinct, evidently stronger subdistal setae and inconspicuous proximal ones due to much weaker median setation (Fig. 14A) **19**
– Paramere with dorsal setae uniform, inconspicuous or distinct, or with proximal setae distinct and long, sometimes stronger than subdistal (Fig. 14B) **21**
19 Median lobe almost parallel-sided, often narrowed distally before or to apex or broadened subdistally; its apex usually with thickened sides, slightly or distinctly enlarged ("swollen", often in shape of a baby pacifier), rounded, truncate, or slightly concave in ventral view (Fig. 15)................. ***casuarina* group (in part)**
– Median lobe different. Apex without such modifications............................... **20**
20 Median lobe thinner in apical half; in ventral view, evenly attenuated to pointed apex and, in lateral view, evenly broad, with rounded apex; its lateral margins slightly thickened (Fig. 16A)......................***morobensis* group (*E. morobensis*)**
– Median lobe more robust; evenly attenuated to bluntly pointed apex in ventral and lateral views; lateral margins not thickened, right one can be slightly concave distally in lateral view (Fig. 16B) .... ***warasera* group**

21 Median lobe in lateral view slender, almost straight, only apex distinctly curved downwards; in ventral view, with apex very broadly rounded (Fig. 16C). Setae of paramere very fine, inconspicuous. Beetle dorsally matt, with distinct to strong punctation and microreticulation .... ***ransikiensis* group (*E. ransikiensis*)**

– Median lobe in lateral view broader, more strongly curved, more or less evenly attenuated to thinner apex; in ventral view, apex bluntly pointed (Fig. 16D). Setae of paramere more distinct. Dorsal surface sculpture different, usually very fine .... ***bacchus* group**

22 Median lobe with discontinuous outline in ventral and often in lateral views (Fig. 4) .... ***ekari* group (in part)**

– Median lobe with continuous outline **23**

23 Male antennomeres extremely modified: antennomeres 4–6 excessively large, 3 and 7 strongly enlarged (Fig. 17)................................ ***bagus* group (*E. bagus*)**

– Male antennomeres simple or slightly enlarged **24**

24 Apex of median lobe with two lateral and one dorsal prolongations (Fig. 18).... .... ***iratoi* group (*E. iratoi*)**

– Apex of median lobe without such modifications.. **25**

25 Paramere with numerous small spines, no long setae. Apex of median lobe thick, short and slightly curved downwards, its minuscule tip curved upwards in lateral view (Fig. 19)... ***mekilensis* group (*E. mekilensis*)**

– Paramere with long setae. Apex of median lobe pointed or rounded, without such modifications **26**

26 Median lobe with distinct subapical setae.. **27**

– Median lobe without setae, in some species with minuscule spines................ **28**

27 Beetle larger, TL–H > 4.5 mm. Apex of median lobe pointed in lateral view and rounded in ventral view (Fig. 20A) ...... ***ascendens* group (in part: *E. tombansi*)**

– Beetle smaller, TL–H < 3.6 mm. Apex of median lobe roundly truncate in lateral view and concave in ventral view (Fig. 20B) .... ***pui* group (*E. pui*)**

28 Apex of median lobe with thickened sides, often distinctly enlarged ("swollen"), in lateral and ventral views often of shape of a baby pacifier, rounded, truncate, or slightly concave in ventral view (Fig. 20C, D)..... ***casuarina* group (in part)**

– Apex of median lobe of different shape, relatively thin, elongate in lateral view and broadly truncate in ventral view **29**

29 Beetle larger, TL–H 3.7–4.35 mm. Male antennomeres enlarged. Median lobe longer. Paramere with numerous small and few large proximal setae; large setae with basal prolongations (Fig. 21A) .... ***wigodukensis* group**

– Beetle smaller, TL–H 3.2–3.6 mm. Male antennomeres simple. Median lobe shorter. Paramere only with small proximal setae (Fig. 21B)............................. .... ***likui* group (*E. likui*)**

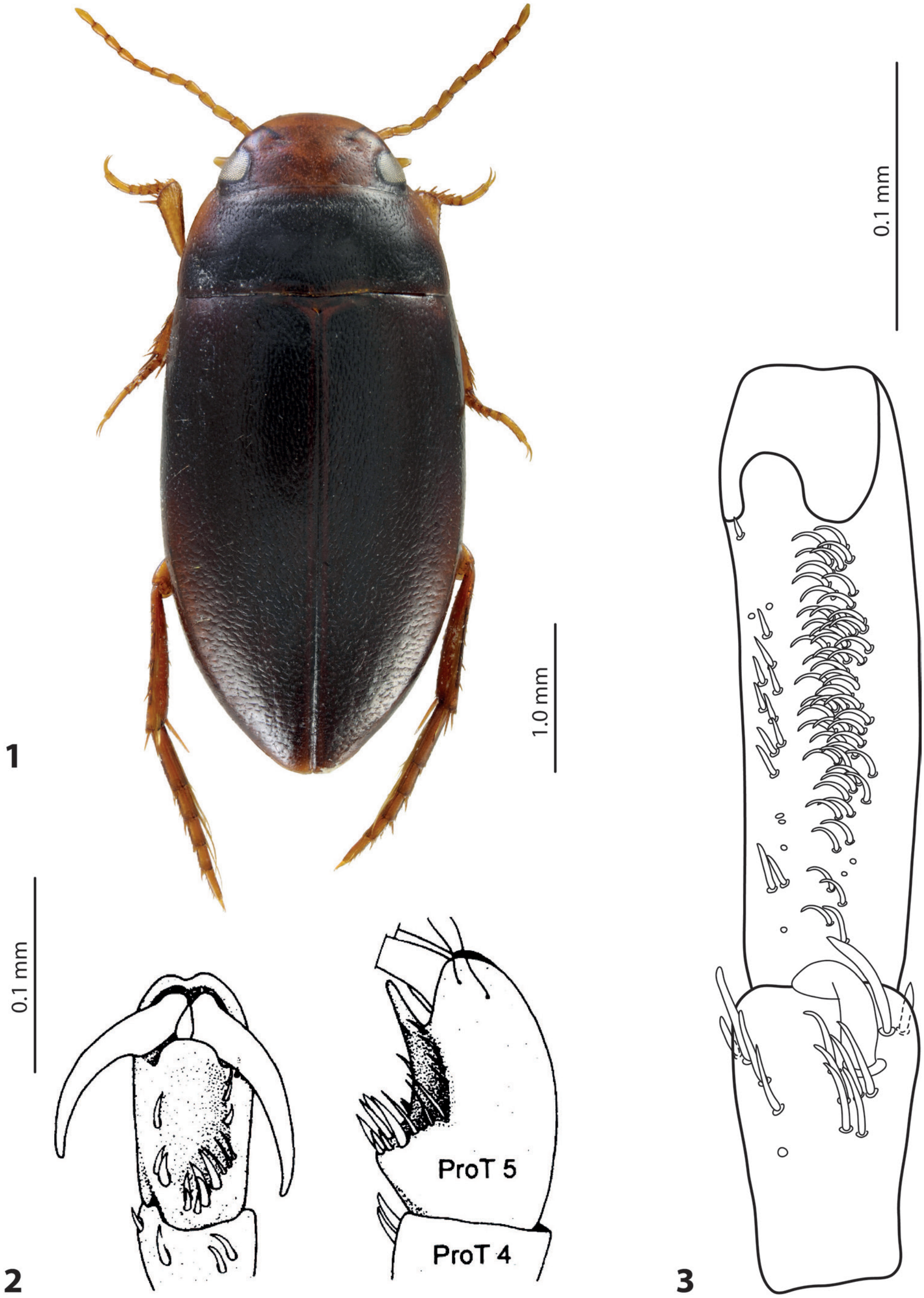

Figures 1–3. 1 Habitus of *Exocelina baliem* Shaverdo, Hendrich & Balke, 2013, female (Shaverdo et al. 2013: 86, fig. 1) **2** Structure of male protarsomeres 4 and 5 of *E. aipo* (Balke, 1998) in ventral and lateral views (Balke 1998: 319, fig. 25) **3** Male protarsomeres 4 and 5 of *E. mimika* Shaverdo & Balke, 2020 in ventrolateral view (Shaverdo et al. 2020b: 140, fig. 9B).

4

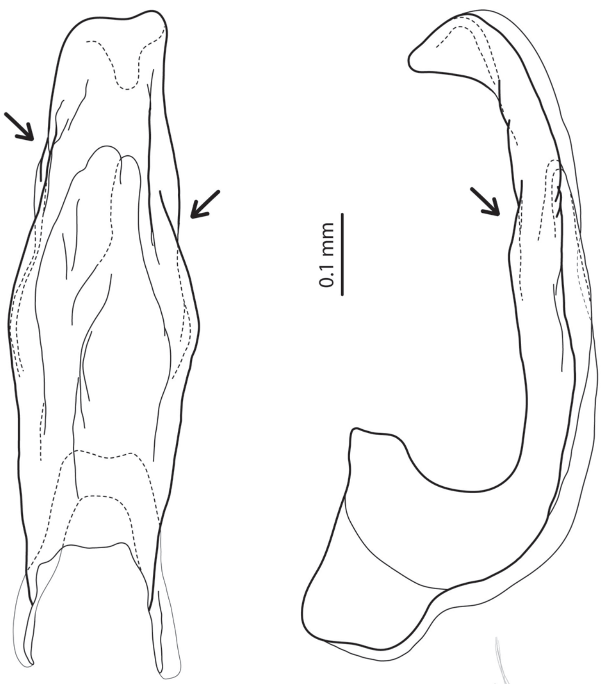

5

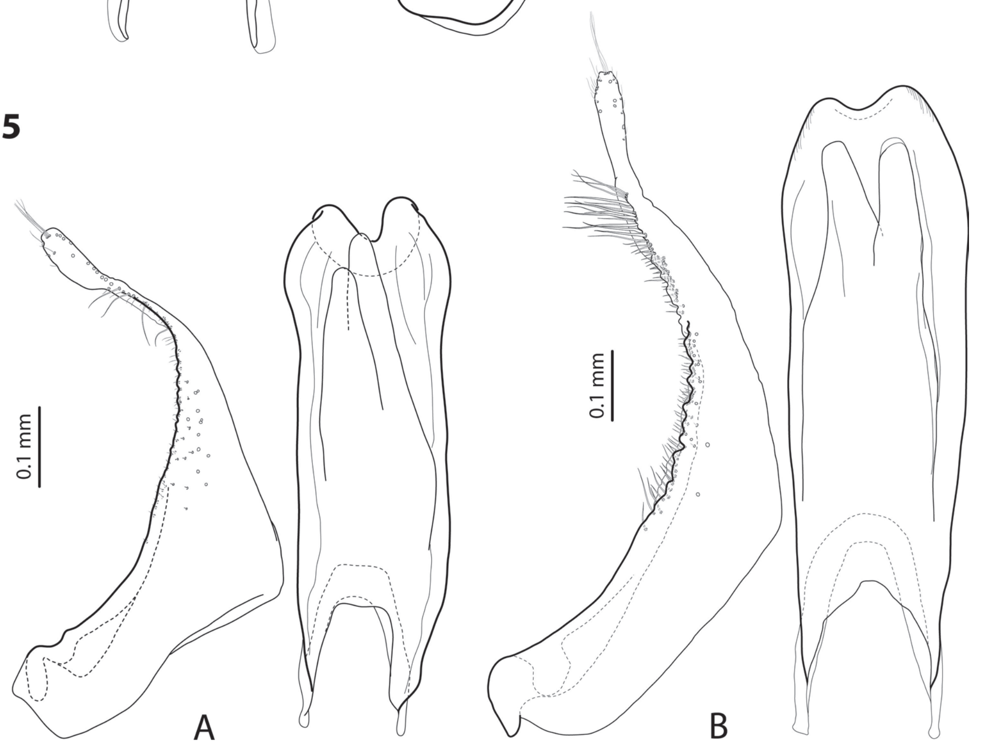

Figures 4, 5. 4 Discontinuous outlines (see arrows) of median lobe of aedeagus of *Exocelina oceai* Shaverdo, Hendrich & Balke, 2012 in ventral and lateral views (Shaverdo et al. 2012: 46, fig. 1) **5** Paramere and median lobe in ventral view of **A** *E. skalei* Shaverdo & Balke, 2014 (Shaverdo et al. 2014: 51, fig. 1C, D) **B** *E. mimika* Shaverdo & Balke, 2020 (Shaverdo et al. 2020b: 140, fig. 9C, A).

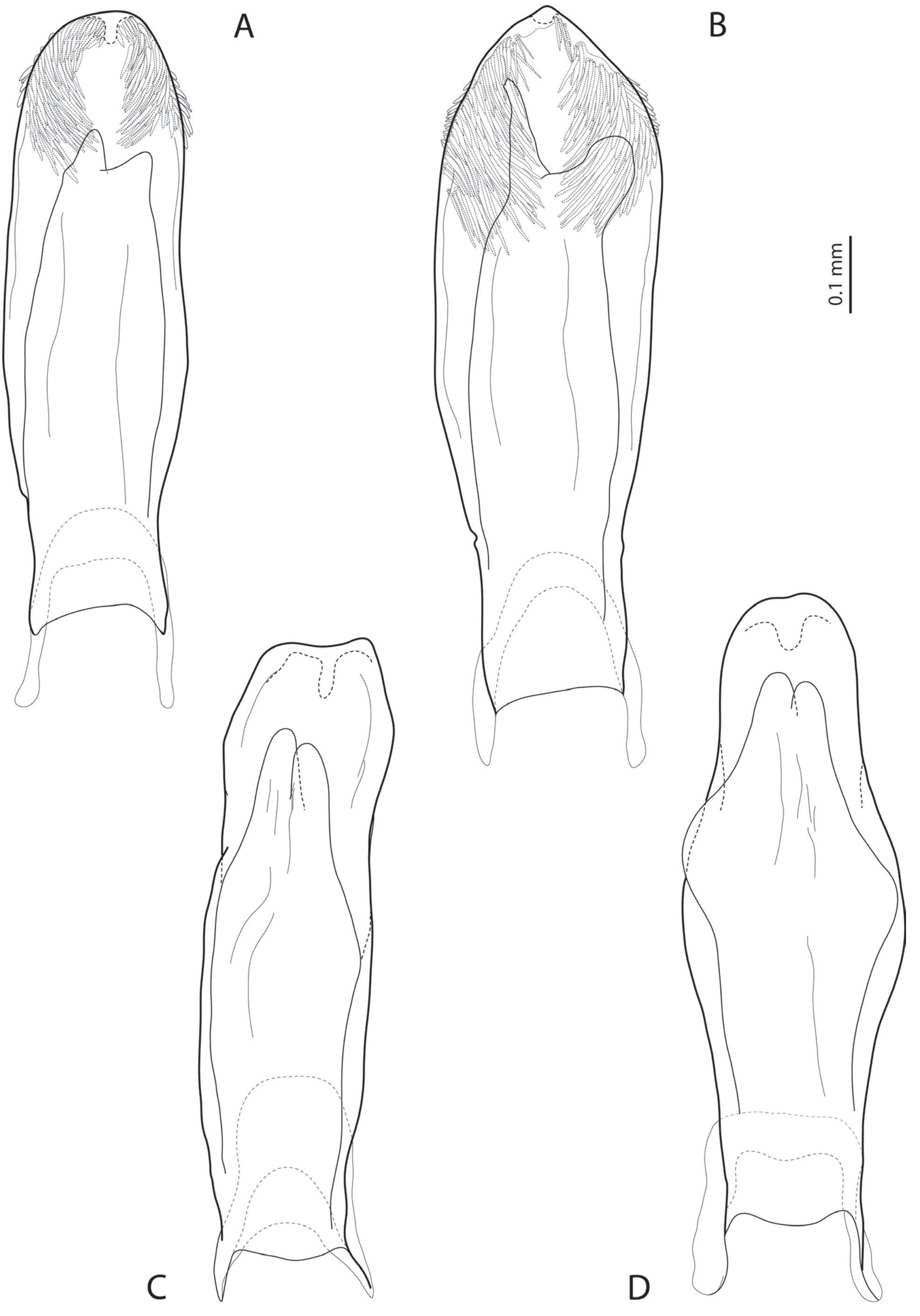

Figure 6. Median lobe in ventral view of **A** *Exocelina broschii* (Balke, 1998) (Shaverdo et al. 2016c: 134, fig. 8B) **B** *E. mondmillensis* Shaverdo, Sagata & Balke, 2016 (Shaverdo et al. 2016c: 139, fig. 11B) **C** *E. gorokaensis* Shaverdo & Balke, 2014 (Shaverdo et al. 2014: 63, fig. 14C) **D** *E. ksionseki* Shaverdo & Balke, 2014 (Shaverdo et al. 2014: 67, fig. 18C).

7

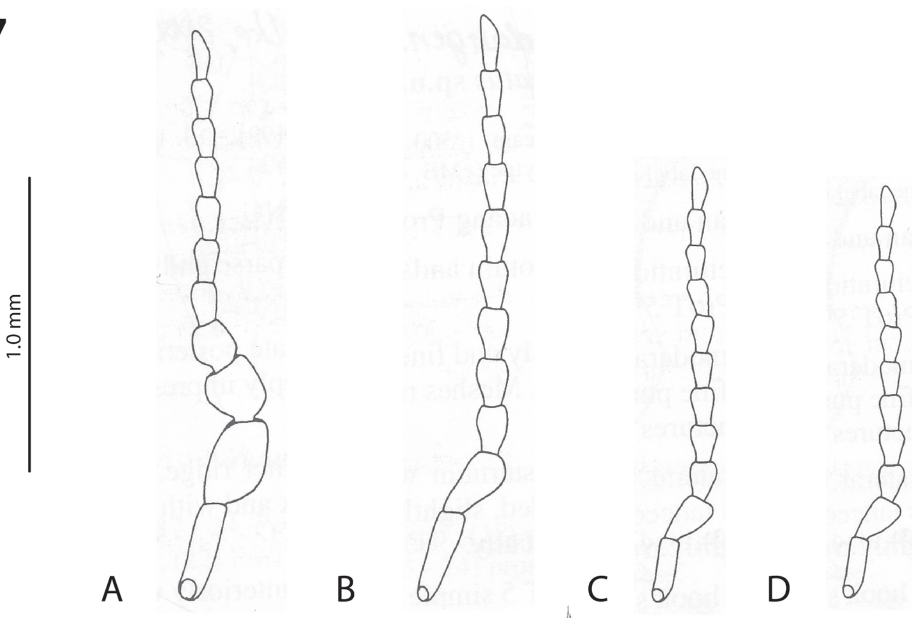

8

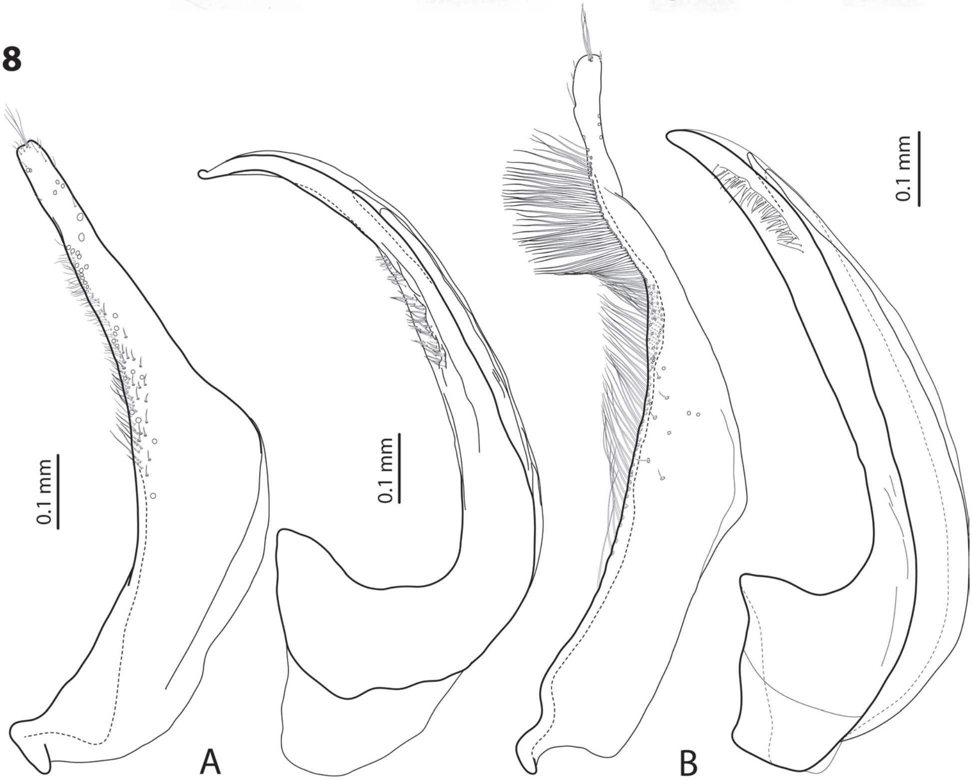

Figures 7, 8. 7 Male antennae of **A** *Exocelina kainantuensis* (Balke, 2001) **B** *E. ullrichi* (Balke, 1998) **C** *E. miriae* (Balke, 1998) **D** *E. rufa* (Balke, 1998) (Balke 1998: 315, figs 12–15) **8** Paramere and median lobe in lateral view of **A** *E. kinibeli* Shaverdo & Balke, 2014 (Shaverdo and Balke 2014: 35, fig. 3; p. 36, fig. 4) **B** *E. miriae* (Shaverdo et al. 2016d: 81, fig. 2C, B).

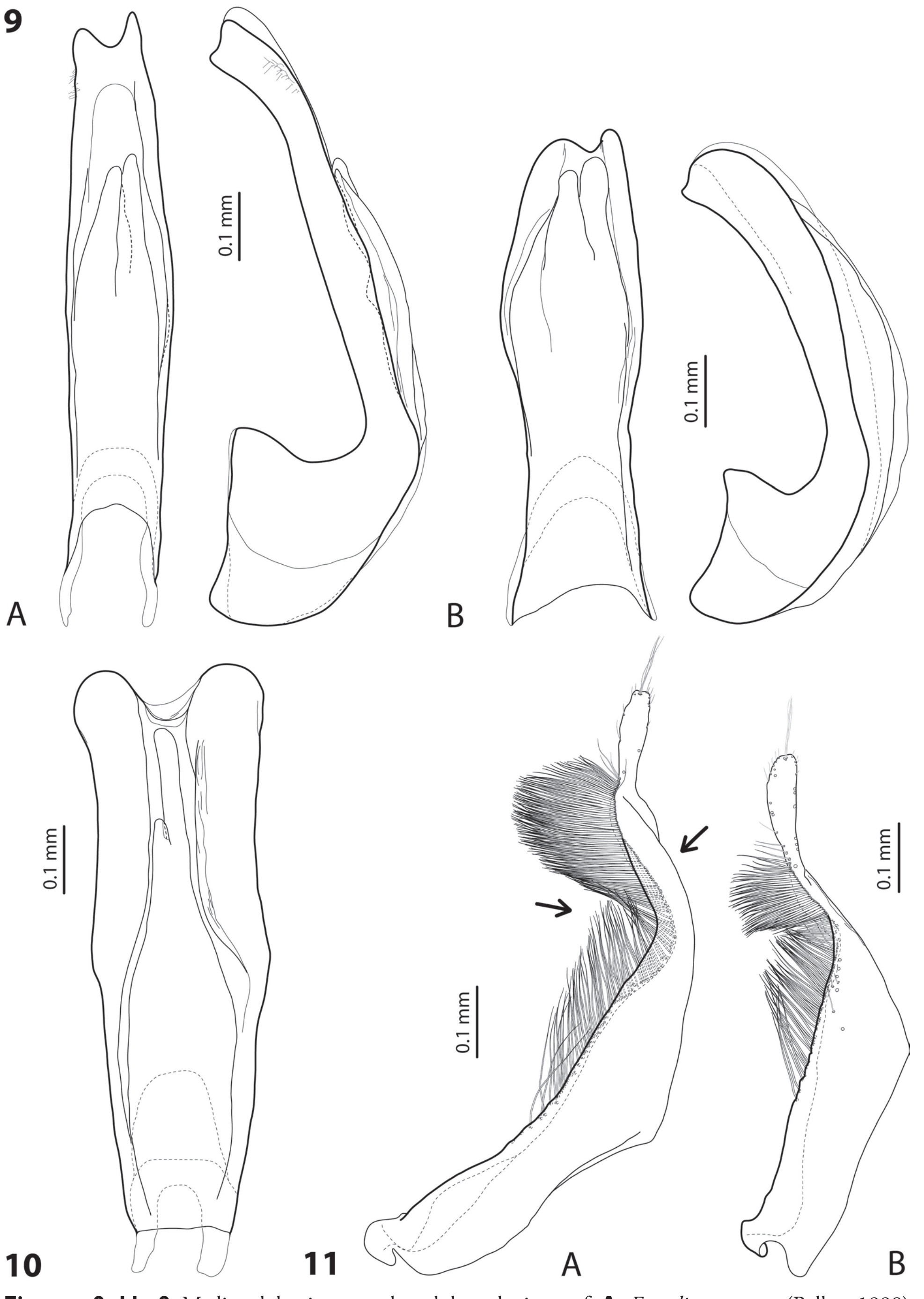

Figures 9–11. 9 Median lobe in ventral and lateral views of **A** *Exocelina monae* (Balke, 1998) **B** *E. jaseminae* (Balke, 1998) (Shaverdo et al. 2019: 114, fig. 31A, B) **10** Median lobe in ventral view of *E. larsoni* (Balke, 1998) (Shaverdo et al. 2019: 126, fig. 40B) **11** Paramere of **A** *E. aipomek* (Balke, 1998) (Shaverdo et al. 2019: 79, fig. 5C) **B** *E. casuarina* (Balke, 1998) (Shaverdo et al. 2018: 54, fig. 26C).

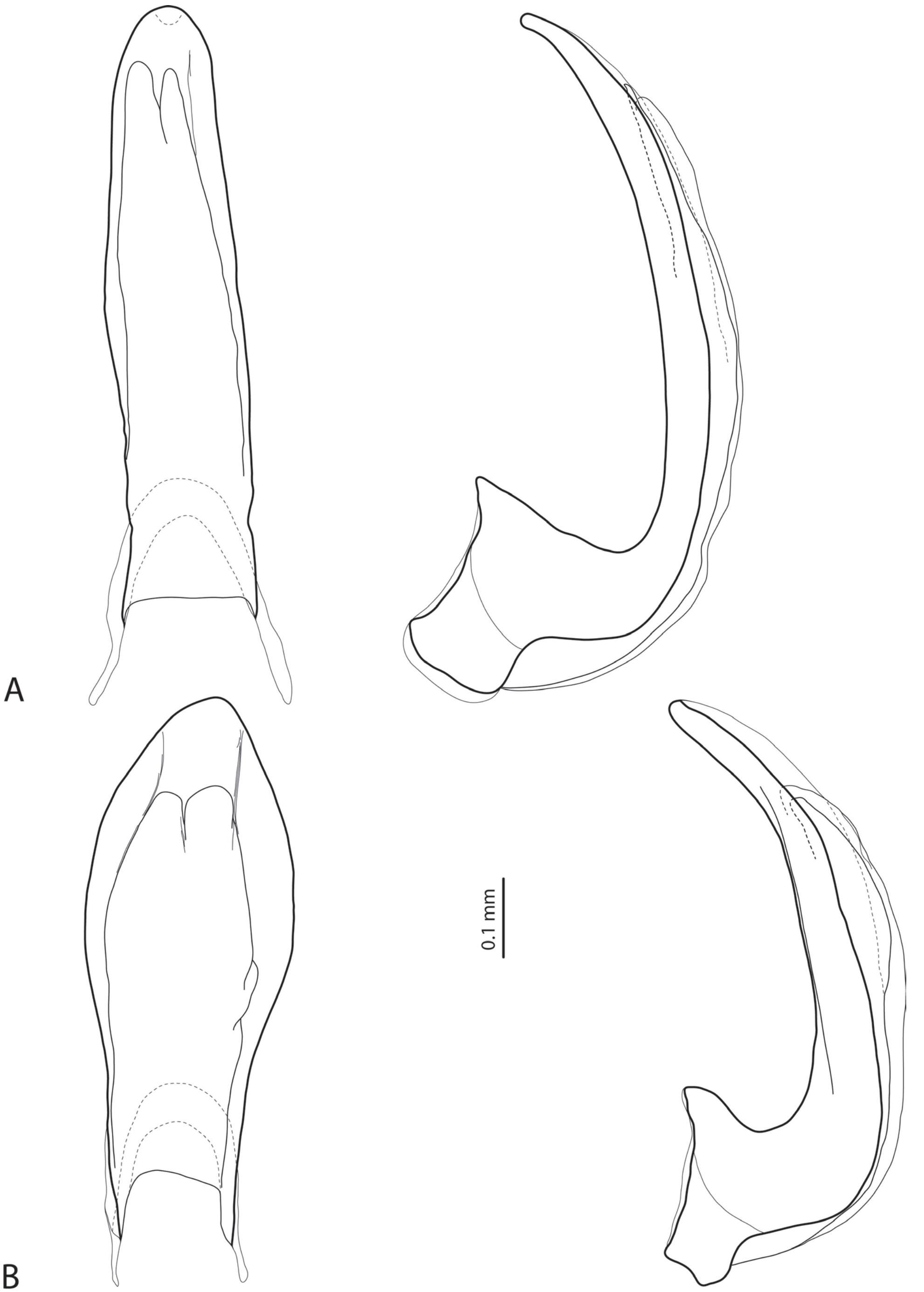

Figure 12. Median lobe in ventral and lateral views of **A** *Exocelina aipomek* (Balke, 1998) (Shaverdo et al. 2019: 79, fig. 5A, B) **B** *E. takime* (Balke, 1998) (Shaverdo et al. 2019: 131, fig. 44A, B).

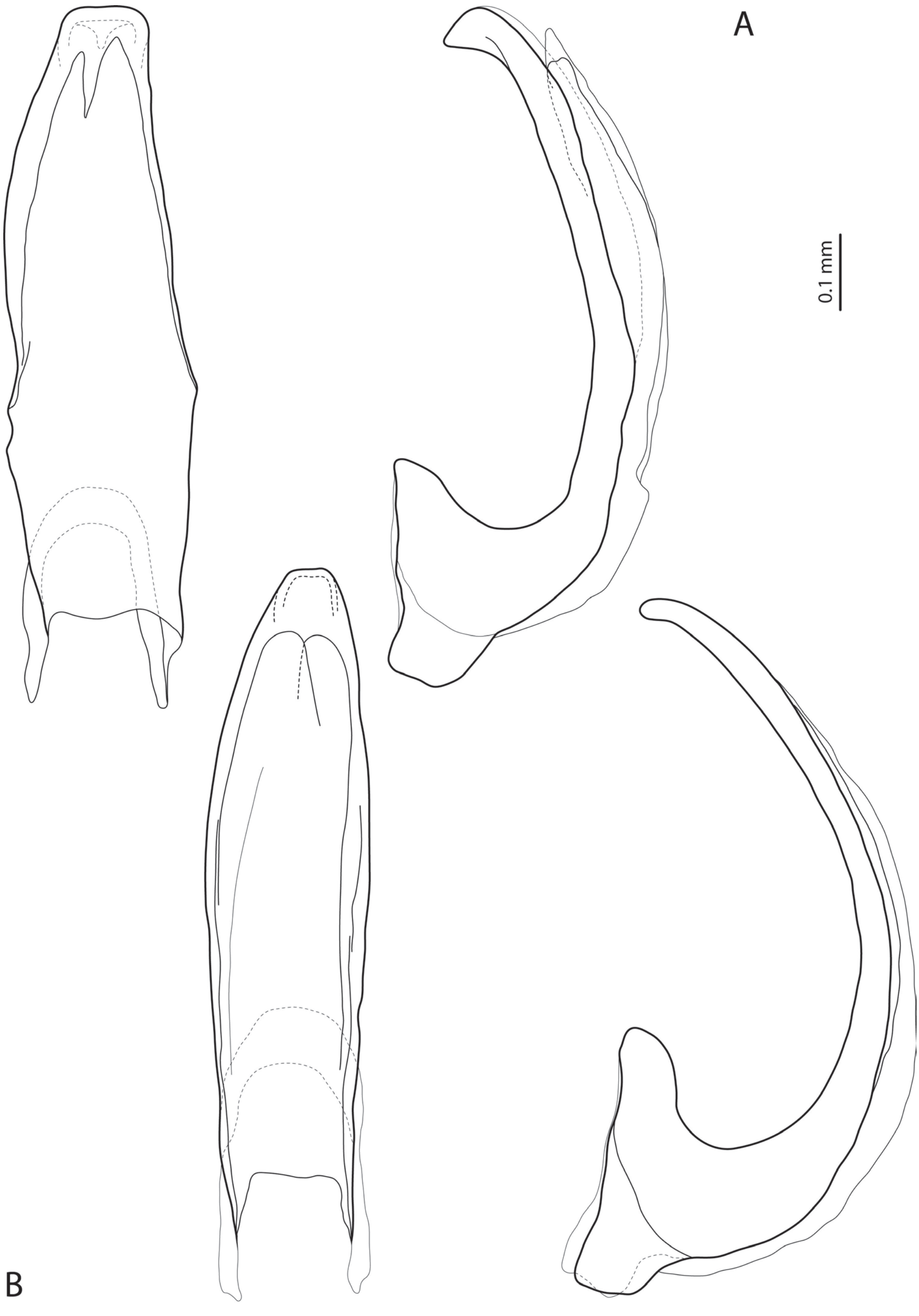

Figure 13. Median lobe in ventral and lateral views of **A** *Exocelina koroba* Shaverdo & Balke, 2019 (Shaverdo et al. 2019: 82, fig. 8B, C) **B** *E. okbapensis* Shaverdo & Balke, 2017 (Shaverdo et al. 2017a: 23, fig. 5B, C).

14

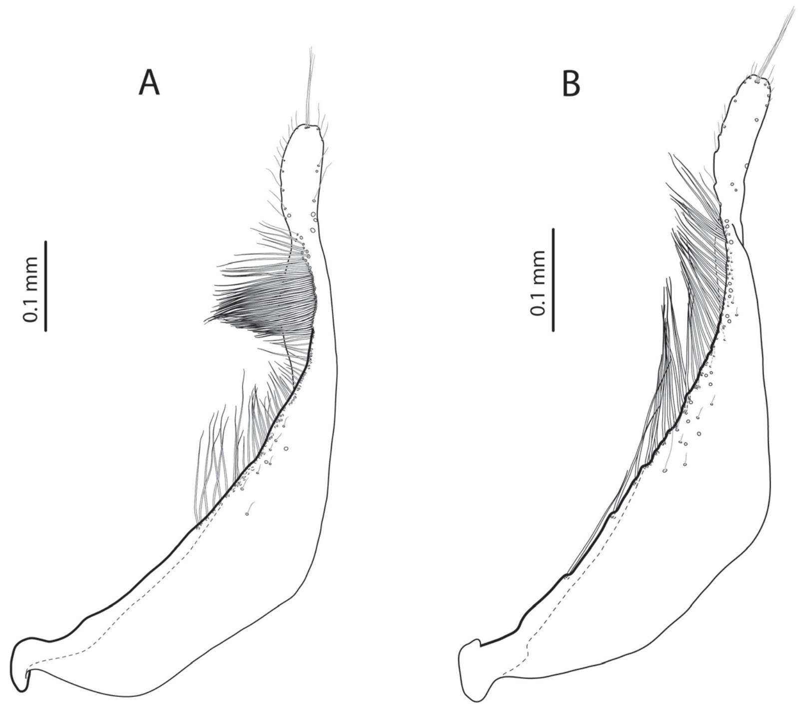

15

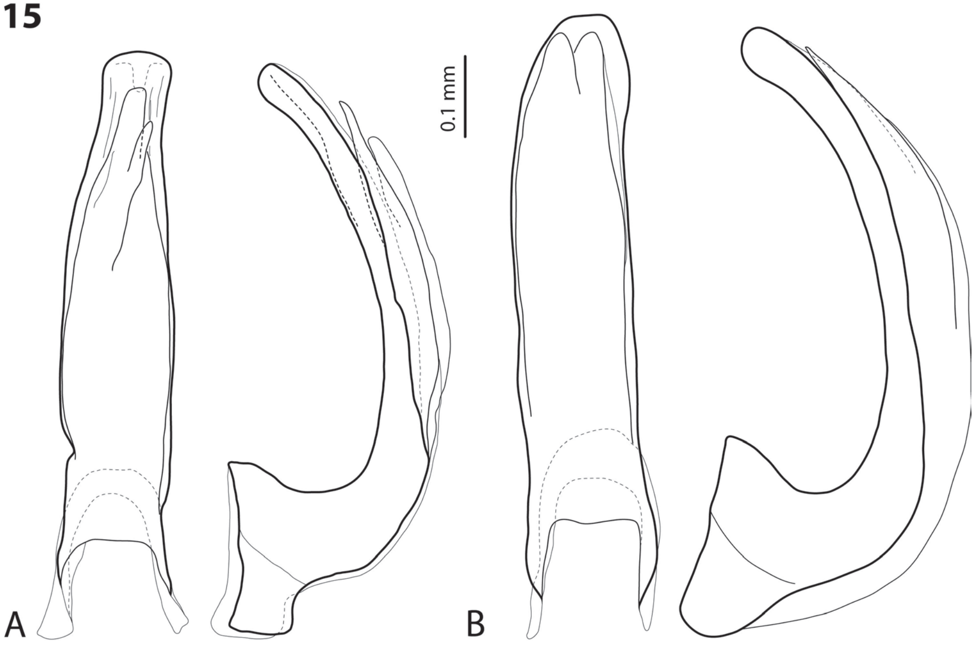

Figures 14–15. 14 Paramere of **A** *Exocelina pseudopusilla* Shaverdo & Balke, 2018 (Shaverdo et al. 2018: 63, fig. 42C) **B** *E. bacchusi* (Balke, 1998) (Shaverdo et al. 2019: 104, fig. 22C) **15** Median lobe in ventral and lateral views of **A** *E. sumokedi* Shaverdo & Balke, 2018 (Shaverdo et al. 2018: 58, fig. 34A, B) **B** *E. desii* (Balke, 1998) (Shaverdo et al. 2018: 61, fig. 39A, B).

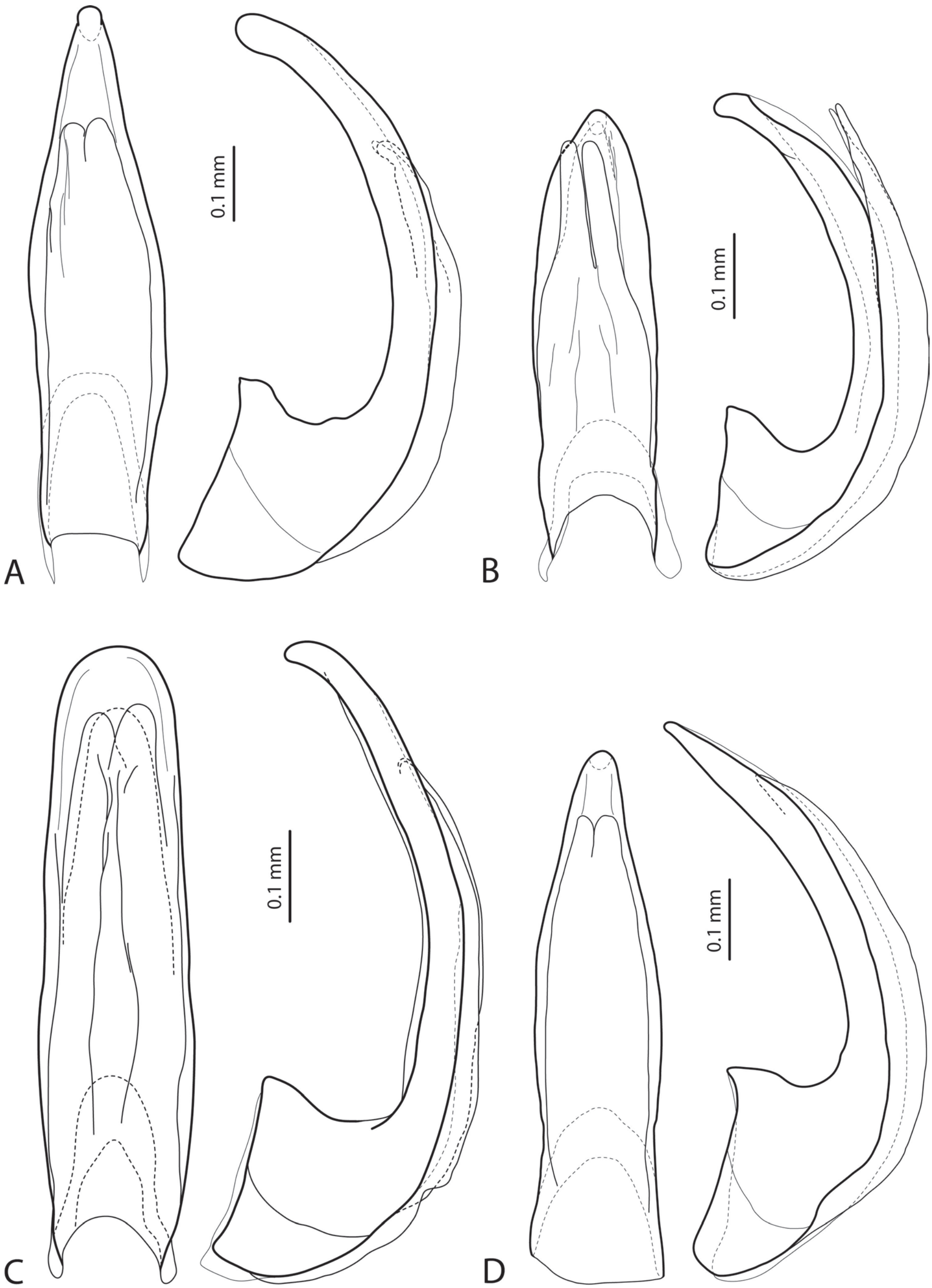

Figure 16. Median lobe in ventral and lateral views of **A** *Exocelina morobensis* Shaverdo & Balke, 2019 (Shaverdo et al. 2019: 88, fig. 10A, B) **B** *E. warasera* Shaverdo & Balke, 2019 (Shaverdo et al. 2019: 140 fig. 52A, B) **C** *E. ransikiensis* Shaverdo, Panjaitan & Balke, 2016 (Shaverdo et al. 2016b: 106, figs 4, 5) **D** *E. bacchusi* (Balke, 1998) (Shaverdo et al. 2019: 104, fig. 22A, B).

17

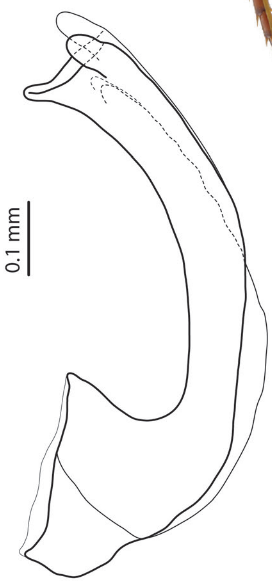

18

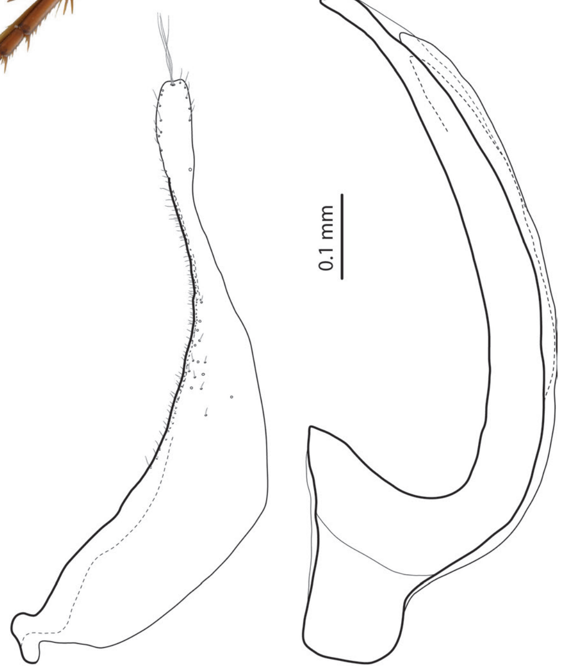

19

Figures 17–19. 17 Habitus of *Exocelina bagus* (Balke & Hendrich, 2001) (Shaverdo et al. 2017b: 111, fig. 6) **18** Median lobe in lateral view of *E. iratoi* Shaverdo & Balke, 2017 (Shaverdo et al. 2017b: 115, fig. 13B) **19** Paramere and median lobe in lateral view of *E. mekilensis* Shaverdo & Balke, 2019 (Shaverdo et al. 2019: 85, fig. 9C, B).

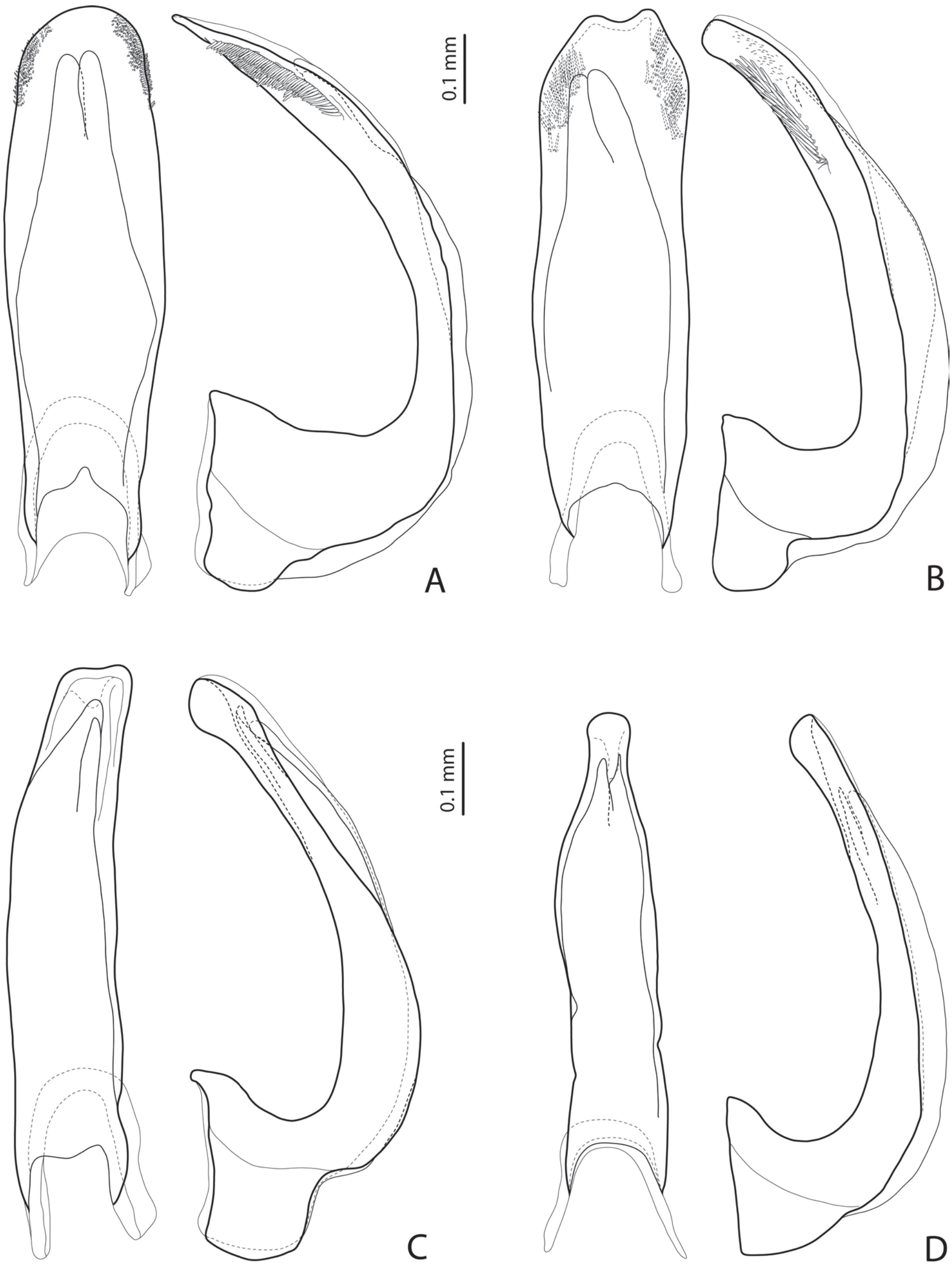

Figure 20. Median lobe in ventral and lateral views of **A** *Exocelina tomhansi* Shaverdo & Balke, 2017 (Shaverdo et al. 2017b: 114, fig. 12A, B) **B** *E. pui* Shaverdo & Balke, 2017 (Shaverdo et al. 2017b: 116, fig. 16A, B) **C** *E. casuarina* (Balke, 1998) (Shaverdo et al. 2018: 54, fig. 26A, B) **D** *E. keki* Shaverdo & Balke, 2018 (Shaverdo et al. 2018: 56, fig. 30A, B).

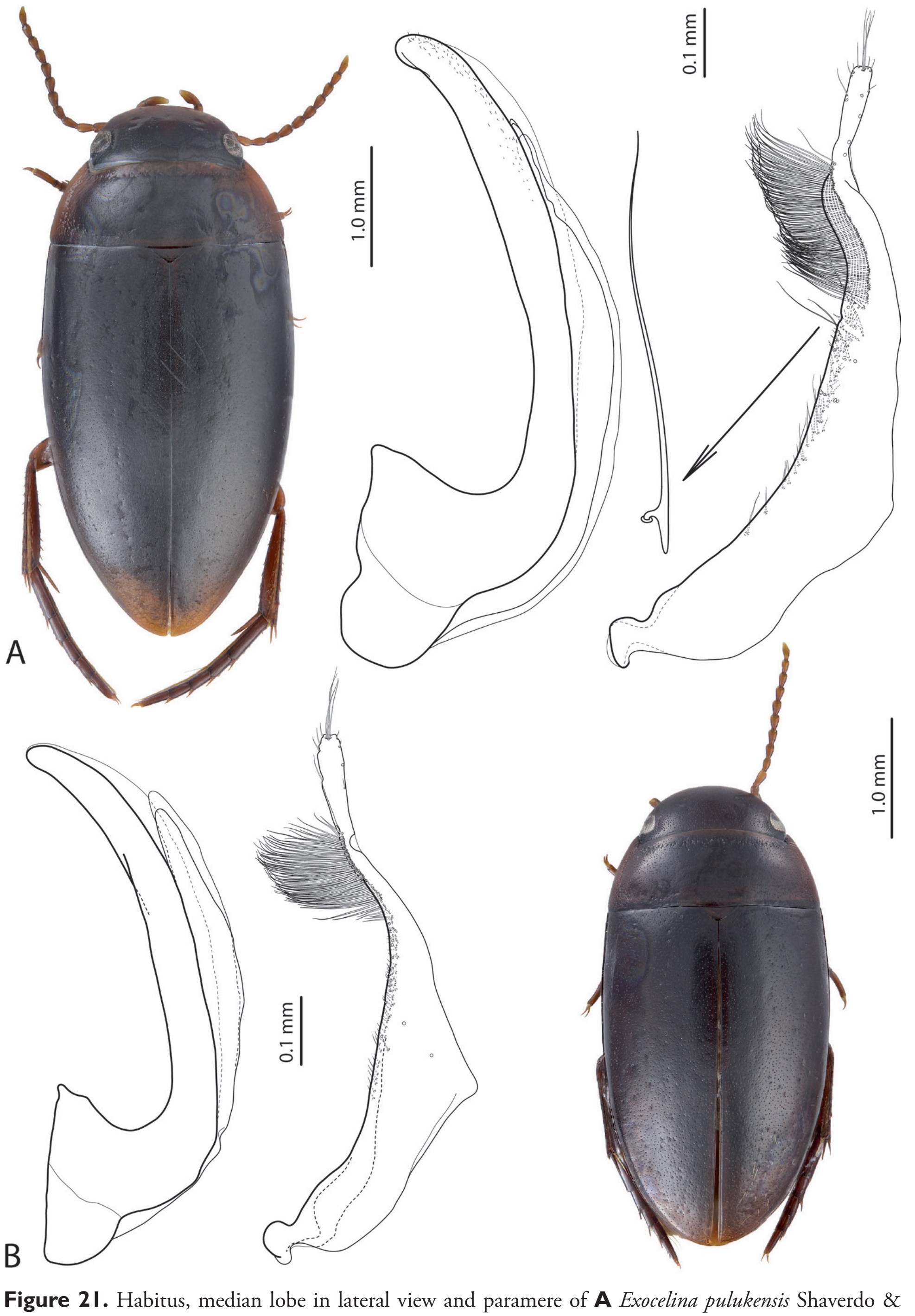

Figure 21. Habitus, median lobe in lateral view and paramere of **A** *Exocelina pulukensis* Shaverdo & Balke, 2017 (Shaverdo et al. 2017b: 112, fig. 10; 117, fig. 18B, C) **B** *E. likui* Shaverdo & Balke, 2017 (Shaverdo et al. 2017b: 112, fig. 7; 116, fig. 15A, B).

Phylogeny and infrageneric structure

The infrageneric structure of New Guinean *Exocelina* is largely based on the molecular phylogeny of the group, most of the species groups being represented as monophyletic clades on the phylogenetic tree (Fig. 22). We consider this approach to be very useful for understanding the taxonomy and evolution of such a species-rich group.

Earlier phylogenetic analyses based on molecular data substantiated the lotic New Guinean *Exocelina* as a monophyletic group, which emerged from a single colonization event by an Australian lineage and led to a rich species radiation on the island (Balke et al. 2004, 2007). More recent investigations suggested an origin of New Guinean *Exocelina* during the late Miocene, ca 5 or 9 million years ago (Toussaint et al. 2014, 2015), or even in the mid-Miocene, ca 17 Ma, when the New Guinean orogeny was at an early stage (Toussaint et al. 2021) and inferred a constant process of lineage diversification with a continuous slowdown in speciation.

A second colonization event was by a lentic species, evident from the presence of only one extant species, i.e., *E. baliem* from wetlands in the Baliem Valley of Papua Province (Shaverdo et al. 2013). According to an unpublished molecular phylogenetic analysis, this species forms a clade with the Australian *E. ferruginea* and the New Caledonian *E. inexpectata* and is placed together with them in the *E. ferruginea* group (Fig. 23).

The 151 lotic New Guinean *Exocelina* species form a monophyletic group, which contains two clades: the smaller clade I with only six species groups and the distinctly larger clade II with 19 species groups (Fig. 22). In clade I, only the monophyly of the *E. ullrichi* group and two monotypic groups (*E. mekilensis* group and *E. koroba* group) is well resolved. The majority of the remaining species are placed in the *E. casuarina* group, whose phylogeny is discussed in details in Shaverdo et al. (2018). With 24 species, this group is the second largest species group of New Guinean *Exocelina*. Interestedly, the *E. aipo* and *E. okbapensis* groups together form a monophyletic clade despite having rather distinct morphologies.

Clade II itself also consists of two large subclades (1 and 2 in Fig. 22). Subclade 1 is very heterogeneous and includes 10 species groups (all species-poor); seven represented as monophyletic clades. The *E. danae* group, the most speciose group of the clade, is inferred as polyphyletic, and the *E. bacchus* and *E. warasera* groups are both paraphyletic. Subclade 2 is the most species-rich clade since it contains the largest species group of New Guinean *Exocelina*, the *E. ekari* group. This group includes 62 species and is monophyletic, forming a monophyletic clade with the *E. skalei* group. The remaining seven groups also form a monophyletic clade (the *E. ascendens* complex) and represent rather different morphological lineages. Whilst species placement into species groups using morphology worked well for the other groups and was later confirmed by phylogenetic analysis, species of the *E. ascendens* complex can mainly be placed using molecular data. Without these data, the groups would probably never be organised in a way that reflects their evolutionary history (see below).

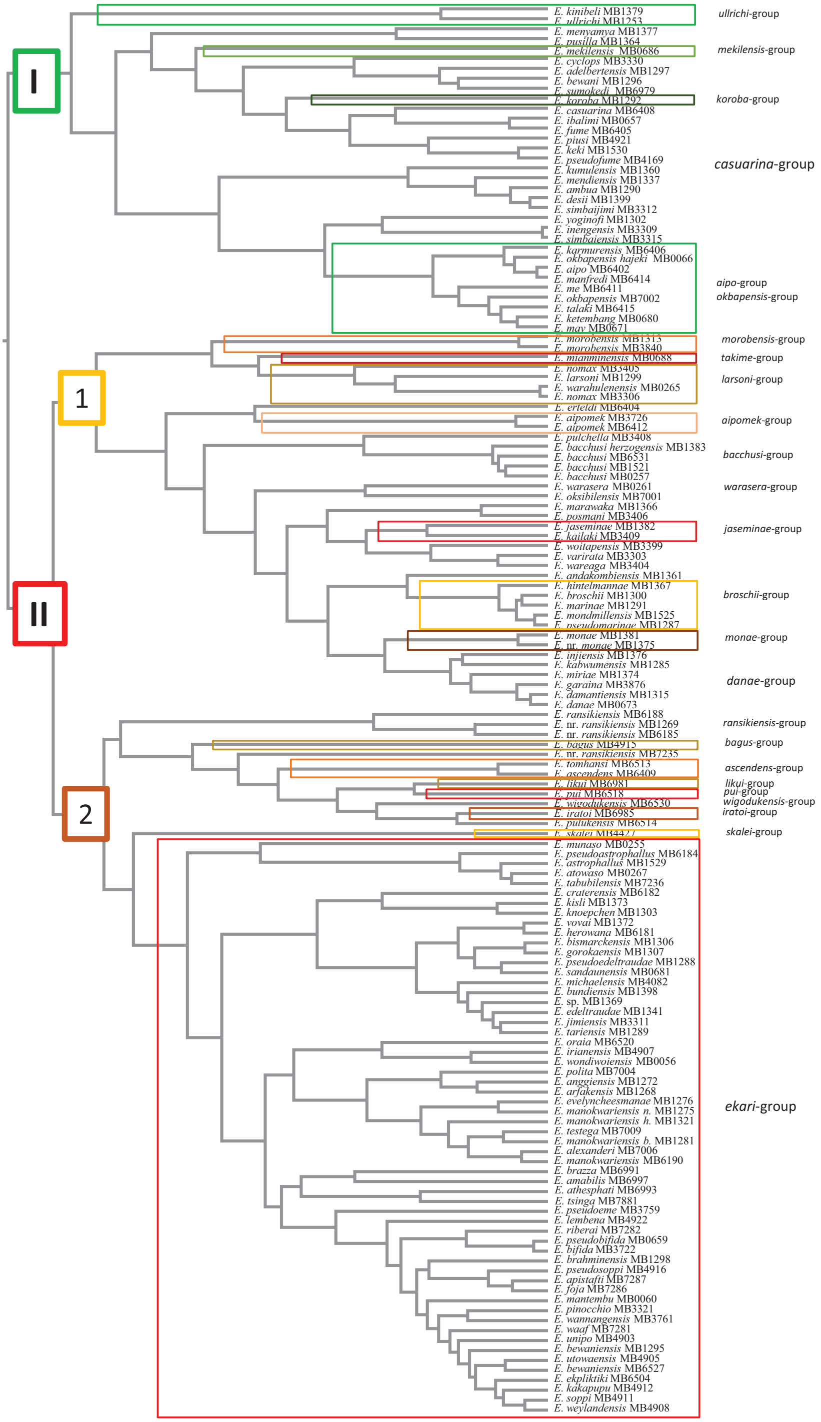

Figure 22. Phylogenetic relationships and species-group structure of *Exocelina* species of New Guinea. Monophyletic groups are highlighted. *Exocelina baliem* Shaverdo, Hendrich & Balke, 2013 is excluded.

Figure 23. Phylogenetic position of *Exocelina baliem* Shaverdo, Hendrich & Balke, 2013 amongst Australian species in the *E. ferruginea* group.

Notes on character evolution

More than 20 different morphological characters were used to describe species and organise species into a species-group structure. Some characters are very diverse and have more than 10 different states, e.g., antennal shape (9 states), shape of the median lobe (14 states), setation of the dorsal side of the parameres (12 states). Here, we briefly discuss characters, which we think are the most taxonomically and phylogenetically important and worthy of further study, not only as separate characters but also in combination.

Structure of the male genitalia

The shape of the median lobe and paramere and their setation are very diverse and serve as the basic characters for species-group structure in New Guinean *Exocelina*. These characters were primarily used to group the species. The most divergent on these characters is the *E. ekari* group with a discontinuous outline of the median lobe, which could be considered an autoapomorphic character; only *E. skalei* with its slight apical discontinuity of the median lobe belongs to the *E. skalei* group. Together with the recently described *E. mimika* Shaverdo & Balke, 2020, this former member of the *E. ekari* group, was placed into the *E. skalei* group based on the reduced setation of its paramere. Representatives of *E. ekari* group have the most complicated and diverse shape and setation of the median lobe and paramere of all New Guinean *Exocelina*. Most likely, this results from strong sexual selection, or adaptive evolution for sexual isolation, since many species of the group co-occur (up to six species) which is not the case in other species groups.

Almost every species group has its own characteristic shape of the median lobe and paramere and their setation or combination of these characters. As already mentioned above, the most problematic was the placement of species of the *E. ascendens* complex that have male genitalia similar to some species of the *E. casuarina*-, *E. aipo*- and *E. okbapensis* groups.

Lateral bead of the pronotum

Presence and part or complete reduction of the lateral pronotal bead are states of this actively used in the key character. It is helpful for species identification, but could not be used reliably for phylogenetic purposes. Absence of the lateral pronotal bead is obviously homoplastic. It has developed independently probably up to eight times within New Guinean *Exocelina* (Fig. 24). Interestingly, absence of the lateral pronotal bead is characteristic for some representatives of the largest species groups: *E. ekari* group and *E. casuarina* group. A few species demonstrate a very narrow pronotal lateral bead or presence of its traces.

Modification of the male antennae

New Guinean *Exocelina* includes more species with modified antennae than any other genus of Dytiscidae; 45 species have them, mainly in males. The degree of modification and number of antennomeres involved are specific for certain species and/or species groups and strongly vary (up to nine different character states) from almost all antennomeres slightly stout to some of them extravagantly enlarged or extremely reduced (Fig. 17). Half of the species (31 spp.) of the *E. ekari* group have modified antennae, whilst this character is absent in the second largest group, the *E. casuarina* group. For the *E. ullrichi* group, it is a group-diagnostic character, as well as for the *E. miriae* subgroup of the *E. danae* group (Fig. 7). Modified male antennae evolved independently up to 10 times in different groups, including five different lineages within the *E. ekari* group (Fig. 24) and could be used for delimitation of the subgroups within it. It is worth noting that, in some species, modification of the antennae is correlated with stronger dorsal surface structure (especially in females) or/and sometimes with diminution of the hook-like setae of the male protarsomere 4. This may indicate association with sexual processes.

Anterolateral seta of the male protarsomere 4

Hook-like anterolateral seta of male protarsomere 4 is the main diagnostic character of the genus *Exocelina* and its unique morphological autoapomorphy. However, secondary diminution or differences in shape are observed in many New Guinean species of the different species groups and have obviously independently involved (Fig. 24). It is currently impossible to postulate why certain species show such characters, although as with other features, sexual selection is likely involved. In the *E. ekari* group, diminution of the seta often occurs in species with enlarged male antennomeres and sometimes also with stronger dorsal surface structure, e.g., species close to *E. polita* (Sharp, 1882). In the *E. casuarina*-, *E. danae*-, *E. jaseminae*-, *E. warasera*-, or *E. bacchusi* groups, representatives of which have simple antennae, reduction of the hook-like seta does not correlate with this character, however, and can be found in species with shiny or matt dorsal surfaces. Although all representatives of the *E. ekari* group without lateral pronotal bead have rather strongly developed hook-like seta on male protarsomere 4, diminution of the hook-like seta was observed in some species of the *E. casuarina* group without the pronotal bead.

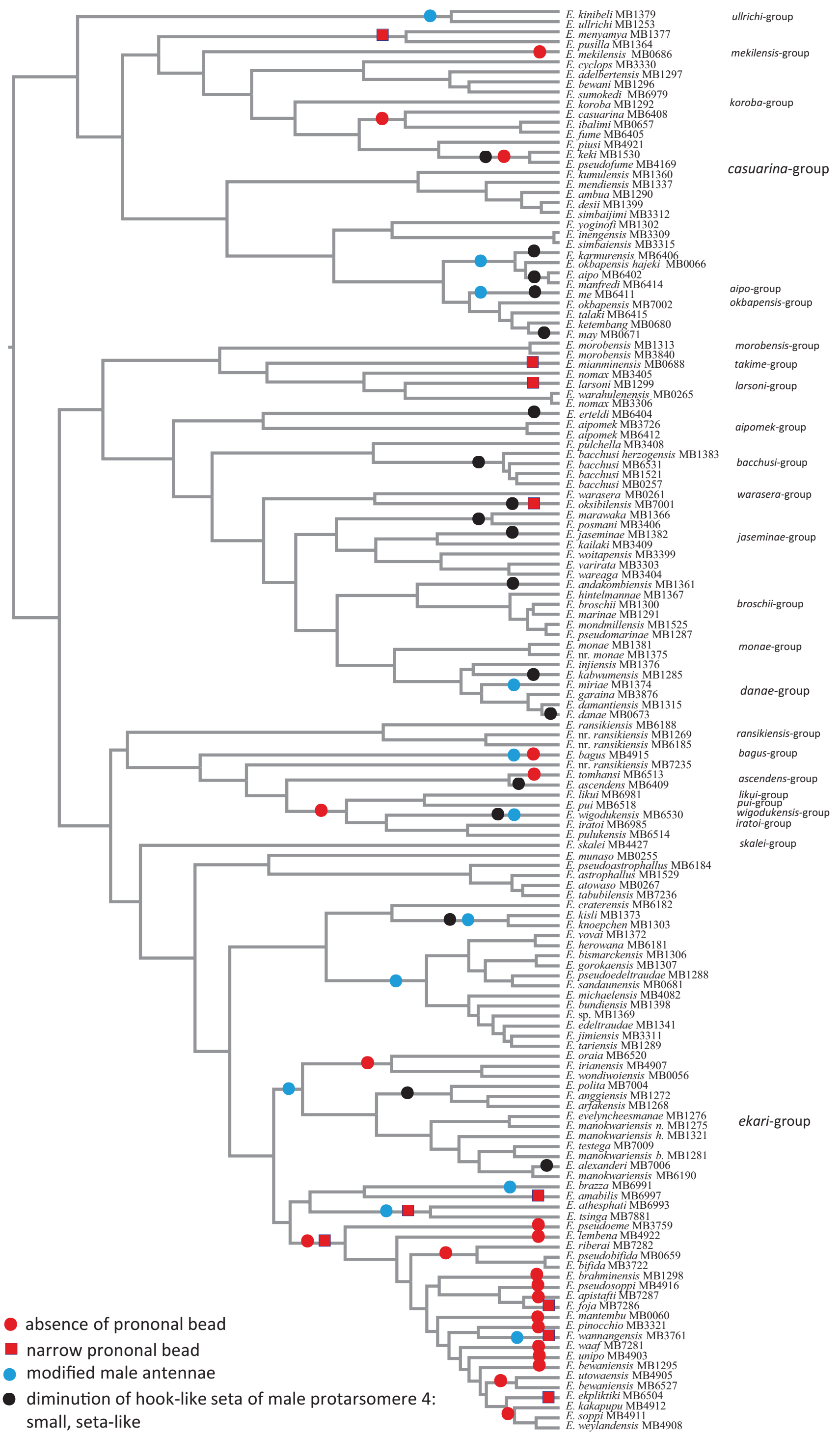

Figure 24. Allocation of four more significant morphological characters amongst *Exocelina* species of New Guinea.

Conclusion

New Guinean *Exocelina* represent a large and diverse group of Copelatinae beetles. Here, and in our previous publications (Table 1), we provide comprehensive taxonomic and faunistic treatments for this radiation. Further investigation of the group will definitely lead to more new species descriptions, some degree of restructuring of the species-group classification and better understanding of species distributions across the island. Having very diverse and intriguing character combinations, New Guinean *Exocelina* are an excellent potential model system for detailed studies on the evolution of homoplastic characters, co-evolution of different species, sexual dimorphism, and sexual conflict during mating.

Acknowledgements

We are grateful to Prof. David Bilton (Plymouth) for a linguistic review of the manuscript, Dr Lars Hendrich (Munich) for data on Australian *Exocelina* species, and Dr Jiří Hájek (Prague) and Dr Günther Wewalka (Vienna) for their comments on the manuscript. Financial support for the study was provided by the FWF (Fonds zur Förderung der wissenschaftlichen Forschung – the Austrian Science Fund) through a project P 24312-B17 and P 31347-B25 to Helena Shaverdo. Michael Balke was supported by the German Science Foundation (DFG BA2152/11-1, 11-2, 19-1, 19-2). We acknowledge support from the SNSB-Innovative scheme, funded by the Bayerisches Staatsministerium für Wissenschaft und Kunst.

References

Balfour-Browne J (1939) On the aquatic Coleoptera of the New Hebrides and Banks Islands. Dytiscidae, Gyrinidae, and Palpicornia. The Annals and Magazine of Natural History (Series 11) 3: 459–479. https://doi.org/10.1080/03745481.1939.9723627

Balke M (1998) Revision of New Guinea *Copelatus* Erichson, 1832 (Insecta: Coleoptera: Dytiscidae): The running water species, Part I. Annalen des Naturhistorischen Museum Wien 100B: 301–341. https://www.zobodat.at/pdf/ANNA_100B_0301-0341.pdf

Balke M (1999) Two new species of the genus *Copelatus* Erichson, 1832, subgenus *Papuadytes* Balke, 1998, from Papua New Guinea (Insecta: Coleoptera: Dytiscidae). Annalen des Naturhistorischen Museum Wien 101B: 273–276. https://www.zobodat.at/pdf/ANNA_101B_0273-0276.pdf

Balke M (2001) Replacement names for three New Guinea species of *Copelatus*, subgenus *Papuadytes* Balke, 1998 (Coleoptera: Dytiscidae). Annalen des Naturhistorischen Museum Wien 103B: 361–362. https://www.zobodat.at/pdf/ANNA_103B_0361-0362.pdf

Balke M, Bergsten J (2003) Dytiscidae: *Papuadytes shizong* sp.n. from Yünnan (China), the first member of *Papuadytes* Balke found west of the Wallace Line (Coleoptera). In: Jäch MA, Ji L (Eds) Water Beetles of China. Vol. III. Zoologisch-Botanische Gesellschaft in

Österreich and Wiener Coleopterologenverein, Wien, 89–94. https://www.zobodat.at/pdf/WB-China_3_0089-0094.pdf

Balke M, Ribera I (2020) A subterranean species of *Exocelina* diving beetle from the Malay Peninsula filling a 4,000 km distribution gap between Melanesia and southern China. Subterranean Biology 34: 25–37. https://doi.org/10.3897/subtbiol.34.50148

Balke M, Ribera I, Vogler AP (2004) MtDNA phylogeny and biogeography of Copelatinae, a highly diverse group of tropical diving beetles (Dytiscidae). Molecular Phylogenetics and Evolution 32(3): 866–880. https://doi.org/10.1016/j.ympev.2004.03.014

Balke M, Pons J, Ribera I, Sagata K, Vogler AP (2007) Infrequent and unidirectional colonization of megadiverse *Papuadytes* diving beetles in New Caledonia and New Guinea. Molecular Phylogenetics and Evolution 42(2): 505–516. https://doi.org/10.1016/j.ympev.2006.07.019

Balke M, Hájek J, Hendrich L, Wewalka G (2014) *Exocelina nehoue* n. sp. from New Caledonia, with a new synonym and new collecting records for other species in the genus (Coleoptera: Dytiscidae). In: Guilbert É, Robillard T, Jourdan H, Grandcolas P (Eds) Zoologia Neocaledonica 8. Biodiversity in New Caledonia. Mémoires du Muséum national d'Histoire naturelle, Paris 206: 181–189.

Bilton D, Toussaint EFA, Turner C, Balke M (2015) *Capelatus prykei* gen. et sp. n. (Coleoptera: Dytiscidae: Copelatinae)–a phylogenetically isolated diving beetles from the Western Cape of South Africa. Systematic Entomology 40(3): 520–531. https://doi.org/10.1111/syen.12128

Boisduval JBA (1835) Faune entomologique de l'océan Pacifique, avec l'illustration des insectes nouveaux recueillis pendant le voyage. 2. Coléoptères et autres ordres. Voyage de découvertes de l'Astrolabe exécuté par ordre du Roi, pendant les années 1826–1827–1828–1829, sous le commandement de M.J. Dumont d'Urville. J. Tastu, Paris, [vii +] 716 pp.

Branden van den C (1884) Catalogue des coléoptères carnassiers aquatiques (Haliplidae, Amphizoidae, Pelobiidae et Dytiscidae). Annales de la Société Entomologique de Belgique 29(1): 5–118.

Broun T (1886) Manual of the New Zealand Coleoptera. Parts III and IV. Government Printer, Wellington, 817–973.

Broun T (1893) Manual of the New Zealand Coleoptera. Parts V–VII. Government Printer, Wellington, 975–1504.

Clark H (1863) Catalogue of the Dytiscidae and Gyrinidae of Australasia, with descriptions of new species. The Journal of Entomology. Descriptive and Geographical 2(1863–1866): 14–23.

Nilsson AN (2007) *Exocelina* Broun, 1886, is the valid name of *Papuadytes* Balke, 1998. Latissimus 23: 33–34.

Nilsson AN, Fery H (2006) World Catalogue of Dytiscidae – corrections and additions, 3 (Coleoptera: Dytiscidae). Koleopterologische Rundschau 76: 55–74.

Nilsson A, Hájek J (2022) A world catalogue of the family Dytiscidae, or the diving beetles (Coleoptera, Adephaga). Version 1. I. 2022, 315 pp. http://www.waterbeetles.eu/documents/W_CAT_Dytiscidae_2022.pdf [Accessed on: 2022-10-31]

Sharp D (1882) On aquatic carnivorous Coleoptera or Dytiscidae. The Scientific Transactions of the Royal Dublin Society, Series II 2: 179–1003. [pls 7–18] https://doi.org/10.5962/bhl.title.9530

Shaverdo HV, Balke M (2014) *Exocelina kinibeli* sp. n. from Papua New Guinea, a new species of the *E. ullrichi*-group (Coleoptera: Dytiscidae). Koleopterologische Rundschau 84: 31–40. https://www.zobodat.at/pdf/KOR_84_2014_0031-0040.pdf

Shaverdo H, Balke M (2019) A new species of the *Exocelina ekari* group and new faunistic data on 12 species of *Exocelina* Broun, 1886 from New Guinea (Coleoptera: Dytiscidae). Koleopterologische Rundschau 89: 1–10. https://www.zobodat.at/pdf/KOR_89_2019_0001-0010.pdf

Shaverdo HV, Sagata K, Balke M (2005) Five new species of the genus *Papuadytes* Balke, 1998 from New Guinea (Coleoptera: Dytiscidae). Aquatic Insects 27(4): 269–280. https://doi.org/10.1080/01650420500290169

Shaverdo HV, Surbakti S, Hendrich L, Balke M (2012) Introduction of the *Exocelina ekari*-group with descriptions of 22 new species from New Guinea (Coleoptera, Dytiscidae, Copelatinae). ZooKeys 250: 1–76. https://doi.org/10.3897/zookeys.250.3715

Shaverdo HV, Hendrich L, Balke M (2013) *Exocelina baliem* sp. n., the only known pond species of New Guinea *Exocelina* Broun, 1886 (Coleoptera, Dytiscidae, Copelatinae). ZooKeys 304: 83–99. https://doi.org/10.3897/zookeys.304.4852

Shaverdo H, Sagata K, Panjaitan R, Menufandu H, Balke M (2014) Description of 23 new species of the *Exocelina ekari*-group from New Guinea, with a key to all representatives of the group (Coleoptera, Dytiscidae, Copelatinae). ZooKeys 468: 1–83. https://doi.org/10.3897/zookeys.468.8506

Shaverdo H, Panjaitan R, Balke M (2016a) A new, widely distributed species of the *Exocelina ekari*-group from West Papua (Coleoptera, Dytiscidae, Copelatinae). ZooKeys 554: 69–85. https://doi.org/10.3897/zookeys.554.6065

Shaverdo H, Panjaitan R, Balke M (2016b) *Exocelina ransikiensis* sp. nov. from the Bird's Head of New Guinea (Coleoptera: Dytiscidae: Copelatinae). Acta Entomologica Musei Nationalis Pragae 56: 103–108.

Shaverdo H, Sagata K, Balke M (2016c) Description of two new species of the *Exocelina broschii*-group from Papua New Guinea, with revision and key to all representatives of this species group (Coleoptera, Dytiscidae, Copelatinae). ZooKeys 577: 125–148. https://doi.org/10.3897/zookeys.577.7254

Shaverdo H, Sagata K, Balke M (2016d) Taxonomic revision of New Guinea diving beetles of the *Exocelina danae* group, with description of ten new species (Coleoptera, Dytiscidae, Copelatinae). ZooKeys 619: 45–102. https://doi.org/10.3897/zookeys.619.9951

Shaverdo H, Sumoked B, Balke M (2017a) Description of two new species and one new subspecies from the *Exocelina okbapensis*-group, and notes on the *E. aipo*-group (Coleoptera, Dytiscidae, Copelatinae). ZooKeys 715: 17–37. https://doi.org/10.3897/zookeys.715.15913

Shaverdo H, Wild M, Sumoked B, Balke M (2017b) Six new species of the genus *Exocelina* Broun, 1886 from Wano Land, New Guinea (Coleoptera, Dytiscidae, Copelatinae). ZooKeys 665: 93–120. https://doi.org/10.3897/zookeys.665.11792

Shaverdo H, Sagata K, Balke M (2018) Introduction of the *Exocelina casuarina*-group, with a key to its representatives and descriptions of 19 new species from New Guinea (Coleoptera, Dytiscidae, Copelatinae). ZooKeys 803: 7–70. https://doi.org/10.3897/zookeys.803.28903

Shaverdo H, Surbakti S, Warikar EL, Sagata K, Balke M (2019) Nine new species groups, 15 new species, and one new subspecies of New Guinea diving beetles of the genus *Exocelina* Broun, 1886 (Coleoptera, Dytiscidae, Copelatinae). ZooKeys 878: 73–143. https://doi.org/10.3897/zookeys.878.37403

Shaverdo H, Surbakti S, Sumoked B, Balke M (2020a) Two new species of the *Exocelina ekari* group from New Guinea with strongly modified male antennae (Coleoptera, Dytiscidae, Copelatinae). ZooKeys 960: 63–78. https://doi.org/10.3897/zookeys.960.55007

Shaverdo H, Surbakti S, Sumoked B, Balke M (2020b) Three new species of *Exocelina* Broun, 1886 from the southern slopes of the New Guinea central range, with introduction of the *Exocelina skalei* group (Coleoptera, Dytiscidae, Copelatinae). ZooKeys 1007: 129–143. https://doi.org/10.3897/zookeys.1007.59351

Shaverdo H, Surbakti S, Sumoked B, Balke M (2021) Seven new species of the *Exocelina ekari* group from New Guinea central and coastal mountains (Coleoptera, Dytiscidae, Copelatinae). ZooKeys 1026: 45–67. https://doi.org/10.3897/zookeys.1026.61554

Toussaint EFA, Hall R, Monaghan MT, Sagata K, Ibalim S, Shaverdo HV, Vogler AP, Pons J, Balke M (2014) The towering orogeny of New Guinea as a trigger for arthropod megadiversity. Nature Communications 5: 4001. [1: 1–10 + 10 supplements] https://doi.org/10.1038/ncomms5001

Toussaint EFA, Henrich L, Shaverdo H, Balke M (2015) Mosaic patterns of diversification dynamics following the colonization of Melanesian islands. Scientific Reports 5(1): 16016. https://doi.org/10.1038/srep16016

Toussaint EF, White LT, Shaverdo H, Lam A, Surbakti S, Panjaitan R, Sumoked B, von Rintelen T, Sagata K, Balke M (2021) New Guinean orogenic dynamics and biota evolution revealed using a custom geospatial analysis pipeline. BMC Ecology and Evolution 21(1): 1–28. https://doi.org/10.1186/s12862-021-01764-2

Watts CHS, Humphreys WF (2009) Fourteen new Dytiscidae (Coleoptera) of the genera *Limbodessus* Guignot, *Paroster* Sharp, and *Exocelina* Broun from underground waters in Australia. Transactions of the Royal Society of South Australia 133(1): 62–107. https://doi.org/10.1080/03721426.2009.10887112

Watts CHS, Hendrich L, Balke M (2016) A new interstitial species of diving beetle from tropical northern Australia provides a scenario for the transition of epigean to stygobitic life (Coleoptera, Dytiscidae, Copelatinae). Subterranean Biology 19: 23–29. https://doi.org/10.3897/subtbiol.19.9513

Wewalka G, Balke M, Hendrich L (2010) Dytiscidae: Copelatinae (Coleoptera). In: Jäch MA, Balke M (Eds) Water Beetles of New Caledonia (part I). Monographs on Coleoptera 3. Zoologisch-Botanische Gesellschaft in Österreich and Wiener Coleopterologenverein, Wien, 45–128.

Zimmermann A (1920) Pars 71. Dytiscidae, Haliplidae, Hygrobiidae, Amphizoidae. In: Schenkling S (Ed.) Coleopterorum Catalogus, Volumen IV. Junk, Berlin, 326 pp.

ZooKeys 1131: 59–70 (2022)
doi: 10.3897/zookeys.1131.95246
https://zookeys.pensoft.net

RESEARCH ARTICLE

A peer-reviewed open-access journal
ZooKeys
Launched to accelerate biodiversity research

A new digamasellid mite of the subgenus *Longoseiulus* Lindquist (Acari, Mesostigmata) from Slovakia

Peter Mašán[1]

1 *Institute of Zoology, Slovak Academy of Sciences, Dúbravská cesta 9, 845-06 Bratislava, Slovakia*

Corresponding author: Peter Mašán (peter.masan@savba.sk, uzaepema@savba.sk)

Academic editor: Farid Faraji | Received 23 September 2022 | Accepted 9 November 2022 | Published 22 November 2022

https://zoobank.org/7016F0AA-8A8F-4612-A76C-CE93CD7070C5

Citation: Mašán P (2022) A new digamasellid mite of the subgenus *Longoseiulus* Lindquist (Acari, Mesostigmata) from Slovakia. ZooKeys 1131: 59–70. https://doi.org/10.3897/zookeys.1131.95246

Abstract
A new digamasellid mite, *Longoseius* (*Longoseiulus*) *disparisetus* **sp. nov.**, was described from females found in the wood detritus of tree cavity of freshly felled elm (*Fraxinus* sp.) in a park in southwestern Slovakia. The new species differs from known congeners by the number of setae on some leg segments (genu II with eight setae, tibiae II and III with seven and six setae, respectively) and by the unusual presence of three pairs of conspicuously shortened setae (*J3*, *J4*, and *Z3*) on the posterior dorsal shield. In other known *Longoseiulus* species, the genu II has 11 setae, the tibiae II and III have 10 and seven setae, respectively, and almost all dorsal setae are of similar length (except for the elongated *Z4* and *S4*), none of which is formed as a microseta. A dichotomous key for females is provided to identify species classified worldwide in *Longoseiulus*.

Keywords
Description, Digamasellidae, *Fraxinus*, morphology, saproxylic habitat, systematics

Introduction

Longoseiulus was originally described by Lindquist (1975) as a subgenus of *Longoseius* Chant, 1961 and later treated at the subgenus level in *Longoseius* by Hirschmann and Wiśniewski (1982) and Castilho et al. (2012), or *Dendrolaelaps* Halbert, 1915 by Shcherbak (1980) and Barilo (1989). Karg (1993) considered *Longoseiulus* to be a synonym of the valid genus *Longoseius*.

The concept of *Longoseiulus* adopted here is largely based on the diagnosis of Lindquist (1975) and mainly on the following characters: (1) leg III with four setae on trochanter instead of normally five setae, and with seven or fewer setae on genu and tibia instead of eight or nine setae; (2) basitarsi II and III each with two or three setae instead of normally four setae, basitarsus IV with one to three setae instead of normally three or four setae; (3) hypostomal furrow of gnathosoma with most proximal fifth row of denticles not distinctly wider than preceding rows (in other genera this fifth row of denticles is conspicuously wider than preceding rows, or six rows of denticles of similar width are rarely present); (4) four-toothed movable digit of female chelicerae; (5) setae *j2* transversely aligned with *j1* and *z1* on podonotal shield; (6) sclerotized anterior margin of opisthonotal shield with a deep double incision in the middle; (7) peritreme of adults and deutonymphs similar in length, shortened and extending at most only slightly beyond posterior margin of coxa II.

The subgenus *Longoseiulus* Lindquist, 1975 is a small group of digamasellid mites and currently includes only seven known species from Europe (*aberrans*, *longuloides*, *longulus*, *ornatus*), Asia (*nobilis*, *ornatosimilis*), and North America (*brachypoda*), which are almost always found in saproxylic habitats, especially in decomposing wood of various coniferous and broad-leaved deciduous trees, and in subcortical spaces associated with galleries of bark- and wood-boring beetles. Phoretic activity of deutonymphs is common in many xylophagous beetles such as Cerambycidae, Cleridae, Elateridae, Scolytinae, and Pyrochroidae (Hirschmann and Wiśniewski 1982).

The aim of this study is to describe a new species of the subgenus *Longoseius* (*Longoseiulus*) from Slovakia and thus to contribute to the knowledge of the fauna of Digamasellidae in Europe. This work is part of a project aimed at increasing our collective knowledge of the mite fauna of Slovakia. In this sense, the finding of the new species also represents a first record of the genus *Longoseius* for Slovakia.

Materials and methods

Mites were extracted from decomposing wood detritus using a modified Berlese-Tullgren funnel equipped with a 40-W lamp and preserved in ethyl alcohol. For identification, the mites were mounted on slides with Swan's medium (gum arabic/chloral hydrate). A Leica DM 1000 light microscope with a Leica EC3 digital camera was used for measurements and micrographs. The photomicrographs were processed using Adobe Photoshop Elements 8 software. Measurements were made on specimens mounted on a microscope slide. Idiosoma and shield lengths were measured along their midlines, and widths were measured at their widest point (unless otherwise noted in the description). The lengths of the ventral idiosomal shields are midline, from the anterior to the posterior margin of each structure, including the hyaline anterior extension of the epigynal shield and excluding the posterior cribrum of the anal shield. Legs were measured excluding the ambulacral apparatus. Setae were measured from the bases of their attachments to their tips. The dimensions of the structures are given as ranges (minimum to maximum). The number of teeth on the cheliceral digits does not include the apical hook. Setal notation symbols for the idiosoma follow Lindquist and Evans (1965), slightly modified by Lindquist (1994), and notation symbols for leg setae follow Evans (1963). Terminology for the other anatomical structures follows Evans and Till (1979). The chaetotaxy symbols used here are shown in Figs 1, 2.

Results

***Longoseius* (*Longoseiulus*) *disparisetus* sp. nov.**
https://zoobank.org/B759A60A-49EF-400D-8823-33B336AA41EF
Figs 1–11

Type material examined. *Holotype* female: SW Slovakia, Podunajská Rovina Flatland, Bratislava Capital, Petržalka Settlement, Sad Janka Kráľa Park (48°08'N, 17°06'E), elev. 135 m, 25 October 2020, wood detritus from a cavity in the trunk of an old and freshly felled elm (*Fraxinus* sp.), colonised by an unidentified ant species (Hymenoptera: Formicidae). ***Paratypes*:** five females, with the same data as the holotype. The type material is deposited in the Institute of Zoology of the Slovak Academy of Sciences, Bratislava, Slovakia.

Diagnosis (female). The presence of three pairs of microsetae (*J3*, *J4*, and *Z3*) on the posterior dorsal shield of the new species is unique and distinctly different from all other known species of the subgenus *Longoseiulus*. Some displacement of *J3* toward the bases of *J4*, making the bases of *J3* and *Z3* almost transversely aligned, also makes the idiosomal chaetotaxy of *Longoseius* (*Longoseiulus*) *disparisetus* sp. nov. peculiar. Most of the dorsal setae are of approximately equal length in all other congeneric species, with the exception of *Z5* and *S5*, which are conspicuously long in most representatives of the family and are located at the posterior margin of the opisthonotum.

There are other important diagnostic characters for this new species: (1) the absence of dorsal setae *r5* (these setae are present on the soft cuticle in females of the related species whose setae *Z3* are prominent and moderately elongate), (2) the absence of many leg setae that Lindquist (1975) indicated in his original definition as being present in *Longoseiulus* species, possibly based on the chaetotaxy of the type species *Longoseius* (*Longoseiulus*) *longulus*. There is one other species of *Longoseiulus* for which Hurlbutt (1967) originally reported the chaetotaxy of the legs, namely *L.* (*L.*) *brachypoda*. In comparison with the above species, the new species was found to have setal deficiencies in the following leg segments: genu II with eight instead of 11 setae, tibia II with seven instead of 10 setae, tibia III with six instead of seven setae, and telotarsi II and III with 11 instead of 12 setae. For a further comparison of the chaetotaxy of the legs of the new species with those of the subgenus *Longoseius*, see Table 1.

Table 1. Number of setae on selected leg segments of *Longoseius* [based on Hurlbutt (1967), Lindquist (1975) and own data]. Explanations: * – new information for a diagnosis of the subgenus *Longoseiulus*, ** – new information for a diagnosis of the genus *Longoseius*.

Leg segment	Taxon	Number of setae			
		Leg I	Leg II	Leg III	Leg IV
Femur	subgen. *Longoseius*	10	10	5	6
	disparisetus sp. nov.	12	10	6	6
	subgen. *Longoseiulus*	12–13	10	6	6
Genu	subgen. *Longoseius*	8	5	4	3
	disparisetus sp. nov.	11	8*	7	7
	subgen. *Longoseiulus*	11–12	11	7	7–8
Tibia	subgen. *Longoseius*	9	7	7	7
	disparisetus sp. nov.	12	7*	6**	7
	subgen. *Longoseiulus*	12	10	7	7
Telotarsus	subgen. *Longoseius*	–	11	10	10
	disparisetus sp. nov.	–	11*	11*	12
	subgen. *Longoseiulus*	–	12	12	12

Description (female). ***Dorsal idiosoma*** (Figs 1, 8). Idiosoma 310–335 µm long and 140–155 µm wide (six measured specimens), narrowly oval, only moderately elongate, rounded anteriorly and posteriorly, suboval, widest in anterior part, at level of anterior ends of peritremes. Dorsal shield completely divided into podonotal and opisthonotal parts, not completely covering the dorsal surface, exposing narrow strips of lateral soft cuticle. Podonotal shield 153–167 µm long and 106–121 µm wide, anteriorly and posteriorly broadly rounded, with smooth and unornamented surface (not considering sigillae, sclerotic nodules, and some fine and very short lines on anterolateral areas), 18 pairs of setae (*j1–j6*, *z1–z6*, *s1–s6*) and two pairs of usually crescent-shaped subsurface sclerotic nodules between setae *z5* (the outer pair with larger and more conspicuous nodules than the inner pair of contiguous nodules arranged anteriorly). Two pairs of anterior marginal setae present, namely *r3* on peritrematal shields and *r4* on soft cuticle between podonotum and peritrematal shields. Opisthonotal shield 147–166 µm long and 76–93 µm wide (excluding lateral strips of scutal elements), anteriorly and posteriorly broadly rounded, laterally straight and nearly parallel, largely smooth except for a small foveolate area between setae *Z4*, with 15 pairs of setae (*J1–J5*, *Z1–Z5*, *S1–S5*); anterior margin of well-sclerotized part of shield with two deep medial incisions, flanked by narrow band with nearly desclerotized margin. Four pairs of posterior marginal setae present: *R1* on soft cuticle adjacent to anterolateral margins of opisthonotum; *R3* and *R4* on narrow longitudinal bands of scutal elements parallel to lateral margins of opisthonotal shield and narrowly fused to posterolateral margins of shield; *R5* usually on soft integument on ventral side near setae *JV5* or rarely on margin of opisthonotal shield. All dorsal setae smooth and needle-like, usually similar in length; three pairs of setae (*J3*, *J4*, and *Z3*) conspicuously reduced in length and each formed as a microseta (2–4 µm long); *S5* longest (37–48 µm); lengths of other dorsal setae as follows: *j1–j6*, *z1–z6*, *s1–s6*, *r4*, *J1*, *J2*, *Z1*, *Z2*, and *S1–S4* = 7–11 µm; *J5*, *Z4*, *R1*, *R3*, and *R4* = 5–7 µm; *Z5* = 22–30 µm; *r3* and *R5* = 10–14 µm.

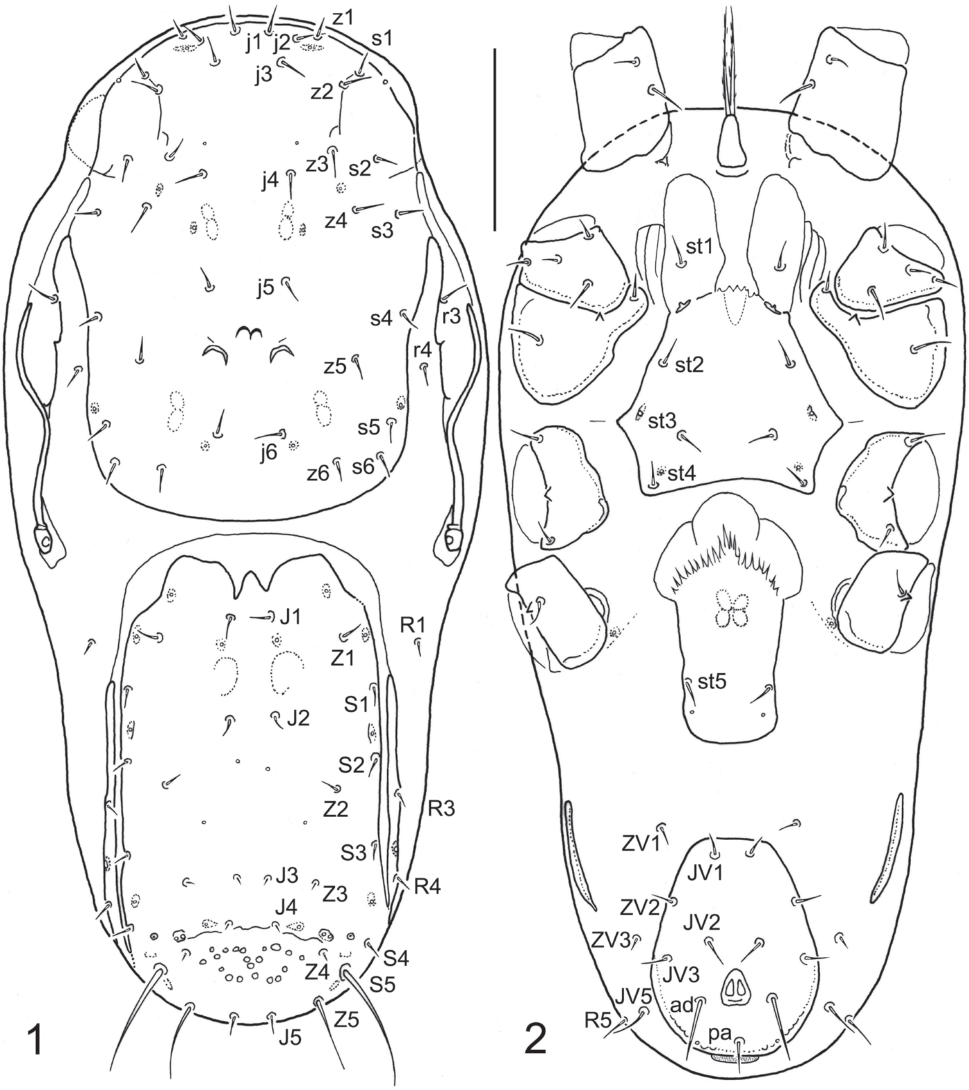

Figures 1, 2. *Longoseius* (*Longoseiulus*) *disparisetus* sp. nov., female, with symbols for chaetotactic notation of idiosomal setae **1** dorsal idiosoma **2** ventral idiosoma. Scale bar: 50 µm.

Ventral idiosoma (Figs 2, 3, 9, 10). Tritosternum with short columnar base and two laciniae; laciniae divided to base, each sparsely, finely and shortly pilose. Sternal shield weakly sclerotized and defined (compared to epigynal and ventrianal shields), longer than wide, with two lobe-shaped anterior extensions each bearing a seta (*st1*), four pairs of sternal setae (*st1–st4*), and three pairs of poroidal structures; *st3* more closely spaced than the other pairs of sternal setae; posterior margin moderately concave and shaped into posterolateral angles, each bearing a metasternal seta (*st4*); shield smooth over entire surface, except for small desclerotized areas lateral to *st1*, each with three to five short lines (Figs 3, 9). Epigynal shield elongate, 81–93 µm long, widest at anterior hyaline part (48–55 µm), formed as convex and moderately trilobate marginal structure, narrowest at level of *st5* (27–33 µm), slightly rounded posteriorly, with a pair of genital setae (*st5*) near posterolateral margins and a pair of genital poroids posterior to *st5*. Exopodal and endopodal plates or platelets not developed, absent. Peritremes usually with dorsolateral to lateral position on idiosoma (Fig. 1), shortened, 67–84 µm long, each with anterior end extending slightly beyond posterior margin of coxa II. Peritrematal shield developed only along anterior part of peritreme (*r3* captured by shield), narrowly connected to podonotal shield at level of *s3*, completely reduced along posterior part of peritreme and weakly developed near stigma, with very short poststigmatic part. A pair of strongly elongated and longitudinally oriented metapodal platelets present; platelets narrow, 34–42 µm long and slightly curved. Ventrianal shield expanded posteriorly, vase-shaped, distinctly longer than wide (69–80 µm long and 49–58 µm wide), with nearly straight anterior margin, broadly rounded posterior margin, smooth surface, four pairs of preanal setae (*JV1–JV3*, *ZV2*) in addition to three circum-anal setae and one pair of gland pores located near posterior margin at level of postanal seta (*pa*); adanal setae (*ad*) at least twice as long as postanal seta (*ad* 18–25 µm, *pa* 8–12 µm); anus and cribrum relatively small. Soft opisthogastric cuticle with three pairs of preanal setae (*ZV1*, *ZV3*, and *JV5*). Ventral setae similar in form to those on dorsal side of idiosoma, with the following lengths: *st1–st5*, *JV1–JV3*, *ZV1* and *ZV2* = 8–11 µm, *ZV3* = 5–7 µm, *JV5* = 12–16 µm.

Sperm induction system (Fig. 4). Sperm duct relatively well sclerotized, long and wide, located within the coxa, trochanter, and femur of legs III, apparently bifurcate near its terminal part, and opened at level of distal part of femur III.

Gnathosomal structures (Figs 5–7). Epistome triramous; median process short, thin, straight, usually with obtuse tip; lateral rami conspicuously longer and thicker than median process, each sharply pointed and usually with a small subapical denticle or tine (Fig. 5). Hypostomal furrow relatively narrow, with five transverse rows of denticles connected laterally by a line; all transverse rows of denticles uniformly narrow and fifth (most proximal) row not noticeably wider than preceding rows, each row with few (3–7) sparsely to regularly spaced denticles; corniculi horn-like and divergent; internal malae extending beyond corniculi and formed as pointed projections with serrated outer margins (Fig. 6). Subcapitular setae smooth and needle-like, *h2* shortest and *h3* longest. Palptrochanter with five setae, palptarsal apotele two-tined. Chelicerae relatively large (compared to size of gnathosoma or idiosoma), with middle article 68–78 µm long; cheliceral digits dentate, similar in size; movable digit quadridentate, with most proximal tooth largest; fixed digit with 5–8 teeth in addition to terminal hook bearing small subapical tooth, and with minute setiform *pilus dentilis* (Fig. 7); a coronet-like fringe, dorsal cheliceral seta, and antiaxial lyrifissure not discernible.

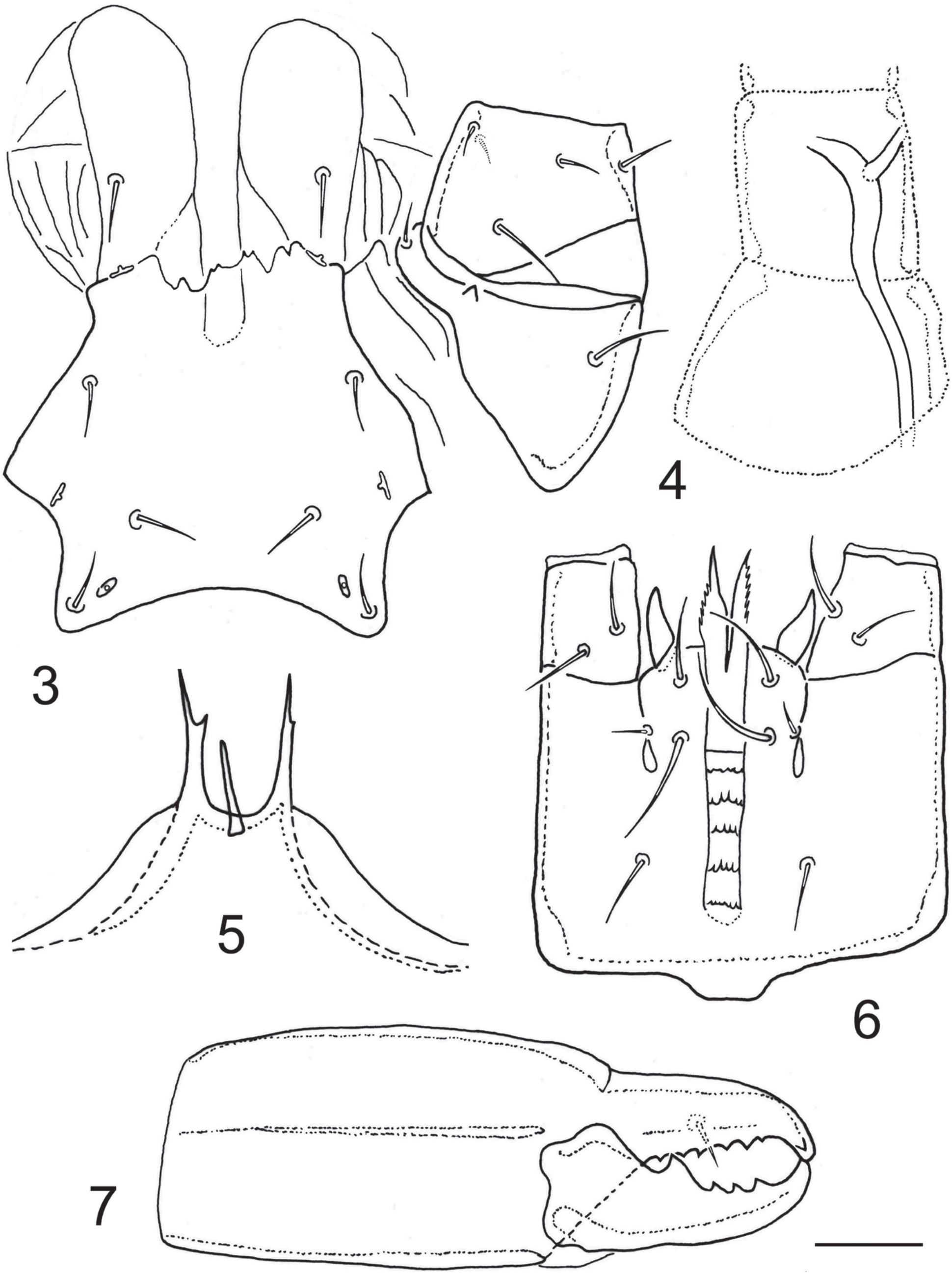

Figures 3–7. *Longoseius* (*Longoseiulus*) *disparisetus* sp. nov., female **3** sternal shield and adjacent coxa with trochanter of leg II **4** tubular part of sperm access system in proximal segments of leg III **5** epistome **6** gnathosoma, ventral view **7** chelicera, lateral view. Scale bar: 20 µm.

Figures 8–10. *Longoseius* (*Longoseiulus*) *disparisetus* sp. nov., photomicrographs of female **8** dorsal idiosoma **9** sternal region **10** ventral idiosoma. Not to scale.

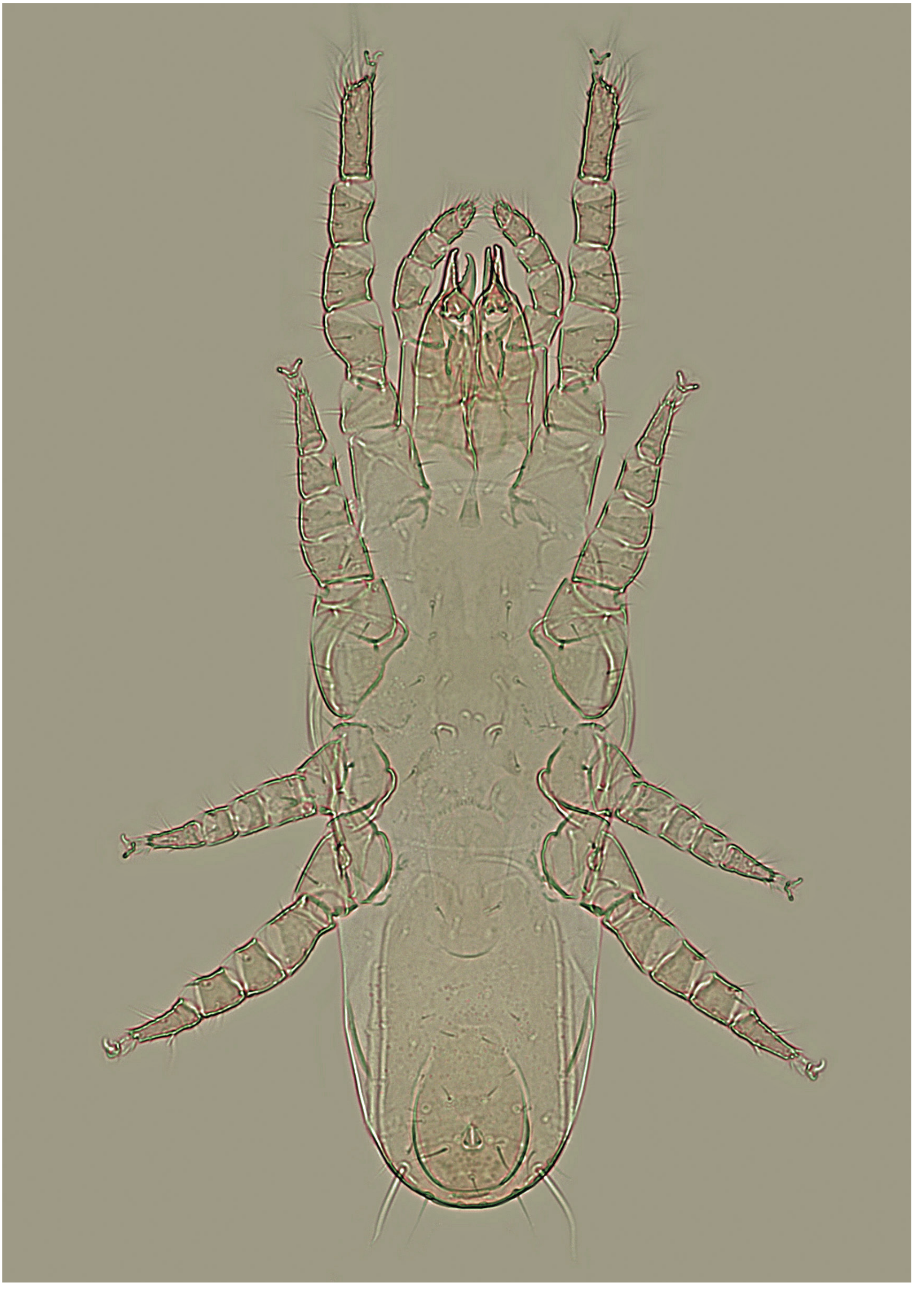

Figure 11. *Longoseius* (*Longoseiulus*) *disparisetus* sp. nov., dorso-ventral habitus of female (photomicrograph). Not to scale.

Legs (Fig. 11). All legs with well-developed pretarsus and ambulacral apparatus (including pulvillus and two claws), distinctly shorter than idiosoma: legs I 180–205 µm, legs II 135–155 µm, legs III 105–120 µm, and legs IV 135–160 µm long. Leg segments not spurred ventrally, with smooth and needle-like setae, except telotarsi II–IV with setae *ad1*, *pd1*, *av1*, *pv1*, and *md* (when present) shortened and thickened, spine-like, and *pd2* thickened. Chaetotactic formulae for each leg segment as follows: leg I – coxa (2), trochanter (6), femur 2-3/1, 2/2-2 (12), genu 2-2/1, 2/2-2 (11), tibia 2-2/1, 3/2-2 (12); leg II – coxa (2), trochanter (5), femur 2-2/1, 1/2-2 (10), genu 1-2/1, 2/1-1 (8), tibia 1-1/1, 2/1-1 (7); leg III – coxa (2), trochanter (4), femur 1-2/1, 1/0-1 (6), genu 1-2/1, 2/0-1 (7), tibia 1-1/1, 2/1-0 (6); leg IV – coxa (1), trochanter (5), femur 1-2/0, 1/1-1 (6), genu 1-2/1, 2/0-1 (7), tibia 1-1/1, 2/1-1 (7). Tibia I without one anterodorsal seta (*ad3*), tibia III without both posterolateral setae (*pl1*, *pl2*), and genua III and IV each with only one ventral seta (*pv* absent). Basitarsi of legs II and III each with two dorsal setae (*al3* and *pl3* absent), basitarsus IV with only one dorsal seta (*al3*, *pd3*, and *pl3* absent). Setation of telotarsi II-III-IV, respectively, 11-11-12 (excluding the pair of dorsodistal seta-like processes); telotarsi II and III each lacking a mediodorsal seta (*md*), but telotarsus IV with seta *md* present.

Taxonomic note. Among the closest relatives with known chaetotaxy of the legs, the new species is easily recognised by the specific number of setae on several leg segments (see Table 1 and the above diagnosis). It lacks many leg setae that Lindquist (1975) indicated in his original definition as being present in *Longoseiulus* species, namely *al*, *ad3*, *pl* on the genu II; *al*, *ad2*, *pl* on the tibia II; *pl* on the tibia III; and *md* on the telotarsi II and III. This requires some amendments to the diagnosis introduced by Lindquist (1975) for *Longoseiulus* and partially for the genus *Longoseius* (a *pl* seta found on the tibia III in *Longoseius cuniculus* Chant, 1961 is absent in the new species).

Etymology. The specific name is derived from the Latin words *dispār* (unequal or dissimilar) and *sēta* (bristle or hair) and refers to the striking differences in length between the setae on the opisthonotal shield of the female of this new mite (three pairs of setae are greatly reduced and formed as microsetae).

Key to the worldwide species of the subgenus *Longoseiulus* (females)

Longoseiulus includes seven described species, all known from the Holarctic. Only *Longoseius* (*Longoseiulus*) *aberrans* Hirschmann, 1960 is not included in the following key because its description is based solely on the male stage (it is one of the species with 21 pairs of setae on the anterior dorsal surface, including *r5*). It is not possible to reliably subdivide the individual species of *Longoseiulus* known to date based on literature data alone, without examining the type specimens. They should be thoroughly revised, redescribed, and compared in future studies to obtain a more accurate and reliable identification key than the one presented in this study. The original descriptions of most *Longoseiulus* species were not elaborated with the necessary precision (for example, they lack information on the chaetotaxy of the legs or on the measurement of important setal or scutal structures). Therefore, it is not currently possible to define and delimit some species morphologically on the basis of reliable characters. It is likely that a future revision will reveal the conspecificity of some species now placed in this subgenus.

1 Anterior dorsum with 20 pairs of setae, including two pairs of marginal setae on peritrematal shields (*r3*) or soft cuticle (*r4*); setae *Z3* short (*Z3≤Z2*, *Z3≤j5*), never reaching beyond posterolateral margins of opisthonotal shield; idiosoma relatively small, 290–335 µm long **2**

– Anterior dorsum with 21 pairs of setae, including three pairs of marginal setae on peritrematal shields (*r3*) or soft cuticle (*r4*, *r5*); setae Z3 long (*Z3*≥2×*Z2*, *Z3*≥2×*j5*), reaching beyond posterolateral margins of opisthonotal shield; idiosoma relatively large, 330–390 µm long **3**

2. Three pairs of opisthonotal setae (*J3*, *J4*, and *Z3*) conspicuously shortened, formed as microsetae (2–4 µm long), at least twice shorter than other dorsal setae; inner pair of sclerotic nodules on hexagonal dorsal area with anterior position as outer pair; tibia III with 6 setae (without posterolateral setae) .... ***Longoseius* (*Longoseiulus*) *disparisetus* sp. nov.** [Slovakia]

– Three pairs of opisthonotal setae (*J3*, *J4*, and *Z3*) never shortened and almost as long as other dorsal setae (except *Z5* and *S5*); two pairs of sclerotic nodules on hexagonal dorsal area in a transverse row; tibia III with 7 setae (with one posterolateral seta) .... ***L.* (*L.*) *longulus* (Hirschmann, 1960)** [Germany]. ***L.* (*L.*) *longuloides* Hirschmann & Wiśniewski, 1982** [Ukraine]

3 Ventrianal shield with three pairs of preanal setae (*JV1*, *JV2*, and *ZV2*).............. .... ***L.* (*L.*) *ornatus* (Hirschmann, 1960)** [Germany]

– Ventrianal shield with four pairs of preanal setae (*JV1–JV3* and *ZV2*) .... ***L.* (*L.*) *brachypoda* (Hurlbutt, 1967)** [U.S.A., Louisiana]. ***L.* (*L.*) *ornatosimilis* (Shcherbak, 1980)** [Russia, Buryat]. ***L.* (*L.*) *nobilis* (Barilo, 1989)** [Uzbekistan]

Acknowledgements

This work was fully supported by the Scientific Grant Agency of the Ministry of Education of the Slovak Republic and the Academy of Sciences [VEGA grant no. 2/0007/22: Mesostigmatic mites associated with subcorticolous habitats and wood-destroying insects in Slovakia – taxonomy, ecology and chorology of the species of Digamasellidae (Acari: Parasitiformes)].

References

Barilo AB (1989) More on central Asian mites of the Rhodacaridae family (Parasitiformes). Zoologicheskii jurnal 68: 138–143. [In Russian with English abstract]

Castilho RC, de Moraes GJ, Halliday B (2012) Catalogue of the mite family Rhodacaridae Oudemans, with notes on the classification of the Rhodacaroidea (Acari: Mesostigmata). Zootaxa 3471(1): 1–69. https://doi.org/10.11646/zootaxa.3471.1.1

Chant DA (1961) A new genus and species of mite in the family Digamasellidae Evans (Acarina). Acarologia 3: 11–13.

Evans GO (1963) Observations on the chaetotaxy of the legs in the free-living Gamasina (Acari: Mesostigmata). Bulletin of the British Museum (Natural History). Zoology (Jena, Germany) 10: 275–303. https://doi.org/10.5962/bhl.part.20528

Evans GO, Till WM (1979) Mesostigmatic mites of Britain and Ireland (Chelicerata: Acari – Parasitiformes). An introduction to their external morphology and classification. Transactions of the Zoological Society of London 35(2): 145–270. https://doi.org/10.1111/j.1096-3642.1979.tb00059.x

Halbert JN (1915) Clare Island Survey. 39. Acarinida. Section II. Terrestrial and marine Acarina. Proceedings of the Royal Irish Academy 31: 45–136. [+ 7 pls.]

Hirschmann W (1960) Gangsystematik der Parasitiformes. Teil 3. Die Gattung *Dendrolaelaps* Halbert, 1915. Acarologie. Schriftenreihe für Vergleichende Milbenkunde 3: 1–27.

Hirschmann W, Wiśniewski J (1982) Weltweite revision der Gattungen *Dendrolaelaps* Halbert, 1915 und *Longoseius* Chant, 1961 (Parasitiformes). Acarologie. Schriftenreihe für Vergleichende Milbenkunde 29(1): 1–190, 29(2): 1–48. [+ pls I–XIV, pls 1–94]

Hurlbutt HW (1967) Digamasellid mites associated with bark beetles and litter in North America. Acarologia 9: 497–534.

Karg W (1993) Acari (Acarina), Milben. Parasitiformes (Anactinochaeta). Cohors Gamasina Leach. Raubmilben. 2. Überarbeitete Auflage. Die Tierwelt Deutschlands 59: 1–523.

Lindquist EE (1975) *Digamasellus* Berlese, 1905, and *Dendrolaelaps* Halbert, 1915, with description of new taxa of Digamasellidae (Acarina: Mesostigmata). Canadian Entomologist 107(1): 1–43. https://doi.org/10.4039/Ent1071-1

Lindquist EE (1994) Some observations on the chaetotaxy of the caudal body region of gamasine mites (Acari: Mesostigmata), with a modified notation for some ventrolateral body setae. Acarologia 35: 323–326.

Lindquist EE, Evans GO (1965) Taxonomic concept in the Ascidae, with a modified setae nomenclature for the idiosoma of the Gamasina (Acarina: Mesostigmata). Memoirs of the Entomological Society of Canada 47: 1–64. https://doi.org/10.4039/entm9747fv

Shcherbak GI (1980) The Palearctic Mites of the Family Rhodacaridae. Naukova Dumka, Kiev, 216 pp. [In Russian with English abstract]

ZooKeys 1131: 71–97 (2022)
doi: 10.3897/zookeys.1131.91017
https://zookeys.pensoft.net

RESEARCH ARTICLE

A peer-reviewed open-access journal
ZooKeys
Launched to accelerate biodiversity research

Two new species of *Centroptilum* Eaton, 1869 from North Africa (Ephemeroptera, Baetidae)

Thomas Kaltenbach[1,2], Laurent Vuataz[1,2], Boudjéma Samraoui[3,4], Sara El Yaagoubi[5], Majida El Alami[5], Jean-Luc Gattolliat[1,2]

1 *Museum of Zoology, Palais de Rumine, Place Riponne 6, CH-1005 Lausanne, Switzerland* **2** *University of Lausanne (UNIL), Department of Ecology and Evolution, CH-1015 Lausanne, Switzerland* **3** *Laboratoire de Conservation des Zones Humides, Université 8 Mai 1945 Guelma, Guelma, Algeria* **4** *Department of Biology, University Badji Mokhtar Annaba, Annaba, Algeria* **5** *Laboratoire Ecologie, Systématique, Conservation de la Biodiversité (LESCB), Unité de Recherche Labellisée CNRST N°18, Université Abdelmalek Essaâdi, Faculté des Sciences, Département de Biologie, B.P.2121 93002 Tétouan, Morocco*

Corresponding author: Thomas Kaltenbach (thomas.kaltenbach@bluewin.ch)

Academic editor: L. Pereira-da-Conceicoa | Received 29 July 2022 | Accepted 26 October 2022 | Published 22 November 2022

https://zoobank.org/EF181E5C-2947-41A1-9594-2756591C9A7F

Citation: Kaltenbach T, Vuataz L, Samraoui B, El Yaagoubi S, El Alami M, Gattolliat J-L (2022) Two new species of *Centroptilum* Eaton, 1869 from North Africa (Ephemeroptera, Baetidae). ZooKeys 1131: 71–97. https://doi.org/10.3897/zookeys.1131.91017

Abstract

Based on recently collected larvae from Algeria and Morocco, the species delimitation within the genus *Centroptilum* Eaton, 1869 in that region is validated. Two new species are described and illustrated, one from north-eastern Algeria, and one from North Morocco, using an integrated approach with morphological and molecular evidence. A table summarising the morphological differences between the new species and *Centroptilum luteolum* (Müller, 1776) from Central Europe is provided. Further, molecular evidence for additional undescribed species of *Centroptilum* in other regions of the West Palearctic is provided and discussed.

Keywords

Algeria, biogeography, COI, mayflies, Morocco, Palearctic, taxonomy

Introduction

Thomas (1998) provided a provisional checklist of the mayflies from the Maghreb including 69 species: 41 from Morocco, 50 from Algeria, and 29 from Tunisia. This checklist included 17 species of Baetidae, nine additional species of this family needed to be confirmed. During the last two decades, important improvements were made in the knowledge of North African mayflies. A few new species of Baetidae, Leptophlebiidae, Heptageniidae, and Prosopistomatidae were described from Tunisia, Algeria, and Morocco (Soldán et al. 2005; Zrelli et al. 2011; Benhadji et al. 2018; Kechemir et al. 2020; Dambri et al. 2022; El Alami et al. 2022b), and new reports were provided for countries or basins, especially for Tunisia (Zrelli et al. 2011, 2012, 2016), East and West Algeria (Benhadji et al. 2020; Samraoui et al. 2021a, b), and Morocco (Khadri et al. 2017; Mabrouki et al. 2017; El Alami et al. 2022a; Zerrouk et al. 2021). A few species were morphologically revised including in some cases the description of previously unknown stages (Soldán et al. 2005; Zrelli et al. 2012; Godunko et al. 2018). However, the status of several species needs confirmation, especially concerning widely distributed Palearctic species originally described from Central Europe. An integrative approach, based on multiple evidence like morphological, molecular, ecological, and biogeographical data, should be widely used to solve this riddle. Among these problematic cases are the various reports of *Centroptilum luteolum* (Müller, 1776) from Algeria, Morocco, and Tunisia that need to be confirmed.

The genus *Centroptilum* Eaton, 1869 originally encompassed only the two species distributed in Europe and North America. It was, at that time, mainly defined by imaginal characters, adults being mostly similar to *Cloeon* Leach, 1815, but different by the presence of narrow hindwings with a long costal process. The generic concept was rapidly broadened to encompass all Baetidae with single intercalary veins and presence of hindwings. Species from all biogeographical regions, including Australasia, were assigned to this genus with the highest diversity in the Afrotropical and Nearctic regions. The generic concept was step by step circumscribed mainly by excluding the Afrotropical species and creating new genera to accommodate them (Gillies 1990; Lugo-Ortiz and McCafferty 1998). In the Maghreb, the species *Centroptilum dimorphicum* (Soldán & Thomas, 1985) was assigned to the Afrotropical genus *Cheleocloeon* Wuillot & Gillies, 1993 (Lugo-Ortiz and McCafferty 1997). Finally, the concept of *Centroptilum* was restricted to the type species *C. luteolum* (Kluge 2012, 2016). All species previously attributed to *Centroptilum* were either assigned to other genera such as *Anafroptilum*, *Neocloeon*, and *Cloeon* or considered as *Incertae sedis* (*Centroptilum collendum* Harker, 1957 and *Centroptilum elongatum* Suter, 1986 from Australia) or species *inquirenda* (*Centroptilum pirinense* Ikonomov, 1962 from the Balkans). The history and concept of the genus *Centroptilum* were recently summarised in detail by Martynov et al. (2022). In the same article, the authors described a new species from the South Caucasus. They provided a table with all reliable characters to securely separate the species within *Centroptilum*. They also gave genetic evidence that the European populations of *C. luteolum* are most probably diphyletic and correspond to two putative species.

The genus *Centroptilum* was reported from the whole Maghreb. In Tunisia, the genus seems to be extremely rare as Boumaïza and Thomas (1995) only reported a single larva in their extensive survey of the country; they also considered it to be the most sensitive species to ionic concentration. In Algeria, the genus has a very limited distribution as it was recently only collected in the El Kala basin (Samraoui et al. 2021a); it seems to be absent from surrounding basins in East Algeria and other parts of the country (Benhadji et al. 2020; Samraoui et al. 2021b). Its distribution is also limited in Morocco as it was only collected in the northern part of the country (El Alami et al. 2022a). As already previously stated (Samraoui et al. 2021a; El Alami et al. 2022a), the genus *Centroptilum* needs to be revised in North Africa. In the present study, we use recently collected specimens from north-eastern Algeria and North Morocco to validate the species delimitation, and to describe two new species; we use an integrative approaches combining morphological and molecular evidence.

Materials and methods

The specimens from Algeria were collected between 2018 and 2020 by BS, and the specimens from Morocco in 2014 and 2021 by MEA and collaborators. Comparative material from Switzerland was collected by André Wagner (MZL). The larvae were preserved in 70%–96% ethanol.

The dissection of larvae was done in Cellosolve (2-Ethoxyethanol) with subsequent mounting on slides with Euparal liquid, using an Olympus SZX7 stereomicroscope.

Drawings were made using an Olympus BX43 microscope. To facilitate the determination of the new species and the comparison of important structures with other species, we partly used a combination of dorsal and ventral aspects in the same drawing (see Kaltenbach et al. 2020: fig. 1c).

Photographs of larvae were taken using a Canon EOS 6D camera and processed with Adobe Photoshop Lightroom (http://www.adobe.com) and Helicon Focus v. 5.3 (http://www.heliconsoft.com). Photographs of body parts of the larvae were taken with an Olympus BX51 microscope equipped with an Olympus SC50 camera and processed with Olympus (recently Evident) software Stream Basic v. 1.3. All pictures were subsequently enhanced with Adobe Photoshop Elements 13.

Distribution maps were generated with SimpleMappr (https://simplemappr.net, Shorthouse 2010). The GPS coordinates of the sample locations are given in Table 1. The terminology follows Hubbard (1995) and Kluge (2004). Table 2 of this study was partly developed based on Martynov et al. (2022: table II).

For the molecular part of the study, we first downloaded all *Centroptilum* cytochrome oxidase subunit 1 (COI) sequences available on GenBank as on 13.04.2022 using a custom script, resulting in 99 records. We then manually removed all sequences from specimens collected outside the Western Palearctic, resulting in 34 European sequences for further analyses. We also examined the sequences available on the BOLDSYSTEMS data portal as on 13.04.2022, but excluded all sequences shared with GenBank, those from specimens collected outside the Western Palearctic, and one sequence that did not blast with *Centroptilum* (i.e., most probably resulting from a misidentification or a contamination). As a result, no additional sequence could be obtained. We also included three sequences from the European mayfly FREDIE project (unpublished; https://wp.fredie.eu/). Finally, seven specimens were newly sequenced for this study (Table 1; the nomenclature of gene sequences follows Chakrabarty et al. (2013)), for a total of 44 *Centroptilum* sequences in our molecular data set. The DNA of the sequenced specimens was extracted using non-destructive methods allowing subsequent morphological analysis (see Vuataz et al. 2011 for details). We amplified a 658 bp fragment of the COI gene using the primers LCO 1490 and HCO 2198 (Folmer et al. 1994, see Kaltenbach and Gattolliat 2020 for details). Sequencing was done with Sanger's method (Sanger et al. 1977). Forward and reverse sequencing reads were assembled and edited in CodonCode Aligner 10.0.2 (Codon-Code Corporation, Dedham, MA), and aligned using MAFFT (Katoh et al. 2019) with default settings as implemented in Jalview 2.11.2.2 (Waterhouse et al. 2009). The best evolutionary model (HKY+ Γ +I) was selected following the second-order Akaike information criterion (AICc; Hurvich and Tsai 1989) implemented in JModelTest 2.1.10 (Darriba et al. 2012) with seven substitution schemes and all other parameters set to default. In order to accommodate different substitution rates among COI codon positions, we analysed our data set in two partitions, one with first and second codon positions and one with third positions (1 + 2, 3). Bayesian inference (**BI**) gene tree reconstruction was conducted in MrBayes 3.2.7a (Ronquist et al. 2012). Two independent analyses of four MCMC chains run for five million generations with trees sampled every 1'000 generations were implemented, and 500'000 generations were discarded as a burn in after visually verifying run stationarity and convergence in Tracer 1.7.2 (Rambaut et al. 2018). One representative of four species belonging to the same subfamily as *Centroptilum* (i.e., Cloeoninae sensu Bauernfeind and Soldán 2012) were used as outgroup. The consensus tree was visualised and edited in iTOL 6.5.7 (Letunic and Bork 2021).

To explore COI evolutionary divergence and compare it to our morphological identifications, we applied three single-locus species delimitation methods to our CO1 data set: the distance-based **ASAP** (Assemble Species by Automatic Partitioning; Puillandre et al. 2020), the tree-based **GMYC** (General Mixed Yule-Coalescent; Pons et al. 2006; Fujisawa and Barraclough 2013), and **mPTP** (multi-rate Poisson Tree Processes; Kapli et al. 2017) approaches. The ASAP method, which is an improvement of the widely used **ABGD** (Automatic Barcode Gap Discovery; Puillandre et al. 2012) approach, has the advantage of providing a score that designates the most likely number of hypothetical species. The GMYC model, which requires a time-calibrated ultrametric tree as input, implements a Maximum Likelihood (ML) approach that defines a threshold separating the branches modelled under speciation events (Yule process) from those described by allele neutral coalescence. The **mPTP** approach, which is a multi-rate extension of the PTP (Poisson Tree Processes; Zhang et al. 2013), also exploits intra- and interspecies phylogenetic differences, but with the advantage of

Table 1. Examined and sequenced specimens.

Species	Country	Location	Coordinates	Specimen catalogue #	GenBank #(CO1)	GenSeq Nomenclature
Centroptilum samraouii sp. nov.	Algeria	Louar inf.	36°37'03"N, 08°22'49"E	GBIFCH00763735	OP113123	genseq-2 COI
		Guitna sup.	36°36'42"N, 08°21'19"E	GBIFCH00895417	OP113124	genseq-2 COI
				GBIFCH00895418	OP113125	genseq-2 COI
				GBIFCH00654969	OP113126	genseq-2 COI
		Guitna inf.	36°37'05"N, 08°20'47"E	GBIFCH00975621	n/a	n/a
Centroptilum alamiae sp. nov.	Morocco	Oued Kelâa	35°14'32"N, 05°10'10"W	GBIFCH00980875	OP113127	genseq-2 COI
				GBIFCH00980876	OP113128	genseq-2 COI
		Oued Jnane Niche	35°15'29"N, 04°52'42"W	GBIFCH00975647	n/a	n/a
Centroptilum sp.	Iran	Javarem	36°13'43"N, 52°54'32"E	GBIFCH00763741	OP113129	genseq-4 COI

directly using the number of substitutions from a phylogenetic tree, eliminating the need for time calibration.

ASAP was applied to our COI alignment using the ASAP webserver available at https://bioinfo.mnhn.fr/abi/public/asap/asapweb.html, computing the genetic distances under the Kimura 2-parameter substitution model (K2P; Kimura 1980) with all other settings set to default. Input BI ultra-metric tree for GMYC was generated in BEAST 1.10.4. (Suchard et al. 2018). To avoid potential biases in threshold estimation, the outgroups were removed, and identical CO1 haplotypes were pruned (see Talavera et al. 2013) using Collapsetypes 4.6 (Chesters 2013). Input BEAST file was created in BEAUTi (Suchard et al. 2018), implementing the best model of evolution and the partition scheme specified above, and selecting a relaxed molecular clock (uncorrelated lognormal) model, a coalescent (constant size) prior (see Monaghan et al. 2009) and a UPGMA starting tree. Two independent MCMC chains were run for 50 million generations, sampling trees every 1'000 generations. Run convergence was visually verified in Tracer and the independent log and tree files were combined using LogCombiner 1.10.4 (Suchard et al. 2018) after discarding 10% of the trees as burn-in. The maximum clade credibility tree, generated in TreeAnnotator 1.10.4 (Suchard et al. 2018) with all options set to default, was used as input for GMYC, which was run in R 4.2.0 (R Core Team 2022) using the SPLITS package 1.0-20 (Ezard et al. 2009). We favoured the single-threshold version of the GMYC model because it was shown to outperform the multiple-threshold version (Fujisawa and Barraclough 2013). Input ML tree for mPTP was generated in RAxML-NG 1.1.0 (Kozlov et al. 2019) from our CO1 alignment (outgroup included), selecting the all-in-one (ML search + bootstrapping) option and MRE-based bootstrap convergence criterion. The best model of evolution and the partition scheme specified above, as well as 50 random and 50 parsimony starting trees were implemented. mPTP was conducted on the web service available at https://mptp.h-its.org. Finally, the number of parsimony-informative sites and the mean COI genetic distances between and within species were calculated in MegaX (Kumar et al. 2018; Stecher et al. 2020) under the K2P model.

Abbreviations:

MZL Musée de Zoologie Lausanne (Switzerland);
LESCB Laboratoire Ecologie, Systématique, Conservation de la Biodiversité, Tétouan (Morocco).

Results

Taxonomy

Centroptilum samraouii **Kaltenbach, Vuataz & Gattolliat, sp. nov.**
https://zoobank.org/C04FC672-92F6-4E55-8B48-FB4D5BDD93BD
Figs 1–3, 4a, d, 5a, 6

Differential diagnosis to other species of *Centroptilum*. Larva. Following combination of characters: A) labrum with anterior margin nearly straight; ratio width vs. length ca. 1.6× (Fig. 1a); B) maxillary palp ca. 1.9× as long as galea-lacinia, segment III apically pointed; segment III ca. 1.3× as long as segment II (Fig. 1g); C) inner distal margin of labial palp segment III concave (Fig. 1j); D) dorsal margin of fore femur with occasional short, spine-like setae (Fig. 2a); E) fore tarsus slightly longer than tibia (1.1×; Fig. 2a) F) claw with two rows of denticles, each with ca. 20 small to minute denticles (Fig. 2b); G) paraproct with 17–23 pointed spines, plus some additional submarginal spines (Fig. 2j).

Description. Larva (Figs 1–3, 4a, d, 5a). Body length 3.8–4.2 mm. Cerci: ca. 2/3 of body length. Paracercus: nearly as long as cerci. Antennae reaching apex of fore protoptera.

Colouration (Fig. 3a, b). Head, thorax and abdomen dorsally brown, with dark grey-brown pattern as in Fig. 3a. Head and thorax ventrally brown, with dark grey-brown lateral marks on thorax (Fig. 3b). Abdomen ventrally light brown. Legs light brown, apex of femur and claw darker. Caudalii ecru, brown annulated.

Labrum (Fig. 1a). Rectangular, width ca. 1.6× maximum length. Distal margin with broad, angulated, medial emargination. Anterior margin nearly straight. Dorsal surface scattered with long, medium and short, simple setae; setae not arranged in a submarginal arc. Ventrally with marginal row of setae composed of anterolateral long, simple, pointed setae and medial long, apically blunt, pectinate setae; ventral surface with ca. seven short, stout setae near lateral and anterolateral margin.

Right mandible (Fig. 1b, c). Incisor and kinetodontium separated. Incisor with three denticles; kinetodontium with two denticles. Prostheca stick-like, distally with two denticles. Margin between prostheca and mola almost straight, with two tufts of long setae. Tuft of setae at apex of mola present.

Left mandible (Fig. 1d, e). Incisor and kinetodontium separated. Incisor with four denticles; kinetodontium with three denticles. Prostheca stick-like, distally denticulate. Margin between prostheca and mola straight, with large brush-like tuft of long setae.

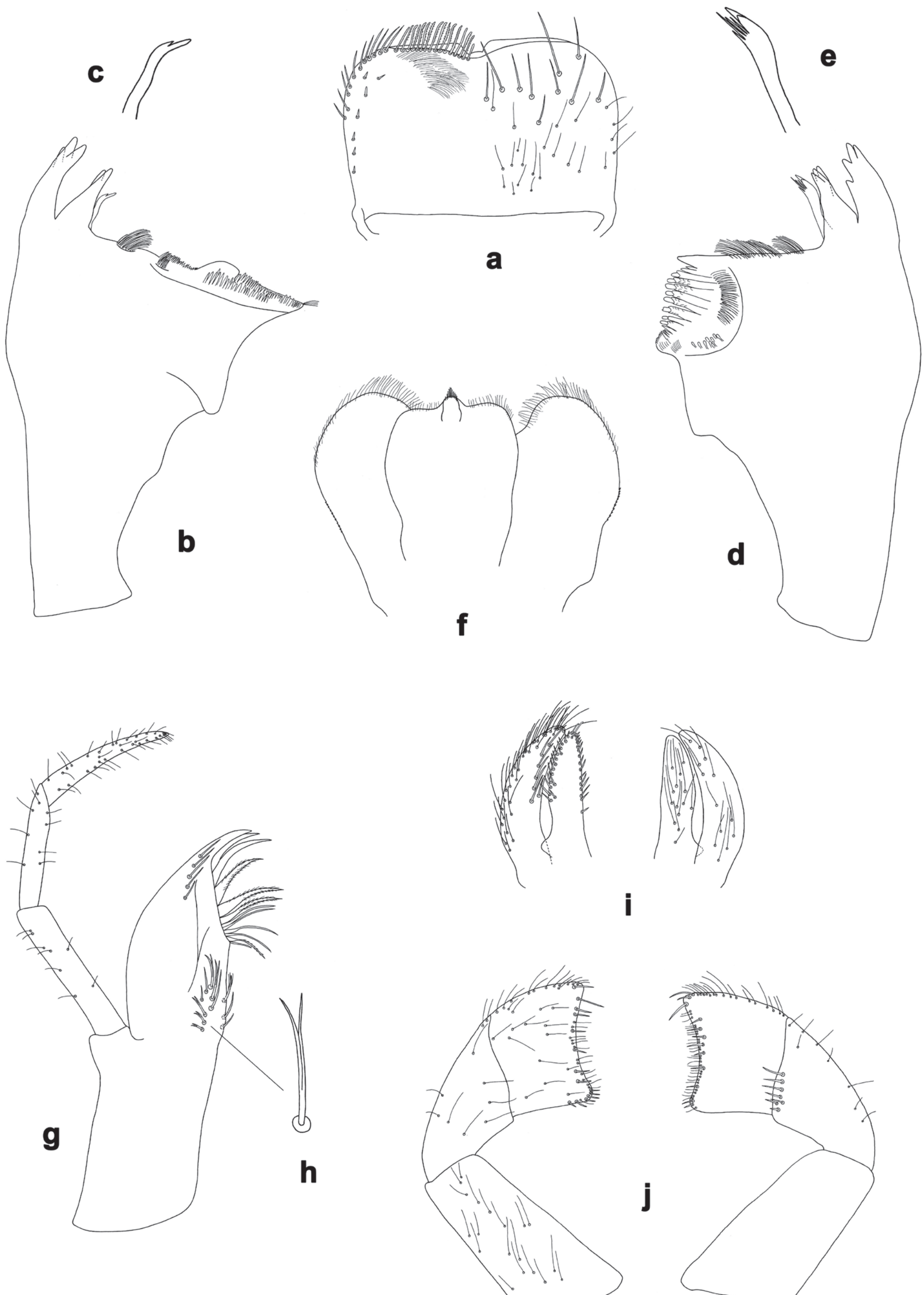

Figure 1. *Centroptilum samraouii* sp. nov., larva morphology **a** labrum (left: ventral view; right: dorsal view) **b** right mandible **c** right prostheca **d** left mandible **e** left prostheca **f** hypopharynx and superlinguae **g** maxilla **h** seta, ventrolateral **i** glossa and paraglossa (left: ventral view; right: dorsal view) **j** labial palp (left: ventral view; right: dorsal view).

Subtriangular process short, on level of area between prostheca and mola. Tuft of setae at apex of mola absent.

Hypopharynx and superlinguae (Fig. 1f). Lingua as long as superlinguae. Lingua longer than broad; distal half laterally not expanded; distal margin with short, fine setae, tuft of stout setae short. Superlinguae distally rounded; lateral margins rounded; fine, short to long, simple setae along distal margin.

Maxilla (Fig. 1g, h). Galea-lacinia ventrally with 3–5 simple, apical setae under canines. Canines long and slender. With three denti-setae, distal denti-seta canine-like, middle and proximal denti-setae slender, bifid and pectinate. Medially with one pectinate, spine-like seta and two simple, spine-like setae (dorsolateral insertions); and ca. eight long setae with bifurcated tips (bifurcation often difficult to see; ventrolateral insertions). Maxillary palp 3-segmented, ca. 1.9× as long as length of galea-lacinia; palp segment III ca. 1.3× length of segment II; setae on maxillary palp fine, simple, scattered over surface of segments I, II, and III; apex of last segment pointed.

Labium (Fig. 1i, j). Glossa nearly as broad and slightly shorter than paraglossa; inner and outer margins with many short, spine-like setae; apex with two medium, robust setae; dorsal surface with long, fine, simple, scattered setae. Paraglossa curved inward; ventrally with many long setae along outer lateral and apical margin, and row of long, stout, pointed, simple setae along inner lateral margin; dorsal surface with long, fine, simple, scattered setae. Labial palp 3-segmented. Segment III nearly trapezoidal with rounded distal corners, distal margin concave; outer lateral margin with short to medium, fine, simple setae, distal margin with short, spine-like and short, fine, simple setae; ventral surface with medium, fine, simple, scattered setae. Segment II with medium, fine, simple, scattered setae along outer lateral margin and on ventral surface; dorsally with 5–7 short, spine-like setae along distal margin. Segment I with medium, fine, simple setae scattered on ventral surface.

Hind protoptera well developed.

Foreleg (Fig. 2a, b) very slender. Ratio of foreleg segments 1.6:1.0:1.1:0.4. *Femur*. Length ca. 5× maximum width. Dorsal margin with occasional short, spine-like setae. Apex slightly rounded. Short, stout, pointed setae scattered along ventral margin; femoral patch absent. *Tibia.* Dorsal margin bare. Ventral margin with row of short, curved, spine-like setae and additional stout, pointed setae along margin. Anterior surface scattered with few stout, pointed, and partly serrate setae along ventral margin. Patellatibial suture present in basal ¼ area. *Tarsus.* Dorsal margin bare. Ventral margin with dense row of short, curved, serrate, spine-like setae. *Claw* with two rows of 17–20 minute denticles each, in basal ca. 1/3 area, increasing in size distally; subapical setae absent.

Terga (Figs 4a, d, 5a). Posterior margin of terga: I smooth, without spines; II with rudimentary spines; III with small, triangular spines; IV–IX with triangular spines.

Sterna. Posterior margin of sterna I–VI smooth, without spines. Posterior margin of sterna VII–VIII with small, triangular spines.

Tergalii (Figs 2c–i, 3c). Present on segments I–VII. Costal margins with minute denticles and short, fine, simple setae, anal margins almost smooth. Tracheae extending from main trunk to inner and outer margins. Tergalius I as long as length of segments

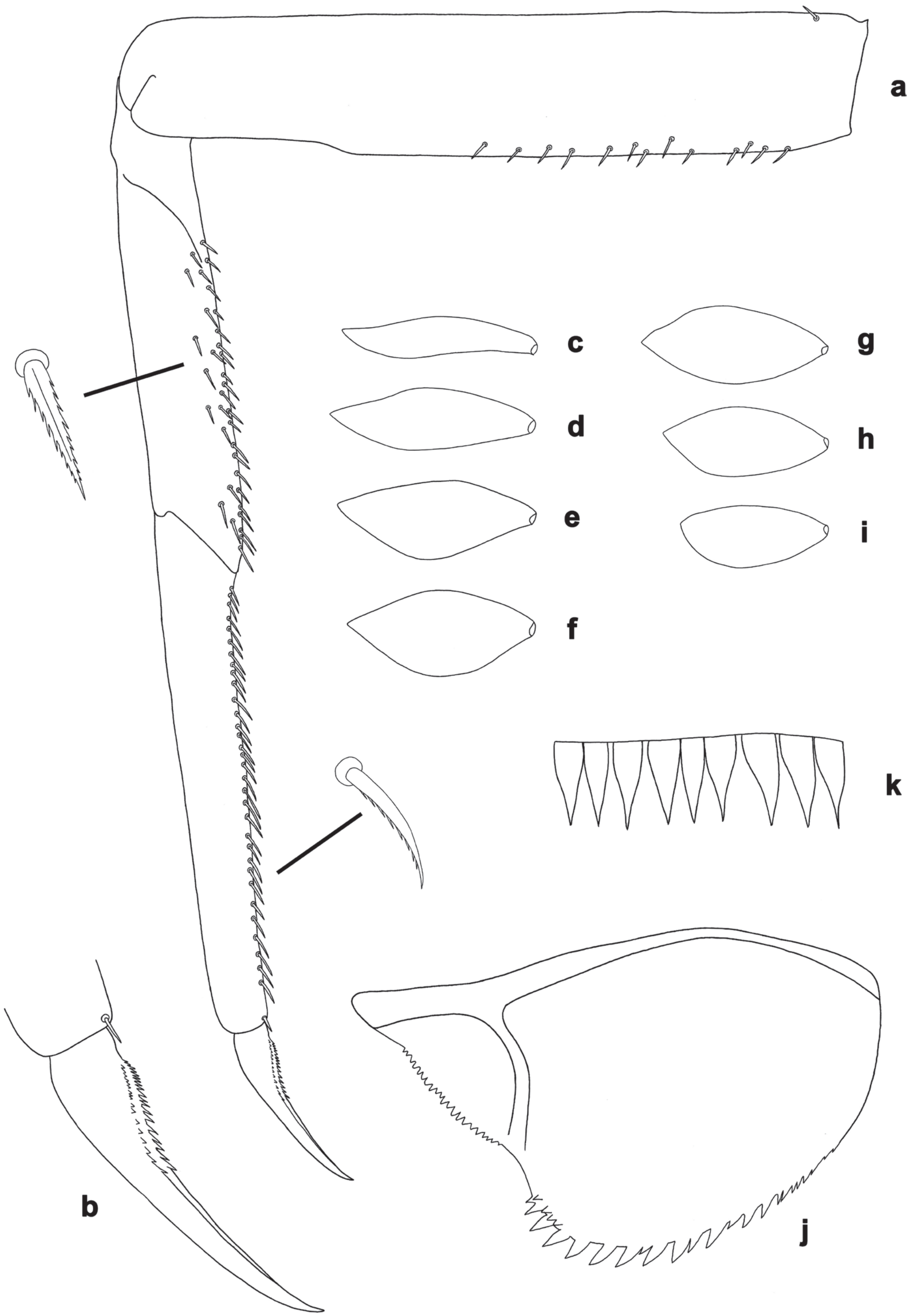

Figure 2. *Centroptilum samraouii* sp. nov., larva morphology **a** foreleg **b** fore claw **c** tergalius I **d** tergalius II **e** tergalius III **f** tergalius IV **g** tergalius V **h** tergalius VI **i** tergalius VII **j** paraproct **k** caudalii, spines on posterior margin of segments.

Figure 3. *Centroptilum samraouii* sp. nov., larva **a** habitus, dorsal view **b** habitus, ventral view **c** tergalius IV. Scale bars: 1 mm (**a, b**); 0.1 mm (**c**).

II–IV combined; tergalius IV as long as length of segments V and VI combined; tergalius VII as long as length of segments VIII and IX combined.

Paraproct (Fig. 2j). With 17–23 pointed marginal spines of different size, and some additional spines in second row. Cercotractor with minute, irregular, marginal spines.

Caudalii (Fig. 2k). Spines at posterior margins of segments elongated triangular with long points.

Subimago. Judging from subimaginal tarsomeres developing under cuticle of last instar female larvae, all tarsomeres of all legs of female subimago have pointed microlepids on surface (see Kluge 2022).

Imago. Unknown.

Etymology. Dedicated to Prof. Boudjéma Samraoui, committed researcher on aquatic insects in Algeria, and collector of the new species; in recognition to his substantial contribution to the knowledge of the ecology and distribution of Algerian mayflies.

Biological aspects. *Centroptilum samraouii* sp. nov. occupies the headwaters of steep, narrow and intermittent streams (Fig. 6c, d; Samraoui et al. 2021b, c).

Distribution (Fig. 6e). Algeria.

Type-material. ***Holotype.*** Algeria • larva; Guitna sup., Ghora; 36°36'42"N, 08°21'19"E; 22.01.2020; leg. B. Samraoui; on slides; GBIFCH00592552, GBIFCH00592551, GBIFCH00592622; MZL. ***Paratypes.*** Algeria • 2 larvae; Guitna sup., Ghora; 36°36'42"N, 08°21'19"E; 05.11.2019; leg. B. Samraoui; on slides; GBIFCH00895417, GBIFCH00895418; MZL • 3 larvae; Guitna sup.; 36°36'42"N, 08°21'19"E; 09.10.2019; leg. B. Samraoui; on slide; GBIFCH00592553; 2 in alcohol; GBIFCH00975620, GBIFCH00975623; MZL • larva; Louar inf., Ghora; 36°37'03"N, 08°22'49"E; 05.11.2019; leg. B. Samraoui; on slide; GBIFCH00592555; MZL • larva; Algeria; Guitna inf.; 07.11.2018; leg. B. Samraoui; in alcohol; GBIFCH00975621; MZL.

Centroptilum alamiae **Kaltenbach, Vuataz & Gattolliat, sp. nov.**
https://zoobank.org/0468CE29-CFF8-4DF7-ABB9-562D1C9B099F
Figs 4b, e, 5b, 6–9

Differential diagnosis to other species of *Centroptilum*. Larva. Following combination of characters: A) labrum with anterior margin slightly concave; ratio width vs. length ca. 1.5× (Fig. 7a); B) maxillary palp ca. 1.7× as long as galea-lacinia, segment III apically rounded; segment III ca. 1.6× as long as segment II (Fig. 7g); C) inner distal margin of labial palp segment III slightly concave (Fig. 7k); D) dorsal margin of fore femur with occasional short, spine-like setae; row of stout, pointed setae near margin (Fig. 8a); E) tarsus approx. as long as tibia (Fig. 8a); F) claw with two rows of denticles, each row with ca. 20 small to minute denticles (Fig. 8b); G) paraproct with 30–45 pointed spines, sometimes with split tips, few additional, submarginal spines (Fig. 8j).

Description. Larva (Figs 4b, e, 5b, 7–9). Body length 5.6–7.0 mm. Caudalii broken. Antennae reaching apex of fore protoptera.

Colouration (Fig. 9a–c). Head, thorax and abdomen dorsally brown, with dark grey-brown pattern as in Fig. 9a. Head, thorax and abdomen ventrally light brown, with dark grey-brown lateral marks on thorax (Fig. 9c). Legs light brown, femur distomedially slightly darker, tarsus basally and distally slightly darker, claw basally darker. Caudalii light brown, darker annulated.

Labrum (Fig. 7a). Rectangular, width ca. 1.5× maximum length. Distal margin with broad, angulated, medial emargination. Anterior margin slightly concave. Dorsal surface scattered with long, medium and short, simple setae; setae not arranged in a submarginal arc. Ventrally with marginal row of setae composed of anterolateral long, simple, pointed setae and medial long, apically blunt, pectinate setae; ventral surface with ca. nine short, stout setae near lateral and anterolateral margin.

Right mandible (Fig. 7b, c). Incisor and kinetodontium separated. Incisor with three denticles; kinetodontium with two denticles. Prostheca stick-like, distally with three denticles. Margin between prostheca and mola almost straight, with two tufts of long setae. Tuft of setae at apex of mola present.

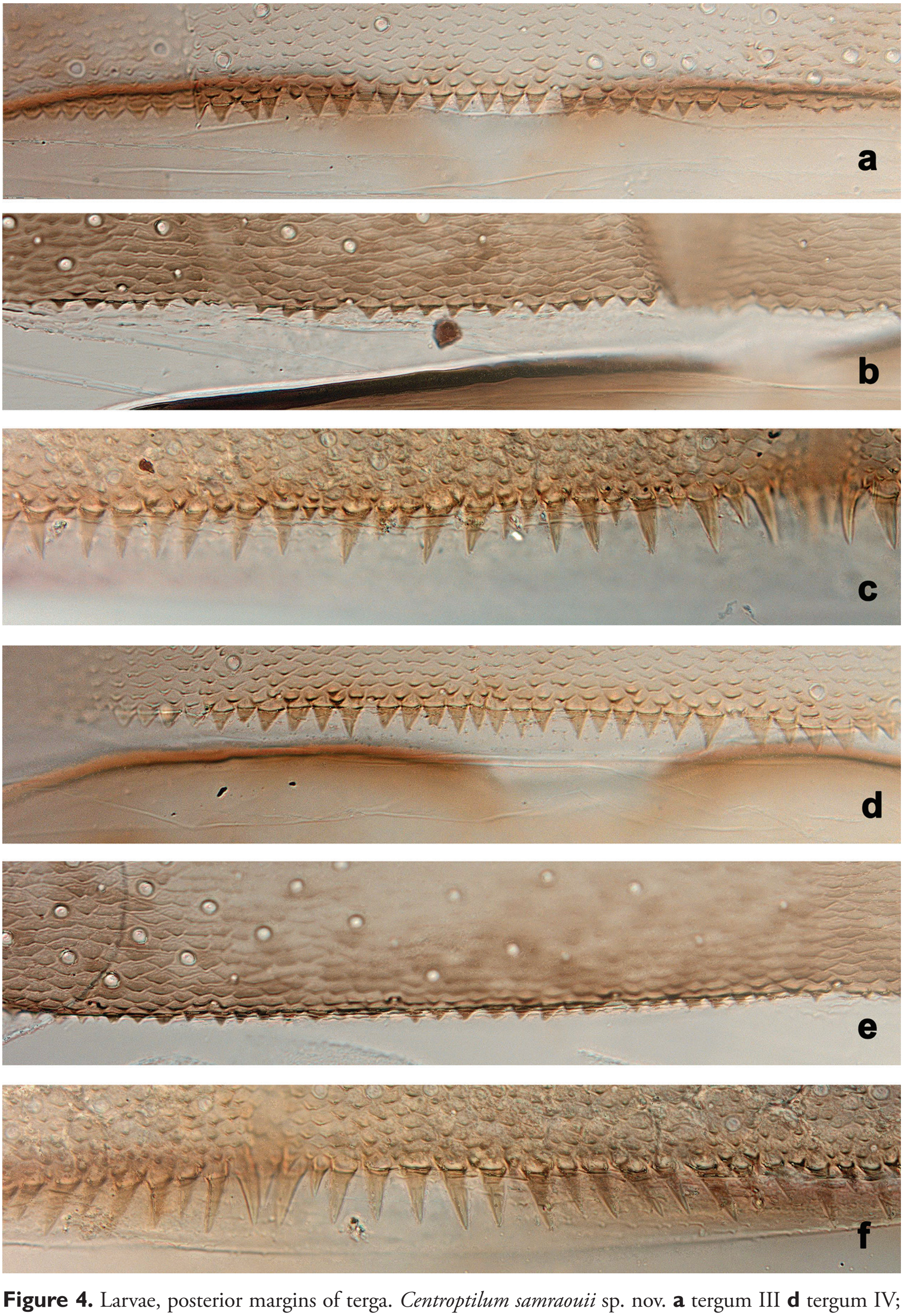

Figure 4. Larvae, posterior margins of terga. *Centroptilum samraouii* sp. nov. **a** tergum III **d** tergum IV; *Centroptilum alamiae* sp. nov. **b** tergum III **e** tergum IV; *Centroptilum luteolum*: **c** tergum III **f** tergum IV.

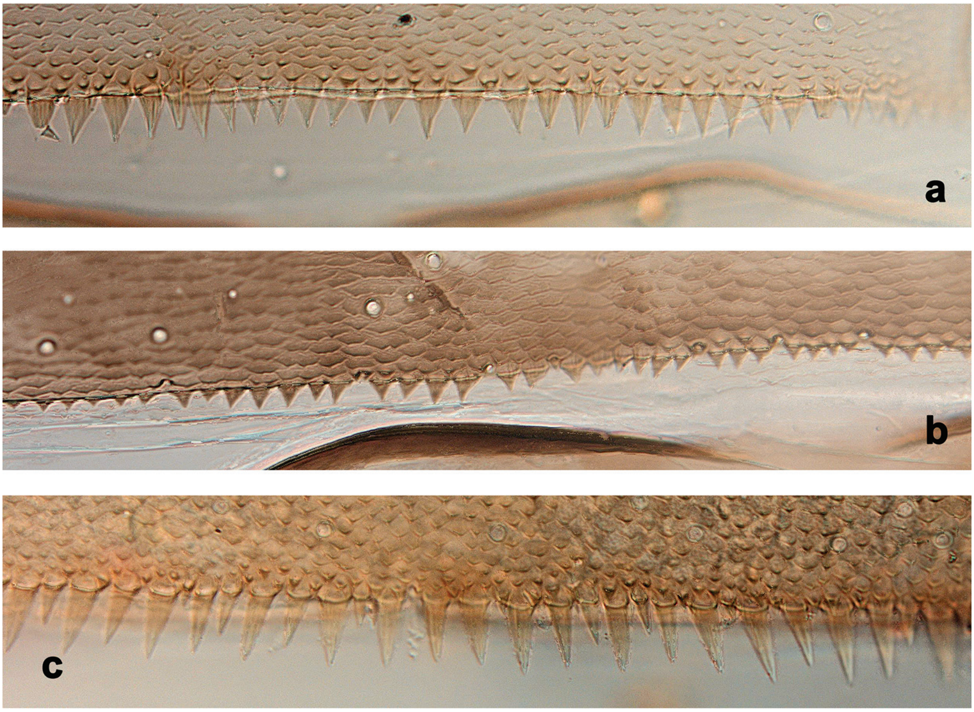

Figure 5. Larvae, posterior margins of terga VII **a** *Centroptilum samraouii* sp. nov. **b** *Centroptilum alamiae* sp. nov. **c** *Centroptilum luteolum*.

Left mandible (Fig. 7d, e). Incisor and kinetodontium separated. Incisor with four denticles; kinetodontium with three denticles. Prostheca stick-like, distolaterally denticulate. Margin between prostheca and mola straight, with large brush-like tuft of long setae. Subtriangular process short, on level of area between prostheca and mola. Tuft of setae at apex of mola absent.

Hypopharynx and superlinguae (Fig. 7f). Lingua as long as superlinguae. Lingua longer than broad; distal half laterally not expanded; distal margin with short, fine setae, tuft of stout setae short. Superlinguae distally rounded; lateral margins rounded; fine, short to long, simple setae along distal margin.

Maxilla (Fig. 7g). Galea-lacinia ventrally with four or five simple, apical setae under canines. Canines long and slender. With three denti-setae, distal denti-seta canine-like, middle and proximal denti-setae slender, bifid and pectinate. Medially with one pectinate, spine-like seta and three simple, spine-like setae (dorsolateral insertions); and ca. six long setae, partly with bifurcated tips (bifurcation often difficult to see; ventrolateral insertions). Maxillary palp 3-segmented, ca. 1.7× as long as length of galea-lacinia; palp segment III ca. 1.6× length of segment II; setae on maxillary palp fine, simple, scattered over surface of segments I, II, and III; apex of last segment rounded.

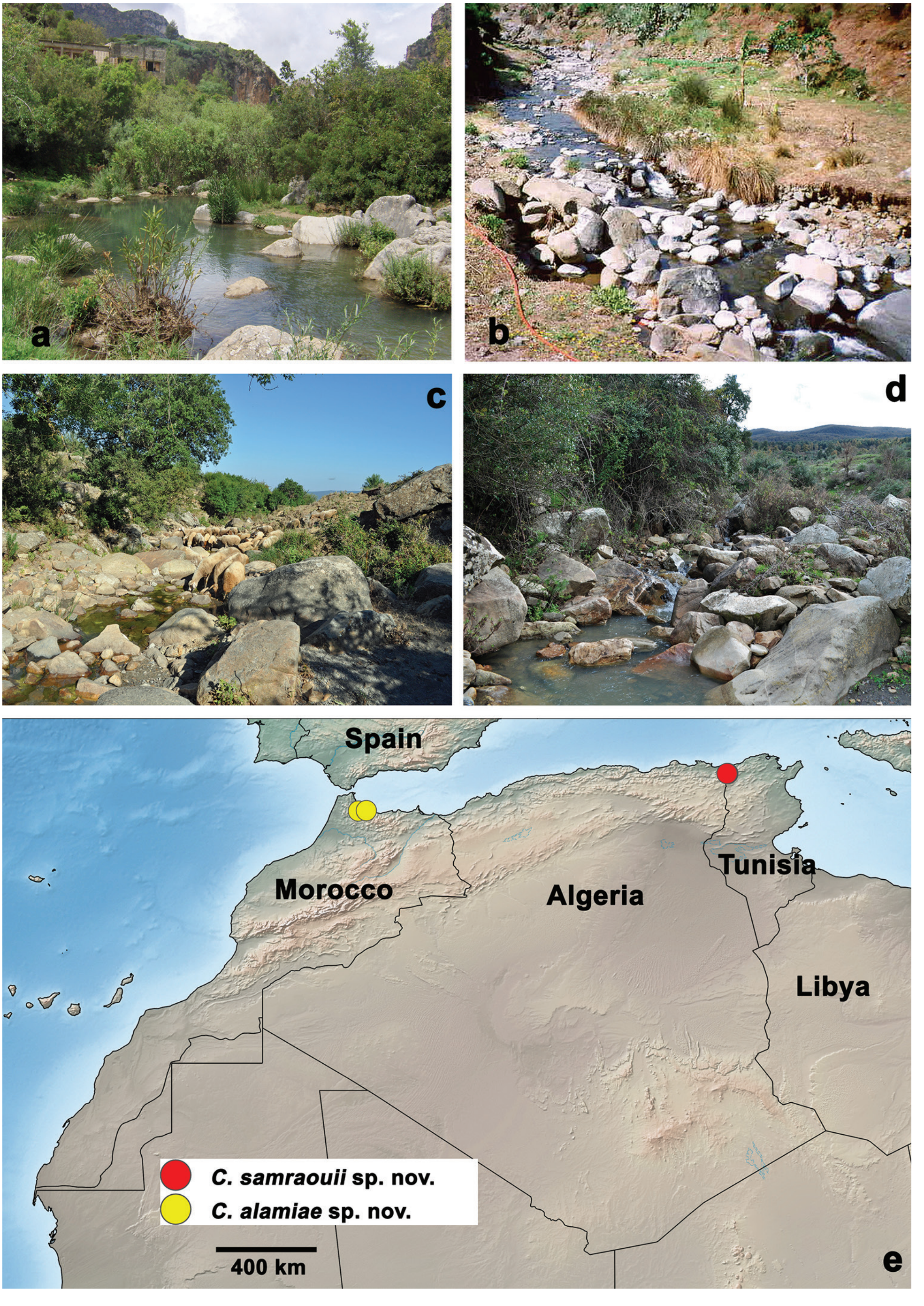

Figure 6. Habitats and distribution of the new species **a, b** *Centroptilum alamiae* sp. nov., habitats **a** Oued Kelâa (type locality) **b** Oued Jnane Niche **c, d** *Centroptilum samraouii* sp. nov., habitats **c** Guitna sup. (type locality) **d** Louar inf. **e** distribution map.

Labium (Fig. 7h–k). Glossa nearly as broad and slightly shorter than paraglossa; inner and outer margins with many short, spine-like setae; apex with two medium, robust setae; dorsal surface with long, fine, simple, scattered setae. Paraglossa curved inward; ventrally with many long setae along outer lateral and apical margin, and row of long, stout, pointed, simple setae along inner lateral margin; dorsal surface with long, fine, simple, scattered setae. Labial palp 3-segmented. Segment III nearly trapezoidal with rounded distal corners, distal margin slightly concave; outer lateral margin with short to medium, fine, simple setae, distal margin with short, spine-like and short, fine, simple setae; ventral surface with medium, fine, simple, scattered setae. Segment II with medium, fine, simple, scattered setae along outer lateral margin and on ventral surface; dorsally with seven or eight short, spine-like setae along distal margin. Segment I with medium, fine, simple setae scattered on ventral surface and on outer lateral margin.

Hind protoptera well developed.

Foreleg (Fig. 8a, b) very slender. Ratio of foreleg segments 1.6:1.0:1.0:0.4. *Femur*. Length ca. 5× maximum width. Dorsal margin with occasional short, spine-like setae, row of short, pointed setae near margin. Apex slightly rounded. Short, stout, pointed setae scattered along ventral margin; femoral patch absent. *Tibia.* Dorsal margin bare. Ventral margin with row of short, curved, spine-like setae and some aditional stout, pointed setae along margin. Anterior surface scattered with short, stout, pointed, and partly serrate setae along ventral margin. Patellatibial suture present in basal 1/3 area. *Tarsus.* Dorsal margin bare. Ventral margin with dense row of short, curved, serrate, spine-like setae. *Claw* with two rows of 17–20 minute denticles each, in basal ca. 1/3 area, increasing in size distally; subapical setae absent.

Terga (Figs 4b, e, 5b). Posterior margin of terga: I smooth, without spines; II–VI (VII) with small triangular spines; VII–IX with triangular, pointed spines.

Sterna. Posterior margin of sterna I–VI smooth, without spines. Posterior margin of sterna VII–VIII with small, triangular spines.

Tergalii (Figs 8c–i, 9d). Present on segments I–VII. Costal margins with minute denticles and short, fine, simple setae, anal margins almost smooth. Tracheae extending from main trunk to inner and outer margins. Tergalius I as long as length of segments II and III combined; tergalius IV as long as length of segments V and VI combined; tergalius VII as long as length of segments VIII and IX combined.

Paraproct (Fig. 8j). With irregular row of 30–45 pointed marginal spines of different size, some with split tips, and few additional spines in second row. Cercotractor with minute, irregular, marginal spines.

Caudalii (Fig. 8k). Spines at posterior margins of segments short triangular, pointed.

Subimago. Judging from subimaginal tarsomeres developing under cuticle of last instar female larvae, all tarsomeres of all legs of female subimago have pointed microlepids on surface (see Kluge 2022).

Imago. Unknown.

Etymology. Dedicated to Prof. Majida El Alami, committed researcher on aquatic insects in Morocco, and collector of some of the specimens; in recognition of her substantial contribution to the knowledge of the systematics, ecology, and distribution of Moroccan mayflies.

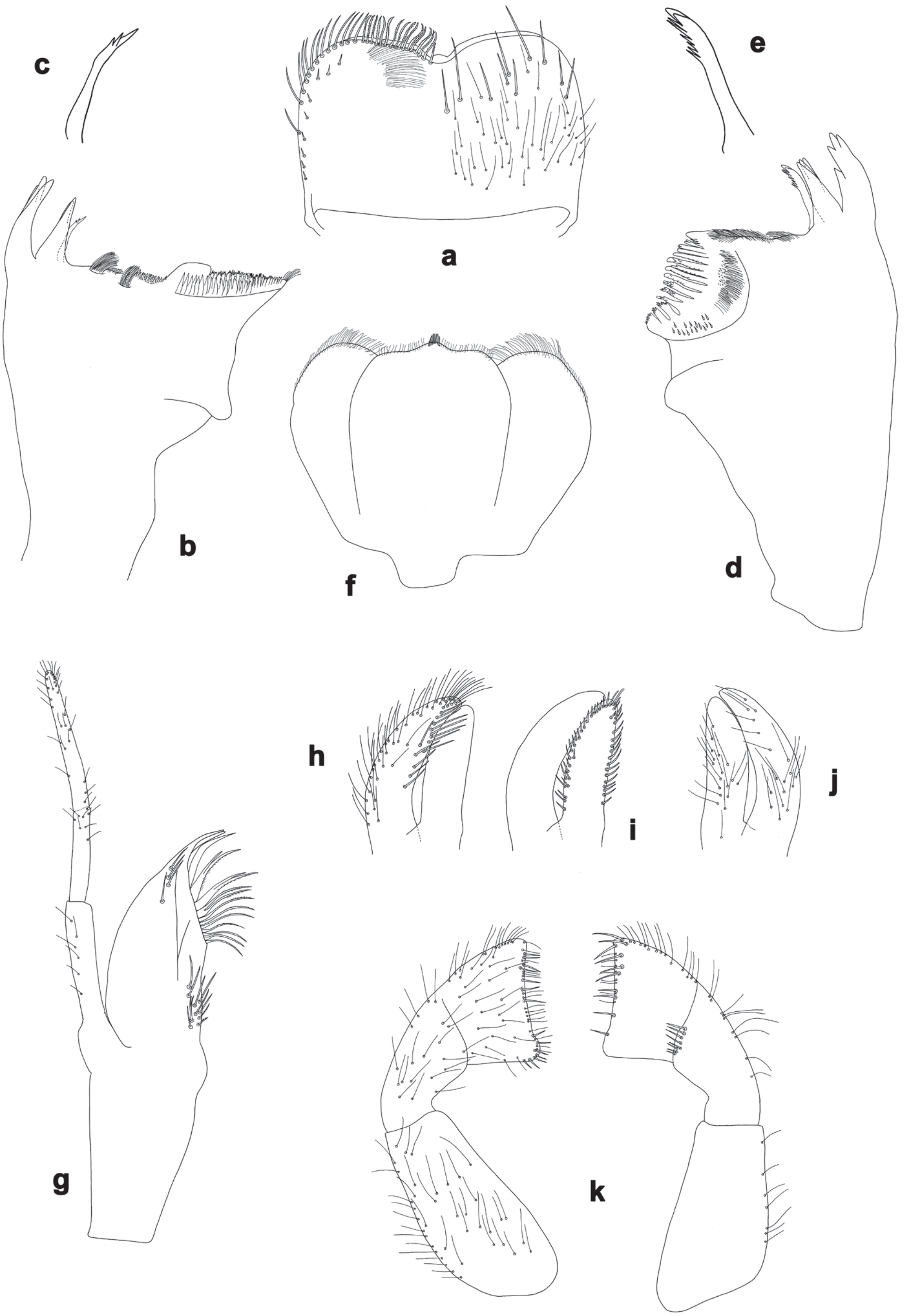

Figure 7. *Centroptilum alamiae* sp. nov., larva morphology **a** labrum (left: ventral view; right: dorsal view) **b** right mandible **c** right prostheca **d** left mandible **e** left prostheca **f** hypopharynx and superlinguae **g** maxilla **h** glossa and paraglossa (ventral view) **i** glossa and paraglossa (ventral view) **j** glossa and paraglossa (dorsal view) **k** labial palp (left: ventral view; right: dorsal view).

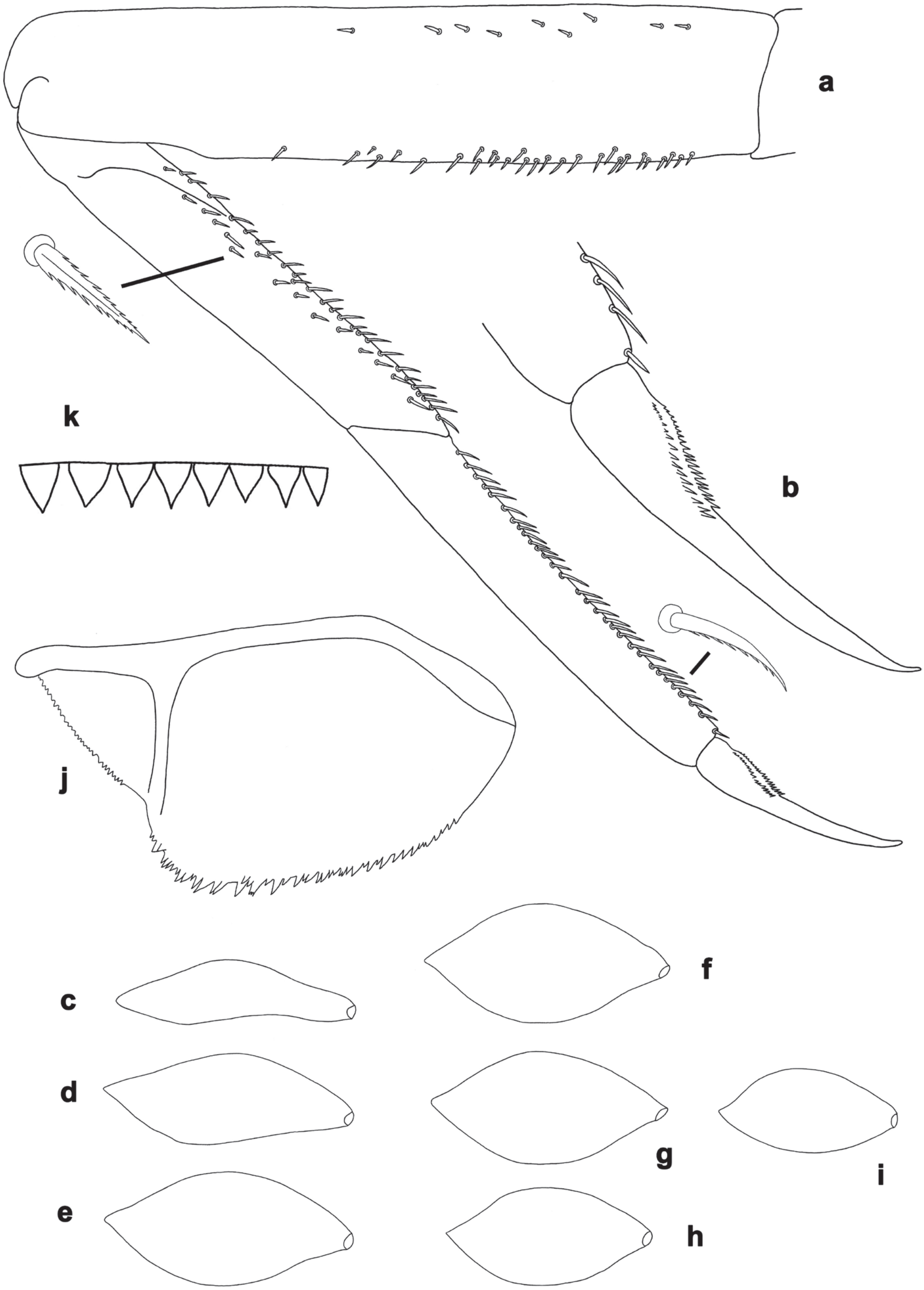

Figure 8. *Centroptilum alamiae* sp. nov., larva morphology **a** foreleg **b** fore claw **c** tergalius I **d** tergalius II **e** tergalius III **f** tergalius IV **g** tergalius V **h** tergalius VI **i** tergalius VII **j** paraproct **k** caudalii, spines on posterior margins of segments.

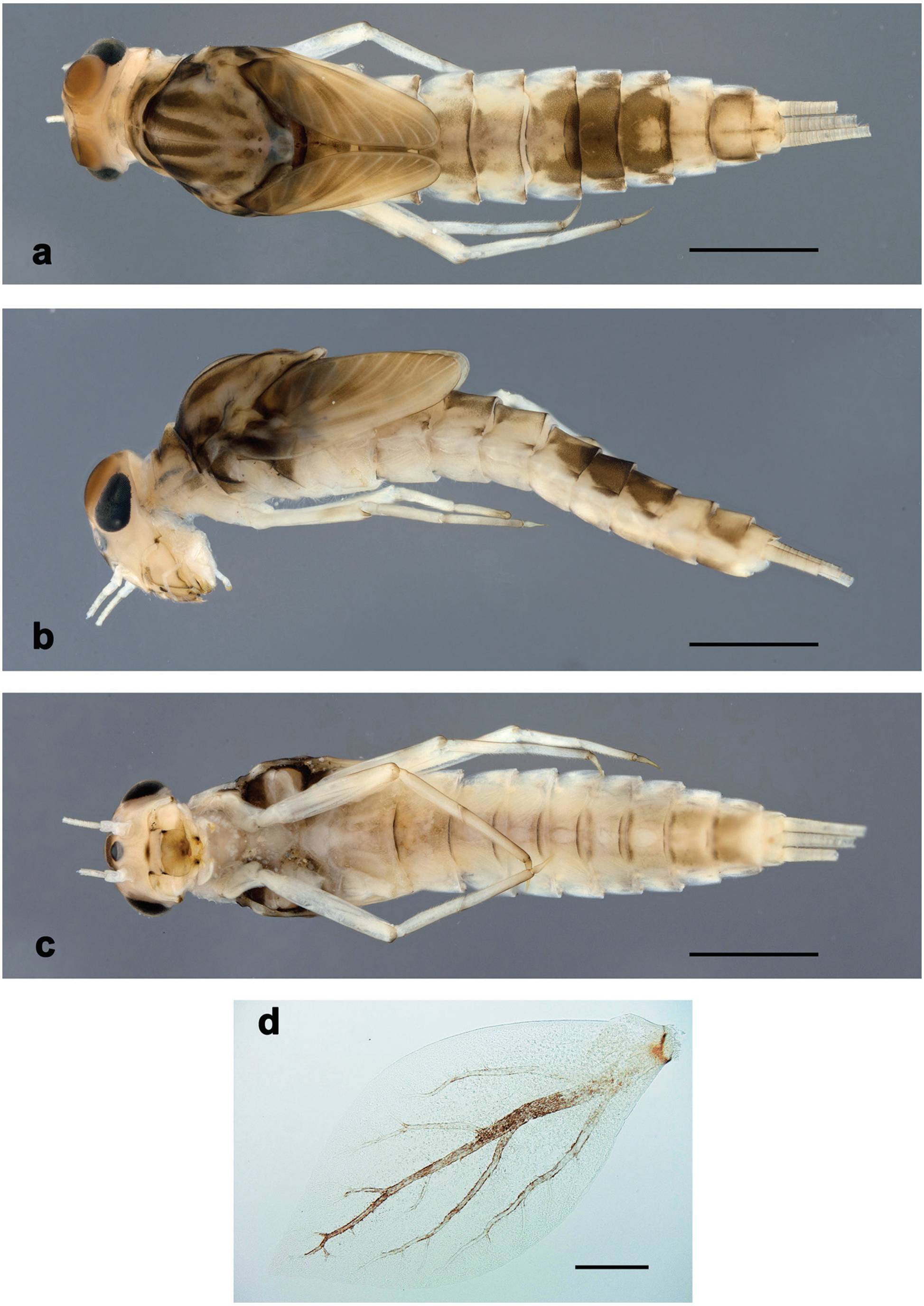

Figure 9. *Centroptilum alamiae* sp. nov., larva **a** habitus, dorsal view **b** habitus, lateral view **c** habitus, ventral view **d** tergalius IV. Scale bars: 1 mm (**a–c**); 0.1 mm (**d**).

Biological aspects. The specimens were collected in calm edge waters, loose substrate, low to moderate current, high temperatures, and sites rich in filamentous algae and mosses (Fig. 6a, b; El Alami et al. 2022a).

Distribution (Fig. 6e). Morocco.

Type-material. *Holotype.* Morocco • larva; Oued Kelâa, Akchour; 35°14'32"N, 05°10'10"W; 13.03.2021; leg. S. El Yaagoubi; on slide; GBIFCH00592619, GBIFCH00592620, GBIFCH00592621; MZL. ***Paratypes.*** Morocco • 6 larvae; same data as holotype; 2 on slides; GBIFCH00980875, GBIFCH00980876; 4 in alcohol; GBIFCH00975645, GBIFCH00975646; MZL • 7 larvae; Oued Jnane Niche (sup.); 16.03.2014; leg. M. El Alami; in alcohol; GBIFCH00975647; MZL • 12 larvae; Oued Jnane Niche (sup.); 17.05.2015; leg. M. El Alami; 1 on slide; 11 in alcohol; LESCB.

Genetics

The COI ingroup data set was 98% complete and included 34% of parsimony informative sites. The missing data almost exclusively resulted from nine GenBank sequences that lacked 5' and/or 3' end. All main CO1 gene tree relationships were resolved and well supported, except for the placement of the three clades *Centroptilum* sp. 1, *C.* sp. 2, and *C. luteolum* 1 (Fig. 10). The four sequences of *C. samraouii* sp. nov. were grouped in a well-supported monophyletic clade, supported as a distinct species in the ASAP, GMYC and mPTP species delimitation analyses (Fig. 10). Similarly, the two sequences of *C. alamiae* sp. nov. were grouped in a well-supported monophyletic clade, supported as a distinct species in all species delimitation analyses. The K2P mean genetic distance within the four *C. samraouii* sp. nov. and the two *C. alamiae* sp. nov. sequences were 0.08% and 0%, respectively. The K2P mean genetic distance between *C. samraouii* sp. nov. and the other six species (or putative species) ranged from 22.1% (mean distance to *C. alamiae* sp. nov.) to 25.2% (mean distance to *C.* sp. 1), whereas it ranged from 9.2% (mean distance to *C. luteolum* 1) to 25.7% (mean distance to *C. volodymyri*) for *C. alamiae* sp. nov. The three species delimitation methods were congruent, except for one slightly divergent sequence within the *C. luteolum* 1 cluster that was isolated by the GMYC, and the three *C. volodymyri* sequences that were all considered as distinct putative species according to ASAP and GMYC.

Discussion

Differentiating characters between species of *Centroptilum*

The characters differentiating the geographically relatively close species *Centroptilum luteolum*, *C. samraouii* sp. nov. and *C. alamiae* sp. nov. are summarised in Table 2. Most important are the spines on posterior margin of abdominal terga and the

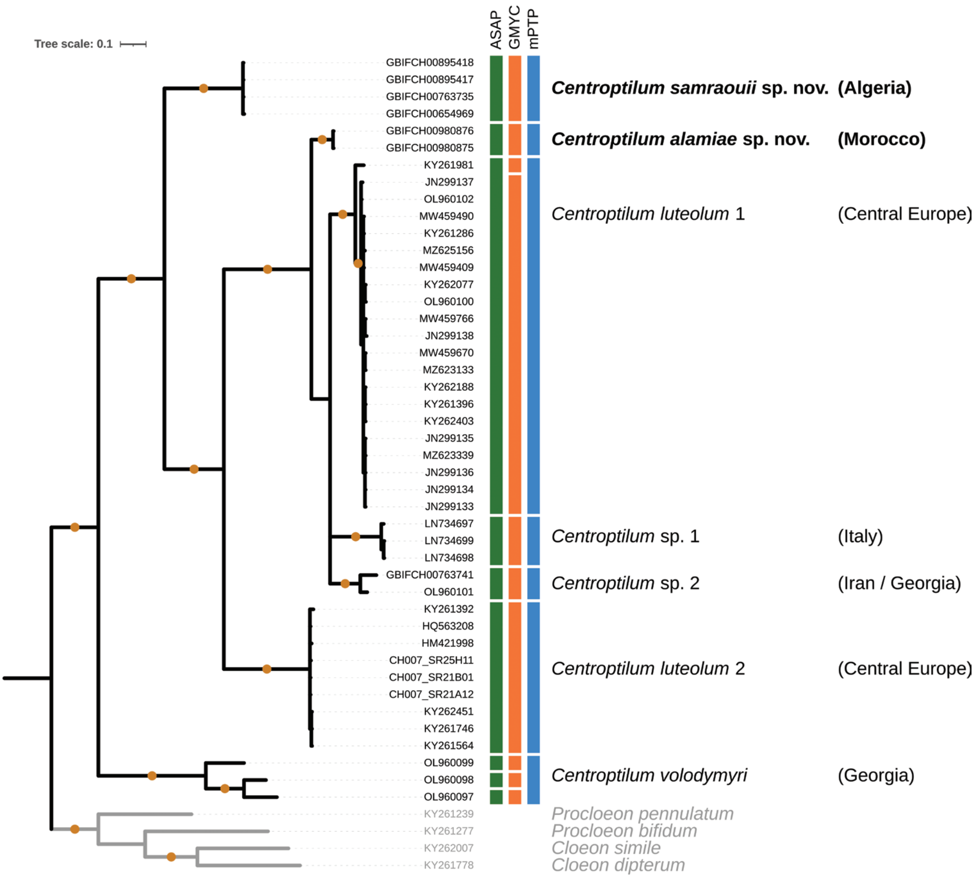

Figure 10. Bayesian majority-rule consensus tree reconstructed from the CO1 data set. Coloured vertical boxes indicate species delimitation hypothesis according to the ASAP, GMYC and mPTP methods. Tips labelled with GBIF codes indicate newly sequenced specimens, CH007_SR codes designate sequences from the FREDIE project, and other codes correspond to previously published GenBank sequences. For each mPTP species hypothesis, the corresponding species names (where available) and the country of origin is provided. Circles on branches indicate Bayesian posterior probabilities > 0.95. Outgroup branches, tips labels, and species names are presented in grey.

spines on paraproct margin (see Table 2). Further reliable characters to differentiate both new species from North Africa are the distal margin of the labrum (straight in *C. samraouii* sp. nov., slightly concave in *C. alamiae* sp. nov.); the distal margin of labial palp segment III (concave in *C. samraouii* sp. nov., slightly concave in *C. alamiae* sp. nov.); the relative length of maxillary palp segment III vs. segment II (1.3× in *C. samraouii* sp. nov., 1.6× in *C. alamiae* sp. nov.); and the setation on dorsal margin of femur (only occasional setae in *C. samraouii* sp. nov., additional row of short, pointed setae near margin in *C. alamiae* sp. nov.) (see Table 2).

The recently described species *C. volodymyri* (Georgia, Turkey, Iran) differs from *C. samraouii* sp. nov. and *C. alamiae* sp. nov. by several distinct characters: maxillary palp much

Table 2. Differentiating characters of new species of *Centroptilum* and *C. luteolum* (Switzerland, VD, Le Chenit, 18 Aug 2001, leg. A. Wagner) (M: 11B and M: 11F refer to figures in Martynov et al. 2022: fig. 11B, F).

Characters	No. in Martynov et al. 2022	*C. luteolum*	Figs	*C. samraouii* sp. nov.	Figs	*C. alamiae* sp. nov.	Figs
Larva							
Head, mouthparts							
Labrum, width/ length ratio	II.1	1.4–1.6		ca. 1.6	1a	ca. 1.5	7a
Labrum, anterior margin	II.3	nearly straight, medial emargination angular		nearly straight, medial emargination angular	1a	slightly concave, medial emargination angular	7a
Maxillary palp, segment III	II.5	(bluntly) pointed apex ca. 1.2× as long as segment II		pointed apex ca. 1.3× as long as segment II	1g	bluntly pointed/rounded apex ca. 1.6× as long as segment II	7g
Maxillary palp, length		ca. 1.8× as long as galea-lacinia		ca. 1.9× as long as galea-lacinia	1g	ca. 1.7× as long as galea-lacinia	7g
Rhight mandible, denticles	II.6	3 + 2		3 + 2	1b	3 + 2	7b
Left mandible, denticles	II.7	4 + 2 (rarely 4 + 3)		4 + 3	1d	4 + 3	7d
Labial palp segment III	II.12	Distal (inner) margin concave		Distal (inner) margin concave	1j	Distal (inner) margin slightly concave	7k
Thorax, legs							
Legs, colour pattern	III.4	femur with brown band distally; tibia proximally darker		legs light brown; claw darker	3b	femur distomedially darker, tarsus basally and distally darker; claw basally darker	9a–c
Fore femur, dorsal margin	III.6	occasional short, pointed setae on margin		occasional short, pointed setae on margin	2a	occasional short, pointed setae on margin; row of short, pointed, setae near margin	8a
Fore tibia, length vs. tarsus		ca. equal length		slightly longer (ca. 1.1×)	2a	ca. equal length	7a
Abdomen							
Terga, posterior margin (spines)	IV.5, 6	I: no spines II–IX: long, narrow triangular, pointed	4c, f 5c	I: no spines II–III: small triangular IV–IX: medium triangular	4a, d 5a	I: no spines II–VI (VII): small triangular VII–IX: medium triangular	4b, e 5b
Terga VII–IX, posterolateral part	IV.7	VII: no spines VIII: ca. 3 spines IX: 10–13 spines		VII: no spines VIII: ca. 5 spines IX: ca. 8 spines		VII: no spines VIII: ca. 4 spines IX: ca. 12 spines	
Sterna, posterior margin (spines)	IV.10	I–IV: no spines V: rudimentary spines VI–IX: medium triangular		I–VI: no spines VII–IX: very small triangular		I–V: no spines VI: rudimentary VII–IX: very small triangular	
Paraproct, distal margin	IV.14	23–30 pointed spines plus some spines in 2nd row	M: 11B	17–23 pointed spines plus few smaller in 2nd row	2j	30–45 pointed spines partly split tips plus few in 2nd row	7j
Caudalii, posterior margin of segments (spines)	IV.17	elongated, triangular spines	M: 11F	elongated, triangular spines with long points	2k	triangular spines with short points	8k

longer than galea-lacinia (ca. 2.3×); maxillary palp segment I distinctly wider than segment II (only slightly wider in all other species); labrum much wider than long (1.8–2.0×); claw with more than 60 minute denticles in two rows (ca. 30 per row) (Martynov et al. 2022; for respective character states of *C. samraouii* sp. nov. and *C. alamiae* sp. nov. see Table 2).

The poorly known species *C. pirinense* (Pirin Mountains, Bulgaria) differs from *C. samraouii* sp. nov. and *C. alamiae* sp. nov. at least in the very wide labrum (ca. 2.0×

wider than long; Martynov et al. 2022: table II), whereas in *C. samraouii* sp. nov. it is ca. 1.6× and in *C. alamiae* sp. nov. ca. 1.5× (see Table 2).

Microlepids of subimago

Judging from tarsomeres of subimagos developing under cuticle of female last instar larvae, at least female subimagos of both new species of *Centroptilum* have all their tarsomeres of all legs covered with pointed microlepids. This is in line with *C. luteolum*, which has pointed microlepids on all tarsomeres of all legs of male and female subimagos (Kluge 2022).

Genetics and biogeography

The two new North African species described here are highly supported by our CO1-based analyses. First, the minimum mean genetic distance of 9.2% (mean distance between *Centroptilum alamiae* sp. nov. to *C. luteolum* 1) is much higher than the generally accepted intra-/interspecific threshold value of ca. 3% divergence for mayflies (e.g., Ball et al. 2005; Kjærstad et al. 2012; Gattolliat et al. 2015). Second, both new species are well supported in their own monophyletic clade, and third, all three species delimitation analyses are congruent and support the morphological results. Interestingly, the two new species are not supported as closely related, despite their geographical proximity, suggesting a distinct origin. Rather, *C. alamiae* sp. nov., and the European species *C.* sp. 1, *C.* sp. 2, and *C. luteolum* 1 are included in the same well-supported clade sister to the others, which possibly indicates a more recent colonisation event from Europe to Morocco. This hypothesis is supported by the presence of *C. luteolum* 1 in the Pyrenees and in the south of Spain (unpublished sequences from the project FREDIE; not shown in Fig. 10). The type locality of *C. alamiae* sp. nov. in Morocco is geographically closer to the south of Spain than to the type locality of *C. samraouii* sp. nov. in Algeria. All examined specimens of *Centroptilum* in Morocco and Algeria belong to one of the new species and not to *C. luteolum* or any other species of *Centroptilum*. The genus *Centroptilum* seems to be extremely rare in Tunisia, no specimen from this country could be investigated in this study. In conclusion, we cannot formally exclude the presence of *C. luteolum* in the Maghreb at this point in time, but it seems unlikely.

Acknowledgements

We are very thankful to André Wagner (Museum of Zoology Lausanne) for the collection of Swiss material for comparison.

Furthermore, we are thankful to Michel Sartori (Museum of Zoology Lausanne) for his constant interest and support for our projects and to Céline Stoffel (Museum of Zoology Lausanne) for her support with lab work and preparation of the COI barcodes.

Lastly, the authors are grateful to the reviewers Roman J. Godunko and Pavel Sroka for their valuable recommendations and comments on the manuscript.

References

Ball SL, Hebert PD, Burian SK, Webb JM (2005) Biological identifications of mayflies (Ephemeroptera) using DNA barcodes. Journal of the North American Benthological Society 24(3): 508–524. https://doi.org/10.1899/04-142.1

Bauernfeind E, Soldán T (2012) The Mayflies of Europe (Ephemeroptera). Apollo Books, Ollerup, Denmark, 781 pp. https://doi.org/10.1163/9789004260887

Benhadji N, Hassaine KA, Sartori M (2018) *Habrophlebia hassainae*, a new mayfly species (Ephemeroptera: Leptophlebiidae) from North Africa. Zootaxa 4403(3): 557. https://doi.org/10.11646/zootaxa.4403.3.8

Benhadji N, Sartori M, Abdellaoui Hassaine K, Gattolliat J-L (2020) Reports of Baetidae (Ephemeroptera) species from Tafna Basin, Algeria and biogeographic affinities revealed by DNA barcoding. Biodiversity Data Journal 8: e55596(14). https://doi.org/10.3897/BDJ.8.e55596

Boumaïza M, Thomas AGB (1995) Distribution and ecological limits of Baetidae vs. the other mayfly families in Tunisia: A first evaluation (Insecta, Ephemeroptera). Bulletin de la Société d`Histoire Naturelle 131: 27–33.

Chakrabarty P, Warren M, Page LM, Baldwin CC (2013) GenSeq: An updated nomenclature and ranking for genetic sequences from type and non-type sources. ZooKeys 346: 29–41. https://doi.org/10.3897/zookeys.346.5753

Chesters D (2013) collapsetypes.pl [computer software]. http://sourceforge.net/projects/collapsetypes/

Dambri BM, Benhadji N, Vuataz L, Sartori M (2022) *Ecdyonurus aurasius* sp. nov. (Insecta, Ephemeroptera, Heptageniidae, Ecdyonurinae), a new micro-endemic mayfly species from Aurès Mountains (north-eastern Algeria). ZooKeys 1121: 17–37. https://doi.org/10.3897/zookeys.1121.89613

Darriba D, Taboada GL, Doallo R, Posada D (2012) jModelTest 2: More models, new heuristics and parallel computing. Nature Methods 9(8): 772–772. https://doi.org/10.1038/nmeth.2109

El Alami M, El Yaagoubi S, Gattolliat J-L, Sartori M, Dakki M (2022a) Diversity and distribution of mayflies from Morocco (Ephemeroptera, Insecta). Diversity 14(6): 498. https://doi.org/10.3390/d14060498

El Alami M, Benlasri M, Sartori M, Vuataz L, Ghamizi M (2022b) A new species of the genus *Prosopistoma* Latreille, 1833 (Ephemeroptera: Prosopistomatidae) from Morocco. ZooKeys 1117: 203–218. https://doi.org/10.3897/zookeys.1117.83539

Ezard T, Fujisawa T, Barraclough TG (2009) SPLITS: Species' Limits by Threshold Statistics. R-package. https://rdrr.io/rforge/splits/

Folmer O, Black M, Hoeh W, Lutz R, Vrijenhoek R (1994) DNA primers for amplification of mitochondrial cytochrome c oxidase subunit I from diverse metazoan invertebrates. Molecular Marine Biology and Biotechnology 3: 294–299. http://www.mbari.org/staff/vrijen/PDFS/Folmer_94MMBB.pdf

Fujisawa T, Barraclough TG (2013) Delimiting species using single-locus data and the Generalized Mixed Yule Coalescent approach: A revised method and evaluation on simulated data sets. Systematic Biology 62(5): 707–724. https://doi.org/10.1093/sysbio/syt033

Gattolliat J-L, Cavallo E, Vuataz L, Sartori M (2015) DNA barcoding of Corsican mayflies (Ephemeroptera) with implications on biogeography, systematics and biodiversity. Arthropod Systematics & Phylogeny 73(1): 3–18.

Gillies MT (1990) A revision of the African species of *Centroptilum* Eaton (Baetidae, Ephemeroptera). Aquatic Insects 12(2): 97–128. https://doi.org/10.1080/01650429009361395

Godunko RJ, Martynov AV, Gattolliat J-L (2018) Redescription of *Nigrobaetis rhithralis* (Soldán & Thomas, 1983) (Ephemeroptera: Baetidae). Zootaxa 4462: 041–072. https://doi.org/10.11646/zootaxa.4462.1.2

Hubbard MD (1995) Towards a standard methodology for the description of mayflies (Ephemeroptera). In: Corkum LD, Ciborowski JJH (Eds) Current directions in research on Ephemeroptera. Canadian Scholar's Press, Toronto, 361–369.

Hurvich CM, Tsai CL (1989) Regression and time series model selection in small samples. Biometrika 76(2): 297–307. https://doi.org/10.1093/biomet/76.2.297

Kaltenbach T, Gattolliat J-L (2020) *Labiobaetis* Novikova & Kluge in Borneo (Ephemeroptera, Baetidae). ZooKeys 914: 43–79. https://doi.org/10.3897/zookeys.914.47067

Kaltenbach T, Garces JM, Gattolliat J-L (2020) The success story of *Labiobaetis* Novikova & Kluge in the Philippines (Ephemeroptera, Baetidae), with description of 18 new species. ZooKeys 1002: 1–114. https://doi.org/10.3897/zookeys.1002.58017

Kapli P, Lutteropp S, Zhang J, Kobert K, Pavlidis P, Stamatakis A, Flouri T (2017) Multi-rate Poisson tree processes for single-locus species delimitation under maximum likelihood and Markov chain Monte Carlo. Bioinformatics 33(11): 1630–1638. https://doi.org/10.1093/bioinformatics/btx025

Katoh K, Rozewicki J, Yamada KD (2019) MAFFT online service: Multiple sequence alignment, interactive sequence choice and visualization. Briefings in Bioinformatics 20(4): 1160–1166. https://doi.org/10.1093/bib/bbx108

Kechemir LH, Sartori M, Lounaci A (2020) An unexpected new species of *Habrophlebia* from Algeria (Ephemeroptera, Leptophlebiidae). ZooKeys 953(2): 31–47. https://doi.org/10.3897/zookeys.953.51244

Khadri O, El Alami M, El Bazi R, Slimani M (2017) Ephemeroptera's diversity and ecology in streams of the ultramafic massif of Beni Bousera and in the adjacent non-ultramafic sites (NW, Morocco). Journal of Materials & Environmental Sciences 8: 3508–3523.

Kimura M (1980) A simple method for estimating evolutionary rate of base substitutions through comparative studies of nucleotide sequences. Journal of Molecular Evolution 16(2): 111–120. https://doi.org/10.1007/BF01731581

Kjærstad G, Webb JM, Ekrem T (2012) A review of the Ephemeroptera of Finnmark–DNA barcodes identify Holarctic relations. Norwegian Journal of Entomology 59(2): 182–195.

Kluge NJ (2004) The phylogenetic system of Ephemeroptera. Academic Publishers, Dordrecht, 1–442. https://doi.org/10.1007/978-94-007-0872-3

Kluge NJ (2012) Non-African representatives of the plesiomorphon Protopatellata (Ephemeroptera: Baetidae). Russian Entomological Journal 20(1): 361–376. https://doi.org/10.15298/rusentj.20.4.02

Kluge NJ (2016) Redescription of the genus *Cheleocloeon* Wuillot & Gillies, 1993 (Ephemeroptera: Baetidae) with descriptions of three new species from Zambia and Uganda. Zootaxa 4067(2): 135–167. https://doi.org/10.11646/zootaxa.4067.2.2

Kluge NJ (2022) Taxonomic significance of microlepides on subimaginal tarsi of Ephemeroptera. Zootaxa 5159(2): 151–186. https://doi.org/10.11646/zootaxa.5159.2.1

Kozlov AM, Darriba D, Flouri T, Morel B, Stamatakis A (2019) RAxML-NG: A fast, scalable and user-friendly tool for maximum likelihood phylogenetic inference. Bioinformatics 35(21): 4453–4455. https://doi.org/10.1093/bioinformatics/btz305

Kumar S, Stecher G, Li M, Knyaz C, Tamura K (2018) MEGA X: Molecular Evolutionary Genetics Analysis across computing platforms. Molecular Biology and Evolution 35(6): 1547–1549. https://doi.org/10.1093/molbev/msy096

Letunic I, Bork P (2021) Interactive Tree Of Life (iTOL) v. 5: An online tool for phylogenetic tree display and annotation. Nucleic Acids Research 49(W1): W293–W296. https://doi.org/10.1093/nar/gkab301

Lugo-Ortiz CR, McCafferty WP (1997) Contribution to the systematics of the genus *Cheleocloeon* (Ephemeroptera: Baetidae). Entomological News 108(4): 283–289.

Lugo-Ortiz CR, McCafferty WP (1998) The *Centroptiloides* complex of Afrotropical small minnow mayflies (Ephemeroptera: Baetidae). Annals of the Entomological Society of America 91(1): 1–26. https://doi.org/10.1093/aesa/91.1.1

Mabrouki Y, Taybi AF, El Alami M, Berrahou A (2017) New and interesting data on distribution and ecology of Mayflies from Eastern Morocco (Ephemeroptera). Journal of Materials & Environmental Sciences 8: 2839–2859.

Martynov AV, Palatov DM, Gattolliat J-L, Bojková J, Godunko RJ (2022) Remarkable finding of *Centroptilum* Eaton, 1869 (Ephemeroptera: Baetidae) in Georgia, Turkey and Iran: one new species evidenced by morphology and DNA. The European Zoological Journal 89(1): 827–855. https://doi.org/10.1080/24750263.2022.2090625

Monaghan MT, Wild R, Elliot M, Fujisawa T, Balke M, Inward DJ, Vogler AP (2009) Accelerated species inventory on Madagascar using coalescent-based models of species delineation. Systematic Biology 58(3): 298–311. https://doi.org/10.1093/sysbio/syp027

Pons J, Barraclough TG, Gomez-Zurita J, Cardoso A, Daniel PD, Hazell S, Kamoun S, William DS, Vogler AP (2006) Sequence-Based Species Delimitation for the DNA Taxonomy of Undescribed Insects. Systematic Biology 55(4): 595–609. https://doi.org/10.1080/10635150600852011

Puillandre N, Lambert A, Brouillet S, Achaz G (2012) ABGD, Automatic Barcode Gap Discovery 643 for primary species delimitation. Molecular Ecology 21(8): 1864–1877. https://doi.org/10.1111/j.1365-294X.2011.05239.x

Puillandre N, Brouillet S, Achaz G (2020) ASAP: Assemble species by automatic partitioning. Molecular Ecology Resources 21(2): 609–620. https://doi.org/10.1111/1755-0998.13281

R Core Team (2022) R: A language and environment for statistical computing. R Foundation for Statistical Computing, Vienna, Austria. https://www.R-project.org/

Rambaut A, Drummond AJ, Xie D, Baele G, Suchard MA (2018) Posterior summarization in Bayesian phylogenetics using Tracer 1.7. Systematic Biology 67(5): 901–904. https://doi.org/10.1093/sysbio/syy032

Ronquist F, Teslenko M, Van Der Mark P, Ayres DL, Darling A, Höhna S, Larget B, Liu L, Suchard MA, Huelsenbeck JP (2012) MrBayes 3.2: Efficient Bayesian phylogenetic inference and model choice across a large model space. Systematic Biology 61(3): 539–542. https://doi.org/10.1093/sysbio/sys029

Samraoui B, Bouhala Z, Chakri K, Márquez-Rodríguez J, Ferreras-Romero M, El-Serehy HA, Samraoui F, Sartori M, Gattolliat J-L (2021a) Environmental determinants of mayfly assemblages in the Seybouse River, north-eastern Algeria (Insecta: Ephemeroptera). Biologia 76(8): 2277–2289. https://doi.org/10.1007/s11756-021-00726-9

Samraoui B, Márquez-Rodríguez J, Ferreras-Romero M, El-Serehy HA, Samraoui F, Sartori M, Gattolliat J-L (2021b) Biogeography, ecology, and conservation of mayfly communities of relict mountain streams, north-eastern Algeria (Insecta: Ephemeroptera). Aquatic Conservation 31(12): 3357–3369. https://doi.org/10.1002/aqc.3719

Samraoui B, Vinçon G, Marquez-Rodriguez J, El-Serehy HA, Ferreras-Romero M, Mostefai N, Samraoui F (2021c) Stonefly assemblages as indicators of relict North African mountain streams (Plecoptera). Wetlands 41(6): 78. https://doi.org/10.1007/s13157-021-01477-8

Sanger F, Nicklen S, Coulson AR (1977) DNA sequencing with chain-terminating inhibitors. Proceedings of the National Academy of Sciences of the United States of America 74(12): 5463–5467. https://doi.org/10.1073/pnas.74.12.5463

Shorthouse DP (2010) SimpleMappr, an online tool to produce publication-quality point maps. https://www.simplemappr.net [Accessed June 2022]

Soldán T, Godunko R, Thomas A (2005) *Baetis chelif* n. sp., a new mayfly from Algeria with notes on *B. sinespinosus* Soldán & Thomas, 1983, n. stat. (Ephemeroptera: Baetidae). Genus 16: 155–165.

Stecher G, Tamura K, Kumar S (2020) Molecular Evolutionary Genetics Analysis (MEGA) for macOS. Molecular Biology and Evolution 37(4): 1237–1239. https://doi.org/10.1093/molbev/msz312

Suchard MA, Lemey P, Baele G, Ayres DL, Drummond AJ, Rambaut A (2018) Bayesian phylogenetic and phylodynamic data integration using BEAST 1.10. Virus Evolution 4(1): vey016. https://doi.org/10.1093/ve/vey016

Talavera G, Dincă V, Vila R (2013) Factors affecting species delimitations with the GMYC model: Insights from a butterfly survey. Methods in Ecology and Evolution 4(12): 1101–1110. https://doi.org/10.1111/2041-210X.12107

Thomas AGB (1998) A provisional checklist of the mayflies of North Africa (Ephemeroptera). Bulletin de la Société d`Histoire Naturelle 134: 13–20.

Vuataz L, Sartori M, Wagner A, Monaghan MT (2011) Toward a DNA taxonomy of Alpine *Rhithrogena* (Ephemeroptera: Heptagenidae) using a mixed Yule-Coalescent Analysis of mitochondrial and nuclear DNA. PLoS ONE 6(5): 1–11. https://doi.org/10.1371/journal.pone.0019728

Waterhouse AM, Procter JB, Martin DMA, Clamp M, Barton GJ (2009) Jalview Version 2-a multiple sequence alignment editor and analysis workbench. Bioinformatics 25(9): 1189–1191. https://doi.org/10.1093/bioinformatics/btp033

Zerrouk M, Dakki M, Bennas N, El Agbani MA, El Alami M, Ghamizi M, L'Mohdi O, Qninba A, Himmi O (2021) Nouvelles données sur les macroinvertébrés du Bassin versant du Haut Sebou (Moyen Atlas, Maroc): Insectes, Mollusques et Crustacés. Boletin de la SEA 69: 29–44.

Zhang J, Kapli P, Pavlidis P, Stamatakis A (2013) A general species delimitation method with applications to phylogenetic placements. Bioinformatics 29(22): 2869–2876. https://doi.org/10.1093/bioinformatics/btt499

Zrelli S, Boumaiza M, Bejaoui M, Gattolliat J-L, Sartori M (2011) New reports of mayflies (Insecta: Ephemeroptera) from Tunisia. Revue Suisse de Zoologie 118: 3–10.

Zrelli S, Gattolliat J-L, Boumaïza M, Thomas A (2012) First record of *Alainites sadati* Thomas, 1994 (Ephemeroptera: Baetidae) in Tunisia, description of the larval stage and ecology. Zootaxa 3497(1): 60. https://doi.org/10.11646/zootaxa.3497.1.6

Zrelli S, Boumaiza M, Bejaoui M, Gattolliat J-L, Sartori M (2016) New data and revision of the Ephemeroptera of Tunisia. Inland Water Biology 3: 99–106.

ZooKeys 1131: 99–134 (2022)
doi: 10.3897/zookeys.1131.95038
https://zookeys.pensoft.net

RESEARCH ARTICLE

A peer-reviewed open-access journal
ZooKeys
Launched to accelerate biodiversity research

Review of Chinese species of the genus *Thoracostrongylus* Bernhauer, 1915 (Coleoptera, Staphylinidae, Staphylininae)

Mei-Hua Xia[1], Liang Tang[1], Harald Schillhammer[2]

1 *College of Life Sciences, Shanghai Normal University, 100 Guilin Road, 1st Educational Building 423 – A Room, Shanghai, 200234, China* **2** *Naturhistorisches Museum Wien, Burgring 7, A – 1010 Wien, Austria*

Corresponding author: Liang Tang (staphylinidae@shnu.edu.cn)

Academic editor: Jan Klimaszewski | Received 18 September 2022 | Accepted 3 November 2022 | Published 22 November 2022

https://zoobank.org/EE89E8CF-4B76-4FBC-821A-79BC51D28D67

Citation: Xia M-H, Tang L, Schillhammer H (2022) Review of Chinese species of the genus *Thoracostrongylus* Bernhauer, 1915 (Coleoptera, Staphylinidae, Staphylininae). ZooKeys 1131: 99–134. https://doi.org/10.3897/zookeys.1131.95038

Abstract

Species of the genus *Thoracostrongylus* Bernhauer, 1915 occurring in China are reviewed. Four new species and one new subspecies are described: *T. baishanzuensis* **sp. nov.** (Zhejiang), *T. bicolor* **sp. nov.** (Guangdong, Guangxi, Hunan, Yunnan), *T. brachypterus* **sp. nov.** (Sichuan), *T. chrysites* **sp. nov.** (Fujian), and *T. formosanus flavipes* **ssp. nov**. (Zhejiang, Fujian, Hubei, Hunan, Sichuan, Guangxi, Guangdong, Anhui, Jiangxi). A new synonymy is proposed: *T. baoxingensis* Yang, Zhou & Schillhammer, 2011 **syn. nov.** is in fact *T. acerosus* Yang, Zhou & Schillhammer, 2011. New provincial records for *T. acerosus* Yang, Zhou & Schillhammer, 2011 are reported. A key to Chinese species of the genus is provided.

Keywords

Identification key, new records, new species, rove beetle, *Thoracostrongylus*

Introduction

Thoracostrongylus Bernhauer, 1915 is a genus strictly distributed in east and southeast Asia. It was originally established as a subgenus of *Ontholestes* Ganglbauer, 1895, and later regarded as a separate genus (Blackwelder 1952). *Thoracostrongylus* can be readily distinguished from *Ontholestes* by the obtuse anterior angles of the pronotum (Smetana and Davies 2000), from *Lesonthotes* by the sparse, simple punctation of the forebody, and the sharply defined temples of the head (Brunke and Smetana 2019). Most species of *Thoracostrongylus* from China are very similar to each other in appearance. Recognition of some species is further complicated by the fact that the coloration is subject to a certain degree of variability. Dissection of male specimens should therefore be mandatory for identification of similar species. Additionally, the shape of the apex of the median lobe and paramere, which would normally be regarded as reliable characters for distinguishing species in related groups, is also variable in some species. Therefore, descriptions of new species in this genus should be based on very careful examination.

At present, sixteen species of the genus have been described worldwide, eleven of them recorded from China: *T. acerosus* Yang, Zhou & Schillhammer, 2011 from Hubei and Sichuan; *T. aduncatus* Yang, Zhou & Schillhammer, 2011 from Yunnan; *T. baoxingensis* Yang, Zhou & Schillhammer, 2011 from Sichuan; *T. birmanus* (Fauvel, 1895) from Hainan and Yunnan; *T. diaoluoensis* Yang, Zhou & Schillhammer, 2011 from Hainan; *T. formosanus* Shibata, 1982 from Zhejiang, Fujian, Hubei, Hunan, Sichuan and Taiwan; *T. fujianensis* Yang, Zhou & Schillhammer, 2011 from Fujian; *T. malaisei* Scheerpeltz, 1965 from Yunnan; *T. miyakei* Bernhauer, 1943 from Sichuan and Taiwan; *T. sarawakensis* (Bernhauer, 1915) from Hainan; and *T. velutinus* Scheerpeltz, 1965 from Yunnan. *Thoracostrongylus baoxingensis* Yang, Zhou & Schillhammer, 2011 syn. nov. is here synonymized with *T. acerosus* Yang, Zhou & Schillhammer, 2011. The records of *T*. *formosanus* from mainland China, however, have turned out to be a distinct subspecies. Thus, including four new species described herein, the total number of *Thoracostrongylus* species is increased to 20 and the number of Chinese species is increased to 14 plus one subspecies.

Materials and methods

The specimens examined in this paper were collected by sifting leaf litter, and by flight intercept traps and pitfall traps. They were subsequently killed with ethyl acetate. For examination of the genitalia, the last three abdominal segments were detached from the body after relaxing in hot water. The aedeagus together with other dissected pieces, were mounted in Euparal (Chroma Gesellschaft Schmidt, Koengen, Germany) on plastic slides beneath the card-mounted specimens. Photographs of sexual characters were taken with a Canon G9 camera attached to an Olympus SZX 16 stereoscope; habitus photographs were taken with a Canon macro lens MP-E 65 mm attached to a Canon EOS 7D camera and stacked with Zerene Stacker (http://www.zerenesystems.com/cms/stacker).

The specimens treated in this study are deposited in the following public and private collections:

ASC Aleš Smetana Collection, the National Museum of Nature and Science, Toshiba, Japan;
BFC Collection of Benedikt Feldmann, Münster, Germany;

IZCAS Institute of Zoology, Chinese Academy of Sciences, Beijing, P. R. China;
MSC Michael Schülke Collection, in Museum für Naturkunde, Berlin, Germany;
NMW Naturhistorisches Museum Wien, Austria;
SHNU Department of Biology, Shanghai Normal University, P. R. China;
VAC Volker Assing Collection, Hannover, Germany† (will be deposited in Zoologisches Museum, Berlin).

Body measurements are abbreviated as follows:

BL body length, measured from the anterior margin of the clypeus to the posterior margin of abdominal tergite X;
CL length of eye;
EL length of elytra, measured from humeral angle;
EW width of elytra at the widest point;
FL forebody length, measured from the anterior margin of the clypeus to the apex of the elytra (apicolateral angle);
HL length of head along the midline;
HW width of head including eyes;
PL length of pronotum along the midline;
PO length of post-ocular region;
PW width of pronotum at the widest point.

Taxonomic account

Thoracostrongylus acerosus Yang, Zhou & Schillhammer, 2011

Figs 1–14, 108
刺茎钝胸隐翅虫

Thoracostrongylus acerosus Yang, Zhou & Schillhammer, 2011: 410.
Thoracostrongylus baoxingensis Yang, Zhou & Schillhammer, 2011: 415. syn. nov.

Material examined. China – **Sichuan Prov.** • 2♂♂, 1♀; Baoxing County, Fengtongzhai; 30°32'10"N, 102°54'20"E; alt. 1490 m; 22 July 2015; Jiang, Peng, Tu & Zhou leg.; SHNU • 1♂, 1♀; Baoxing County, Fengtongzhai N.R., Dengchigou; 30°32'N, 102°56'E; alt. 1870 m; 01 August 2016; Zhou, Jiang, Liu & Gao leg.; SHNU • 1♀; Baoxing County, Fengtongzhai N.R., Dengchigou; 30°29'N, 102°51'E; alt. 1692 m; 02 August 2016; Zhou, Jiang, Liu & Gao leg.; SHNU • 2♀♀; Tianquan County, Liangluxiang Village; 29°56'N, 102°23'E; alt. 1500–1700 m; 10 July 2012; Peng, Dai & Yin leg.; SHNU • 1♀; Tianquan County, Liangluxiang; 29°56'N, 102°23'E; alt. 1900–2000 m; Peng, Dai & Yin leg.; SHNU • 5♀♀; Tianquan County, Lianglu County; alt. 1400 m; 01 August 2011; Hao Huang leg.; SHNU • 2♂♂, 1♀; Dayi County, Xiling Snow Mt.; 30°38'6.25"N, 103°10'99.08"E;

alt. 1250 m; 31 July 2021; Zhao & Cai leg.; SHNU. – **Shaanxi Prov.** • 1♀; Hanzhong, Tiantaishan; 33°16'20"N, 107°04'52"E; alt. 1326 m; 08 May 2021; Juan Li et al. leg.; SHNU • 2♀♀; Liuba, Huoshaodian; 33°30'08"N, 106°56'08"E; alt. 1041 m; 08 July 2021; Juan Li et al. leg.; SHNU • 2♀♀; Zhouzhi Coun., Houzhenzi, Qinling, west Sangongli Gou; 33°50'6.13"N, 107°48'52.4"E; alt. 1336 m; 17–19 May 2008; Huang & Xu leg.; SHNU • 1♀; Zhouzhi Coun., Houzhenzi, Qinling; 33°51'20.3"N, 107°50'18.3"E; alt. 1260 m; 05–10 May 2008; Huang & Xu leg.; SHNU • 1♂; Baoji City, Jiulongdong; 34°19'56"N, 106°52'22"E; alt. 986 m; 26 May 2021; Juan Li et al. leg.; SHNU • 1♀; Baoji City, Jiulongdong; 34°19'59"N, 106°52'21"E; alt. 975 m; 05 August 2021; Juan Li et al. leg.; SHNU • 1♀; Baoji City, Jiulongdong; 34°20'10"N, 106°51'51"E; alt. 969 m; 05 August 2021; Juan Li et al. leg.; SHNU • 1♂; Liuba, Zhangliang Temple; 33°41'51"N, 106°47'15"E; alt. 1476 m; 11 July 2021; Juan Li et al. leg.; SHNU • 1♀; Lueyang, Wulongdong; 33°31'16"N, 106°16'22"E; alt. 1107 m; 20 July 2021; Juan Li et al. leg.; SHNU • 1♀; Lueyang, Wulongdong; 33°30'51"N, 106°15'04"E; alt. 1237 m; 20 July 2021; Juan Li et al. leg.; SHNU • 2♂♂; Ankang City, Ningshan, Guanghuojie Town; 33°45'81"N, 108°46'48"E; alt. 1176 m; 07–08 May 2011; Bao-Xiang Zhan leg.; SHNU. – **Gansu Prov.** • 1♂; Hui County, Gaoqiaolinchang; 34°05'44"N, 105°57'42"E; alt. 1305 m; 18 May 2021; Juan Li et al. leg.; SHNU • 1♀; Hui County, Yanpinglinchang; 33°40'36"N, 106°16'51"E; alt. 1483 m; 18 July 2021; Juan Li et al. leg.; SHNU. – **Henan Prov.** • 1♂; Funiu Shan, Baotianman; alt. 1500–1700 m; 33°31'N, 111°56'E; 15 June 2009; J. Turna leg.; NMW.

Measurements. Male: BL: 8.2–9.7 mm, FL: 4.5–5.2 mm. HL: 1.28–1.45 mm, HW: 1.78–1.95 mm, CL: 0.89–0.95 mm, PO: 0.22–0.28 mm, PL: 1.61–1.78 mm, PW: 1.45–1.50 mm, EL: 1.95–2.11 mm, EW: 1.95–2.11 mm. HL/HW: 0.70–0.78, CL/PO: 3.20–4.00, PL/PW: 1.12–1.23, EL/EW: 0.95–1.00, HW/EW: 0.87–0.94, PW/EW: 0.68–0.74, HW/PW: 1.23–1.31. **Female:** BL: 9.2–10.4 mm, FL: 4.8–5.3 mm. HL: 1.39–1.50 mm, HW: 2.00–2.17 mm, CL: 0.89–1.06 mm, PO: 0.22–0.28 mm, PL: 1.72–1.95 mm, PW: 1.50–1.72 mm, EL: 2.00–2.50 mm, EW: 2.11–2.50 mm. HL/HW: 0.68–0.72, CL/PO: 3.60–4.00, PL/PW: 1.00–1.19, EL/EW: 0.95–1.00, HW/EW: 0.84–0.95, PW/EW: 0.69–0.71, HW/PW: 1.23–1.33.

Distribution. China (Hubei, Sichuan, Shaanxi, Gansu, Henan). New to Shaanxi, Gansu, and Henan.

Diagnosis. In general appearance, *T. acerosus* is similar to *T. aduncatus* Yang, Zhou & Schillhammer, 2011, *T. fujianensis* Yang, Zhou & Schillhammer, 2011, and *T. diaoluoensis* Yang, Zhou & Schillhammer, 2011, but it can be recognized by the sharply pointed tip of aedeagal median lobe.

Remarks. The apical portion of the median lobe and the paramere are subject to some variability (Figs 3–14). This may be observed not only in populations from different localities but also within one population. A closer inspection of the types of *T. baoxingensis* and *T. acerosus* revealed that this is the case here as well and that both species are conspecific.

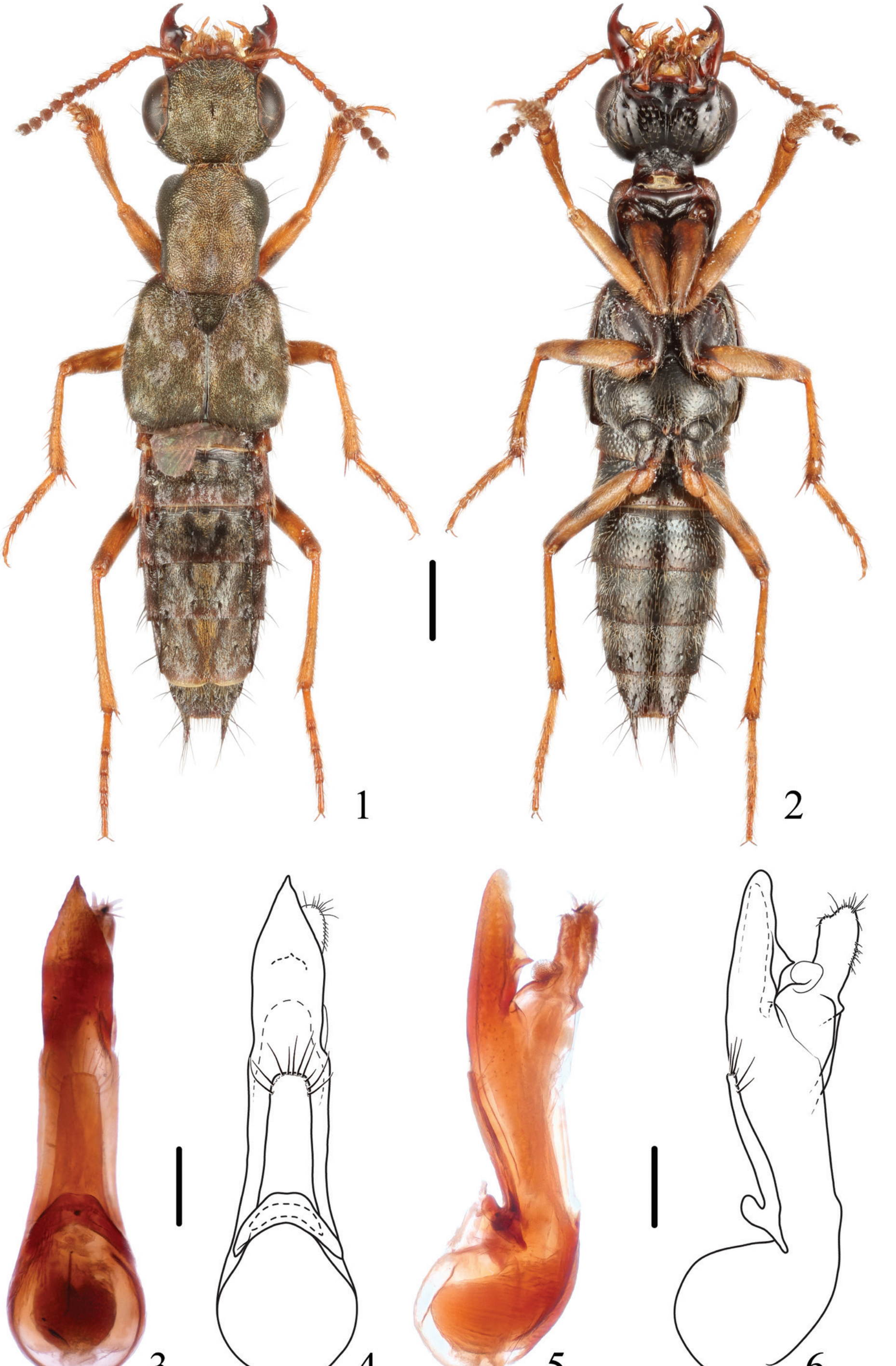

Figures 1–6. *Thoracostrongylus acerosus* **1, 2** habitus **3–6** aedeagus, ventral (**3, 4**) and lateral (**5, 6**) views. Scale bars: 1 mm (**1, 2**); 0.2 mm (**3–6**).

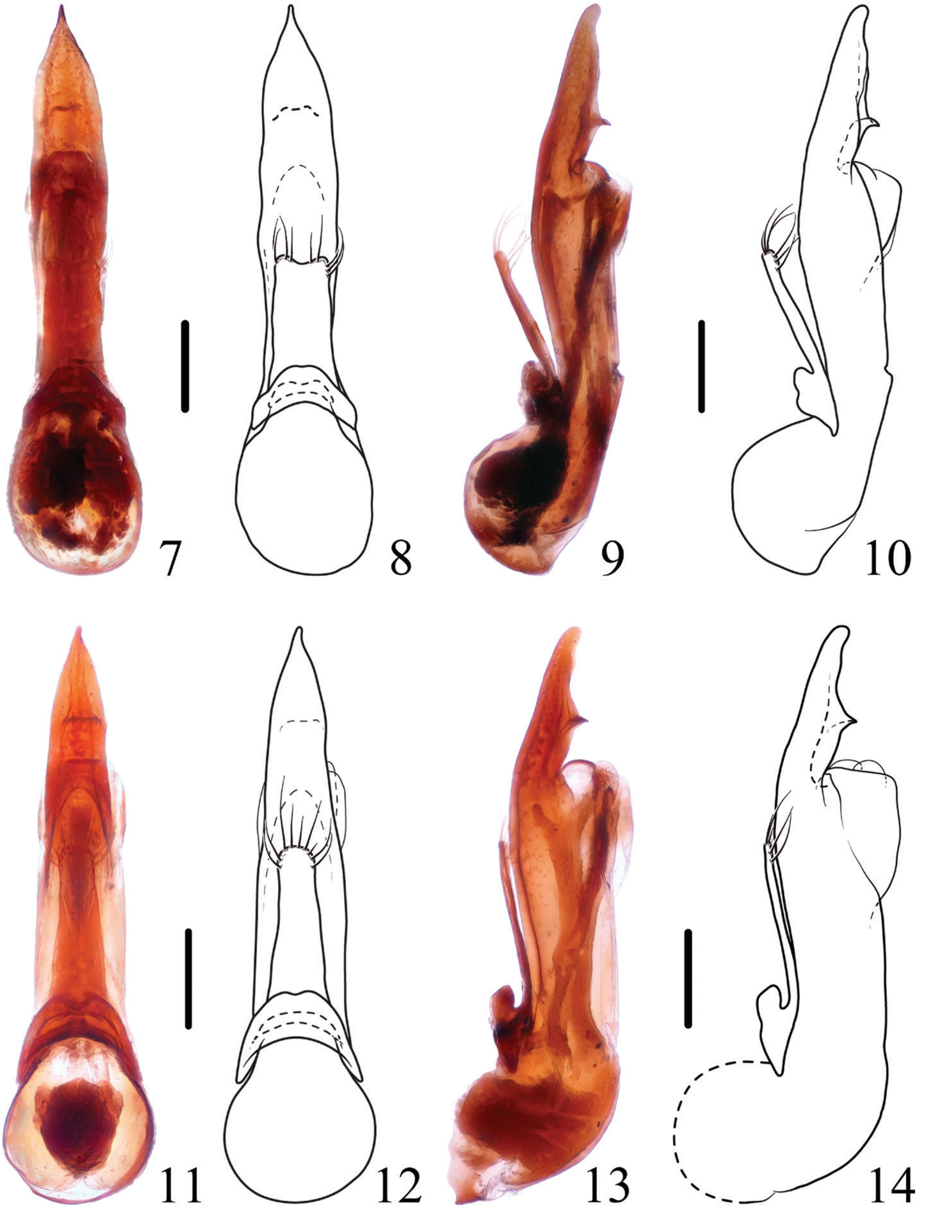

Figures 7–14. *Thoracostrongylus acerosus* **7–10** aedeagus from Xiling Snow Mountain, ventral (**7, 8**) and lateral (**9, 10**) views **11–14** aedeagus from Jiulongdong, ventral (**11, 12**) and lateral (**13, 14**) views. Scale bars: 0.2 mm.

Thoracostrongylus aduncatus Yang, Zhou & Schillhammer, 2011

Figs 15–32, 109
钩茎钝胸隐翅虫

Thoracostrongylus aduncatus Yang, Zhou & Schillhammer, 2011: 413.

Material examined. China – **Yunnan Prov.** • 1♂; Xishuangbanna, Menglong Town, Mengsong; 20°30'41"N, 100°30'19"E; alt. 1700 m; 03 April 2018; Peng, Shen & Cheng leg.; SHNU • 1♂; Nabanhe N.R., Chuguohe, Bengganghani; alt. 1750 m; 28 April 2009; Hu & Yin leg.; SHNU • 1♂; Nabanhe N.R., Bengganghani, Nanmugaha; alt. 1650 m; 30 April 2009; Hu & Yin leg.; SHNU • 1♂, 1♀; Nabanhe N.R., Shanshenmiao, Bengganghani; alt. 1700 m; 27 April 2009; Hu & Yin leg.; SHNU • 2♀♀; Nabanhe N.R., Bengganghani; alt. 1750 m; 03 May 2009; Hu & Yin leg.; SHNU • 4♂♂, 1♀; Baoshan City, Mangkuan Town, Baihualing; 25°18'11"N, 98°47'38"E; alt. 1900 m; 21 April 2013; Dai, Peng & Song leg.; SHNU.

Measurements. Male: BL: 7.0–8.3 mm, FL: 4.2–5.1 mm. HL: 1.17–1.39 mm, HW: 1.61–1.89 mm, CL: 0.83–0.95 mm, PO: 0.17–0.28 mm, PL: 1.50–1.78 mm, PW: 1.22–1.50 mm, EL: 1.78–2.11 mm, EW: 1.78–2.11 mm. HL/HW: 0.70–0.77, CL/PO: 3.00–5.00, PL/PW: 1.12–1.27, EL/EW: 0.97–1.00, HW/EW: 0.84–0.91, PW/EW: 0.66–0.71, HW/PW: 1.24–1.32. **Female:** BL: 8.0–9.6 mm, FL: 4.8–5.3 mm. HL: 1.33–1.50 mm, HW: 1.83–2.06 mm, CL: 0.95–1.00 mm, PO: 0.22–0.28 mm, PL: 1.72–1.83 mm, PW: 1.39–1.56 mm, EL: 2.00–2.11 mm, EW: 2.11–2.22 mm. HL/HW: 0.73, CL/PO: 3.60–4.25, PL/PW: 1.18–1.24, EL/EW: 0.95, HW/EW: 0.87–0.93, PW/EW: 0.66–0.70, HW/PW: 1.32.

Diagnosis. The species is similar to *T. acerosus* Yang, Zhou & Schillhammer, 2011, *T. fujianensis* Yang, Zhou & Schillhammer, 2011, and *T. diaoluoensis* Yang, Zhou & Schillhammer, 2011 in general appearance, but it can be distinguished from them by the apex of median lobe pointed dorsad forming an apical tooth in lateral view, and from *T. diaoluoensis* also by the aedeagal median lobe with a subapical tooth on the dorsal side. Aedeagal variation (Figs 17–32) occurs in the apical parts of median lobe and paramere.

Distribution. China (Yunnan).

***Thoracostrongylus birmanus* (Fauvel, 1895)**

Figs 33–39, 110

缅甸钝胸隐翅虫

Leistotrophus birmanus Fauvel, 1895: 246.
Ontholestes birmanus: Bernhauer & Schubert, 1914: 392.
Thoracostrongylus birmanus: Cameron, 1932: 214; Yang et al. 2011: 422.

Material examined. China – **Yunnan Prov.** • 1♂; Xishuangbanna, Nabanhe N.R.; 18 June 2009; Ling-Zeng Meng leg.; SHNU • 1♂; Nabanhe N.R., Manfei; 22°09'30.5"N, 100°41'29.1"E; alt. 620 m; 18 November 2008; Hu & Tang leg.; SHNU • 1♂, 1♀; Nabanhe Conv., Manfei; 10 January 2004; Li & Tang leg.; SHNU • 1♂, 1♀; Nabanhe Conv., Manfei; 09 January 2004; Li & Tang leg.; SHNU • 1♀; Mengla County, Menglun Town; alt. 550 m; 26 April 2014; Jian-Yue Qiu leg.; SHNU • 2♂♂; Baoshan City, Baihualing; 25°17'39"N, 98°48'09"E; alt. 1350–1450 m; 19 April 2013; Song, Peng & Dai leg.; SHNU • 1♂, 1♀; Xishuangbanna, Jinghong City; 22°02'19"N, 100°55'23"E; alt. 1000–1080 m; 29 November 2016; Jiang, Liu, Huang & Liu leg.; SHNU • 1♂; Lincang, Shuibatou Village; 24°38'16"N, 100°29'17"E; alt. 1281 m; 20 June 2019; Zi-Chun Xiong leg.; SHNU

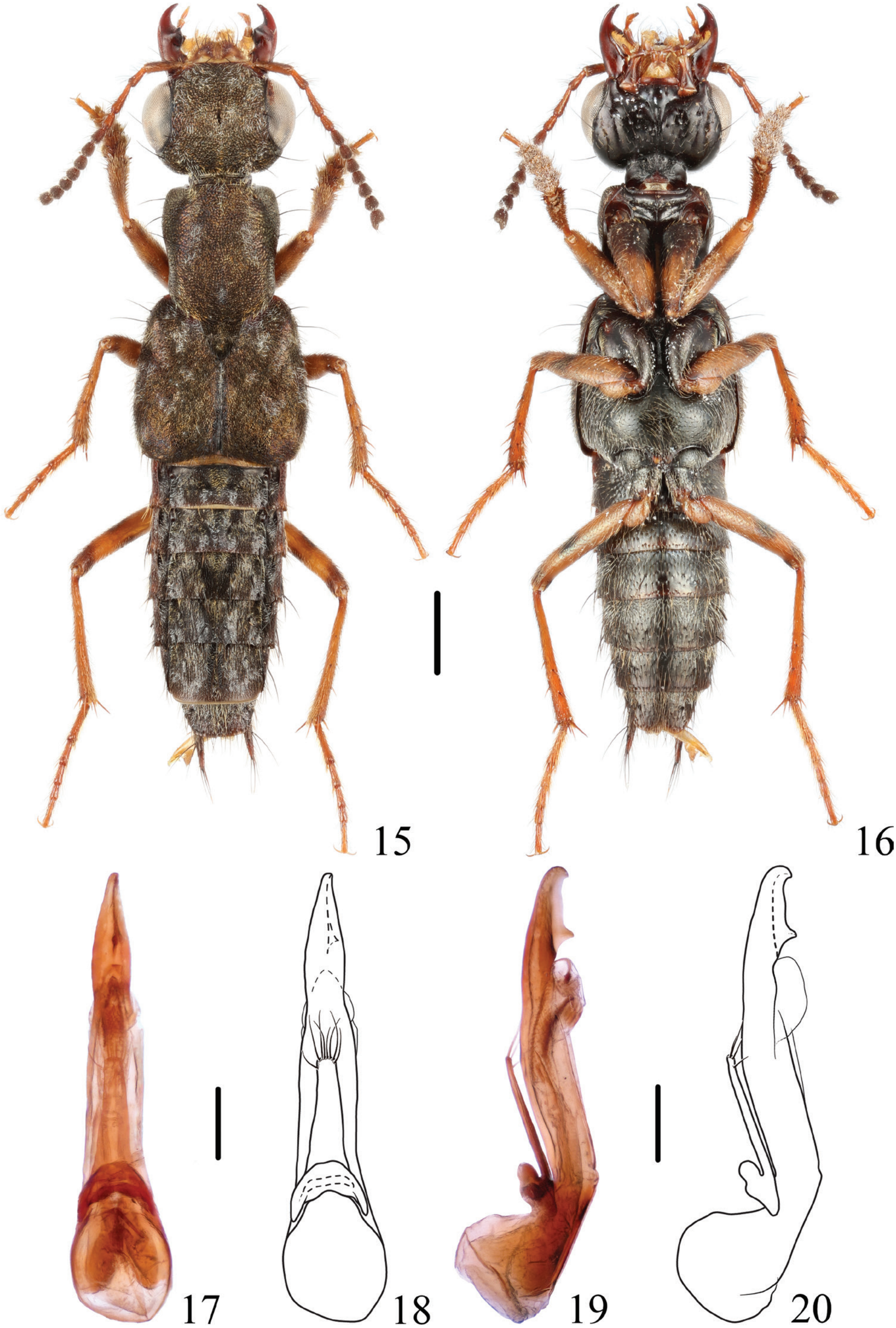

Figures 15–20. *Thoracostrongylus aduncatus* **15, 16** habitus **17–20** aedeagus, ventral (**17, 18**) and lateral (**19, 20**) views. Scale bars: 1 mm (**15, 16**); 0.2 mm (**17–20**).

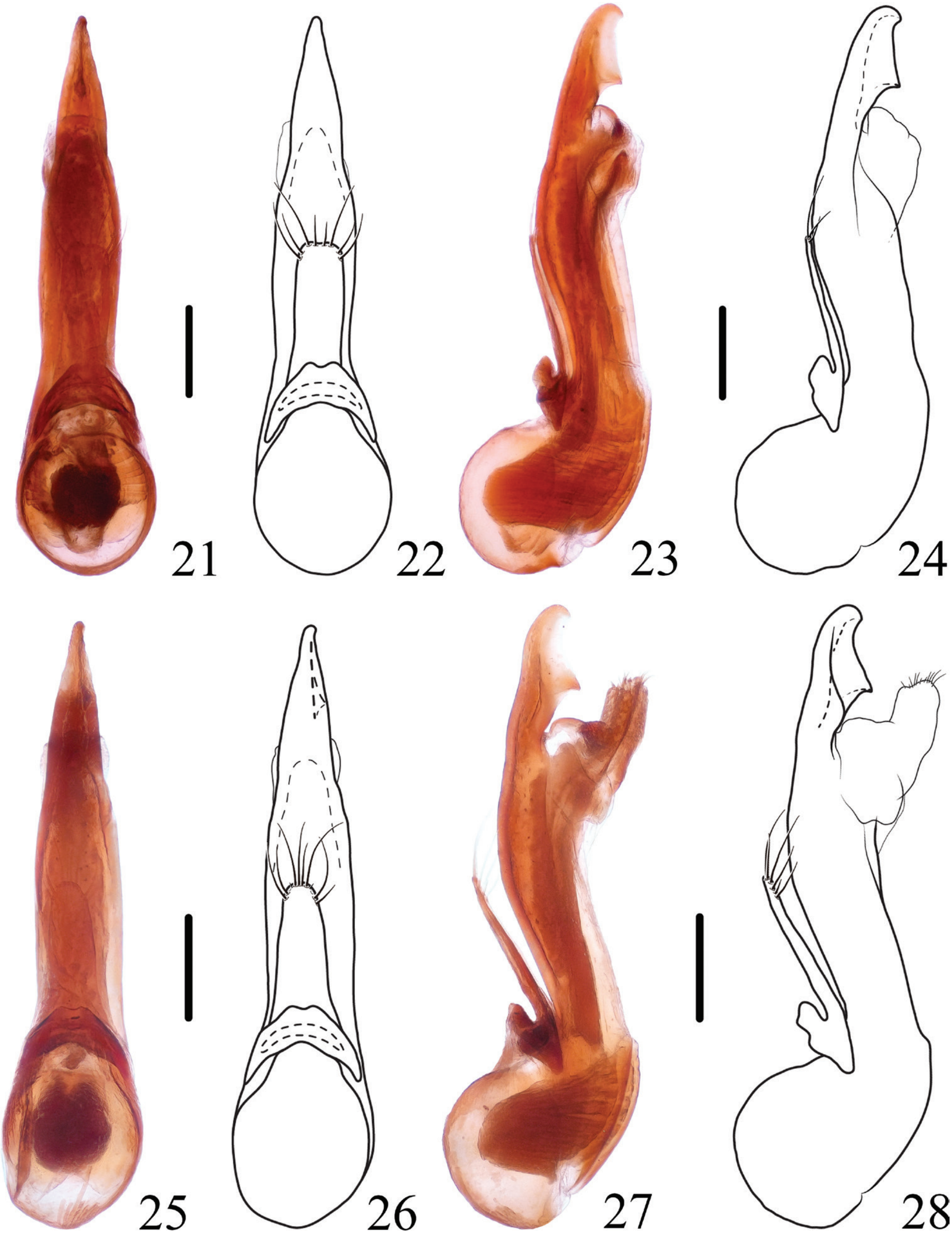

Figures 21–28. *Thoracostrongylus aduncatus* **21–24** aedeagus from Baihualing, ventral (**21, 22**) and lateral (**23, 24**) views **25–28** aedeagus from Baihualing, ventral (**25, 26**) and lateral (**27, 28**) views. Scale bars: 0.2 mm.

• 1♀; Baoshan, Longyang baihualing; 25°20'35"N, 98°49'01"E; alt. 1400–1900 m; 20–23 June 2020; Lu Qiu leg.; SHNU. – **Hainan Prov.** • 2♂♂, 2♀♀; Ledong County, Jianfengling, Mingfenggu; 18°44'43"N, 108°50'20"E; alt. 956–1048 m; 20–21 April 2018;

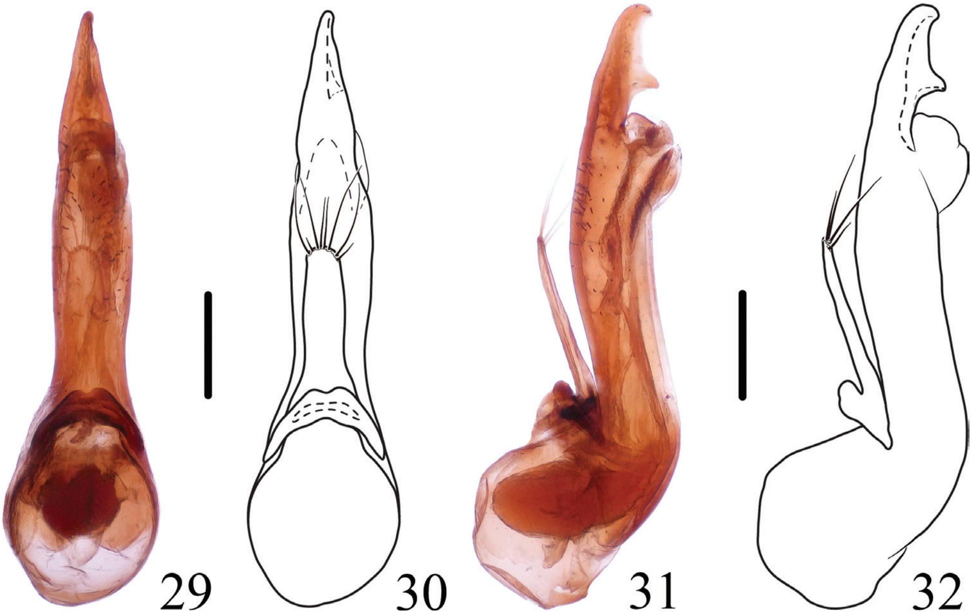

Figures 29–32. *Thoracostrongylus aduncatus* **29–32** aedeagus from Nabanhe, ventral (**29, 30**) and lateral (**31, 32**) views. Scale bars: 0.2 mm.

Ri-Xin Jiang leg.; SHNU • 1♂, 1♀; Wuzhishan City, Mt. Wuzhishan; 18°54'N, 109°41'E; alt. 650–700 m; 20 April 2012; Peng & Dai leg.; SHNU • 1♂; Ledong County, Jianfengling; alt. 950 m; 15 April 2010; Jian-Qing Zhu leg.; SHNU • 2♀♀; Ledong County, Jianfengling N.R.; alt. 910 m; 15 April 2010; Ting Feng leg.; SHNU • 1♂; Wuzhishan Mt., Guanshandian; 18°53'N, 109°41'E; alt. 650 m; 19 April 2012; Pan & Li leg.; SHNU • 1♀; Changjiang County, Bawangling; alt. 1000 m; 14 November 2006; Li-Zhen Li leg.; SHNU • 1♀; Baoshan County, Maoganxiang; 14 April 2015; Lu Qiu leg.; SHNU • 1♀; Qiongzhong County, Limu Mt., N.R.; 19°10'04"N, 109°44'45"E; alt. 625 m; 29 January 2015; Peng, Yin, Tu, Song, Shen, Zhou, Yan & Wang leg.; SHNU.

Measurements. Male: BL: 6.8–9.1 mm, FL: 4.4–5.2 mm. HL: 1.33–1.50 mm, HW: 1.78–2.06 mm, CL: 0.89–1.00 mm, PO: 0.28 mm, PL: 1.56–1.78 mm, PW: 1.39–1.61 mm, EL: 1.83–2.17 mm, EW: 1.95–2.22 mm. HL/HW: 0.70–0.75, CL/PO: 3.20–3.60, PL/PW: 1.10–1.19, EL/EW: 0.92–0.98, HW/EW: 0.90–0.93, PW/EW: 0.68–0.74, HW/PW: 1.24–1.37. **Female:** BL: 7.5–10.8 mm, FL: 4.8–5.8 mm. HL: 1.39–1.67 mm, HW: 1.89–2.22 mm, CL: 0.95–1.11 mm, PO: 0.22–0.28 mm, PL: 1.72–2.00 mm, PW: 1.50–1.67 mm, EL: 1.95–2.39 mm, EW: 2.11–2.45 mm. HL/HW: 0.72–0.75, CL/PO: 3.40–4.50, PL/PW: 1.15–1.21, EL/EW: 0.92–0.98, HW/EW: 0.84–0.91, PW/EW: 0.66–0.71, HW/PW: 1.24–1.33.

Diagnosis. The species may be easily recognized by the combination of following characters: abdominal sternites with longer and denser pubescence, male sternite VIII (Fig. 39) with deep medio-apical emargination, and male sternite VII slightly emarginate medio-apically.

Distribution. China (Yunnan, Hainan), India, and Myanmar.

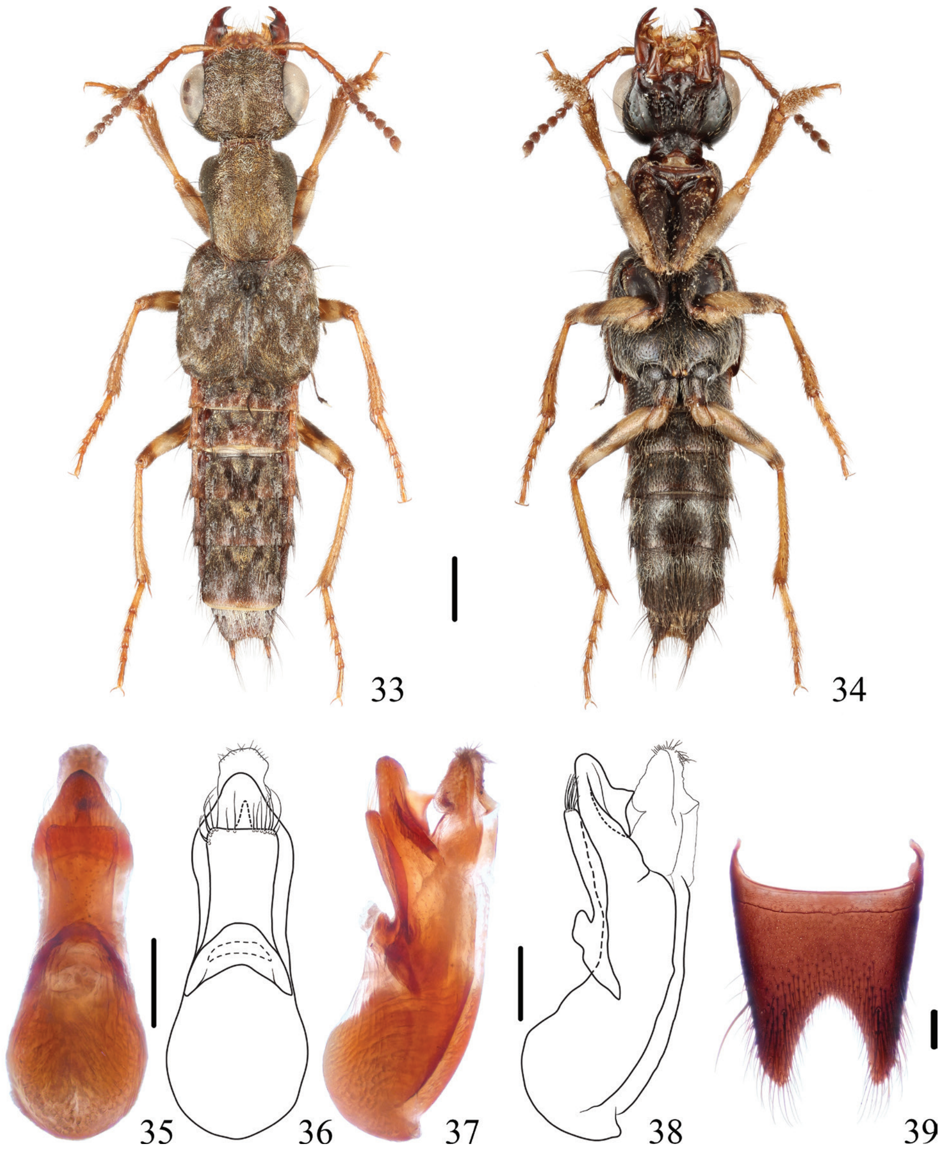

Figures 33–39. *Thoracostrongylus birmanus* **33, 34** habitus **35–38** aedeagus, ventral (**35, 36**) and lateral (**37, 38**) views **39** male abdominal sternite VIII. Scale bars: 1 mm (**33, 34**); 0.2 mm (**35–39**).

Thoracostrongylus diaoluoensis Yang, Zhou & Schillhammer, 2011

Figs 40–45, 111

吊罗钝胸隐翅虫

Thoracostrongylus diaoluoensis Yang, Zhou & Schillhammer, 2011: 418.

Material examined. China – **Hainan Prov.** • 1♂; Changjiang County, Bawangling; alt. 1000 m; 14 November 2006; Li-Zhen Li leg.; SHNU.

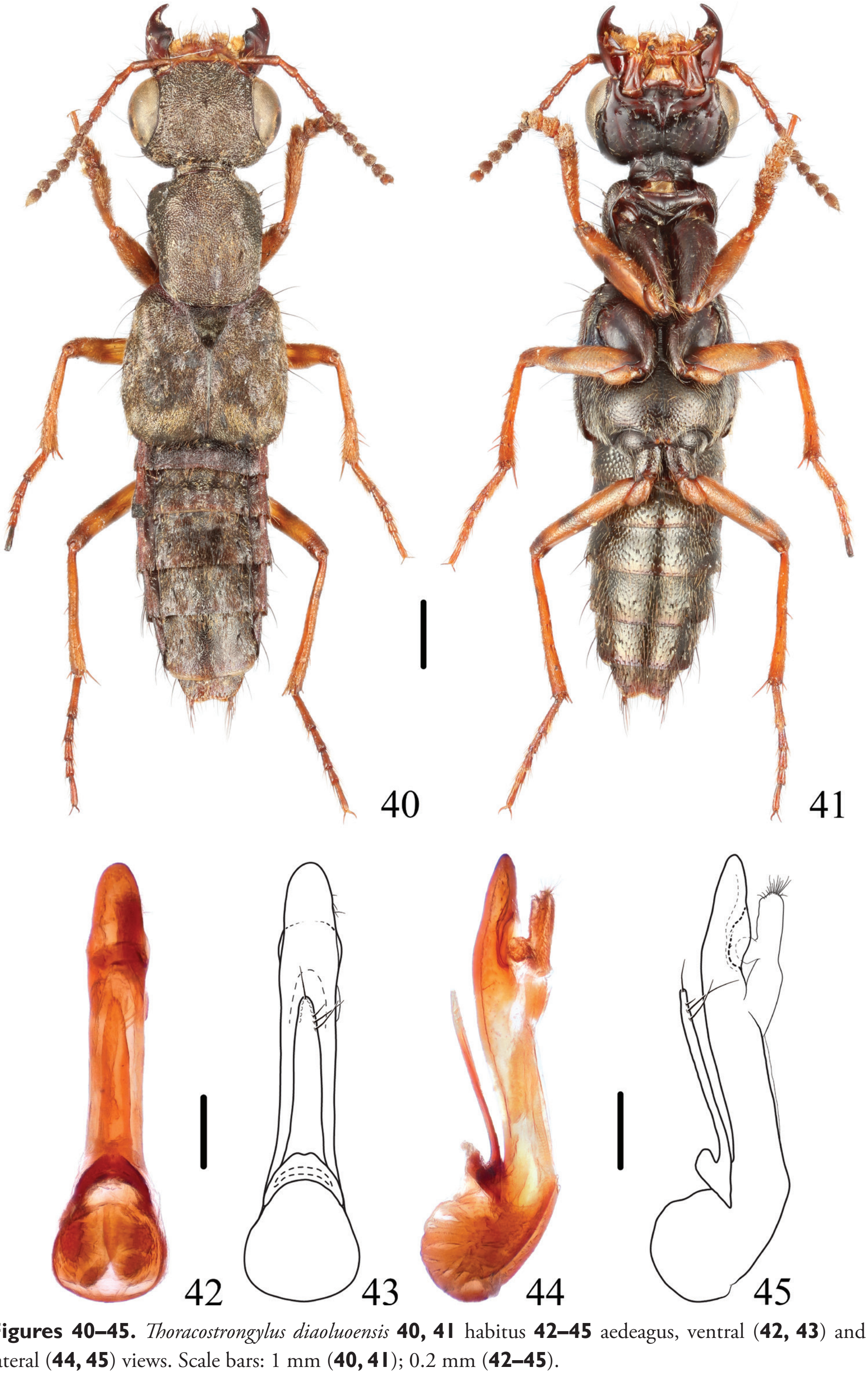

Figures 40–45. *Thoracostrongylus diaoluoensis* **40, 41** habitus **42–45** aedeagus, ventral (**42, 43**) and lateral (**44, 45**) views. Scale bars: 1 mm (**40, 41**); 0.2 mm (**42–45**).

Measurements. Male: BL: 9.2 mm, FL: 5.6 mm. HL: 1.56 mm, HW: 2.28 mm, CL: 1.06 mm, PO: 0.28 mm, PL: 2.06 mm, PW: 1.72 mm, EL: 2.39 mm, EW: 2.39 mm. HL/HW: 0.68, CL/PO: 3.80, PL/PW: 1.19, EL/EW: 1.00, HW/EW: 0.95, PW/EW: 0.72, HW/PW: 1.32.

Diagnosis. The apical portion of the median lobe (Figs 42–45) of the specimen examined here is a little wider than that of the type illustrated in the original description, which is considered as intraspecific variation. The species can be recognized from similar species by median lobe of the aedeagus without an apical or subapical tooth on the dorsal side.

Distribution. China (Hainan).

Thoracostrongylus formosanus formosanus **Shibata, 1982**

Fig. 112

台湾钝胸隐翅虫指名亚种

Thoracostrongylus formosanus Shibata, 1982: 71; Yang et al. 2011: 424; Hu, 2020: 348.

Material examined. China – **Taiwan Prov.** • 10 exs.; Hualien, Guanyuan; 24°11'12"N, 121°20'00"E; alt. 2200–2300 m; 27 June 2006; Y.-F. Hsu leg.; NMW • 16 exs.; Hualien, Pilu; alt. 2100 m; 24°10'58"N, 121°23'16"E; 06 May 2006; Y.-F. Hsu leg.; NMW.

Measurements. BL: 8.5–10.5 mm, FL: 5.0–5.8 mm. HL: 1.25–1.60 mm, HW: 1.8–2.2 mm, CL: 0.85–0.85 mm, PO: 0.3–0.4 mm, PL: 1.75–2.00 mm, PW: 1.5–1.7 mm, EL: 2.1–2.5 mm, EW: 2.20–2.65 mm. HL/HW: 0.69–0.73, CL/PO: 2.38–2.86, PL/PW: 1.16–1.17, EL/EW: 0.94–0.95, HW/EW: 0.81–0.83.

Diagnosis. The subspecies is most similar to *T. velutinus* from Yunnan and Myanmar, but can be easily distinguished by the usually black mid and hind tibiae and tarsi. Both differ from other species from east and southeast China in the abdominal tergites III–VI without triangular mediobasal golden tomentose patch.

Distribution. China (Taiwan).

Thoracostrongylus formosanus flavipes **ssp.nov.**

https://zoobank.org/811E5361-8C24-41BE-8BB2-5C2AF207A456

Figs 46–52, 113

台湾钝胸隐翅虫黄足亚种

Type material. ***Holotype.*** China – **Zhejiang Prov.** • ♂, glued on a card with labels as follows: "China: Zhejiang, Longquan, Fengyang Mt., Guanyintai; alt. 1000 m; 11 May 2019; Tang & Zhao leg." "Holotype / *Thoracostrongylus formosanus flavipes* / Xia, Tang & Schillhammer" [red handwritten label]; SHNU. ***Paratypes***. China – **Zhejiang Prov.** • 4♂♂, 6♀♀; same data as holotype; SHNU • 1♂; Longquan

City, Fengyangshan, Lu'ao Vill.; 27°55'8.95"N, 119°11'55.54"E; alt. 1200–1300 m; 16–17 July 2018; Zi-Wei Yin leg.; SHNU • 2♂♂, 1♀; Longquan City, Fengyangshan N.R., Lu'aocun Village; 27°55'19.66"N, 119°11'38.86"E; alt. 1076 m; 04 May 2016; Jiang, Liu & Zhou leg.; SHNU • 1♂; Longquan City, Fengyangshan N.R., Datianping; 27°54'29.67"N, 119°10'31.45"E; alt. 1350 m; 30 April 2016; Jiang, Liu & Zhou leg.; SHNU • 2♀♀; Longquan City, Fengyangshan N.R., Datianping; 27°54'29.67"N, 119°10'31.45"E; alt. 1350 m; 30 April 2016; Jiang, Liu & Zhou leg.; SHNU • 2♂♂, 1♀; Jinhua City, Pan'an County, Dapanshan N.R.; 28°58'41.03"N, 120°29'19.24"E; alt. 531–783 m; 08 May 2016; Jiang, Liu & Zhou leg.; SHNU • 1♂, 2♀♀; Lishui City, Qingyuan County, Baishanzu, Station to Peak; 27°45'20"N, 119°11'78"E; alt. 1721 m; 24 April 2015; Song & Yan leg.; SHNU • 2♀♀; Longquan City, Fengyangshan N.R., Mihougu, near stream; 27°55'0.18"N, 119°11'52.91"E; alt. 1116 m; 03 May 2016; Jiang, Liu & Zhou leg.; SHNU • 1♀; Wuyanling; alt. 700 m; 09 May 2004; Hu, Tang & Zhou leg.; SHNU. – **Guangxi Prov.** • 7♂♂, 16♀♀; Huanjiang, Jiuwan Mt., Yangmeiao; 25°12'22.15"N, 108°40'32.01"E; alt. 1250 m; 25 April 2021; Tang, Peng, Cai & Song leg.; SHNU • 1♂; Huanjiang, Jiuwan Mt., Yangmeiao; 25°12'22.15"N, 108°40'32.01"E; alt. 1250 m; 08 May 2021; Tang, Peng, Cai & Song leg.; SHNU • 1♀; Huanjiang, Jiuwan Mt., Yangmeiao; 25°12'22.15"N, 108°40'32.01"E; alt. 1250 m; 23 April 2021; Tang, Peng, Cai & Song leg.; SHNU • 1♂; Jinxiu County, Mt. Shengtangshan; alt. 1500 m; 26 July 2011; Zhong Peng leg.; SHNU • 1♀; Guilin City, Huaping N.R., Anjiangping; alt. 1500 m; 18 July 2011; Liang Tang leg.; SHNU. – **Guangdong Prov.** • 4♂♂, 2♀♀; Ruyuan County, Nanling N.R., Qingshui Valley; 24°54'57"N, 113°01'55"E; alt. 900 m; 04 May 2015; Peng, Tu & Zhou leg.; SHNU • 1♂, 2♀♀; Ruyuan County, Nanling N.R., Laopengkeng; 24°56'29"N, 113°00'27"E; alt. 1360 m; 29 April 2015; Peng, Tu & Zhou leg.; SHNU • 6♂♂, 3♀♀; Ruyuan County, Nanling N.R., Baobaoshan Station; 24°55'43"N, 113°00'58"E; alt. 1030 m; 25 April 2015; Peng, Tu & Zhou leg.; SHNU. – **Sichuan Prov.** • 3♂♂, 1♀; Dayi County, Xiling Snow Mt.; 30°38'6.25"N, 103°10'99.08"E; alt. 1250 m; 31 July 2021; Zhao & Cai leg.; SHNU • 1♀; Jiulong County, Hongba; alt. 2000 m; 13 August 2005; Ming Yi leg.; SHNU. – **Anhui Prov.** • 1♀; Huangshan, Tangkou Town, Hougu; 30°05'3.48"N, 118°08'45.96"E; alt. 569–688 m; 29 June–03 July 2020; Chong Li leg.; SHNU. – **Jiangxi Prov.** • 1♂, 1♀; Yichun City, Fengxin County, Baizhang Vill.; 28°42'55"N, 114°46'14"E; alt. 1000–1300 m; 16 July 2013; Hu & Lv leg.; SHNU • 1♂; Longnan County, Jiulianshan, summit of Huangniushi; 24°30'53"N, 114°26'6.72"E; alt. 1000–1230 m; 12 May 2021; Zhou & Li leg.; SHNU • 1♂; Ji'an City, Jinggangshan, Huangyangjie; 26°37'25"N, 114°06'58"E; alt. 1240 m; 28.vii,2014; Chen, Hu, Lv & Yu leg.; SHNU • 1♀; Pingxiang City, Gaozhou County, Gaotianyan; 27°23'51"N, 114°00'54"E; alt. 1025 m; 23 July 2013; Song, Yin & Yu leg.; SHNU. – **Hunan Prov.** • 2♂♂; Liuyang City, Daweishan; 28°25'25"N, 114°05'57"E; alt. 1300 m; 06 June 2014; Peng, Shen, Yu & Yan leg.; SHNU • 2♂♂; Liuyang City, Daweishan, 28°25'25"N, 114°05'57"E; alt. 1300 m, 07 June 2014; Peng, Shen, Yu & Yan leg.; SHNU • 2♂♂, 1♀; Yan-

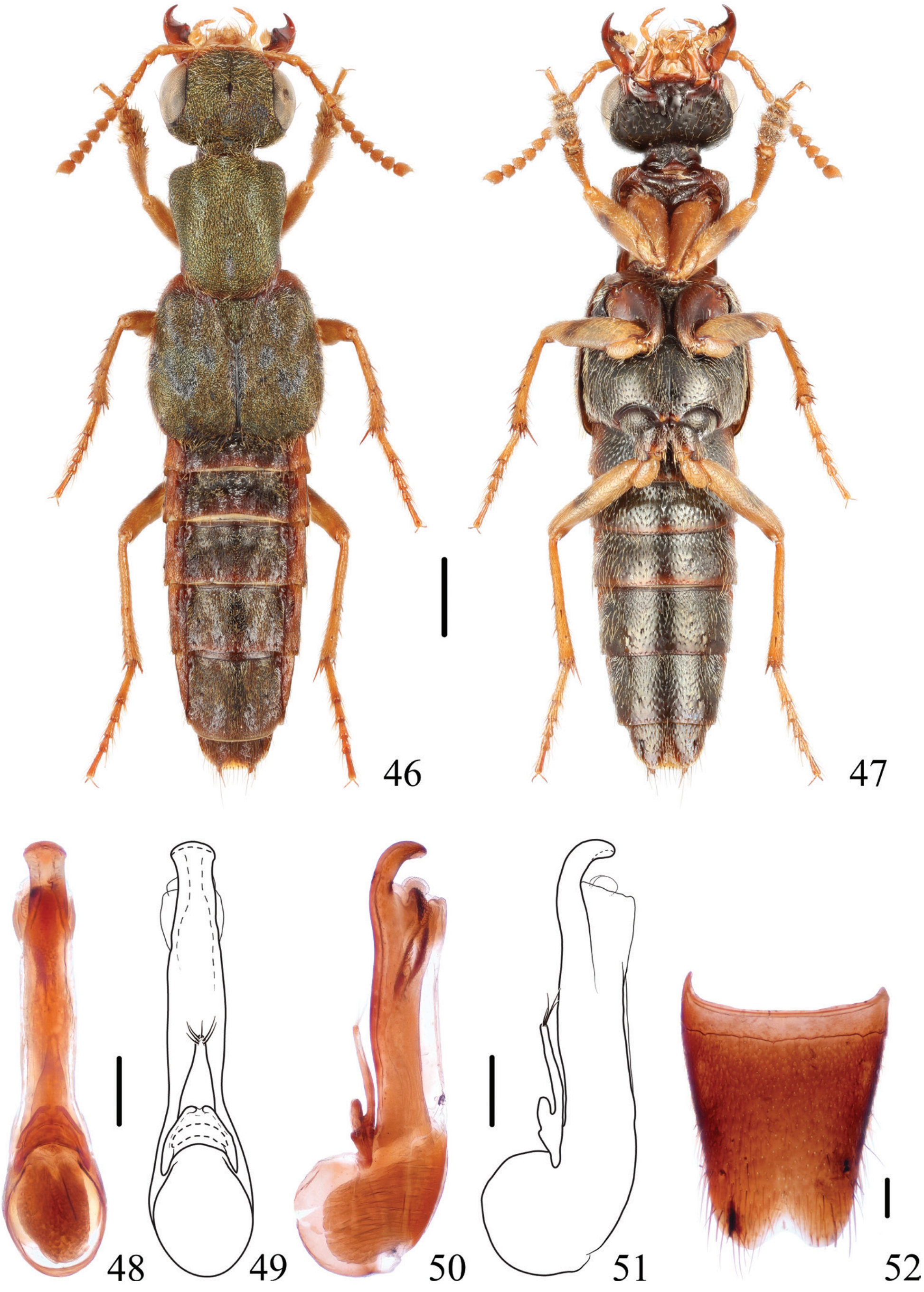

Figures 46–52. *Thoracostrongylus formosanus flavipes* ssp. nov. **46, 47** habitus **48–51** aedeagus, ventral (**48, 49**) and lateral (**50, 51**) views **52** male abdominal sternite VIII. Scale bars: 1 mm (**46, 47**); 0.2 mm (**48–52**).

ling County, Nanfengmian; 26°18'N, 114°01'E; alt. 1855 m; 07 June 2015; Peng, Shen, Tu & Zhou leg.; SHNU • 1♂; Xin'ning County, Shunhuang Mt., Yangheping; 26°23'41.58"N, 111°00'08.16"E; alt. 820 m; 02 May 2021; Yin, Zhang, Pan & Shen leg.; SHNU • 1♂; Xin'ning County, Shunhuang Mt., Yangheping; 26°23'41.58"N, 111°00'08.16"E; alt. 820 m; 30 April 2021; Yin, Zhang, Pan & Shen leg.; SHNU • 1♂; Chengzhou, Yizhang County, Mangshan N.R.; 24°56'26"N, 112°59'18"E; alt. 1400 m; 26 April 2015; Peng, Tu & Zhou leg.; SHNU • 2♀♀; Liuyang City, Daweishan; 28°25'N, 114°05'E; alt. 1000 m; 11 June 2015; Peng, Shen, Tu & Zhou leg.; SHNU • 2♂♂, 3♀♀; Mangshan N.R.; 10 May 2020; SHNU • 6♂♂, 12♀♀; Yanling County, Nanfengmian; 26°18'10"N, 114°00'12"E; alt. 1620 m; 26 May 2014; Peng, Shen, Yu & Yan leg.; SHNU • 1♂, 1♀; Yanling County, Nanfengmian; 26°16'32"N, 113°59'34"E; alt. 1380 m; 27 May 2014; Peng, Shen, Yu & Yan leg.; SHNU • 2♂♂, 1♀; Yanling County, Nanfengmian; 26°18'20"N, 114°00'51"E; alt. 1730 m; 28 May 2014; Peng, Shen, Yu & Yan leg.; SHNU. – **Fujian Prov.** • 15♂♂, 14♀♀; Wuyishan City, Guadun Vill.; 27°44'N, 117°38'E; alt. 1300–1500 m; 27 May 2012; Peng & Dai leg.; SHNU • 2♂♂, 1♀; Wuyishan City, Guadun Vill.; 27°44'N, 117°38'E; alt. 1200–1500 m; 26 May 2012; Peng & Dai leg.; SHNU • 2♂♂, 2♀♀; Wuyishan City, Guadun Vill.; 27°44'N, 117°38'E; alt. 1200–1500 m; 25 May 2012; Peng & Dai leg.; SHNU • 3♀♀; Wuyishan City, Guadun Vill.; 27°44'N, 117°38'E; alt. 1200–1300 m; 24 May 2012; Peng & Dai leg.; SHNU • 1♀; Wuyishan City, Guadun Vill.; 27°44'N, 117°38'E; alt. 1100–1400 m; 29 May 2012; Peng & Dai leg.; SHNU • 1♂, 2♀♀; Wuyishan City, Guadun Vill.; 27°44'N, 117°38'E; alt. 1800 m; 01 June 2012; Peng & Dai leg.; SHNU • 1♂; Guadun Vill.; August 2008; Zhu-Qing He leg.; SHNU • 2♂♂, 1♀; Guihe Vill., Meihua Mt.; alt. 1500 m; 20 May 2007; Huang & Xu leg.; SHNU • 1♂; N. Slope Gouzinao, Meihua Mt.; alt. 1650 m; 29 May 2007; Huang & Xu leg.; SHNU • 1♂; Guihe Vill., Gouzinao, Meihua Mt.; alt. 1500 m; 26 May 2007; Huang & Xu leg.; SHNU.

Measurements. Male: BL: 9.0–10.8 mm, FL: 5.0–5.8 mm. HL: 1.22–1.56 mm, HW: 1.72–2.11 mm, CL: 0.89–1.06 mm, PO: 0.22–0.28 mm, PL: 1.78–2.00 mm, PW: 1.45–1.72 mm, EL: 2.11–2.45 mm, EW: 2.17–2.56 mm. HL/HW: 0.69–0.76, CL/PO: 3.20–4.00, PL/PW: 1.16–1.23, EL/EW: 0.95–0.97, HW/EW: 0.79–0.83, PW/EW: 0.66–0.67, HW/PW: 1.18–1.23. **Female:** BL: 8.2–11.7 mm, FL: 4.7–5.6 mm. HL: 1.22–1.45 mm, HW: 1.61–2.00 mm, CL: 0.83–0.89 mm, PO: 0.22–0.28 mm, PL: 1.67–2.00 mm, PW: 1.33–1.67 mm, EL: 2.00–2.56 mm, EW: 2.00–2.67 mm. HL/HW: 0.70–0.76, CL/PO: 3.00–3.75, PL/PW: 1.20–1.25, EL/EW: 0.95–1.00, HW/EW: 0.75–0.81, PW/EW: 0.63–0.68, HW/PW: 1.18–1.21.

Diagnosis. The new subspecies differs from the nominate subspecies in the slightly shorter tempora, and entirely reddish to yellowish antennae and legs (except a dark band on the femora), while the nominate subspecies has almost entirely dark antennae, and black tibiae and tarsi. Even in paler (teneral) specimens of the nominate subspecies, the antennae and legs are at least partly darkened.

Distribution. The subspecies is widespread in China (Zhejiang, Fujian, Hubei, Hunan, Sichuan, Guangxi, Guangdong, Anhui, Jiangxi).

Thoracostrongylus fujianensis **Yang, Zhou & Schillhammer, 2011**

Figs 53–70, 114
福建钝胸隐翅虫

Thoracostrongylus fujianensis Yang, Zhou & Schillhammer, 2011: 419.

Material examined. China – **Fujian Prov.** • 1♂, 1♀; Wuyishan City, Guadun Vill.; 27°44'N, 117°38'E; alt. 1200–1500 m; 25 May 2012; Peng & Dai leg. (SHNU) • 3♂♂, 1♀; Wuyishan City, Guadun Vill.; 27°44'N, 117°38'E; alt. 1200–1500 m; 26 May 2012; Peng & Dai leg.; SHNU • 1♂; Wuyishan City, Guadun Vill.; 27°44'N, 117°37'E; alt. 1200–1500 m; 28 May 2012; Peng & Dai leg.; SHNU • 1♂; Wuyishan City, Guadun Vill.; 27°44'N, 117°38'E; alt. 1300–1500 m; 27 May 2012; Peng & Dai leg.; SHNU • 1♂; Wuyishan City, Guadun Vill.; 27°44'N, 117°38'E; alt. 1100–1300 m; 30 May 2012; Peng & Dai leg.; SHNU • 2♂♂; Wuyishan City, Guadun Vill.; 27°44'N, 117°38'E; alt. 1300 m; 02 June 2012; Peng & Dai leg.; SHNU • 3♀♀; Guadun; August 2008; Zhu-Qing He leg.; SHNU • 2♀♀; Wuyishan, Guadun; alt. 1200 m; 30 August 2009; Hao Huang leg.; SHNU • 1♂; Mt. Wuyi; 27–31 May 2012; Li-Zhen Li leg.; SHNU • 1♂; Longkeng Vill., Junzifeng; alt. 1400 m; 07 August 2008; Qi & Yin leg.; SHNU • 1♂; Guihe Vill., Meihua Mt.; alt. 1500 m; 27 May 2007; Huang & Xu leg.; SHNU • 1♂; Guihe Vill., Meihua Mt.; alt. 1500 m; 20 May 2007; Huang & Xu leg.; SHNU.

Measurements. Male: BL: 7.7–11.1 mm, FL: 4.4–5.8 mm. HL: 1.22–1.56 mm, HW: 1.72–2.17 mm, CL: 0.83–1.00 mm, PO: 0.22–0.28 mm, PL: 1.50–2.06 mm, PW: 1.33–1.72 mm, EL: 1.83–2.34 mm, EW: 1.83–2.39 mm. HL/HW: 0.70–0.76, CL/PO: 3.00–4.50, PL/PW: 1.13–1.21, EL/EW: 0.95–1.00, HW/EW: 0.85–0.95, PW/EW: 0.69–0.75, HW/PW: 1.22–1.32. **Female:** BL: 8.8–10.3 mm, FL: 5.1–5.6 mm. HL: 1.39–1.61 mm, HW: 1.95–2.22 mm, CL: 0.95–1.11 mm, PO: 0.22–0.28 mm, PL: 1.83–2.06 mm, PW: 1.50–1.72 mm, EL: 2.06–2.39 mm, EW: 2.11–2.45 mm. HL/HW: 0.69–0.74, CL/PO: 3.40–4.25, PL/PW: 1.17–1.22, EL/EW: 0.95–1.00, HW/EW: 0.90–0.95, PW/EW: 0.70–0.72, HW/PW: 1.27–1.33.

Diagnosis. The species shows some intraspecific variability (Figs 55–70) in the shape of the paramere and median lobe of the aedeagus. In general appearance, the species is similar to *T. acerosus*, *T. aduncatus*, and *T. diaoluoensis*, but can be keyed out by the aedeagal characters.

Distribution. China (Fujian).

Thoracostrongylus malaisei **Scheerpeltz, 1965**

Figs 71, 72, 115
马来钝胸隐翅虫

Thoracostrongylus malaisei Scheerpeltz, 1965: 245; Yang et al. 2011: 428.

Material examined. China – **Yunnan Prov.** • 1♀; 100 km W Baoshan, Gaoligongshan Nat. Res.; 14–21 June 1993; E. Jendek & O. Sausa leg.; NMW.

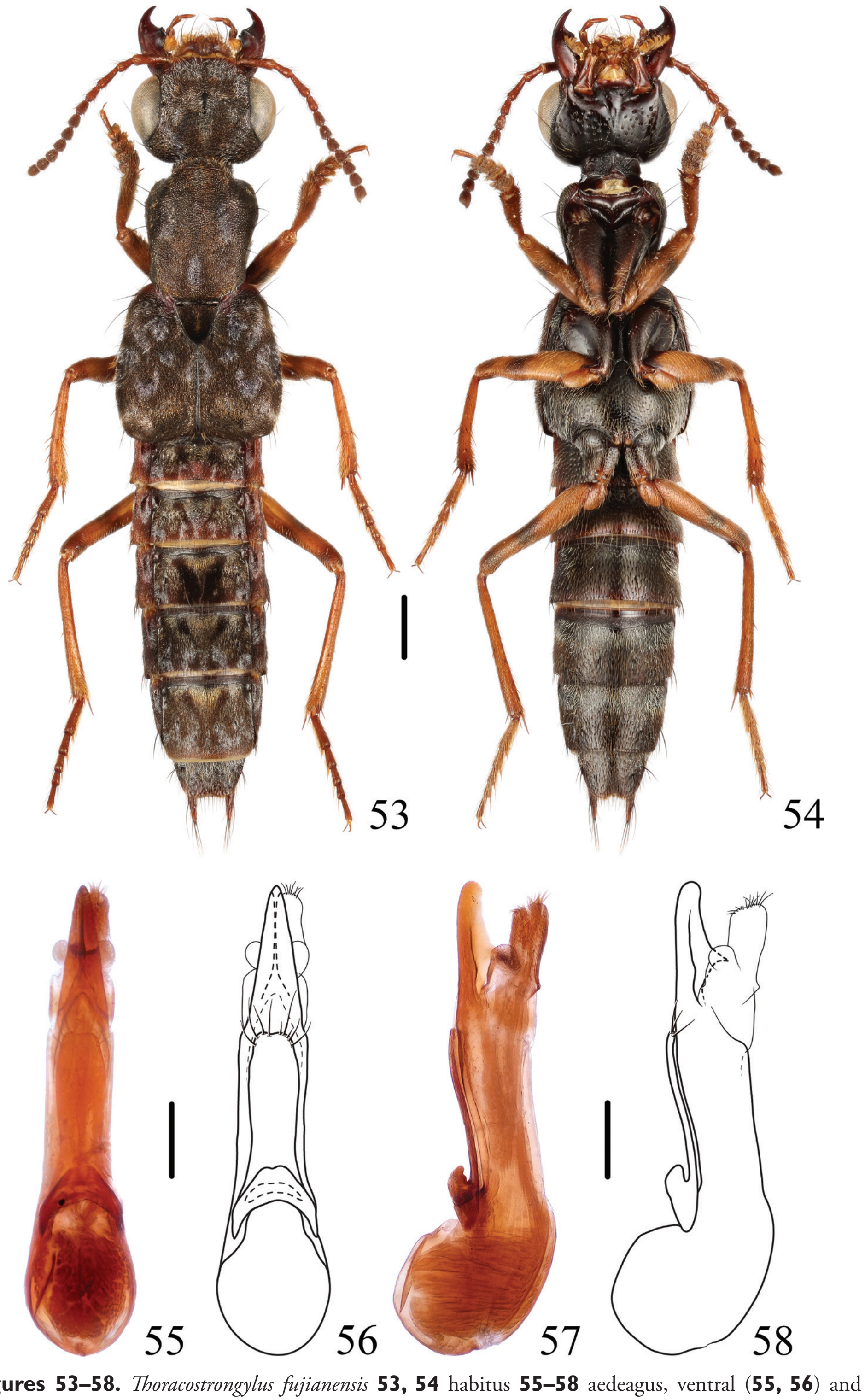

Figures 53–58. *Thoracostrongylus fujianensis* **53, 54** habitus **55–58** aedeagus, ventral (**55, 56**) and lateral (**57, 58**) views. Scale bars: 1 mm (**53, 54**); 0.2 mm (**55–58**).

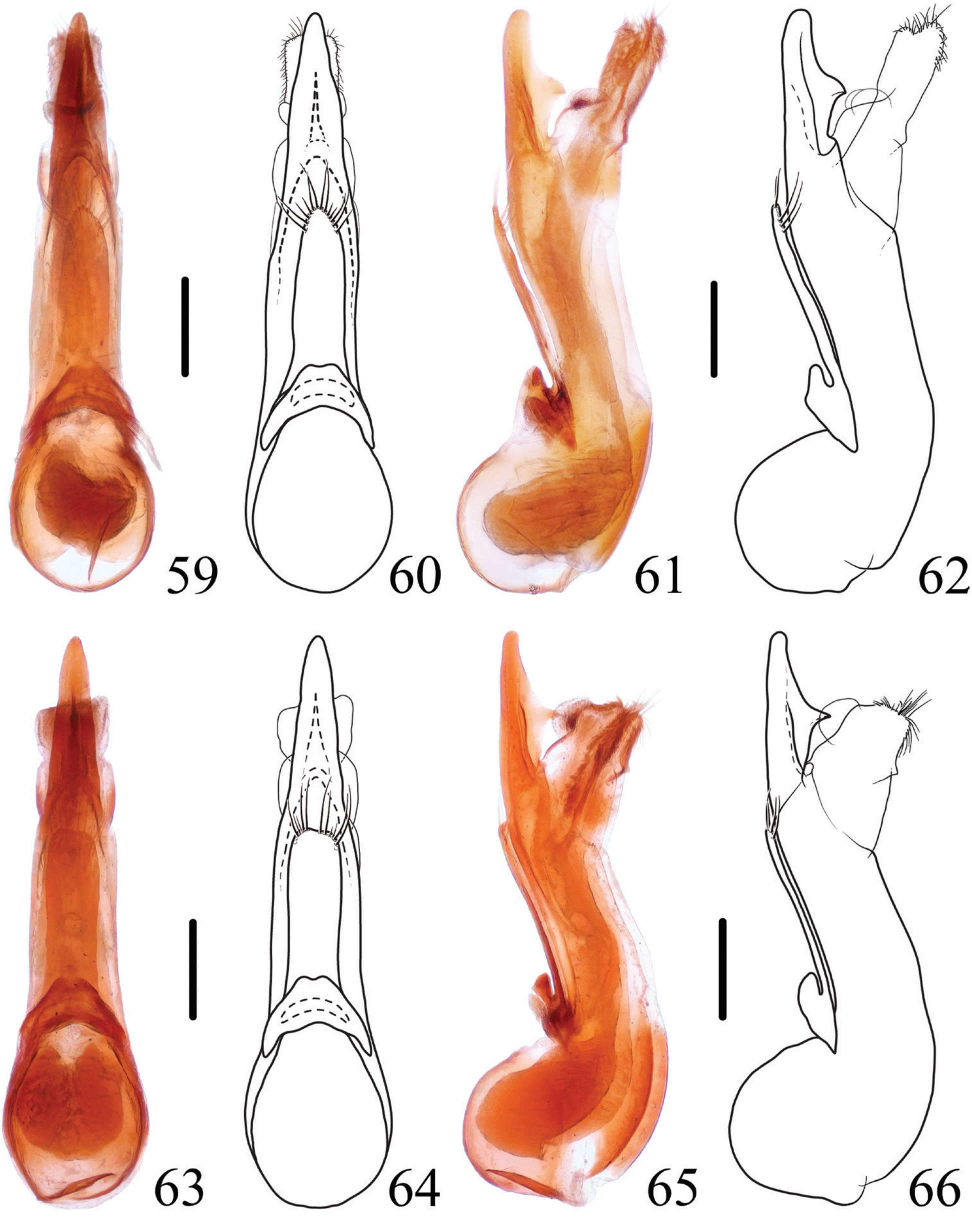

Figures 59–66. *Thoracostrongylus fujianensis* **59–62** aedeagus from Guadun, ventral (**59, 60**) and lateral (**61, 62**) views **63–66** aedeagus from Guadun, ventral (**63, 64**) and lateral (**65, 66**) views. Scale bars: 0.2 mm.

Distribution. China (Yunnan), Myanmar.

Remarks. The species was originally described from Myanmar, and was recorded from China by Yang, Zhou & Schillhammer in 2011 based on the one female mentioned above. However, there were some inconsistencies concerning morphometrics in that paper: The character used in the key "ratio of eye longitudinal diameter to temple length < 3”, applies only to the male. However, the measurements of female *T. malaisei* in the same paper were written as “CL: 0.98; PO: 0.28”, and the ratio of CL/PO should be 3.5 by calculation, which conflicts with the key. *Thoracostrongylus malaisei* is most closely related to *T. brachypterus* sp. nov.; for diagnosis of these two species, see under the latter.

Thoracostrongylus miyakei Bernhauer, 1943

Figs 73, 116
三宅钝胸隐翅虫

Thoracostrongylus miyakei Bernhauer, 1943: 179; Yang et al. 2011: 428; Hu 2020: 349.

Material examined. • 1♀; Taiwan, Taichung Hsien, Anmashan; alt. 2230 m; 30 April –4 May 1990; A. Smetana leg.; ASC.

Distribution. China (Sichuan?, Taiwan).

Remarks. The record for Sichuan reported by Yang et al. (2011) is doubtful: the record was published based on a specimen from Sichuan in coll. NMW. However, such a specimen does not exist, but there is a male (identified as *T. miyakei*) from Yunnan that was not mentioned in Yang et al. (2011). Numerous specimens from the mainland of east China have been examined in this paper and none of them is *T. miyakei*, creating a huge distributional gap between Sichuan and Taiwan. In addition, *T. miyakei* is a brachypterous species, making its occurrence in mainland China very unlikely. Since no male of that species from Taiwan was available for this paper, the solution to this problem must wait until males from Taiwan can be studied.

Thoracostrongylus sarawakensis (Bernhauer, 1915)

Fig. 117
沙捞越钝胸隐翅虫

Amichrotus sarawakensis Bernhauer, 1915h: 233.
Thoracostrongylus sarawakensis: Hammond 1984: 194, 195.
Ontholestes (*Thoracostrongylus*) *doriae* Gridelli, 1924: 207. Synonymized by de Rougemont 2016: 568.
Amichrotus doriae: Hammond 1984: 194, 195.

Material examined. None.

Distribution. China (Hainan?), Borneo.

Remarks. The Chinese record of the species was published by de Rougemont (2016) without detailed locality data. The specimens in coll. Rougemont should be studied to confirm the occurrence of the species on Hainan.

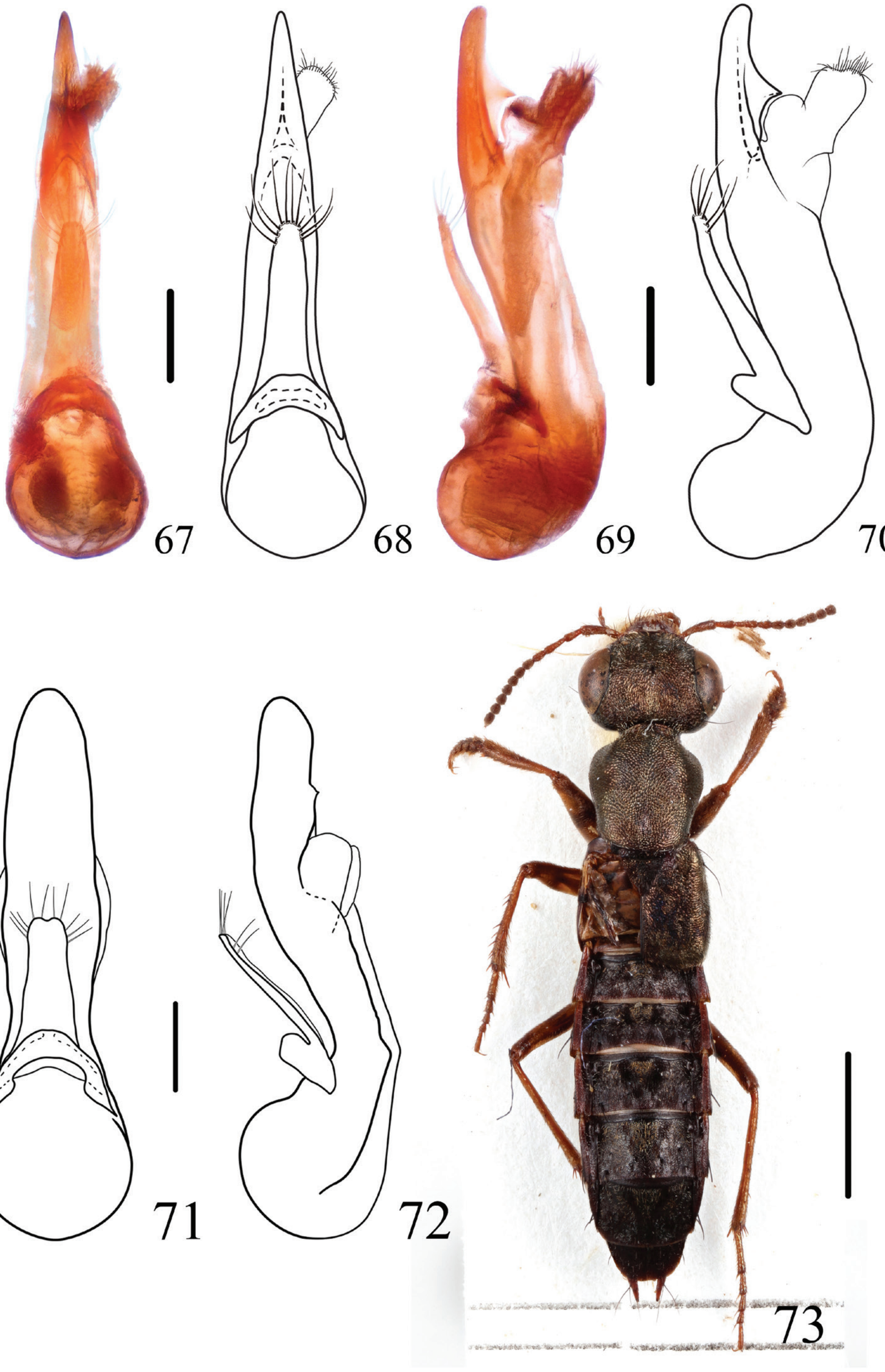

Figures 67–73. *Thoracostrongylus* **67–70** *T. fujianensis* aedeagus from Mt. Meihua, ventral (**67, 68**) and lateral (**69, 70**) views **71–72** *T. malaisei* aedeagus, ventral (**71**) and lateral (**72**) views **73** *T. miyakei* habitus. Scale bars: 0.2 mm (**67–72**); 2 mm (**73**).

Thoracostrongylus velutinus **Scheerpeltz, 1965**
Figs 74–79, 118
绒钝胸隐翅虫

Thoracostrongylus velutinus Scheerpeltz, 1965: 243; Yanget al. 2011: 430.

Material examined. China – **Yunnan Prov.** • 1♂, 1♀; Gongshan County, Qiqi; alt. 2000 m; 29 June 2010; Wen-Xuan Bi leg.; SHNU • 3♀♀; Gongshan County, Qiqi; alt. 1900 m; 02 July 2010; Liang Tang leg.; SHNU • 1♂; Tengchong Coun., Baihualing; 24 May 2005; Hao Huang leg.; SHNU • 1♂; Tengchong County, Mingguang Town, Zizhi Vill; 25°42'N, 98°35'E; alt. 2300–2500 m; 30 April 2013; Song, Dai & Peng leg.; SHNU.

Measurements. Male: BL: 7.3–8.9 mm, FL: 4.7–5.1 mm. HL: 1.22–1.33 mm, HW: 1.61–1.72 mm, CL: 0.83 mm, PO: 0.22–0.28 mm, PL: 1.67–1.78 mm, PW: 1.39–1.50 mm, EL: 2.11 mm, EW: 2.11–2.22 mm. HL/HW: 0.73–0.77, CL/PO: 3.00–3.75, PL/PW: 1.19–1.23, EL/EW: 0.95–1.00, HW/EW: 0.78–0.79, PW/EW: 0.66–0.68, HW/PW: 1.15–1.20. **Female:** BL: 8.4–10.3 mm, FL: 4.7–5.3 mm. HL: 1.28–1.45 mm, HW: 1.72–1.95 mm, CL: 0.89–0.95 mm, PO: 0.22–0.28 mm, PL: 1.67–1.89 mm, PW: 1.39–1.61 mm, EL: 2.00–2.34 mm, EW: 2.00–2.45 mm. HL/HW: 0.73–0.76, CL/PO: 3.20–4.00, PL/PW: 1.17–1.23, EL/EW: 0.95–1.00, HW/EW: 0.76–0.92, PW/EW: 0.63–0.69, HW/PW: 1.17–1.35.

Diagnosis. The species can be easily distinguished from other species from southwest China by the abdominal tergites III–VI without a triangular, mediobasal, golden tomentose patch. In general appearance, *T. velutinus* is most similar to *T. formosanus*, but may be distinguished from the nominate ssp. of the latter by its smaller body size and paler mid and hind legs, and from *T. formosanus flavipes* by the dark antennae.

Distribution. China (Yunnan), Myanmar.

Thoracostrongylus baishanzuensis **sp. nov.**
https://zoobank.org/2BCAB674-45E6-4A5B-BC62-53B506E0EC08
Figs 80–85, 119
百山祖钝胸隐翅虫

Type material. ***Holotype.*** China – **Zhejiang Prov.** • ♂, glued on a card with labels as follows: “China: Zhejiang, Qingyuan, Baishanzu N.R.; 27°45'26"N, 119°12'08"E; alt. 1730 m; 02 May 2014; Peng, Song, Yan & Yu leg.” “Holotype / *Thoracostrongylus baishanzuensis* / Xia, Tang & Schillhammer” [red handwritten label]; SHNU. ***Paratypes.*** China – **Zhejiang Prov.** • 6♂♂, 2♀♀; same data as for the holotype; SHNU • 1♂, 1♀; Qingyuan, Baishanzu N.R.; 27°45'14"N, 119°11'55"E; alt. 1560–1750 m; 01 May 2014; Peng et al. leg.; SHNU • 1♂, 4♀♀; Lishui City, Qingyuan County, Baishanzu, Station to Peak; 27°45'20"N, 119°11'78"E; alt. 1721 m; 22 May 2015; Song & Yan leg.; SHNU • 1♂, 2♀♀; Lishui City, Qingyuan County, Baishanzu, Station to Peak; 27°45'20"N, 119°11'78"E; alt. 1721 m; 24 April 2015; Song &

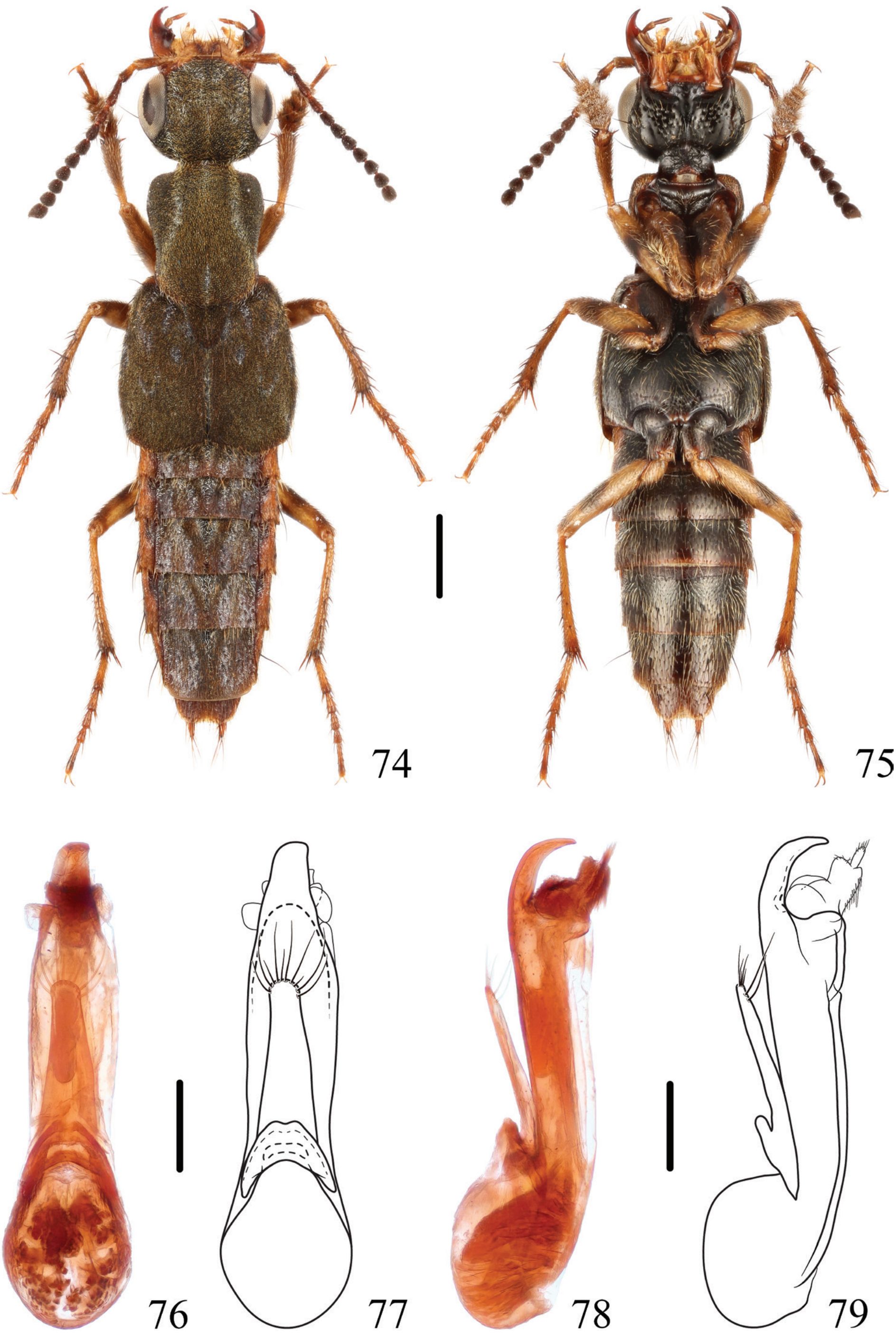

Figures 74–79. *Thoracostrongylus velutinus* **74, 75** habitus **76–79** aedeagus, ventral (**76, 77**) and lateral (**78, 79**) views. Scale bars: 1 mm (**74, 75**); 0.2 mm (**76–79**).

Yan leg.; SHNU • 1♀; Lishui City, Qingyuan County, Baishanzu; alt. 1500 m; 22–23 September 2008; Tang & Zhang leg.; SHNU.

Diagnosis. The new species can be easily recognized by the combination of following characters: legs reddish yellow without dark markings, head slightly wider than or as wide as elytra, apical portion of median lobe of aedeagus (Figs 82–85) curved dorsad into a fin-shape, paramere bilobed.

Measurements. Male: BL: 7.8–8.6 mm, FL: 4.3–4.9 mm. HL: 1.22–1.39 mm, HW: 1.72–1.95 mm, CL: 0.83–0.89 mm, PO: 0.28 mm, PL: 1.56–1.78 mm, PW: 1.33–1.50 mm, EL: 1.72–1.95 mm, EW: 1.72–1.95 mm. HL/HW: 0.71–0.74, CL/PO: 3.00–3.20, PL/PW: 1.15–1.23, EL/EW: 1.00, HW/EW: 1.00–1.03, PW/EW: 0.77–0.79, HW/PW: 1.26–1.31. **Female:** BL: 8.3–9.2 mm, FL: 4.7–5.2 mm. HL: 1.39–1.45 mm, HW: 1.95–2.06 mm, CL: 0.89–0.95 mm, PO: 0.28 mm, PL: 1.72–1.78 mm, PW: 1.45–1.61 mm, EL: 1.89–1.95 mm, EW: 1.89–2.00 mm. HL/HW: 0.68–0.71, CL/PO: 3.20–3.40, PL/PW: 1.10–1.19, EL/EW: 0.94–1.00, HW/EW: 1.00–1.03, PW/EW: 0.75–0.81, HW/PW: 1.28–1.35.

Description. Forebody dark brown with a bronze tint, abdominal segments III and IV reddish brown, remaining segments gradually becoming darker apicad, labrum reddish brown, mandibles reddish brown with medial portions distinctly darker, maxillary and labial palpi reddish brown, antennae reddish brown, antennal club indistinctly darker, legs reddish brown without dark markings, elytra with few small patches of whitish pubescence, scutellum with black pubescence in apical half, abdominal tergites III–VII each with triangular mediobasal golden tomentose patch delimited by pair of dark tomentose spots, dark tomentose spots of tergites III and IV indistinct, dark tomentose spots of tergite V particularly large and dark, confluent apically, forming sagittate patch, dark tomentose spots of tergite VI similar to that of tergite V, but little smaller and distinctly lighter, dark tomentose spots of tergite VII indistinct.

Head slightly wider than or as wide as elytra; vertex with small longitudinal specular spot medially; surface densely covered with umbilicate punctures except specular median spot. Antennae with antennomere 1 longest, antennomeres 2 and 3 almost half as long as antennomere 1, antennomeres 4 and 5 longer than wide, antennomeres 6–10 gradually increasing in width and decreasing in length, antennomere 10 slightly longer than or as long as wide, antennomere 11 distinctly longer than wide, asymmetrical and subacuminate towards tip.

Pronotum widest behind anterior angles; punctation dense and umbilicate, very short and narrow impunctate midline in posterior quarter, pubescence golden, distinct on entire dorsal surface.

Elytra subquadrate, inconspicuously wider than long, slightly dilated posteriad; surface densely and finely, regularly punctate, with brassy pubescence, mixed with grey spots all over the disc. Scutellum triangular, finely and densely punctate, with black, velvety pubescence.

Abdomen with tergites densely punctate; tergites III–VII brown, tergite VII with apical palisade fringe.

Male. Sternite VIII with medio-apical emargination. Aedeagus (Figs 82–85) relatively stout, median lobe gradually narrowed apicad in apical fourth in ventral view, in

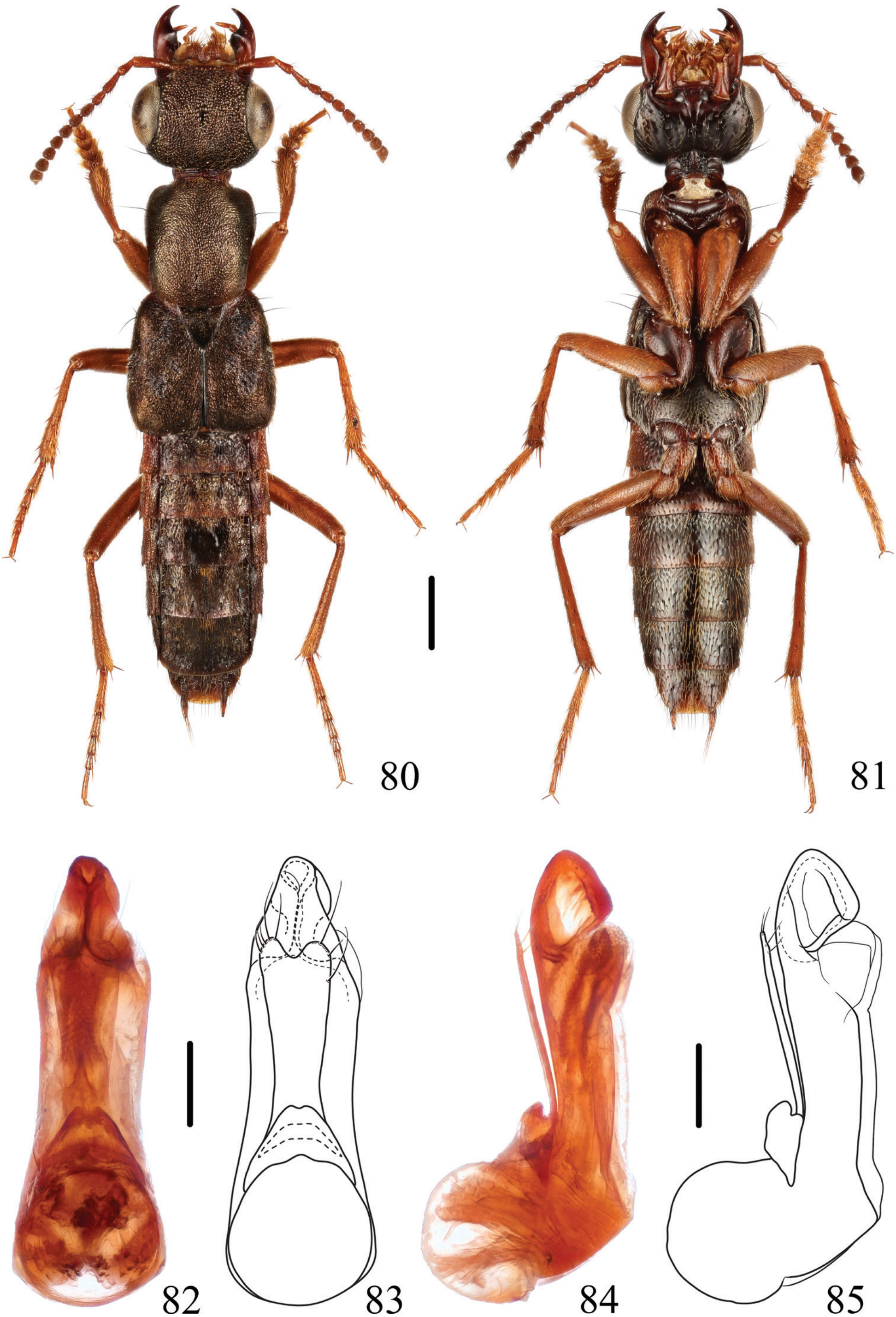

Figures 80–85. *Thoracostrongylus baishanzuensis* sp. nov. **80, 81** habitus **82–85** aedeagus, ventral (**82, 83**) and lateral (**84, 85**) views. Scale bars: 1 mm (**80, 81**); 0.2 mm (**82–85**).

lateral view, apical portion of median lobe curved dorsad forming distinct fin-shape; paramere very long, gradually widened apicad, apex bilobed, each lobe with five to six setae around apical margin.

Female. Sternite VIII with posterior margin entire.

Distribution. China (Zhejiang).

Etymology. This species is named after the type locality, Baishanzu, in Zhejiang Province, China.

Thoracostrongylus bicolor sp. nov.

https://zoobank.org/1F6192BE-17A1-4289-9684-83F45132333E
Figs 86–95, 120
双色钝胸隐翅虫

Type material. ***Holotype.*** China – **Guangdong Prov.** • ♂, glued on a card with labels as follows: “China: Guangdong, Shaoguan, Ruyuan, Nanling N.R., Ruyang; 24°56'10"N, 113°00'18"E; alt. 1050–1200 m; 01–06 May 2021; Hu, Lin, Zhou & Li leg.” “Holotype / *Thoracostrongylus bicolor* / Xia, Tang & Schillhammer” [red handwritten label]; SHNU. ***Paratypes.*** China **– Guangdong Prov.** • 4♂♂, 1♀; same data as for the holotype; SHNU • 1♂, 3♀♀; Shaoguan, Ruyuan County, Nanling N.R., Ruyang; 24°55'49.5"N, 113°01'08"E; alt. 1000 m; 01 May 2021; Zhou & Li leg.; SHNU • 1♀; Ruyuan County, Nanling N.R., Qingshui Valley; 24°54'57"N, 113°01'55"E; alt. 900 m; 04 May 2015; Peng, Tu & Zhou leg.; SHNU. **– Hunan Prov.** • 1♀; Yizhang, Mangshan, Mengkengshi; 24°55'10"N, 112°58'37"E; alt. 1625 m; 26 August 2020; Zhong Peng leg.; SHNU. **– Guangxi Prov.** • 3♂♂, 2♀♀; Huanjiang, Jiuwan Mt., Yangmei’ao; 25°12'22.15"N, 108°40'32.01"E; alt. 1250 m; 25 April 2021; Tang, Peng, Cai & Song leg.; SHNU • 2♂♂; Xing’an County, Mao’er Shan; 25°53'07"N, 110°29'14"E; alt. 1143 m; 31 July 2014; Peng, Song, Yu & Yan leg.; SHNU • 1♀; Xing’an County, Mao’er Shan; 25°53'11"N, 110°28'13"E; alt. 810 m; 28 July 2014; Peng, Song, Yu & Yan leg.; SHNU • 1♂; Mt. Damingshan; 23°23'N, 103°29'E; alt. 1150–1250 m; 31 July 2012; Hu & Song leg.; SHNU • 1♀; Guilin City, Huaping N.R., Yunxi Valley; 25°34'00.62"N, 109°56'19.59"E; alt. 1460–1550 m; 23 April 2021; Yin, Zhang, Pan & Shen leg.; SHNU • 1♀; Jinxiu County, Mt. Shengtangshan; alt. 1200 m; 27 July 2011; Zhong Peng leg.; SHNU. – **Yunnan Prov.** • 5♀♀; NE Kunming; 25°08'40"N, 102°53'48"E; alt. 2290 m; 11 August 2014; mixed forest, sifted; V. Assing leg.; 3 VAC, 2 NMW • 5♀♀; NE Kunming; 25°08'35"N, 102°53'49"E; alt. 2320 m; 13 August 2014; mixed forest, sifted; V. Assing leg.; 4 VAC, 1 NMW • 1♀; Mt. W Xundian; 25°34'58"N, 103°08'42"E; alt. 2300 m; 15 August 2014; sifted; V. Assing leg.; VAC • 2♂♂, 2♀♀; Mt. W Xundian; 25°34'58"N, 103°08'42"E; alt. 2300 m; 16 August 2014; sifted; V. Assing leg.; 3 VAC, 1 NMW • 1 ex.; E Kunming, Xiaobailong Forest Park; 24°55'43"N, 103°05'22"E; alt. 2110 m; secondary pine forest, pine litter and litter at trail margin sifted; 10 August 2014; M. Schülke leg. [CH14-03]; MSC • 1♂, 2exs.; NE Kunming; 25°09'07"N,

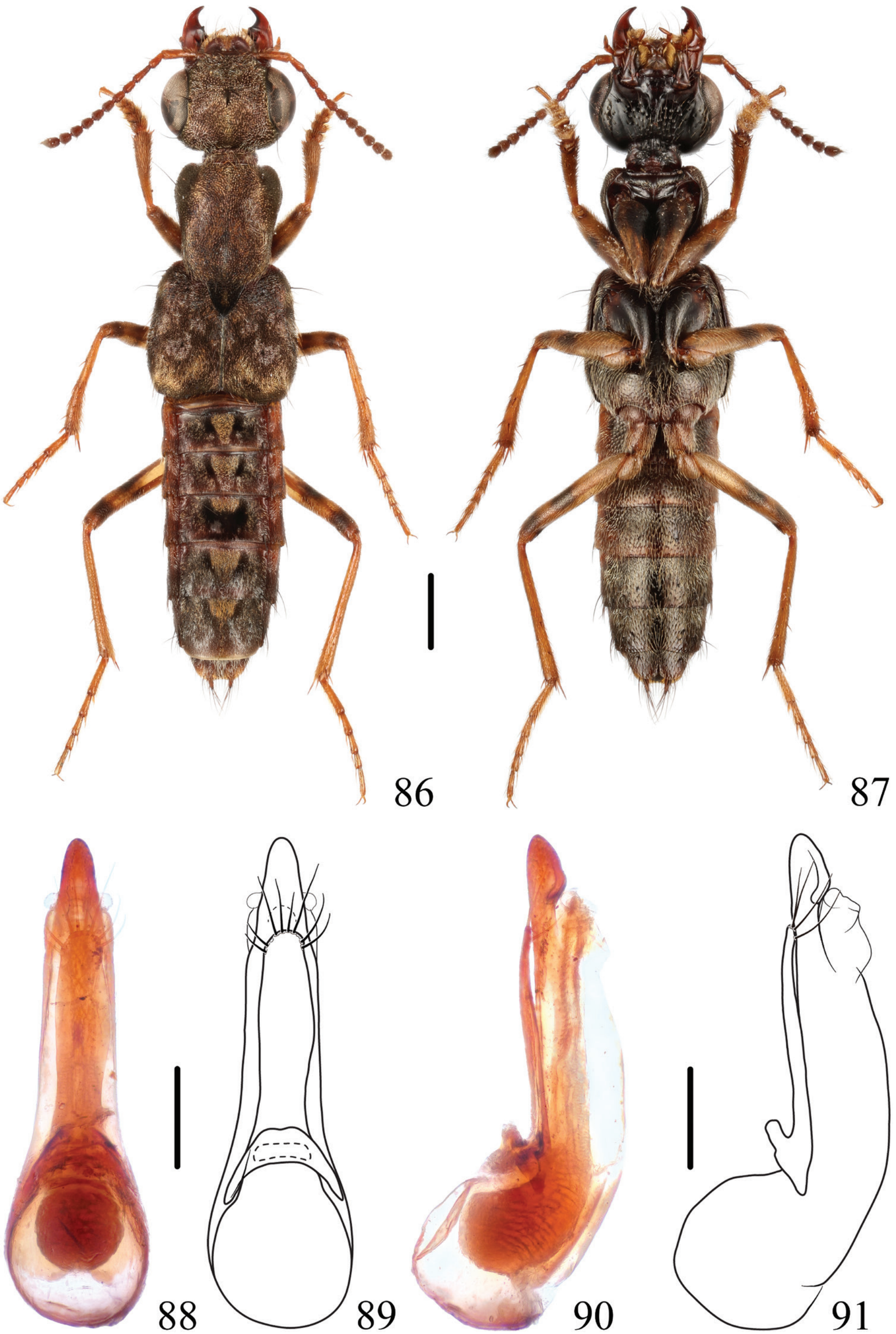

Figures 86–91. *Thoracostrongylus bicolor* sp. nov. **86, 87** habitus **88–91** aedeagus, ventral (**88, 89**) and lateral (**90, 91**) views. Scale bars: 1 mm (**86, 87**); 0.2 mm (**88–91**).

102°53'46"E; alt. 2280 m; secondary pine forest, with scattered old alder, litter, sifted; 11 August 2014; M. Schülke leg. [CH14-04]; MSC • 1♂, 1 ex.; NE Kunming; 25°08'40"N, 102°53'48"E; alt. 2290 m; mixed deciduous forest with scattered pine trees, litter and mushrooms, sifted; 11 August 2014; M. Schülke leg. [CH14-05]; MSC • 1ex.; NE Kunming; 25°08'35"N, 102°53'49"E; alt. 2320 m; mixed forest with alder, oak, and pine, litter and mushrooms, sifted; 13 August 2014; M. Schülke leg. [CH14-06]; MSC • 1ex.; Mt. W Xundian; 25°34'58"N, 103°08'42"E; alt. 2300 m; mixed forest with alder, pine, shrub undergrowth, litter, twigs, and roots of herbs, sifted; 16 August 2014; M. Schülke leg. [CH14-09b]; MSC • 1♂; mountain W Yuxi; 24°27'11"N, 102°29'58"E; alt. 2250 m; secondary mixed forest, litter, roots, and moss sifted; 31 August 2014; M. Schülke leg. [CH14-23]; MSC.

Measurements. Male: BL: 8.1–10.1 mm, FL: 4.5–4.9 mm. HL: 1.22–1.39 mm, HW: 1.78–1.95 mm, CL: 0.83–0.95 mm, PO: 0.22–0.28 mm, PL: 1.67–1.78 mm, PW: 1.39–1.45 mm, EL: 1.78–2.06 mm, EW: 1.95–2.09 mm. HL/HW: 0.69–0.74, CL/PO: 3.20–4.25, PL/PW: 1.15–1.24, EL/EW: 0.91–1.00, HW/EW: 0.91–0.97, PW/EW: 0.69–0.74, HW/PW: 1.23–1.35. **Female:** BL: 7.9–11.0 mm, FL: 4.6–5.4 mm. HL: 1.22–1.50 mm, HW: 1.83–2.11 mm, CL: 0.89–1.06 mm, PO: 0.22–0.28 mm, PL: 1.67–1.89 mm, PW: 1.39–1.61 mm, EL: 1.95–2.22 mm, EW: 1.95–2.28 mm. HL/HW: 0.67–0.74, CL/PO: 3.40–4.75, PL/PW: 1.11–1.26, EL/EW: 0.97–1.00, HW/EW: 0.93–0.97, PW/EW: 0.66–0.73, HW/PW: 1.28–1.41.

Diagnosis. The new species is similar to *T. baishanzuensis* sp. nov., but it can be easily recognized from latter by the bicolored femora. From other species of east and southeast China, it can be easily recognized by the bicolored abdomen.

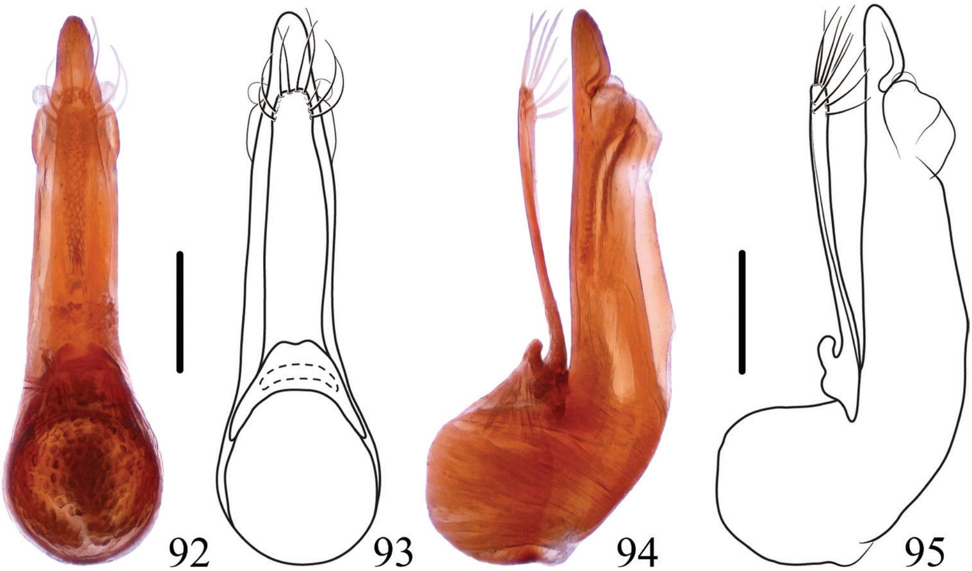

Figures 92–95. *Thoracostrongylus bicolor* sp. nov. **92–95** aedeagus from Guangxi, ventral (**92, 93**) and lateral (**94, 95**) views. Scale bars: 0.2 mm.

Description. The new species is similar to *T. baishanzuensis* sp. nov. in most aspects except for the following characters: abdominal tergites III–VII each with a longer and more distinct triangular, mediobasal, golden tomentose patch; femora each with median dark mark and apical dark mark, although the apical dark markings of the forelegs are less distinct.

Male. Sternite VIII with medioapical emargination. Aedeagus (Figs 88–95) slender, median lobe gradually narrowed apicad with round apex in ventral view, apex of median lobe expanded dorsad in lateral view; paramere relatively long, apex wide and round with approximately 11 setae around the apical margin.

Female. Sternite VIII with posterior margin entire.

Distribution. China (Guangdong, Hunan, Guangxi, and Yunnan).

Etymology. This species is named after its bicolored abdomen.

Thoracostrongylus brachypterus sp. nov.

https://zoobank.org/09964804-5ECF-43BA-817C-6F2A046D2759
Figs 96–101, 121
短翅钝胸隐翅虫

Type material. ***Holotype.*** China – **Sichuan Prov.** •♂, glued on a card with labels as follows: "China: Sichuan, Muli Tibetan Autonomous County, Mianbu Yakou; 27°68'N, 101°22'E; alt. 3100 m; 04 June 2012; Hao Huang. leg." "Holotype / *Thoracostrongylus brachypterus* / Xia, Tang & Schillhammer" [red handwritten label]; SHNU. ***Paratypes.*** China – **Sichuan Prov.** • 1♀; S Sichuan, pass 20km S MULI (BOWA); 27.45°N, 101.13°E; 28–29 June 1998; mixed forest cca. 3500m; Jaroslav Turna leg.; NMW • 21♂♂, 9♀♀; S-Sichuan, pass betw. Yanyuan/Muli; alt. 3244 m; 27.68638°N, 101.22335°E; 11–18 June 2017; C. Reuter leg.; 20 BFC, 10 NMW • 1♂; S-Sichuan, pass ~ 50km NE Yanyuan to Xichang; alt. 2950 m, 27°33'11"N, 101°45'04"E; 07–18 June 2017; C. Reuter leg.; BFC.

Measurements. Male: BL: 7.6–9.3 mm, FL: 4.1–4.6 mm. HL: 1.20–1.30 mm, HW: 1.50–1.70 mm, CL: 0.80–0.89 mm, PO: 0.22–0.25 mm, PL: 1.55–1.78 mm, PW: 1.23–1.45 mm, EL: 1.60–1.72 mm, EW: 1.70–1.89 mm. HL/HW: 0.77–0.80, CL/PO: 3.23–4.00, PL/PW: 1.23–1.26, EL/EW: 0.91–0.94, HW/EW: 0.88–0.90. **Female:** BL: 11.0 mm, FL: 4.8–5.0 mm. HL: 1.35–1.40 mm, HW: 1.80–1.85 mm, CL: 0.80–0.90 mm, PO: 0.30–0.35 mm, PL: 1.75–1.80 mm, PW: 1.55 mm, EL: 1.85 mm, EW: 1.95 mm. HL/HW: 0.73–0.78, CL/PO: 2.33–3.03, PL/PW: 1.13–1.16, EL/EW: 0.95, HW/EW: 0.92–0.95.

Diagnosis. The new species is the only brachypterous species of the genus so far that is known from mainland China, except for a potential record of a brachypterous *T. malaisei*, from which it can be separated as indicated above. The *T. malaisei* specimens from the type locality have rather short elytra and developed hindwings, which may be functional or not since the palisade fringe on tergite VII is very narrow. *Thoracostrongylus miyakei* from Taiwan also has weakly developed, non-functional hind wings and no palisade fringe on tergite VII, which differs from the new species by pronotum without impunctate midline.

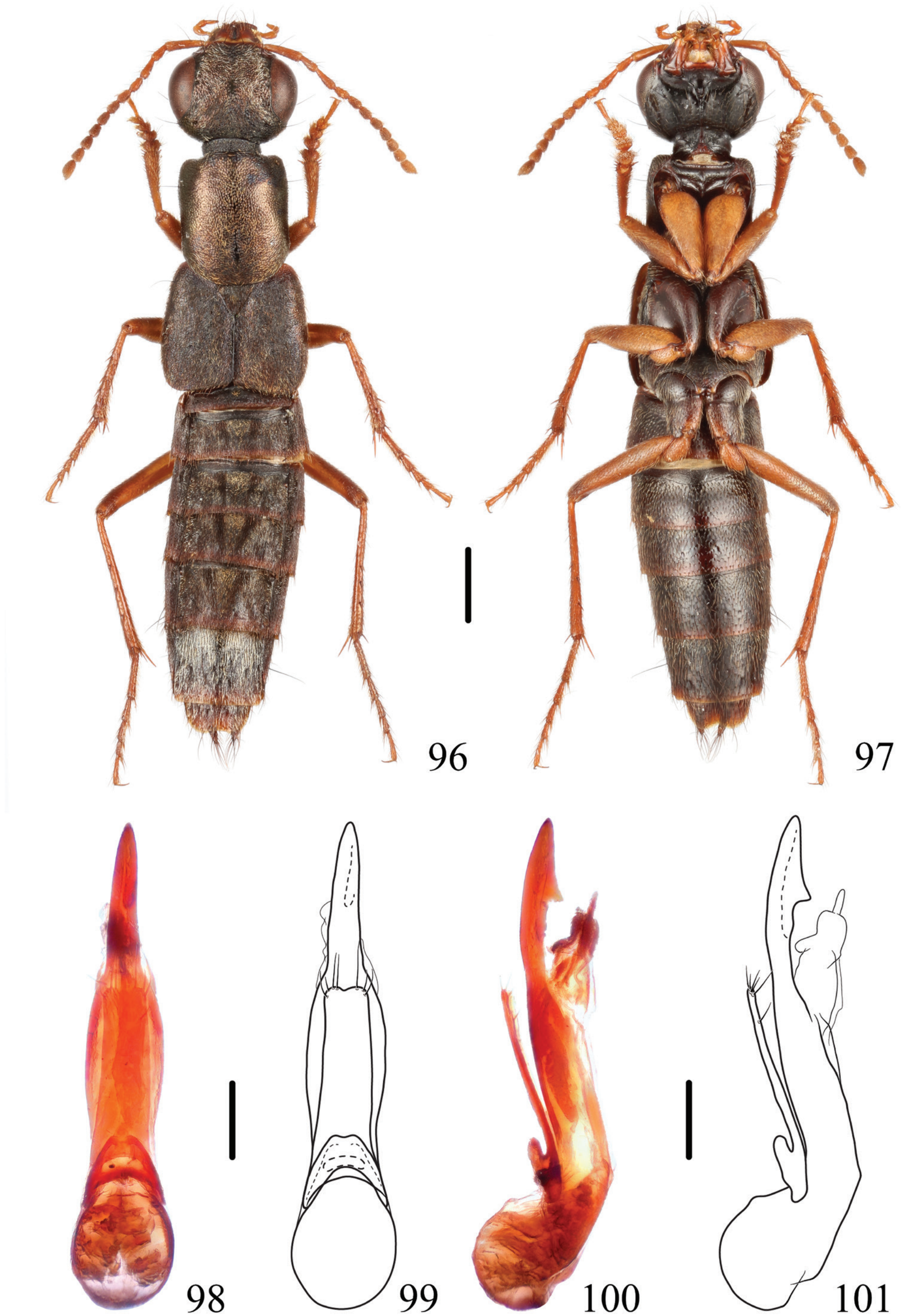

Figures 96–101. *Thoracostrongylus brachypterus* sp. nov. **96, 97** habitus **98–101** aedeagus, ventral (**98, 99**) and lateral (**100, 101**) views. Scale bars: 1 mm (**96, 97**); 0.2 mm (**98–101**).

Description. The new species is almost identical to *T. malaisei*, from which it differs, in addition to the different aedeagus, by the differently colored labrum, which is reddish with each lobe with a large, dark brown, central spot (in *T. malaisei* with a black medial margin along medial excision). Most specimens of *T. malaisei* have at least a very narrow palisade fringe on tergite VII, which is lacking only in the single specimen from Yunnan.

Male. Sternite VIII with medioapical emargination. Aedeagus (Figs 98–101) slender and long, median lobe swollen in middle third and then narrowed apicad in ventral view; in lateral view, median lobe with subapical tooth on dorsal side in apical sixth; paramere rather wide, subparallel-sided, apical margin with slight medial notch, with approximately seven setae.

Female. Sternite VIII with posterior margin entire.

Distribution. China (Sichuan).

Etymology. This specific name (derived from Greek) means "short winged".

***Thoracostrongylus chrysites* sp. nov.**
https://zoobank.org/8DE3842B-DDF8-4AE8-85AE-9E149BDC418B
Figs 102–107, 122
金斑钝胸隐翅虫

Type material. ***Holotype.*** China – **Fujian Prov.** •♂, glued on a card with labels as follows: "China: Fujian, Wuyishan City, Guadun Vill.; 27°45'N, 117°38'E; alt. 1800 m; 01 June 2012; Peng & Dai leg." "Holotype / *Thoracostrongylus chrysites* / Xia, Tang & Schillhammer" [red handwritten label]; SHNU. ***Paratypes.*** China – **Fujian Prov.** • 3♀♀; same data as for the holotype; SHNU • 1♀; Wuyishan City, Guadun Vill.; 27°44'N, 117°38'E; alt. 1700–1800 m; 31 May 2012; Peng & Dai leg.; SHNU.

Measurements. Male: BL: 9.0 mm, FL: 5.0 mm. HL: 1.45 mm, HW: 1.95 mm, CL: 0.95 mm, PO: 0.28 mm, PL: 1.67 mm, PW: 1.45 mm, EL: 1.95 mm, EW: 2.00 mm. HL/HW: 0.74, CL/PO: 3.40, PL/PW: 1.15, EL/EW: 0.97, HW/EW: 0.97, PW/EW: 0.72, HW/PW: 1.35. **Female:** BL: 9.5–10.0 mm, FL: 4.7–5.1 mm. HL: 1.39–1.50 mm, HW: 1.89–2.06 mm, CL: 0.83–1.00 mm, PO: 0.22–0.33 mm, PL: 1.67–1.78 mm, PW: 1.45–1.56 mm, EL: 1.95–2.11 mm, EW: 1.95–2.11 mm. HL/HW: 0.73–0.74, CL/PO: 2.50–4.25, PL/PW: 1.14–1.19, EL/EW: 0.97–1.00, HW/EW: 0.97, PW/EW: 0.72–0.74, HW/PW: 1.31–1.35.

Diagnosis. The new species can be easily recognized by the reddish yellow femora and abdominal tergite VII fully covered with golden pubescence.

Description. The new species is similar to *T. baishanzuensis* sp. nov. except for the following characters: pronotum reddish along posterior margin, elytra reddish at base, abdominal segments with posterior margin reddish, legs reddish yellow without dark markings, although indistinct dark markings may be present near base of profemora; abdominal tergite VI with larger median golden tomentose patch, reaching posterior

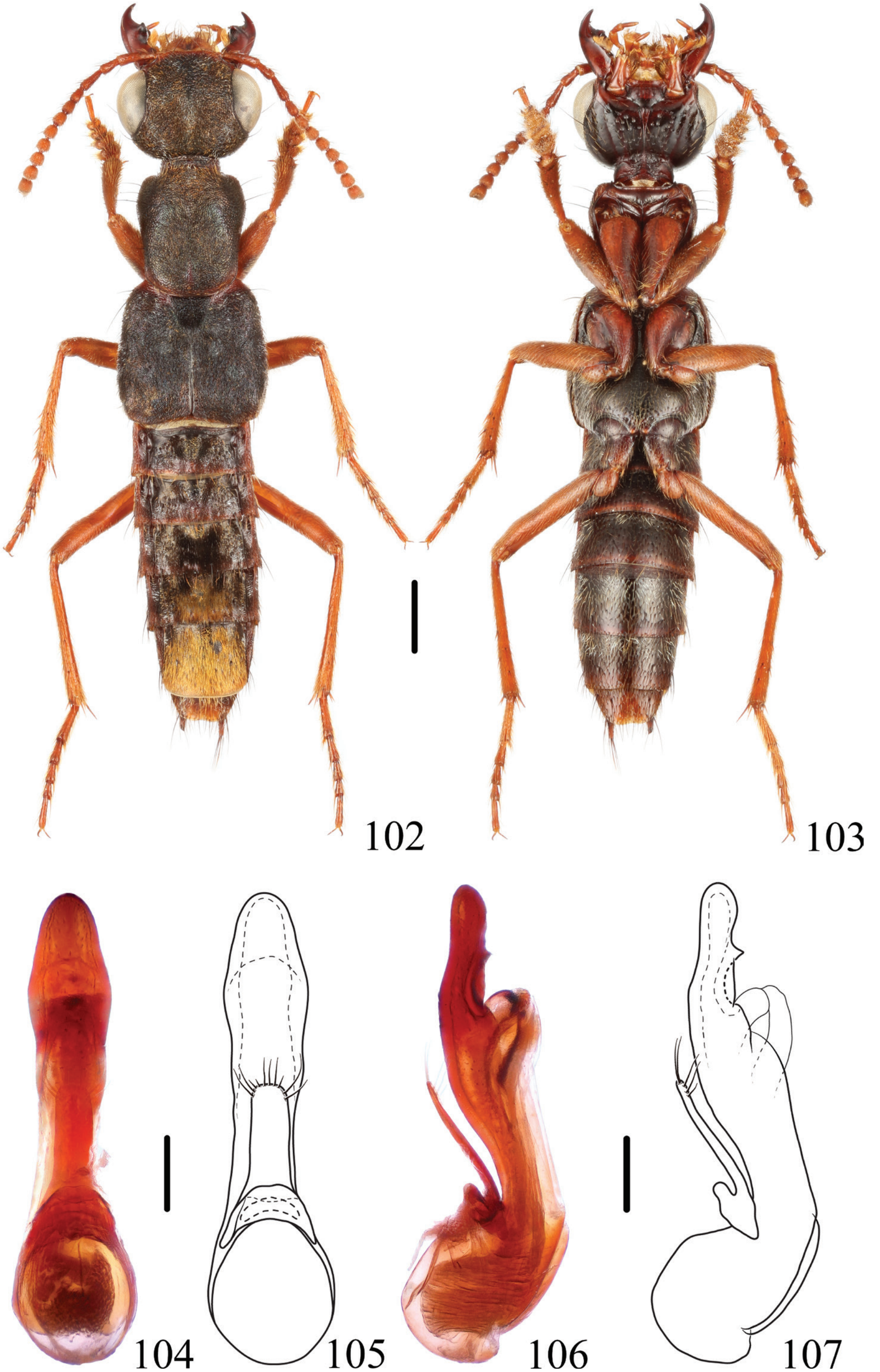

Figures 102–107. *Thoracostrongylus chrysites* sp. nov. **102, 103** habitus **104–107** aedeagus, ventral (**104, 105**) and lateral (**106, 107**) views. Scale bars: 1 mm (**102, 103**); 0.2 mm (**104–107**).

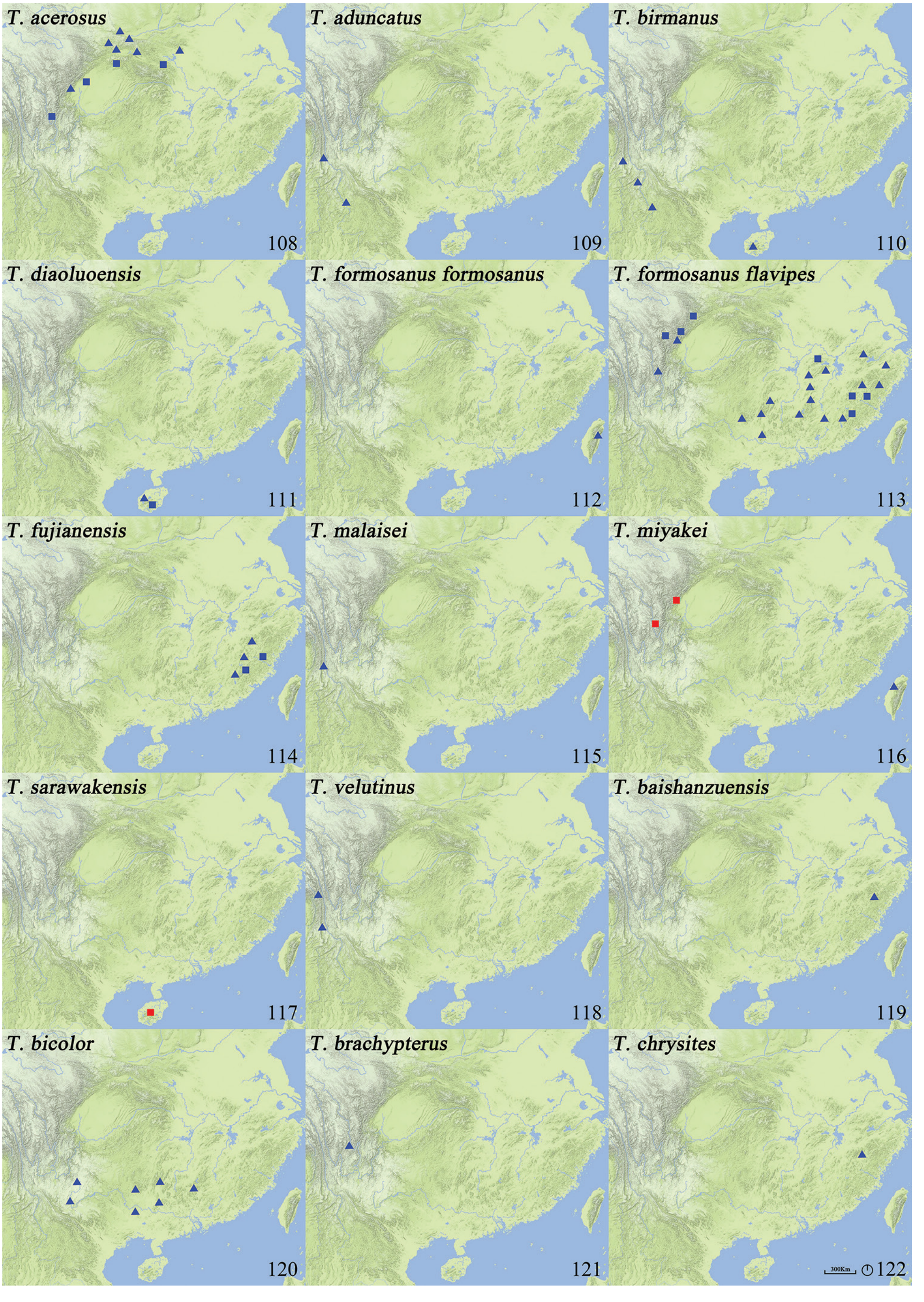

Figures 108–122. Distribution map of *Thoracostrongylus* species of China **108** *T. acerosus* **109** *T. aduncatus* **110** *T. birmanus* **111** *T. diaoluoensis* **112** *T. formosanus formosanus* **113** *T. formosanus flavipes* **114** *T. fujianensis* **115** *T. malaisei* **116** *T. miyakei* **117** *T. sarawakensis* **118** *T. velutinus* **119** *T. baishanzuensis* **120** *T. bicolor* **121** *T. brachypterus* **122** *T. chrysites*. Triangle, localities of specimens examined in this paper; square, localities of specimens listed in previous papers. Red, doubtful localities; blue, trustede localities.

margin of tergite, pair of dark tomentose spots very small; abdominal tergite VII completely covered with golden pubescence.

Male. Sternite VIII with medioapical emargination. Aedeagus (Figs 104–107) slender, in ventral view, median lobe slightly widened in apical fifth, apex broadly rounded; in lateral view, median lobe with subapical dorsal tooth, apex rounded.

Female. Sternite VIII with posterior margin entire.

Distribution. China (Fujian).

Etymology. The species is named after the golden pubescence of abdominal tergite VII.

Key to Chinese species of *Thoracostrongylus*

1 Last three antennomeres whitish, distinctly lighter than previous antennomeres. China (Hainan?), Borneo .... ***T. sarawakensis***
– Last three antennomeres not whitish, similar to or slightly darker than previous antennomeres **2**
2 Posterior margin of abdominal tergite VII without palisade fringe; hindwings reduced **3**
– Posterior margin of abdominal tergite VII with more or less distinct palisade fringe; macropterous **5**
3 Labrum reddish, each lobe with margin along median excision blackish. Specimens of *T. malaisei* without palisade fringe at posterior margin of tergite VII...... **6**
– Labrum reddish, each lobe with variably large dark brown spot in center.......... **4**
4 Pronotum usually with an almost complete, but narrow impunctate midline, rarely with only a specular medio-longitudinal patch in posterior half; China (Sichuan) .... ***T. brachypterus***
– Pronotum without impunctate midline; China (Sichuan?, Taiwan).... ***T. miyakei***
5 Abdominal tergites III–VI without triangular mediobasal golden tomentose patch, instead with some silvery pubescence.. **6**
– Abdominal tergites III–VI each with triangular mediobasal golden tomentose patch.. **9**
6 Fore body with coppery hue, interstices of punctures slightly wider, thus more shiny; palisade fringe at posterior margin of tergite VII very narrow or lacking. China (Yunnan), Myanmar .... ***T. malaisei***
– Fore body with olive greenish hue, punctation extremely dense, fore body thus very matt; palisade fringe at posterior margin of tergite VII distinct **7**
7 Antennae and legs (except for band on femora) entirely reddish. China (Zhejiang, Fujian, Hubei, Hunan, Sichuan, Guangxi, Guangdong, Anhui, Jiangxi).. ***T. formosanus flavipes***
– Antennae with variable number of segments (at least distal six) dark brown or black **8**
8 Meso- and metatibiae and -tarsi usually black. More robust build. China (Taiwan).. ***T. formosanus formosanus***
– Meso- and metatibiae and -tarsi reddish. Body smaller. China (Yunnan), Myanmar .... ***T. velutinus***

9 Femora reddish yellow without black markings **10**
– Femora reddish yellow with black markings **11**
10 Head narrower than elytra in most specimens; abdominal tergite VII fully covered with golden pubescence. China (Fujian) .... ***T. chrysites***
– Head as wide as or slightly wider than elytra; abdominal tergite VII with triangular mediobasal golden tomentose patch. China (Zhejiang)...... ***T. baishanzuensis***
11 Abdominal sternites with long and dense pubescence; posterior margin of male 8th sternite deeply emarginate (Fig. 39). China (Yunnan, Hainan), India, Myanmar .... ***T. birmanus***
– Abdominal sternites with relatively short and sparse pubescence; posterior margin of male 8th sternite shallowly emarginate **12**
12 Abdominal sternites III–V reddish brown, lighter than remaining sternites. China (Guangdong, Hunan, Guangxi, Yunnan) .... ***T. bicolor***
– Abdominal sternites III–V brown, similar to remaining sternites; four species that can be separated with certainty only by the shape of the aedeagus **13**
13 In lateral view, median lobe of aedeagus with an apical or subapical tooth on dorsal side **14**
– In lateral view, median lobe of aedeagus without an apical or subapical tooth on dorsal side (Figs 42–45). China (Hainan)................................... ***T. diaoluoensis***
14 In lateral view, apex of median lobe of aedeagus pointing dorsad, forming a subapical tooth (Figs 17–32). China (Yunnan) .... ***T. aduncatus***
– In lateral view, median lobe of aedeagus without distinct subapical tooth........ **15**
15 In ventral view, apex of median lobe of aedeagus with a sharp tip (Figs 3–14). China (Hubei, Sichuan, Shaanxi, Gansu, Henan) .... ***T. acerosus***
– In ventral view, apex of median lobe of aedeagus with a blunt tip (Figs 55–70). China (Fujian) .... ***T. fujianensis***

Acknowledgements

We express our sincere gratitude to anonymous reviewers for improving the manuscript, to Mr. Qing-Hao Zhao, Miss Yin-Yi Cai, Mr. Wen-Xuan Bi, Mr. Hao Huang, Mr. Lu Qiu, Dr. Zhu-Qing He, Mrs. Jian-Yue Qiu, Mr. Zi-Chun Xiong and Mr. Zhao Pan for donating specimens, and we also thank all the other collectors mentioned in this paper.

References

Bernhauer M (1915) Neue Staphyliniden aus Java und Sumatra. Tijdschrift voor Entomologie 58: 213–243.

Bernhauer M (1943) Neuheiten der palaearktischen Staphylinidenfauna. Mitteilungen der Münchner Entomologischen Gesellschaft 33: 169–188.

Bernhauer M, Schubert K (1914) Staphylinidae IV. In S. Schenkling, Coleopterorum Catalogus, Junk, Berlin 5(57): 289–408.

Blackwelder RE (1952) The generic names of the beetle family Staphylinidae, with an essay on genotypy. Bulletin – United States National Museum 200: [i–iv] 1–483.

Brunke A, Smetana A (2019) A new genus of Staphylinina and a review of major lineages (Staphylinidae: Staphylininae: Staphylinini). Systematics and Biodiversity 17(8): 745–758. https://doi.org/10.1080/14772000.2019.1691082

Cameron M (1932) The fauna of British India including Ceylon and Burma. Coleoptera. Staphylinidae, Taylor and Francis, London. Vol. 3, [xiii +] 1–443.

de Rougemont G-M (2016) New Bornean Staphylinidae (Coleoptera). Linzer Biologische Beitrage 48(1): 559–572. https://sabiis.sabah.gov.my/sites/default/files/uploads/publications/339/guillaume-de-rougemont-new-bornean-staphylinidae-coleoptera.pdf

Fauvel A (1895) Staphylinides nouveaux de l'Inde et de la Malaisie. Revue d'Entomologie 14: 180–286. https://doi.org/10.1017/S102688120005892X

Gridelli E (1924) Ottavo contributo alla conoscenza degli Staphylini. Note su alcune specie di *Ontholestes* Ganglb. della regione orientale. Annali del Museo Civico di Storia Naturale Giacomo Doria 10(3): 204–212.

Hammond PM (1984) An annotated check-list of Staphylinidae (Insecta: Coleoptera) recorded from Borneo. The Sarawak Museum Journal 33(54): 187–218.

Hu F-S (2020) New distributional records of Staphylinina in Taiwan, including a new species of *Miobdelus* Sharp (Coleoptera: Staphylinidae: Staphylininae: Staphylinini). Zootaxa 4768: 334–360. https://doi.org/10.11646/zootaxa.4768.3.2

Scheerpeltz O (1965) Wissenschaftliche Ergebnisse der Schwedischen Expedition 1934 nach Indien und Burma. Coleoptera Staphylinidae (except Megalopsidiinae et Steninae). Arkiv för Zoologi 17(2): 93–371.

Shibata Y (1982) A new species of the genus *Thoracostrongylus* Bernhauer from Taiwan (Coleoptera: Staphylinidae). Transactions of the Shikoku Entomological Society 16: 71–76.

Smetana A, Davies A (2000) Reclassification of the north temperate taxa associated with *Staphylinus sensu lato*, including comments on relevant subtribes of Staphylinini (Coleoptera: Staphylinidae). American Museum Novitates 3787: 1–88. https://doi.org/10.1206/0003-0082(2000)287<0001:ROTNTT>2.0.CO;2

Yang Z, Zhou H-Z, Schillhammer H (2011) Taxonomy of the genus *Thoracostrongylus* Bernhauer (Coleoptera: Staphylinidae) with descriptions of five new species from China. Journal of Natural History 45(7–8): 407–433. https://doi.org/10.1080/00222933.2010.534190

ZooKeys 1131: 135–153 (2022)
doi: 10.3897/zookeys.1131.90392
https://zookeys.pensoft.net

RESEARCH ARTICLE

A peer-reviewed open-access journal
ZooKeys
Launched to accelerate biodiversity research

A revision of the North American genus *Proctorus* (Coleoptera, Curculionidae, Ellescini) with descriptions of two new species

Jake H. Lewis[1,2], Robert S. Anderson[3]

1 *Environmental Science Section, Okinawa Institute of Science and Technology, 1919-1 Tancha, Onna-son, Kunigami-gun, Okinawa, 904-0495 Japan* **2** *Department of Natural History, New Brunswick Museum, 277 Douglas Avenue, Saint John, New Brunswick, E2K 1E5 Canada* **3** *Beaty Centre for Species Discovery, Canadian Museum of Nature, 1740 Chemin Pink, Gatineau, Quebec, J9J 3N7 Canada*

Corresponding author: Jake H. Lewis (jake.lewis@oist.jp)

Academic editor: M. Alonso-Zarazaga | Received 15 July 2022 | Accepted 7 September 2022 | Published 23 November 2022

https://zoobank.org/E32D09D3-C60B-4171-90C5-4393B13F3E47

Citation: Lewis JH, Anderson RS (2022) A revision of the North American genus *Proctorus* (Coleoptera, Curculionidae, Ellescini) with descriptions of two new species. ZooKeys 1131: 135–153. https://doi.org/10.3897/zookeys.1131.90392

Abstract

The rarely collected North American endemic genus *Proctorus* (Coleoptera, Curculionidae, Ellescini) has hitherto contained two described species, *P. armatus* LeConte, 1876 and *P. decipiens* (LeConte, 1876). Here, *Proctorus* is revised and two new species, namely *P. emarginatus* **sp. nov.** and *P. truncatus* **sp. nov.**, are described. Lectotypes for *P. armatus* and *P. decipiens* are designated from known syntypes. All four species in the genus are associated with Salicaceae, but, in addition to differences in external and genital morphology, there is also evidence of differing host plant usage between the species. A photographic key to the four species is provided to facilitate identification.

Keywords

Museology, new species, rare species, species discovery, taxonomy, weevil, willows

Introduction

The genus *Proctorus* LeConte, 1876 (Coleoptera, Curculionidae, Ellescini) has hitherto contained two described species, namely *P. armatus* LeConte, 1876 and *P. decipiens* (LeConte, 1876), which feed on species in the family Salicaceae and are endemic to

North America (O'Brien and Wibmer 1982; Anderson 2002; Bousquet et al. 2013). Members of the genus are rarely collected, and the males possess remarkable modifications (e.g., ventral projections, carinae) on the apical abdominal ventrites (LeConte 1876, 1878). In addition to *Proctorus*, the tribe Ellescini contains several other northern genera that also feed on Salicaceae, namely *Dorytomus* Germar, 1817, *Ellescus* Dejean, 1821, and *Rodotymus* Zumpt, 1932 (Alonso-Zarazaga and Lyal 1999; Anderson 2002; Caldara et al. 2014). The genera *Dorytomus* (100+ species) and *Ellescus* (7 species) are Holarctic in distribution and *Rodotymus* (monotypic) occurs in Kazakhstan and its bordering countries (Alonso-Zarazaga and Lyal 1999; Anderson 2002). Anderson (2002) separated *Proctorus* from the related genera *Dorytomus* and *Ellescus* on the basis of the former possessing basal teeth on the tarsal claws and femoral teeth (*Dorytomus*: simple tarsal claws, with femoral tooth; *Ellescus*: basal teeth on tarsal claws, without femoral tooth). *Proctorus* is currently placed in Ellescina with *Ellescus* (Alonso-Zarazaga and Lyal 1999; Anderson 2002; Bousquet et al. 2013; Caldara et al. 2014; Alonso-Zarazaga et al. 2017) based on shared toothed tarsal claws; the claws are simple in *Dorytomus*, which is generally placed in Dorytomina.

The purpose of this paper is to revise *Proctorus* and describe two new species, *P. emarginatus* sp. nov. and *P. truncatus* sp. nov., from North America.

Materials and methods

Specimens were borrowed from public and private insect collections as well as collected in the field. Institution names and associated acronyms used in this work are presented below:

AFCF Atlantic Forestry Centre, Canadian Forest Service, Natural Resources Canada, Fredericton, New Brunswick, Canada;
CAS California Academy of Sciences, San Francisco, California, U.S.A.;
CBG Center for Biodiversity Genomics, Guelph, Ontario, Canada;
CCCH Claude Chantal Insect Collection, Varennes, Quebec, Canada;
CMNC Canadian Museum of Nature, Ottawa, Ontario, Canada;
CNCI Canadian National Collection of Insects, Arachnids, and Nematodes, Ottawa, Ontario, Canada;
MCZC Museum of Comparative Zoology, Harvard University, Massachusetts, USA;
NBM New Brunswick Museum Insect Collection, Saint John, New Brunswick, Canada;
PdTC Pierre de Tonnancour Collection, Terrasse-Vaudreuil, Quebec, Canada;
RBCM Royal British Columbia Museum, Victoria, British Columbia, Canada;
RWC Reginald Webster Collection, Charters Settlement, New Brunswick, Canada;
UAMIC University of Alaska Museum Insect Collection, Fairbanks, Alaska, USA;
USNM United States National Museum, Washington, District of Columbia, USA.

Specimens were dissected using standard protocols and genitalia were cleared in a water + KOH solution. The sexes were associated primarily by collection event (i.e., same day and locality). All examined specimens have Unique Specimen Identifier (USI) labels attached that read in the form: JHLRSA_PROC_###. All images were taken using a Leica Z16 APOA camera and LAS images stacking software (Leica Microsystems, Wetzlar, Germany).

Results

A taxonomic investigation of the genus *Proctorus* revealed the presence of an additional two species, namely *P. emarginatus* sp. nov. and *P. truncatus* sp. nov., with distinct external and genitalic (male) morphology. The fifth ventrite of males bear modifications (e.g., projections, carinas) that not only define the lineage more broadly, but also contain useful phylogenetic information and allow for unambiguous separation of males of the now four known species. Furthermore, there is some evidence of differing host plant usage between the species (see *P. armatus* species profile). Although females were dissected, no consistent differences in female genitalia were observed and thus females were largely identified by association with males taken during the same collection event (i.e., locality and date). *Proctorus emarginatus* is described here from three male specimens; the female remains unknown. This distinctive species is very rare, apparently restricted to northwestern North America, and has not been collected since 1988, when it was collected in the Northwest Territories. A photographic key to *Proctorus* along with profiles for each species are presented below.

Taxonomy

Genus *Proctorus* LeConte, 1876

Proctorus LeConte, 1876: 212. LeConte 1878: 620. O'Brien and Wibmer 1982: 94. Alonso-Zarazaga and Lyal 1999: 78. Bousquet et al. 2013: 326.

Encalus LeConte, 1876: 213. Type species: *Encalus decipiens* LeConte, 1876 (monotypy).

Type species. *Proctorus armatus* LeConte, 1876, by monotypy.

Gender. Masculine.

Diagnosis. Length 2.9–4.1 mm. Small, rounded, cuticle dark (black) or dark red and some species with dull orange, transverse stripe on elytra. Cuticle with coarse, white and/or yellow hair-like or more broad scales. Rostrum stout, roughly equal in length to pronotum, and often covered in scales up to antennal insertion. Eyes small and circular to oval, extending somewhat onto the rostrum medially. Antennae reddish with small, oval club. Pronotum as wide as long, coarsely punctate, scaled, and with or without prominent smooth, longitudinal midline. Scutellum not covered densely with bright white scales. Elytra oval in dorsal view, striae with large, deep punctures each bearing a scale. Punctures of elytral striae distinctly larger than those of pronotal disk. Interstrial regions of elytra with 2–4 irregular rows of scales. Fifth ventrite of male modified, with various projections and carinae. Fifth ventrite of female unmodified. Legs with femora toothed. Tarsal claws bearing basal tooth. Aedeagus rounded, subquadrate or emarginate at apex. Internal sac with hook-like sclerite.

Species profiles

Proctorus armatus LeConte, 1876

Figs 1D–F, 4, 7C, D, 8A

Proctorus armatus LeConte, 1876: 212 [type locality: south side of Lake Superior (USA)]. LeConte 1878: 620. O'Brien and Wibmer 1982: 94. Alonso-Zarazaga and Lyal 1999: 78. Bousquet et al. 2013: 326.

Material examined. ***Lectotype*** **(here designated): USA:** south side of Lake Superior, Type 5244 (1 female, MCZC), MCZ-ENT00005224.

***Paralectotype*.** **USA:** south side of Lake Superior, Type 2 5244 (1 female, MCZC), MCZ-ENT00529966.

Non-type material. Canada: Alberta: Tp. 39, Rge. 27, 1 April 1985, B.F. & J.L. Carr, on *Populus* (3, CNCI; 1 CMNC), JHLRSA_PROC_313 – JHLRSA_PROC_315, JHLRSA_PROC_321; Calgary, 4–5 July 1974, C.V. Nidek (1, CMNC),

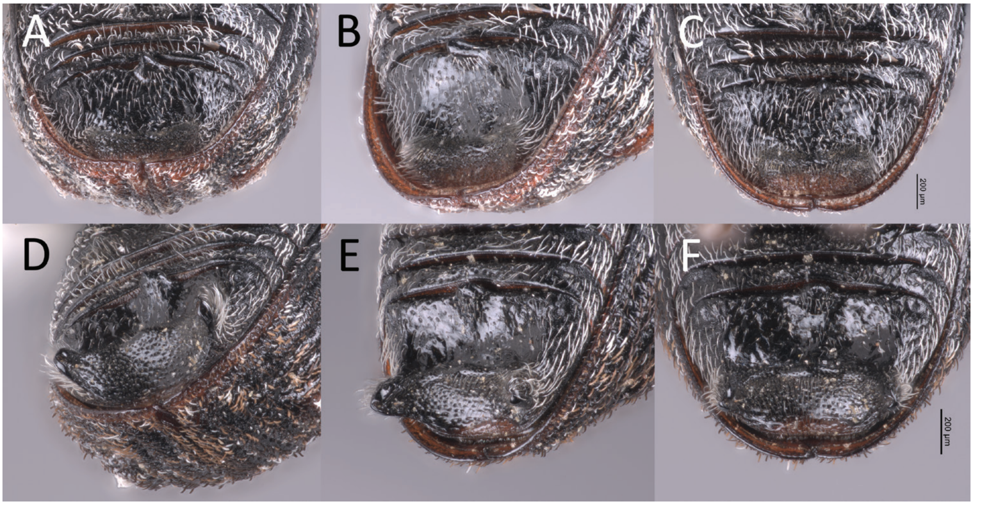

Figure 1. A–C male *Proctorus truncatus* fifth ventrite **A** slightly oblique view **B** oblique view **C** ventral (straight-on) view **D–F** male *Proctorus armatus* fifth ventrite **D** slightly oblique view **E** oblique view **F** ventral (straight-on) view.

JHLRSA_PROC_322; **Manitoba:** Aweme, 7 April 1925, N. Criddle (1, CNCI), JHLRSA_PROC_317; Riding Mountain Park, 9 June 1937, W.J. Brown (1, CNCI), JHLRSA_PROC_319; Winnipeg, 15 April 1916, L.H. Roberts (1, MCZC), MCZ-ENT00726923; **Northwest Territories:** Fort Smith, 13 June 1988, B.F. & J.L. Carr (1, CNCI), JHLRSA_PROC_320; **Ontario:** Moose Factory, 26 June 1948, W.Y. Watson (1, CNCI), JHLRSA_PROC_316. **USA: Alaska:** Willow, Fishhook Road near Deception Creek (61.7622°N, 150.4603°W), 11 August 2014, R. Progar & S. Bresney, on *Populus* (1, UAMIC), UAM100378225; Two Rivers (64.88925°N, 147.0871°W), 24 May 2015, S. Melerotto (1, UAMIC), UAM100430466; **Michigan:** Marquette, (2, MCZC (LeConte and Horn Collection)), MCZ-ENT00772797, MCZ-ENT00772798; Marquette, Hubbard & Schwarz (1, USNM), JHLRSA_PROC_330; **New Mexico:** Cloudcroft, 20 July 1978, J.M. Campbell (1, CNCI), JHLRSA_PROC_318.

Diagnosis. Length 3.8–4.1 mm. Body (especially rostrum and femora) dark, although elytra often with orange stripe extending posteriorly from humerus. Protibiae of male dentate on inner edge. Elytra without clear, distinct x-pattern of white scales. Fifth ventrite of male with two prominent ventral projections apico-laterally which are connected by a transverse ridge; also with a single, smaller ventral projection positioned baso-medially. Apical tooth of metatibiae of male straight. Aedeagus in dorsal view slightly rounded to truncate, not emarginate or significantly expanded laterally.

Notes on types. This species was described based on three specimens collected along the south side of Lake Superior. Two examined syntypes in the MCZC bear several types of labels. Both specimens bear a rectangular brown label reading "J.L. LeConte Coll.", a square red type label reading "Type 5224" and "Type 2 5224", and MCZC unique identifier labels (see specimens examined). One specimen also bears a rectangular brown label reading "Proctorus armatus Lec." and a rectangular white label reading "Jan.-Jul. 2005 MCZ Image Database". The location of the third (male) syntype specimen is unknown; however, the identity (i.e., *P. armatus*) of that specimen is clear, based on LeConte's original description. Here, we designate one of the known *P. armatus* syntypes (MCZ-ENT00005224) as a lectotype to fix the identity of this species.

Taxonomic comments. See same section for *Proctorus truncatus*.

Remarks. This species is likely most closely related to *P. truncatus* as males of both species bear a basomedial projection on the fifth sternite (lacking in other species; males only), have a straight metatibial spur (lacking in *P. decipiens*; only males), and are both large and dark in general form. Furthermore, examined specimens of *P. truncatus* and *P. armatus* were only collected from *Populus* when such data was recorded, whereas examined specimens of *P. decipiens* and *P. emarginatus* have only been collected from *Salix* species. Although more field data should be amassed to support this difference in host plant preference, an emerging pattern of differing host plant preference is apparent and supports the hypothesis that *P. truncatus* and *P. armatus* are closely related.

LeConte (1876) remarked that *P. armatus* lacks femoral teeth. However, we note that the four species treated here all possess a distinct tooth on all femora.

***Proctorus decipiens* (LeConte, 1876)**
Figs 2D–F, 3, 7A, B

Encalus decipiens LeConte, 1876: 213 [type locality: Illinois and Minnesota]. Alonso-Zarazaga and Lyal 1999: 78.
Proctorus decipiens; LeConte, 1878: 620. O'Brien and Wibmer 1982: 94. Bousquet et al. 2013: 326.

Material examined. ***Lectotype* (here designated): USA: Minnesota** (see Notes on types), Type 5349 (1 female, MCZC), MCZ-ENT00005349.

Non-type material. Canada: Alberta: Fitzgerald, 14 June 1988, B.F. & J.L. Carr (1, CNCI), JHLRSA_PROC_096; Lethbridge, 16 May 1930, J.H. Pepper (1, CNCI), JHLRSA_PROC_198; Crow's Nest Pass, 6–7 June 1930, J.H. Pepper (2, CNCI), JHLRSA_PROC_051, JHLRSA_PROC_052; Calgary, 30 June 1957 – 5 July 1958, B.F. & J.L. Carr (4, CNCI), JHLRSA_PROC_191 – JHLRSA_PROC_195; Calgary, 11–12 June 1890, H.C. Fall Collection (1, MCZC), MCZ-ENT00727128; Writing-on-Stone Provincial Park (0.5 miles north), 14 June 1982, R.S. Anderson (3, CMNC), JHLRSA_PROC_041 – JHLRSA_PROC_043; Sturgeon River at Lac Ste. Anne (50°43'N, 114°20'W), 1–3 June 1982, J.S. Richardson (1, CMNC), JHLRSA_PROC_037; Magrath, 20 May 1938, G.S. Walley (1, CNCI), JHLRSA_PROC_140; Medicine Hat, 1 June 1963 – 9 June 1973, B.F. & J.L. Carr (1, CNCI), JHLRSA_PROC_170 – JHLRSA_PROC_173; Edmonton, 8 June 1916 – 1 July 1920, F.S. Carr (2, CNCI; 15 CAS; 1 MCZC; 1 USNM), JHLRSA_PROC_177, JHLRSA_PROC_178, JHLRSA_PROC_210 – JHLRSA_PROC_224, JHLRSA_PROC_337, MCZC00726934; Brule Lake, 29 June 1989, B.F. & J.L. Carr (1, CNCI), JHLRSA_PROC_143; Fort Macleod, 20 June 1976, B.F. & J.L. Carr (2, CNCI), JHLRSA_PROC_101, JHLRSA_PROC_102; Ghost Dam, 1 June 1975, B.F. & J.L. Carr (1, CNCI), JHLRSA_PROC_103; Edson (30 miles west of), 11 June 1950, P. Rubtsoff (1, CAS), JHLRSA_PROC_227; **British Columbia:** Salmon Arm, 9 June 1940, H. Leech (1, MCZC), MCZ-ENT00726945; Brisco, 19 June 1932, O. Bryant (1, CAS), JHLRSA_PROC_241; Terrace, 1927, M.E. Hippisley (2, MCZC), MCZ-ENT0026933; Vancouver, 30 April 1932, G.R. Hopping (4, CAS), JHLRSA_242 – JHLRSA_PROC_245; Vancouver, 24 April 1930, G.H. Larnder (4, RBCM), ENT991-111637, ENT991-111639, ENT991-111640, ENT991-111642; Princeton, Missezula Lake, 16 June 1929, G. Stace Smith, on *Salix* (1, RBCM), ENT991-111638; Harrison, 9 June 1899, A. Hanham (1, RBCM), ENT991112019; Saanich, 12 May 1930, W.H. Preece (1, CNCI), JHLRSA_PROC_067; Creston, 16 June 1950 – 18 April 1956, G. Stace Smith (5, CNCI; 3, CAS), JHLRSA_PROC_109 – JHLRSA_PROC_113, JHLRSA_PROC_246; Revelstoke, 2 June 1978, B.F. & J.L. Carr (1, CNCI), JHLRSA_PROC_196; Fort Steele, 23 May 1977, B.F. & J.L. Carr (3, CNCI), JHLRSA_PROC_188 – JHLRSA_PROC_190; Sicamous, 2 June 1978, B.F. & J.L. Carr (1, CNCI), JHLRSA_PROC_107; Golden (9 miles northwest), 28 August 1973, R.H. Parry (1, CMNC), JHLRSA_PROC_040; Golden, 27 June–30 August 1975, B.F. & J.L. Carr (2, CNCI),

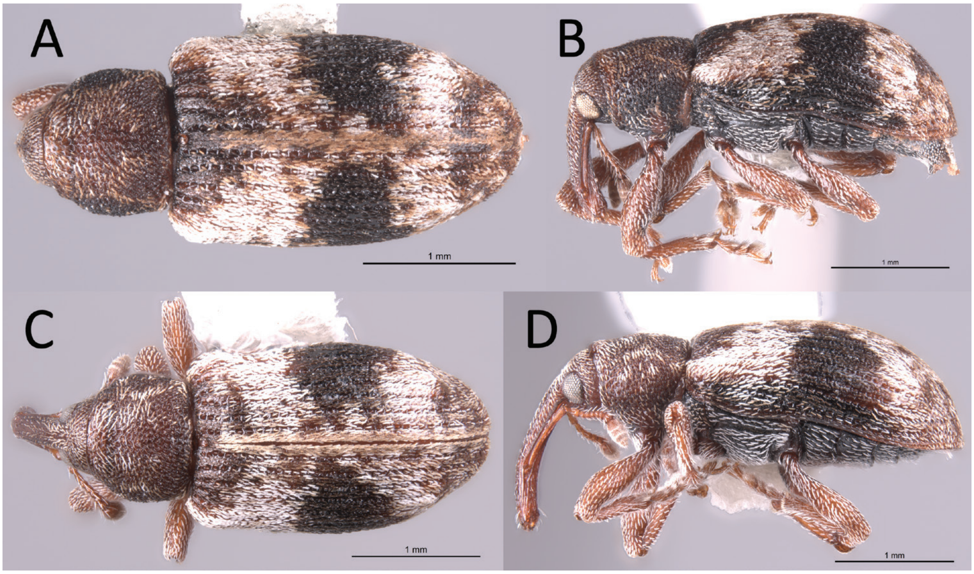

Figure 3. *Proctorus decipiens* habitus (USI: JHLRSA__PROC_095, JHLRSA_PROC_037) **A** dorsal (♂) **B** lateral (♂) **C** dorsal (♀) **D** lateral (♀).

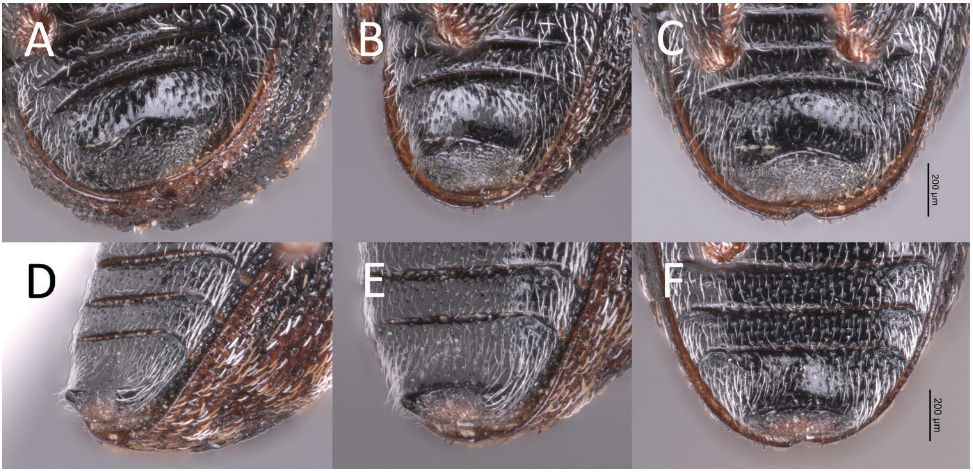

Figure 2. A–C male *Proctorus emarginatus* fifth ventrite **A** slightly oblique view **B** oblique view **C** ventral (straight-on) view **D–F** male *Proctorus decipiens* fifth ventrite **D** slightly oblique view **E** oblique view **F** ventral (straight-on) view.

JHLRSA_PROC_104, JHLRSA_PROC_105; Robson, June 1949 (1, CNCI), JHLRSA_PROC_135; Vancouver, 30 April 1932, G.R. Hopping (4, CNCI), JHLRSA_PROC_131 – JHLRSA_PROC_134; Lake Errock, near Deroche, 2 June – 4 July 1953, S.D. Hicks, on *Salix* (14, CNCI), JHLRSA_PROC_145 – JHLRSA_PROC_158; Blanket Creek, 9 June 1984, B.F. & J.L. Carr (1, CNCI), JHLRSA_PROC_114; **Manitoba:** Aweme, 24 June 1907 – 27 May 1909, N. Criddle (1, MCZC; 1, USNM),

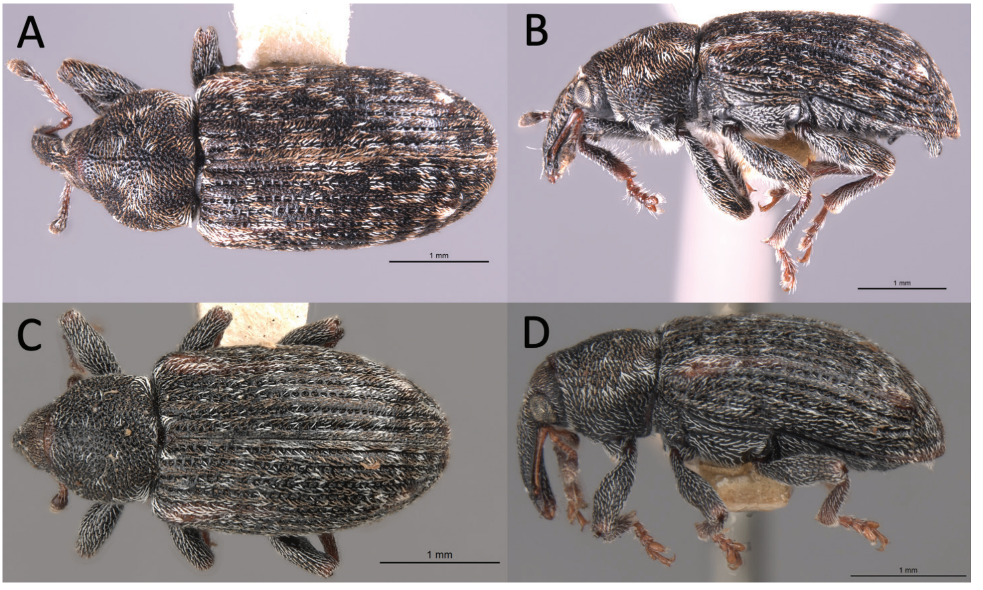

Figure 4. *Proctorus armatus* habitus (USI: JHLRSA_PROC_318, MCZ-ENT00005224) **A** dorsal (♂) **B** lateral (♂) **C** dorsal (♀) **D** lateral (♀).

MCZ-ENT00727134, JHLRSA_PROC_336; Russell, 21 July 1954, Brooks-Wallis (1, CNCI), JHLRSA_PROC_050; Winnipeg, 22 May–5 June 1915, J.B. Wallis (1, CNCI; 1, MCZC), JHLRSA_PROC_205, MCZENT-00727131; Riding Mountain Park, 8 June 1937 – 9 June 1938, W.J. Brown (10, CNCI), JHLRSA_PROC_160 – JHLRSA_PROC_169; **New Brunswick:** Boiestown, 13 July 1928, W.J. Brown (1, CNCI), JHLRSA_PROC_059; Carleton County, Wakefield, Meduxnekeag Valley Nature Preserve (46.1931°N, 67.6825°W), 31 May 2005, M.-A. Giguère & R. Webster (1, RWC), JHLRSA_PROC_002; Madawaska County, Gounamitz Road (47.62250°N, 68.96973°W), 21 June 2011, Martin N. Turgeon (1, NBM), NBM-070118; Restigouche County, Summit Area, 7 June 2011, Martin N. Turgeon (1, NBM), NBM-070119; **Northwest Territories:** Fort Simpson, Manners Creek, 11 June 1972, A. Smetana (1, CNCI), JHLRHS_PROC_095; Highway 5 (2 km east of Junction with Highway 2), 16 June 1988, B.F. & J.L. Carr (3, CNCI), JHLRSA_PROC_200 – JHLRSA_PROC_202; Highway 7 (125 km north of British Columbia border), 25 June 1988, B.F. & J.L. Carr (1, CNCI), JHLRSA_PROC_203; Along Highway 7 (219 km north of British Columbia border), 21 June 1988, B.F. & J.L. Carr (1, CNCI), JHLRSA_PROC_204; **Nova Scotia:** Tusket, 27 June 1947, W.J. Brown (1, CNCI), JHLRSA_PROC_141; Hants County, Mount Uniacke, 14 June 1947, W.J. Brown (4, CNCI), JHLRSA_PROC_136 – JHLRSA_PROC_139; Waverley, 10 June 1947, W.J. Brown (1, CNCI), JHLRSA_PROC_144; Bathurst, July 1915, J.N. Knull (1, CAS), JHLRSA_PROC_233; **Ontario:** Toronto, 25 May 1896, R.J. Crew (1, USNM), JHLRSA_PROC_335; Parry Sound, 14 July 1932, G.S. Walley (1, CNCI), JHLRSA_PROC_199;

Smoky Falls, Mattagami River, 21 June 1934, G.S. Walley (1, CNCI), JHLRSA_PROC_055; Merivale, 4 May 1937, W.J. Brown (2, CNCI), JHLRSA_PROC_053, JHLRSA_PROC_054; Mer Bleue, Ottawa, 28 May 1935, W.J. Brown (1, CNCI), JHLRSA_PROC_060; Black Rapids, Ottawa, 23 May 1927, W.J. Brown (1, CNCI), JHLRSA_PROC_099; Sultan Road, 6.8 km west of junction with Highway 144, 26 June 1996, B.F. & J.L. Carr (2, CNCI), JHLRSA_PROC_064, JHLRSA_PROC_065; Ottawa, 9 May 1930, W.J. Brown (1, CNCI), JHLRSA_PROC_108; Longlac (13 km west) along Highway 11, 10 June 1995, B.F. & J.L. Carr (1, CNCI), JHLRSA_PROC_206; Pass Lass Junction (13 km southwest), 10 June 1995, B.F. & J.L. Carr (1, CNCI), JHLRSA_PROC_181; Prince Edward County, 1 June 1919 – 23 June 1923, J.F. Brimley (2, CNCI), JHLRSA_PROC_179 – JHLRSA_PROC_180; Rainy River District, 18 June – 7 September 1924, J.F. Brimley (3, CNCI), JHLRSA_PROC_174 – JHLRSA_PROC_176; Hastings County, 14 June 1938 (1, CNCI), JHLRSA_PROC_159; Moosonee, 30 June 1973, J.M. Campbell & Parry (1, CMNC), JHLRSA_PROC_039; Pickle Lake (8 miles north), 19–22 June 1973, J.M. Campbell & Parry (5, CMNC), JHLRSA_PROC_045 – JHLRSA_PROC_049; Lake Superior Provincial Park, Frater, 13 June 1973, J.M. Campbell & R. Parry (1, CMNC), JHLRSA_PROC_035; Lake Superior Provincial Park, Noisy Bay, 13 June 1973, J.M. Campbell & R. Parry (1, CMNC), JHLRSA_PROC_034; Carleton County, Constance Bay, 4 May 1982, H. & A. Howden (1, CMNC), JHLRSA_PROC_036; Thunder Bay District, Stanley, 9–17 June 1981, M. Kaulbars (1, CMNC), JHLRSA_PROC_044; **Quebec:** Aylmer, 16 August 1916, J.N. Knull (1, CAS; 1, MCZC), JHLRSA_PROC_234, MCZ-ENT00727133; Duparquet, 11 June 1936 – 21 June 1944, G. Stace Smith, on *Salix* (5, CAS), JHLRSA_PROC_235 – JHLRSA_PROC_239; Duparquet, 11 June 1936, G. Stace Smith (1, USNM), JHLRSA_PROC_333; Montreal, Liebeck Collection (2, MCZC), MCZ-ENT00726926, MCZ-ENT00726927; Sept-Îles, 8 June 1929, W.J. Brown (1, CNCI), JHLRSA_PROC_061; Temiscamingue County, L'Etang, 16 August 1985, Larochelle & Lariviere (1, CNCI), JHLRSA_PROC_062; Cadillac, 2 July 1981 (1, CNCI), JHLRSA_PROC_063; Knowlton, 14 June 1928, G.H. Fisk (1, CNCI), JHLRSA_PROC_097; Cascapedia, 11–20 June 1938, W.J. Brown (25, CNCI), JHLRSA_PROC_068 – JHLRSA_PROC_092; Forillon National Park, trail off of park compound (48.857°N, 64.376°W), 10–17 June 2013, F. Tremblay (1, CBG), BIOUG11159-H04, JHLRSA_PROC_001; Gatineau, Mont Cascades (45.590941°N, 75.850435°W), 13 May 2021, J.H. Lewis, beaten off *Salix* sp. (1, CMNC); Gatineau, Mont Cascades (45.590941°N, 75.850435°W), 12 May 2021, J.H. Lewis, beaten off *Salix* sp. (1, CMNC); Laurentides Wildlife Reserve (km. 145), 16 June 2012, P. de Tonnancour, beating *Salix* sp. (2, CMNC; 11, PdTC), JHLRSA_PROC_004 – JHLRSA_PROC_016; Laurentides Wildlife Reserve, Mre-du-Sault (km. 117), 16 June 2012, P. de Tonnancour, beating *Salix* sp. (10, PdTC), JHLRSA_PROC_017 – JHLRSA_PROC_026; Sainte-Catherine, 5 June 2007, C. Tessier (1, PdTC), JHLRSA_PROC_027; Mont Rigaud, 20 April 2012, P. de Tonnancour, beating *Salix* sp. (1, PdTC), JHLRSA_PROC_028; Grand-Remous, Chemin Baskatong (46.7729°N, 75.8802°W), 27 May 2017, P. de Tonnancour, beating *Salix* sp. (3, PdTC), JHLRSA_PROC_029 – JHLRSA_PROC_31;

Villeroy, 30 May 1990, C. Chantal (1, CCCH), JHLRSA_PROC_032; Quebec, 21 June 1966, C. Chantal (1, CCCH), JHLRSA_PROC_033; **Saskatchewan:** Val Marie, 11 June 1955, A.R. Brooks (1, CNCI), JHLRSA_PROC_100; Elbow, 23 June 1954, Brooks-Wallis (2, CNCI), JHLRSA_PROC_093, JHLRSA_PROC_094; **Yukon:** Eagle River, Dempster Highway, 15 June 1980, R.J. Cannings (1, CMNC), JHLRSA_PROC_038; Kirkman Creek, 13 June 1928 (1, CNCI), JHLRSA_PROC_142; Dempster Highway (mile 123), 2 August 1979, B.F. & J.L. Carr (2, CNCI), JHLRSA_PROC_186, JHLRSA_PROC_187; Dawson, 24–29 June 1924, H.C. Fall Collection (2, MCZC), MCZ-ENT00727135, MCZ-ENT00727136. **USA: Alaska:** Along Wales Highway, Hess Creek (149°10'N, 65°40'W), 10 July 1978, J.M. Campbell & A. Smetana (3, CNCI), JHLRSA_PROC_056 – JHLRSA_PROC_058; Selawik National Wildlife Reserve (66.85873°N, 158.16618°W), 24 June 2010, D.S. Sikes, sweep in open sand dunes (1, UAMIC), UAM100283525; Fairbanks, Chena Ridge (64.79672°N, 148.02143°W), 12 June 2005, D.S. Sikes, silver birch and black spruce forest (4, UAMIC), UAM100361536-UAM100361539; Circle, 21 June 1928 (13, CNCI), JHLRSA_PROC_115 – JHLRSA_PROC_127; Circle Hot Springs, 20 June 1945, J.C. Chamberlin, swept from mustard (1, USNM), JHLRSA_PROC_355; Beaver, 24 June 1928 (3, CNCI; 1, MCZC), JHLRSA_PROC_128 – JHLRSA_PROC_130, MCZ-ENT00727130; **California:** Del Norte County, Smith River Recreational Area (41°47.696'N, 124°02.184'W), 27 June 2002, F.G. Andrews & A.J. Gilbert (1, CMNC), JHLRSA_PROC_003; Trinidad, 7 June 1925, J.O. Martin (1, CAS), JHLRSA_PROC_240; Del Norte County, Gasquet, 21 April 1966, T. Peacock & R.P. Allen, on *Sambucus racemosa* L. (1, USNM), JHLRSA_PROC_347; **Colorado:** Fort Collins, Liebeck Collection (1, MCZC), MCZ-ENT00726929; Garland (3, MCZC Main Collection and Horn Collection), MCZ-ENT00726940, MCZ-ENT00726941, MCZ-ENT00772808; Garland, Hubbard and Schwarz (2, USNM), JHLRSA_PROC_350, JHLRSA_PROC_351; La Veta (1, MCZC (LeConte Collection)), MCZ-ENT00772802; La veta, Hubbard & Schwarz (2, USNM), JHLRSA_PROC_348, JHLRSA_PROC_349; “Colorado”, F.C. Bowditch Collection (1, MCZC), MCZ-ENT00726939; “Col” (2, MCZC (Horn Collection)), MCZ-ENT00772803, MCZ-ENT00772804; **Idaho:** Burley, 2 June 1986, B.F. & J.L. Carr (1, CNCI), JHLRSA_PROC_066; Coolin, Priest Lake, 19 July 1927, E.C. Van Dyke (1, CAS), JHLRSA_PROC_232; Coeurd’ Alene, June, Wickham (2, MCZC), MCZ-ENT00726935, MCZ-ENT00726936; **Maine:** Monmouth, 16 July 1913 – 16 July 1915, C.A. Frost, on *Salix* (2, MCZC), MCZ-ENT00726931, MCZ-ENT00726932; Rockland, July 1893, H.C. Fall Collection (1, MCZC), MCZ-ENT00727129; **Massachusetts:** Stoneham, July 1910, F.A. Sherriff (1, MCZC), MCZ00726943; **Michigan:** Marquette, Hubbard & Schwarz (2, USNM), JHLRSA_PROC_338, JHLRSA_PROC_339; Detroit, Hubbard & Schwarz (1, USNM), JHLRSA_PROC_342; **Minnesota:** Grand Marais, 25 August 1951, Bryant (4, CAS), JHLRSA_PROC_207 – JHLRSA_PROC_209, JHLRSA_PROC_300; Duluth, A. Fenyes Collection (1, CAS), JHLRSA_PROC_231; Ithaca State Park, September 1927, S. Garthside (1, USNM), JHLRSA_PROC_341; **Montana:** Tiber Dam, 28 June 1982, B.F. & J.L. Carr (1, CNCI), JHLRSA_PROC_197; “Mon.” (2, USNM), JHLRSA_PROC_331, JHLRSA_PROC_332; Bear Paw Mountain, Hubbard and

Schwarz (2, USNM), JHLRSA_PROC_352, JHLRSA_PROC_353; Bozeman, 31 May 1907 (1, USNM), JHLRSA_PROC_354; **New Hampshire:** Squam Lake, 2 July 1931, J.W. Green (1, CAS), JHLRSA_PROC_301; New York: Cranberry Lake, 20 June 1922, M.H. Hatch (1, USNM), JHLRSA_PROC_340; **Oregon:** Corvallis, June 1919, Liebeck Collection, on willow (1, MCZC), MCZ-ENT00726930; **Utah:** Tony Grove (2 km west) along Highway 89, 24 June 1986, B.F. & J.L. Carr (1, CNCI), JHLRSA_PROC_106; Utah Lake, June 1919, Hubbard and Schwarz (1, CAS), JHLRSA_PROC_302; Utah Lake (2, MCZC (Horn Collection)), MCZ-ENT00772806, MCZ-ENT00772807; Utah Lake, Hubbard & Schwarz (4, USNM), JHLRSA_PROC_342 – JHLRSA_PROC_346; Duchesne, 23 June 1948, G.F. Knowlton (1, USNM), JHLRSA_PROC_334; **Washington:** Olympia, Liebeck Collection (1, MCZC), MCZ-ENT00726928; Monroe, 4–14 July 1906, Van Dyke Collection (3, CAS), JHLRSA_PROC_225, JHLRSA_PROC_226, JHLRSA_PROC_303; Easton, Koebele Collection (2, CAS), JHLRSA_PROC_228, JHLRSA_PROC_229; Everett, July 1912, A. Fenyes Collection (2, CAS), JHLRSA_PROC_230; Everett, July 1912, Wickham (3, MCZC; 5 USNM), MCZ-ENT00726937, MCZ-ENT00726938, MCZ-ENT00727132, JHLRSA_PROC_356 – JHLRSA_PROC_360; Silver Lake, 28 June 1945, Anderson, on willow (5, USNM), JHLRSA_PROC_361 – JHLRSA_PROC_363; Seattle, on willow (1, USNM), JHLRSA_PROC_364; Montesano, 11 August 1944, Forse & Smith, on willow (4, USNM), JHLRSA_PROC_365 – JHLRSA_PROC_368; Yakima County, White Swan, 1 May 1979, B. McAfee (7, USNM), JHLRSA_PROC_369 – JHLRSA_PROC_375; **Wyoming:** Junctions of Highway 120 and 296, 22–27 June 1982, B.F. & J.L. Carr (4, CNCI), JHLRSA_PROC_182 – JHLRSA_PROC_185; "Wy" (1, MCZC (Horn Collection)), MCZ-ENT00772805; **UNSPECIFIED LOCALITY:** Central United States (1, MCZC (LeConte Collection)), MCZ-ENT00772800.

Notes on types. This species was described based on two specimens collected from Illinois and Minnesota. One syntype specimen is deposited in the MCZC (see specimens examined) and is likely the Minnesota syntype as it bears a circular blue label that LeConte used to indicate specimens collected around Lake Superior. The specimen bears six labels: a circular blue label, a square brown label reading "2008", a square red type label reading "Type. 5349", a rectangular brown ID label reading "P. decipiens Lec. (Encalus)", a rectangular white label reading "Jan.–Jul. 2005 MCZ Image Database", and a rectangular white label reading "MCZ-ENT00005349". The location of the second syntype is unknown. Here, we designate the examined *P. decipiens* syntype (MCZ-ENT00005349) as a lectotype to fix the identity of this species.

Diagnosis. Length 2.9–3.1 mm. Body (especially rostrum and femora) rufous. Protibiae of male not prominently dentate on inner edge. Elytra with clear, distinct x-pattern of white scales. Fifth ventrite of male with two prominent ventral apico-lateral projections which are connected by a transverse ridge; without any baso-medial ventral projection. Apical tooth of metatibiae of male curved. Aedeagus with apex with margins weakly expanded laterally, and coming to weak, rounded point.

Ecology. This species has been collected frequently from *Salix* and is occasionally taken in large numbers. The record of one specimen (JHLRSA_PROC_347) collected from *Sambucus racemosa* L. is likely incidental and does not reflect use of *Sambucus* as a host.

***Proctorus truncatus* Lewis & Anderson, sp. nov.**
https://zoobank.org/172594D2-4FA6-4AEB-B275-91D0172173AD
Figs 1A–C, 5, 7E, F, 8B

Material examined. ***Holotype*: Canada: Ontario:** Constance Bay, 17 May 2003, H. & A. Howden (1 male, CMNC), JHLRSA_PROC_292. ***Paratypes*: Canada: Alberta:** Ghost Dam, 25 May 1983, B.F. & J.L. Carr (1, CNCI), JHLRSA_PROC_299; Tp. 12, Rge. 1, 11 April 1976, B.F. & J.L. Carr (1, CNCI), JHLRSA_PROC_304; Tp. 34, Rge. 4, 21 May 1962, B.F. & J.L. Carr (1, CNCI), JHLRSA_PROC_311; Olds, T.N. Willing (1, USNM), JHLRSA_PROC_328; **British Columbia:** Paul Lake, 24 May 1933, A. Thrupp (3, CAS), JHLRSA_PROC_269 – JHLRSA_PROC_271; Terrace, M.E. Hippisley (1, MCZC), MCZ-ENT00726924; **Manitoba:** Aweme, 5 May 1898 – 12 May 1914, N. Criddle, on *Populus* (1, CNCI; 2 MCZC), JHLRSA_PROC_306, MCZ-ENT00726919, MCZ-ENT00726920; **New Brunswick:** Northumberland County, Parker, 3 June 1959, on Aspen (1, AFCF), AFCF0019835; York County, Durham, 5 May 1958, G.W. Barter, on *Populus tremuloides* Michx. (1, AFCF), AFCF0019834; Fredericton, 29 April 1913 (1, CNCI), JHLRSA_PROC_298; **Ontario:** Constance Bay, 17 May 2003, H. & A. Howden (1, CMNC), JHLRSA_PROC_293; Honey Harbor, 10 June 1932, G.S. Walley (1, CNCI), JHLRSA_PROC_305; Lake Superior Provincial Park, Old Woman Bay, 11 June 1973, M. Campbell and R. Parry (1, CMNC), JHLRSA_PROC_295; Lake Superior Provincial Park, Sand River, 6 June 1973, M. Campbell and R. Parry (1, CMNC), JHLRSA_PROC_294; Bell's Corner, 2 June 1950, S.D. Hicks (1, CNCI), JHLRSA_PROC_297; Rainy River District, 18–20 June 1924, J.F. Brimley (1, CNCI; 1 MCZC), JHLRSA_PROC_309, MCZ-ENT00726925; Rainy River, 11 June 1924, J.F. Brimley (1, USNM), JHLRSA_PROC_326; Sudbury, 1889 (1, CNCI), JHLRSA_PROC_310; **Quebec:** Harrington Lake, 1 June 1954, H.J. Huckel (1, CNCI), JHLRSA_PROC_308; Duparquet, 11 June 1935–26 May 1944, G. Stace Smith, on *Populus tremuloides* Michx. (18, CAS; 2, CMNC; 1, USNM), JHLRSA_PROC_247 – JHLRSA_PROC_266, JHLRSA_PROC_329; St. Rose, 1 June 1939, G. Stace Smith, on *Pinus contorta* Douglas ex Loudon (1, CAS), JHLRSA_PROC_267; Saint Hyppolyte, Biology station of Laurentides (45.9778°N, 74.0039°W), 3 June 2017, P. de Tonnancour, beaten from *Populus grandidentata* Michx. (2, CMNC; 8, PdTC), JHLRSA_PROC_272 – JHLRSA_PROC_281; Saint-Pierre, 3 June 1984, C. Chantal, from *Populus grandidentata* Michx. (2, CMNC; 8, CCCH), JHLRSA_PROC_282 – JHLRSA_PROC_291; **Saskatchewan:** Cut Knife, 29 August 1940, A.R. Brooks (1, CNCI), JHLRSA_PROC_307; Montreal River, 26 May 1954, on *Populus* (1, CNCI), JHLRSA_PROC_296; **USA: Michigan:** Marquette (1, MCZ (Horn Collection))), MCZ-ENT00772799; **Minnesota:** "Min.", H.C. Fall Collection (1, MCZC), MCZ-ENT00726922; **New Hampshire:** Mount Washington (summit), 29 July 1954, Becker, Munroe & Mason (1, CNCI), JHLRSA_PROC_312; **New Mexico:** Santa Fe, 14 June 1935, Van Dyke Collection (1, CAS), JHLRSA_PROC_268; **New York:** Chateaugay Lake, F.C. Bowditch (1, MCZC), MCZ-ENT00726921; **Utah:** Logan, 29 April 1934, T.O. Thatcher (1, USNM), JHLRSA_PROC_327.

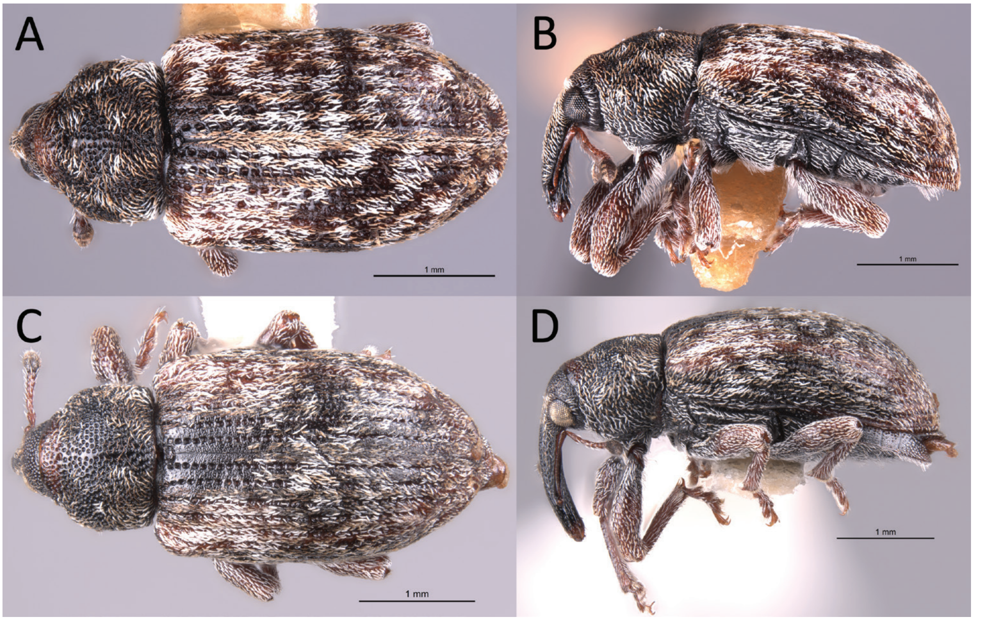

Figure 5. *Proctorus truncatus* habitus (USI: JHLRSA_PROC_305, JHLRSA_PROC_282) **A** dorsal (♂) **B** lateral (♂) **C** dorsal (♀) **D** lateral (♀).

Diagnosis. Length 3.7–4.0 mm. Body (especially rostrum and femora) dark, although elytra often has orange stripe extending posteriorly from humerus. Protibiae of male not prominently dentate on inner edge. Elytra without clear, distinct x-pattern of white scales. Fifth ventrite of male with two low, minutely serrate ridges apico-laterally, which are connected by a transverse ridge; fifth ventrite also with a single, smaller ventral projection positioned baso-medially. Apical tooth of metatibiae of male straight. Aedeagus with apex dorsoventrally flattened and expanded laterally.

Etymology. The specific name refers to the truncate ventral projections on the fifth ventrite of males (compare with *P. armatus* which has long ventral projections).

Ecology. This species has been collected from *Populus grandidentata* Michx. and *P. tremuloides* Michx. The single record of a specimen (JHLRSA_PROC_267) from *Pinus contorta* Douglas ex Loudon is likely incidental.

Taxonomic comments. This species was long confused with the less common *P. armatus* from which it differs in the armature of the fifth ventrite (males), protibia dentation (males), genitalia (males), rostrum length (females) and overall body shape (both sexes). LeConte (1878: 620) wrote of *P. armatus* (two years after describing that species): "Several specimens of this curious insect were found at Marquette, and among them are ♂♂ in which the two processes of the apical edge of the fifth ventral segment are very short, and scarcely apparent, though the anterior tubercle or spine and the large excavation are as well developed as in the other specimens." Clearly, LeConte is referring to our new species *P. truncatus*; however, he apparently assumed that the differences in ventrite armature were cases of intraspecific variation in *P. armatus* as no additional species were described.

Proctorus emarginatus **Lewis & Anderson, sp. nov.**
https://zoobank.org/4BD64D73-88C9-46ED-A0CE-C8FDE063FA01
Figs 2A–C, 6, 7G, H

Material examined. ***Holotype*: CANADA: British Columbia:** Summit Lake (Alaska Highway – mi. 392), 25 June 1959, R.E. Leech, on *Salix* (1 male, CNCI), JHLRSA_PROC_325. ***Paratypes*: CANADA: Alberta:** Tp. 78, Rge. 15, 5 June 1984, B.F.

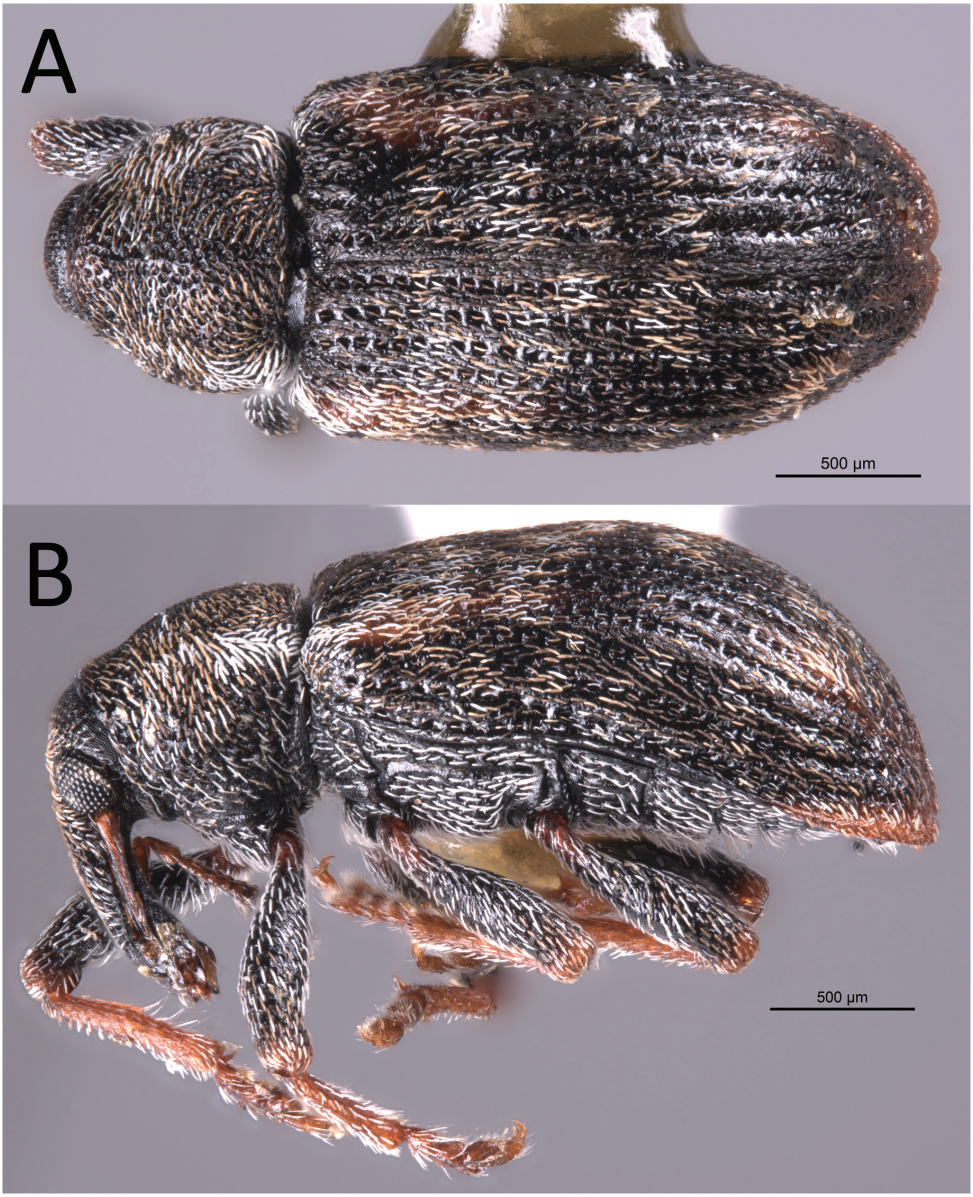

Figure 6. *Proctorus emarginatus* habitus (USI: JHLRSA_PROC_325) **A** dorsal (♂) **B** lateral (♂).

Figure 7. Aedeagi of four *Proctorus* species. *Proctorus decipiens* (USI: JHLRSA_PROC_035) **A** dorsal **B** lateral. *Proctorus armatus* (USI: JHLRSA_PROC_316) **C** dorsal **D** lateral; *Proctorus truncatus* (USI: JHLRSA_PROC_295) **E** dorsal **F** lateral; *Proctorus emarginatus* (USI: JHLRSA_PROC_325) **G** dorsal **H** lateral.

& J.L. Carr (1, CMNC), JHLRSA_PROC_323; **Northwest Territories:** Highway 5 (49 km, east of junction with Highway 2), 16 June 1988, B.F. & J.L. Carr (1, CNCI), JHLRSA_PROC_324.

Diagnosis. Length 2.9–3.1 mm. Body (especially rostrum and femora) dark, although elytra often has orange stripe extending posteriorly from humerus. Protibiae of male not prominently dentate on inner edge. Elytra without clear, distinct x-pattern of white scales. Fifth ventrite of male with a single transverse ridge which peaks medially; without any baso-medial ventral projection. Apical tooth of metatibiae of male straight. Aedeagus with apex distinctly emarginate and with four prominent lobes (two on each side).

Etymology. The specific name refers to the apically emarginate body of the penis.

Ecology. One specimen was collected from *Salix*. However, nothing else is known of the natural history of this species.

Remarks. This species is known only from northwestern North America (only Canada at present), and based on institutional collection records also represents one of the rarer weevils in Canada. The female of *P. emarginatus* is unknown.

Key to the species of *Proctorus* LeConte

Note that the female of *P. emarginatus* is unknown and therefore not included in the key.

1 Fifth ventrite with armature (projections, swellings) (Figs 1, 2, 3B, 4B, 5B, 6B) [males] **2**

– Fifth ventrite unmodified (Figs 3D, 4D, 5D) [females] **5**

2 Fifth ventrite lacking basomedial swelling, but with two apicolateral projections (Figs 2D–F, 3B). Apical tooth of metatibiae curved. Femora and usually rostrum reddish (Fig. 3A, B). Elytra with distinctive x-shaped pattern of white scales (Fig. 3A, B). Apex of penis with edges weakly expanded laterally, and coming to weak, rounded point (Fig. 7A, B)........ ***Proctorus decipiens* (LeConte, 1876) (male)**

– Fifth ventrite never with combination of apicolateral projections and lack of basomedial swelling (Figs 1, 2A–C, 4B, 5B, 6B). Apical tooth of metatibiae straight. Femora and usually rostrum dark (Figs 4A, B, 5A, B, 6A, B). Elytra without discernible pattern of scales (Fig. 4A, B, 5A, B, 6A, B). Penis not as above (Fig. 7C–H) **3**

3 Fifth ventrite with two prominent apicolateral projections and basomedial swelling (Fig. 1D–F, 4B). Apical half of protibiae strongly dentate on ventral side (Fig. 8A). Apex of penis slightly rounded to truncate, not emarginate or significantly expanded laterally (Fig. 7C, D) .... ***Proctorus armatus* LeConte, 1876 (male)**

– Fifth ventrite not as above, always lacking two prominent apicolateral projections (Figs 1A–C, 2A–C, 5B, 6B). Apical half of protibiae not dentate or only with weak dentation ventrally (Fig. 8B). Apex of penis dorsoventrally flattened and expanded laterally (Fig. 7E, F) or emarginate (Fig. 7G, H)........ **4**

4 Fifth ventrite with prominent basomedial swelling and low, apicolateral ridges (Figs 1A–C, 5B). Apex of penis dorsoventrally flattened and expanded laterally (Fig. 7E, F). Length 3.7–4.0 mm .... ***Proctorus truncatus* sp. nov. (male)**

– Fifth ventrite lacking prominent basomedial swelling, but with apical ridge that swells to a peak medially (Figs 2A–C, 6B). Apex of penis distinctly emarginate and with four prominent lobes (two on each side) (Fig. 7G, H). Length 2.9–3.1 mm .... ***Proctorus emarginatus* sp. nov. (male)**

5 Cuticle reddish, with distinctive x-shaped pattern of white scales across elytra (Fig. 3C, D) .... ***Proctorus decipiens* (LeConte, 1876) (female)**

– Cuticle dark, without discernible pattern of scales on elytra (Figs 4C, D, 5C, D).... **6**

6 Body more round in dorsal and lateral view (Fig. 5C, D). Rostrum thinner and longer (Fig. 5D) .... ***Proctorus truncatus* sp. nov. (female)**

– Body more elongate and somewhat flattened dorsoventrally (Fig. 4C, D). Rostrum thicker and shorter (Fig. 4D)...........***Proctorus armatus* LeConte, 1876 (female)**

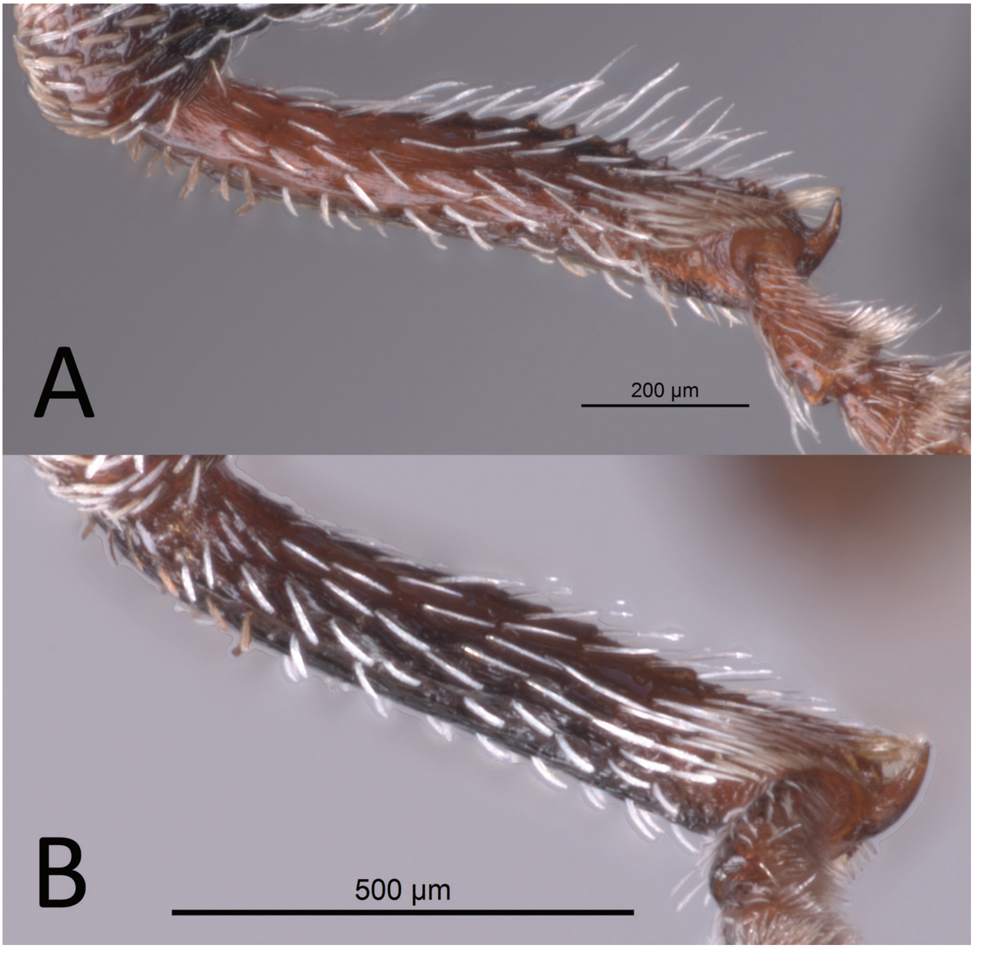

Figure 8. Male protibiae **A** *Proctorus armatus* **B** *Proctorus truncatus*.

Discussion

Proctorus represents a morphologically distinct monophyletic lineage that is endemic to North America. The specific armature on the fifth ventrite of males is unique to the genus within North America; however, we note that the males of the Old World species *Dorytomus dorsalis* (Linnaeus, 1758) also possesses similar structures. Although *Proctorus* is currently placed in the subtribe Ellescina with *Ellescus* (Alonso-Zarazaga and Lyal 1999; Anderson 2002; Bousquet et al. 2013; Caldara et al. 2014; Alonso-Zarazaga et al. 2017), the shared ventral armature in *Proctorus* and *Dorytomus* (subtribe Dorytomina) hints at a closer phylogenetic relationship between those genera than previously thought. Preliminary molecular work suggests that *Proctorus* represents a lineage sister to or nested within *Dorytomus*. However, improved taxon and gene sampling is required to improve branch support and determine which of those phylogenetic hypotheses is correct (unpublished data, Lewis and Anderson). Here, we take a conservative approach and continue to recognize the validity of *Proctorus* as members of that genus are morphologically separable from all *Dorytomus* species (including *D. dorsalis*) by tarsal claw morphology.

Although the species of *Proctorus* are easily distinguished by external and internal morphology, two species described here were long overlooked. This is likely due to the fact that specimens of the genus are rare in institutional collections. Indeed, *P. emarginatus* sp. nov. is only known from three specimens. Future studies of the genus should focus on surveying for the female of *P. emarginatus* and further investigating differing host plant usage amongst the species.

Acknowledgements

We thank Dr Lourdes Chamorro (USNM), Dr Reginald Webster (Fredericton, New Brunswick), Dr Donald McAlpine (NBM), Dr Jon Sweeney (AFCF), Dr Derek Sikes (UAMIC), Dr Mikko Pentinsaari (CBG), Dr Chris Grinter (CAS), Dr Patrice Bouchard (CNCI), Claude Chantal (Varennes, Quebec), Pierre de Tonnancour (Terrasse-Vaudreuil, Quebec), Dr Crystal Maier (MCZC), and Claudia Copley (RBCM) for loaning material used in the present study. We thank Dr Andrew Smith (CMN) and Dr Roberto Caldara for their constructive comments on the manuscript. The Canadian Museum of Nature and University of Ottawa, in particular Dr Julian Starr, are acknowledged for supporting this project and providing access to research facilities.

References

Alonso-Zarazaga MA, Lyal CHC (1999) A World Catalogue of Families and Genera of Curculionoidea (Insecta: Coleoptera) (Excepting Scolytidae and Platypodidae). Entomopraxis, Barcelona, 315 pp.

Alonso-Zarazaga MA, Barrios H, Borovec R, Bouchard P, Caldara R, Colonnelli E, Gúltekin L, Hlavá P, Korotyaev B, Lyal CHC, Machado A, Meregalli M, Pierotti H, Ren L, Sánchez-Ruiz M, Sforzi A, Silfverberg H, Skuhrovec J, Trýzna M, Velázquez de Castro AJ, Yunakov NN (2017) Cooperative Catalougue of Palearctic Coleoptera Curculionoidea. Monografías electrónicas SEA 8. Sociedad Entomológica Aragonesa S.E.A, Zaragoza, 729 pp.

Anderson RS (2002) Curculionidae. In: Arnett RH, Thomas MC, Skelley PE, Frank JH (Eds) American Beetles - Volume 2 - Polyphaga: Scarabaeoidea through Curculionoidea. CRC Press, Boca Raton, 722–815.

Bousquet Y, Bouchard P, Davies AE, Sikes DS (2013) Checklist of Beetles (Coleoptera) of Canada and Alaska. 2nd Edn. Pensoft Series Faunistica No. 109. Pensoft, Sofia, 402 pp. https://doi.org/10.3897/zookeys.360.4742

Caldara R, Franz NM, Oberprieler RG (2014) Curculioninae Latreille, 1802. In: Leschen RAB, Beutel RG (Eds) Handbook of Zoology - Coleoptera, Beetles (Phytophaga: Chrysomeloidea, Curculionoidea): Morphology and Systematics. De Gruyter, Berlin, 589–628.

LeConte JL (1876) The *Rhynchophora* of America north of Mexico. Proceedings of the American Philosophical Society 15(96): 1–455. https://doi.org/10.5962/bhl.title.38329

LeConte JL (1878) The Coleoptera of Michigan. Proceedings of the American Philosophical Society 17(101): 593–669.

O'Brien CW, Wibmer GJ (1982) Annotated checklist of the weevils (Curculionidae sensu lato) of North America, Central America, and the West Indies (Coleoptera: Curculionoidea). Memoirs of the American Entomological Institute 34: 1–382.

ZooKeys 1131: 155–171 (2022)
doi: 10.3897/zookeys.1131.85218
https://zookeys.pensoft.net

RESEARCH ARTICLE

A peer-reviewed open-access journal
ZooKeys
Launched to accelerate biodiversity research

Molecular phylogeny and revision of species groups of Nearctic bombardier beetles (Carabidae, Brachininae, *Brachinus* (*Neobrachinus*))

Raine M. Ikagawa[1], Wendy Moore[2]

1 *Graduate Interdisciplinary Program in Entomology and Insect Science, University of Arizona, Tucson, Arizona, 85721-0036, USA* **2** *Department of Entomology, University of Arizona, 1140 E. South Campus Dr., Tucson, Arizona, 85721-0036, USA*

Corresponding author: Wendy Moore (wmoore@arizona.edu)

Academic editor: Lyubomir Penev | Received 12 April 2022 | Accepted 26 September 2022 | Published 23 November 2022

https://zoobank.org/8582AB45-05F7-4700-B96C-1E9893BD2626

Citation: Ikagawa RM, Moore W (2022) Molecular phylogeny and revision of species groups of Nearctic bombardier beetles (Carabidae, Brachininae, *Brachinus* (*Neobrachinus*)). ZooKeys 1131: 155–171. https://doi.org/10.3897/zookeys.1131.85218

Abstract

Bombardier beetles of the genus *Brachinus* Weber are notorious for their explosive defensive chemistry. Despite ongoing research on their defense mechanism, life history, and ecology, the group lacks a robust molecular-based phylogeny. In this study, three loci from mitochondrial and nuclear genomes (COI, CAD, 28S) are used to reconstruct the phylogeny of the large subgenus *Neobrachinus*, and test species group boundaries hypothesized by Erwin (1970) based on morphological characters. Erwin's *fumans* species group is found to be polyphyletic, and is herein re-defined with eight new species groups erected to reflect clades based on molecular evidence: the *cinctipennis*, *cyanipennis*, *galactoderus*, *gebhardis*, *mexicanus*, *phaeocerus*, *quadripennis*, and *tenuicollis* species groups. Erwin's *cordicollis* group is also expanded to include *Brachinus* (*Neobrachinus*) *medius* and the *americanus* group.

Keywords

molecular phylogenetics, systematics

Introduction

Bombardier beetles of the genus *Brachinus* Weber are famous for their explosive defensive chemistry; when provoked, they generate a 100 °C cloud of benzoquinones and aim the explosion towards their enemy (Eisner 1958; Schildknecht et al. 1964; Aneshansley et al. 1969; Dean et al. 1990; Arndt et al. 2015). *Brachinus* are abundant predators and scavengers in their communities, they offer other carabids (e.g., certain species of *Agonum* Bonelli, *Chlaenius* Bonelli, and *Platynus* Bonelli) well-protected spaces in multispecies aggregations (Schaller et al. 2018), and they have the potential to sustainably manage pest populations in agroecosystems (Scaccini et al. 2020). Previous research has also examined their larval development (Erwin 1967; Juliano 1984; Juliano 1985; Saska and Honek 2004), aggregation behaviors (Brandmayr et al. 2006; Schaller et al. 2018), and microbiome (McManus et al. 2018; Silver et al. 2021).

Species of the *Brachinus* subgenus *Neobrachinus* Erwin have historically been described as difficult to identify. George Ball (1960) wrote: "The taxonomy of the North American species of this group is very poorly understood and it is almost a waste of time at present to attempt to determine individuals to species." Ten years later, Erwin (1970) revised the Nearctic members of the genus after studying more than 28,000 specimens of *Brachinus* and more than 2,000 specimens of other brachinine taxa. He identified many subtle species-specific characters, from the depth of punctures on the pronotum to the shape of the miniscule virga of the endophallus which requires meticulous dissection and processing to observe. He also used morphological characters to classify 62 members of *Neobrachinus* into 14 species groups (representatives in Fig. 1) and to propose a phylogenetic tree. He hypothesized that speciation among *Neobrachinus* was mirrored by the evolution of the shape of the virga, which is the apical sclerite surrounding the gonopore of the male endophallus. He placed the *americanus* group at the base of the tree based on morphological similarities of the virga with a species known from Sikkim, India, *B. dryas* Andrewes (Erwin 1970). The virga of *B. dryas* was regarded as a *Neobrachinus*-type, different from all other virgae of *Brachinus* species outside of the Americas (Erwin 1970); *B. dryas* has since been reclassified and placed in the subgenus *Brachynolomus* Reitter (Akhil et al. 2020).

The vast majority of species examined in Erwin (1970) are endemic to North and Central America. The subgenus also includes 21 *incertae sedis* species from South America that were not examined. Erwin hypothesized that the ancestral lineage of *Neobrachinus* entered North America via the Bering Land Bridge and rapidly invaded South America in a single colonization event before its isolation from Central America during the Eocene. He considered that these *incertae sedis* species were likely members of species groups *brunneus*, *grandis*, *lateralis*, and *texanus*, but stated that further examinations of South American taxa would be necessary before placing them in species groups.

Erwin's work transformed brachinine taxonomy and provided a dichotomous key for identifying brachinine genera and North and Central American *Neobrachinus* species. However, identification of *Neobrachinus* species remains challenging. This is

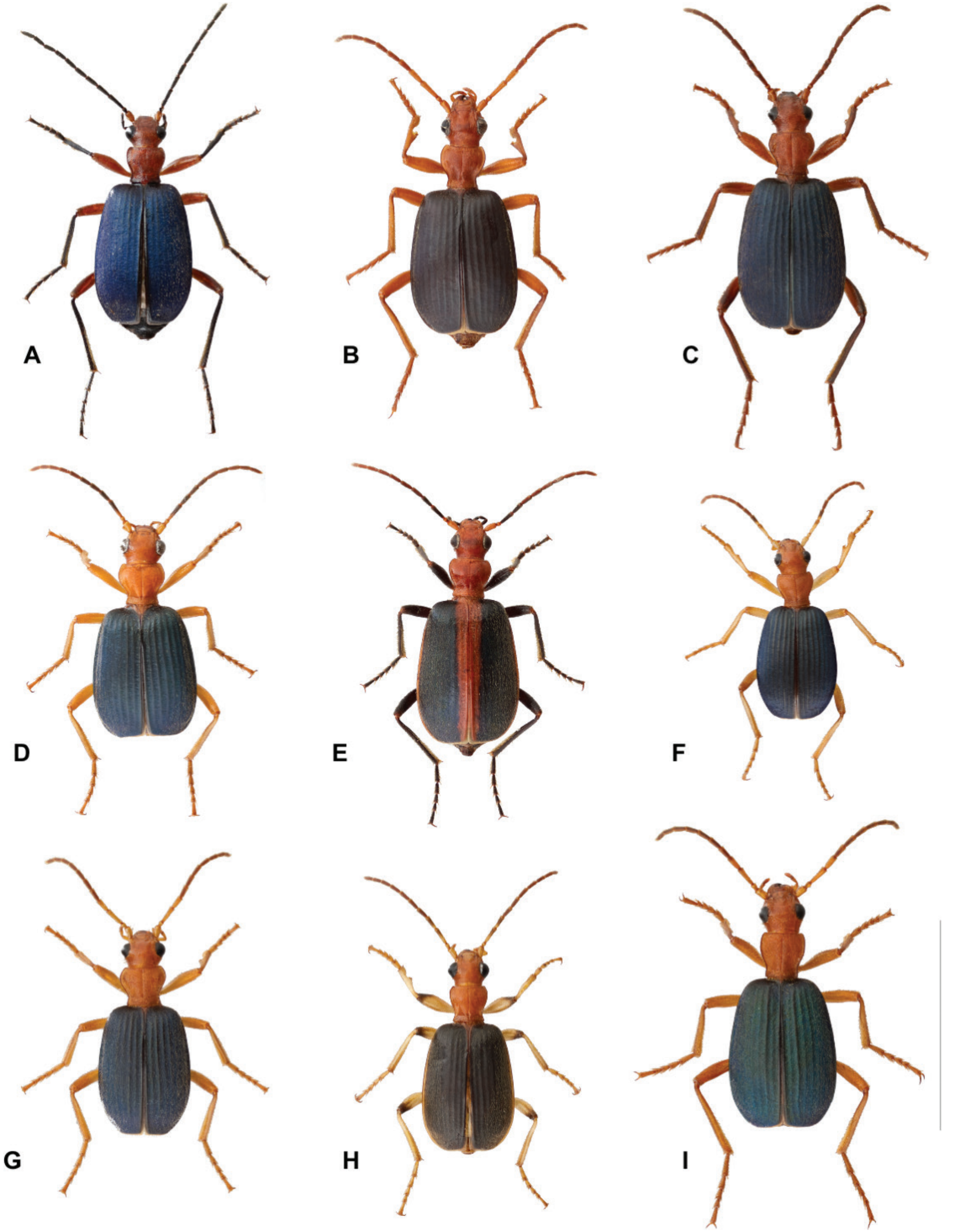

Figure 1. Dorsal habitus view of representatives from several species groups of the subgenus *Neobrachinus* Erwin **A** *B. azureipennis* Chaudoir **B** *B. gebhardis* Erwin **C** *B. elongatulus* Chaudoir **D** *B. mexicanus* Dejean **E** *B. cibolensis* Erwin **F** *B. costipennis* Motschulsky **G** *B. hirsutus* Bates **H** *B. lateralis* Dejean **I** *B. favicollis* Erwin. Scale bar: 1 cm.

largely due to highly conserved morphology; the maintenance of "the *Brachinus* habitus" seems to have been favored over the course of multiple speciation events (e.g., Fig. 1C, D, F, G, I). Furthermore, species-level identification often relies on very subtle characters that can change over in specimens time as colors darken and setae break. Adding to the challenge, members of the same species can vary significantly in size because of their idiobiont ectoparasitoid larval lifestyle (Fig. 2). Upon hatching, the first instar triungulin locates the pupa of an aquatic beetle and consumes it (and only it) during the course of its development. Therefore, adult size is positively correlated to the size of the pupal host, resulting in vast differences in adult body size (Juliano 1985; Saska and Honek 2012). Another barrier to identification is that some species of *Neobrachinus* are only represented by a few specimens collected many decades ago, deposited in a handful of museum collections. Not only does this hinder morphological work, with so few specimens available for comparison, it is also more challenging to acquire molecular sequence data, particularly from single-copy genes.

Neobrachinus are abundant members of riparian arthropod communities in the southwestern US (Moody and Sabo 2017). A recent study documenting and exploring the multispecies aggregation behavior of these species included a molecular phylogeny of many *Neobrachinus* species (Schaller et al. 2018). This work corroborated the monophyly of *Neobrachinus* using molecular sequence data. However, results also suggested that some species groups within *Neobrachinus* may not be monophyletic,

Figure 2. Two specimens of *B. elongatulus* demonstrating adult size variation within the species. Scale bar: 5 mm.

including the *fumans* group, and therefore some diagnostic morphological characters identified by Erwin (1970) may be plesiomorphic. For example, Erwin considered the shape of the virga "with sides curved over ventrally from base to apex, forming a central (ventral) trough" to be the apomorphy of the *fumans* species group (Erwin 1970).

With morphologically challenging taxa, molecular sequence data are often used to determine species boundaries and relationships, and these studies also help to reveal cryptic diversity. This study aims to address the morphological challenges of *Neobrachinus* by using molecular sequence data to infer the phylogeny of the species and to test proposed species groups.

Materials and methods

Taxon sampling and classification

Challenges associated with *Neobrachinus* identification led us to limit our taxon sampling to expertly identified specimens in museum collections (Suppl. material 1: table S1). We targeted material from institutions where Erwin conducted work on *Neobrachinus*. Specimen loans were acquired from the University of Alberta E.H. Strickland Entomological Museum (Edmonton, Alberta, CA), where Erwin deposited his vouchers after completing his PhD research with George E. Ball, culminating in several publications (Erwin 1965, 1967, 1970, 1973). We also used specimens deposited in the University of Arizona Insect Collection (Tucson, Arizona, USA), where Erwin identified *Brachinus* specimens to the species level as a Visiting Arthropod Systematist in 2014.

Efforts were made to sample several species from as many species groups as possible, especially within the large *fumans* group which we hypothesized may not be monophyletic. We also downloaded all available sequences of *Neobrachinus* species from the Barcode of Life Database (BOLD) and GenBank and tested their species identities against sequence data from expertly identified specimens.

DNA extraction and quantification

Total genomic DNA was extracted from the right middle leg of specimens using the Qiagen DNeasy Blood & Tissue Kit (Valencia, CA) following the manufacturer suggested protocol. Extractions on older specimens were conducted in the Schlinger Ancient DNA Laboratory at the University of Arizona Insect Collection using the QIAamp DNA Micro Kit (Qiagen Inc., Valencia, CA) following the manufacturer suggested protocol. The concentration of total genomic DNA in extraction products was measured on a Qubit 3.0 Fluorometer (Thermo Fisher, USA). Samples with quantifiable DNA were used in subsequent PCRs.

Gene selection and PCR

The gene regions CAD (carbamoyl-phosphate synthetase 2, aspartate transcarbamylase, dihydroorotase) and COI (cytochrome c oxidase subunit I) have been shown to be phylogenetically informative in *Neobrachinus* by Schaller et al. (2018), and sequences generated in that study were downloaded from GenBank. Sequences for additional taxa to these datasets were generated following published protocols (Schaller et al. 2018).

Sequence data were also obtained for the D2-3 region of large subunit ribosomal gene (28S) from the total genomic DNA extracted for Schaller et al. (2018) as well as the new taxa added herein. We chose to add 28S to our analyses for several reasons; it has been shown to be phylogenetically informative in other genera of carabid beetles, and as a multicopy gene it is easier to amplify from older museum specimens (Sproul and Maddison 2017). Therefore, we started building a reference library of 28S sequences obtained from expertly identified specimens to facilitate future molecular work with museum material. The D2-3 region of 28S was amplified using primers LS58F and LS998R (Ober 2002) and the following PCR cycling conditions: initial denaturation at 94 °C for 2 min, followed by 35 cycles at 94 °C for 22 s, 57 °C for 22 s, 72 °C for 1 min and 10 s, and a final elongation at 72 °C for 5 min.

Sequencing

PCR products were quantified, normalized, and sequenced in forward and reverse directions using Sanger sequencing at the University of Arizona Genetics Core (UAGC) using an Applied Biosystems 3730 DNA Analyzer (ThermoFisher Scientific). Chromatograms were assembled into contigs, and initial base calls were made using Phred (Green and Ewing 2002) and Phrap (Green 1999) as implemented by the Chromaseq 1.52 module (Maddison and Maddison 2020) within Mesquite 3.61 (Maddison and Maddison 2019). Final base calls were made by visual inspection of the contigs.

Phylogenetic analysis

Three single gene matrices (COI, CAD, and 28S) were assembled. Each matrix contained sequences generated specifically for this study as well as all homologous sequences of *Neobrachinus* publicly available on BOLD and GenBank (databases searched January 2021) (Suppl. material 1: table S1). The COI matrix contained 270 taxa, the CAD matrix contained 70 taxa, and the 28S matrix contained 54 taxa. Sequences in each matrix were aligned using default settings in MAFFT v. 7.474 (Katoh and Standley 2013) within Mesquite. A concatenated matrix with the data from all three genes was also assembled, which contained 282 taxa including 228 *Neobrachinus* (representing 9/15 *Neobrachinus* species groups, and 32/62 *Neobrachinus* species) and 54 outgroups. In the concatenated matrix and single gene matrices, COI and CAD characters were partitioned by codon position. Maximum-likelihood analyses and bootstrap analyses were conducted on single gene matrices and on the concatenated dataset using IQ-TREE v. 1.6.10 (Nguyen et al. 2015). The ModelFinder feature within IQ-TREE (Kalyaanamoorthy et al. 2017) was used to find the optimal character evolution models. The ModelFinder Plus model option was used for 28S, and the TESTMERGE option for the protein-coding genes and for the concatenated dataset. One hundred searches were conducted for the maximum-likelihood tree for each matrix in Mesquite. Bootstrap analyses for the four trees were conducted with 1000 replicates using IQ-TREE v. 1.6.10 (Nguyen et al. 2015), as orchestrated by the CIPRES Science Gateway (Miller et al. 2010). Support for and against clades were calculated for each species group and the subgenus *Neobrachinus* in Mesquite using its "Clade Frequencies in Trees" feature and bootstrap trees generated by IQ-TREE (Maddison et al. 2019; Kavanaugh et al. 2021).

Results

Models and partitions

IQ-Tree ModelFinder and ModelFinder Plus identified the following models of evolution for each character partition: COI codon 1 = K2P+I+G4; COI codon position 2, CAD codon 1, CAD codon 2 = 2K2P+I; COI codon 3 = TIM2+F+G4; CAD codon 3 = HKY+F; and 28S = GTR+F+I+G4.

Molecular phylogeny

The three-gene IQ-Tree analysis resulted in the phylogeny shown in Figs 3–7. The full concatenated tree, and individual gene trees for 28S, CAD, and COI, are shown in Suppl. material 1: figs S1–S4). The COI analysis identified several specimens obtained from public databases that could be misidentified (Suppl. material 1: fig. S4). In all analyses, the following species groups originally proposed by Erwin 1970 were recovered as monophyletic: *cordicollis*, *lateralis*, and *texanus*.

In all analyses the *fumans* species group proposed by Erwin (1970) was polyphyletic (Fig. 3, Suppl. material 1: figs S1–S4). *B. medius* fell within a highly supported clade containing Erwin's *americanus* and *cordicollis* groups (Fig. 6, Table 1). Support for and against the subgenus *Neobrachinus* and each species group are shown in Fig. 8. A revised classification of *Neobrachinus* species that reflects molecular and morphological support for species groups is shown in Table 1.

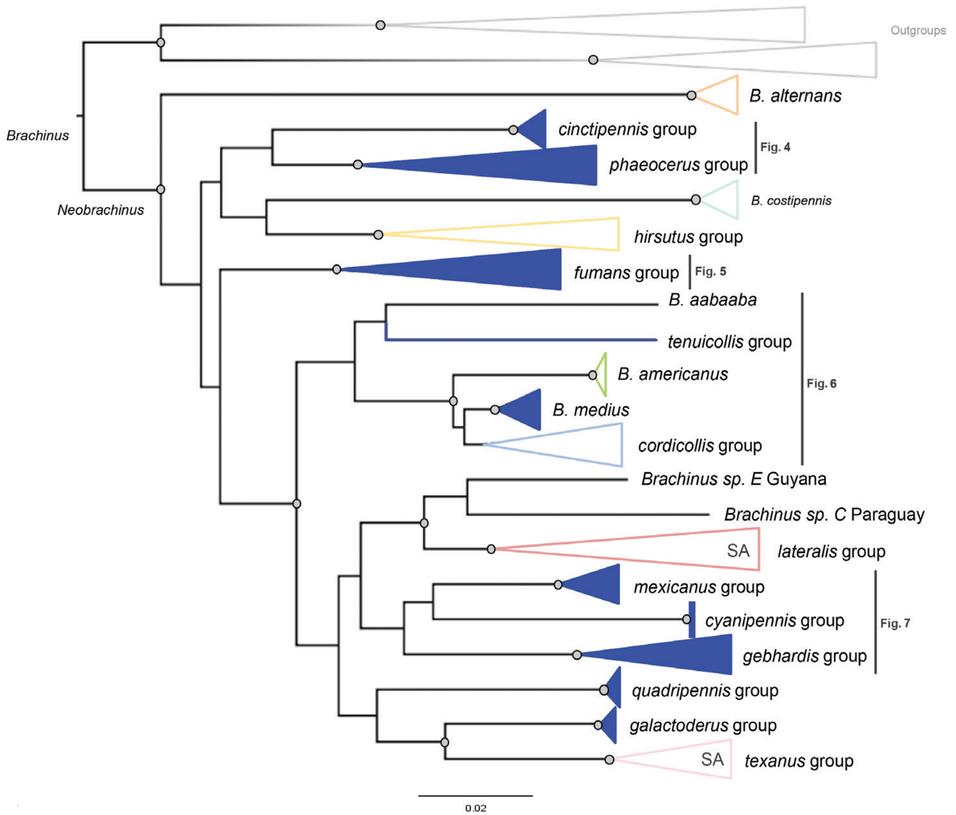

Figure 3. The maximum-likelihood three-gene molecular phylogeny of *Neobrachinus* with clades collapsed. Clades are colored by species group. Clades in solid blue were formerly placed within the *fumans* species group. Nodes with bootstrap values > 0.90 are denoted with grey circles. Clades present in South America are denoted with "SA."

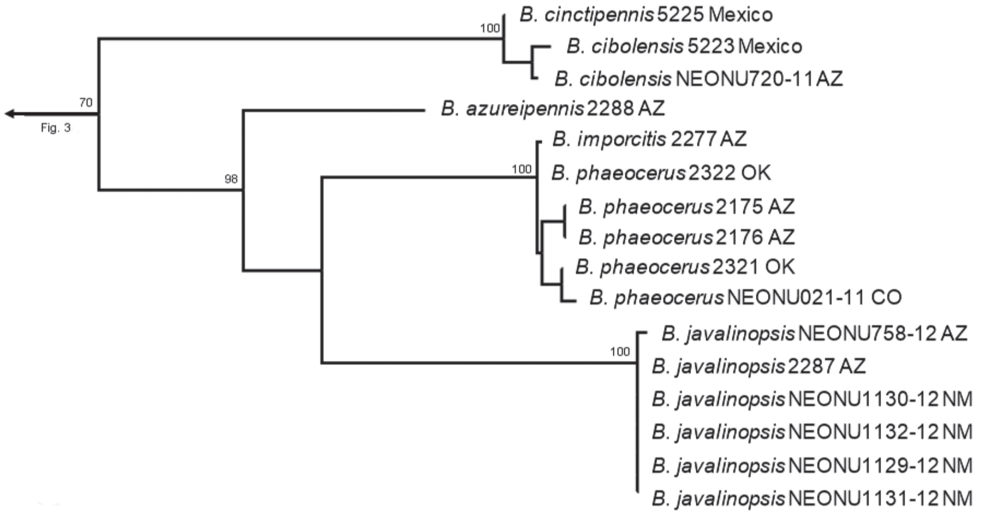

Figure 4. Phylogeny within the *cinctipennis* and *phaeocerus* species groups.

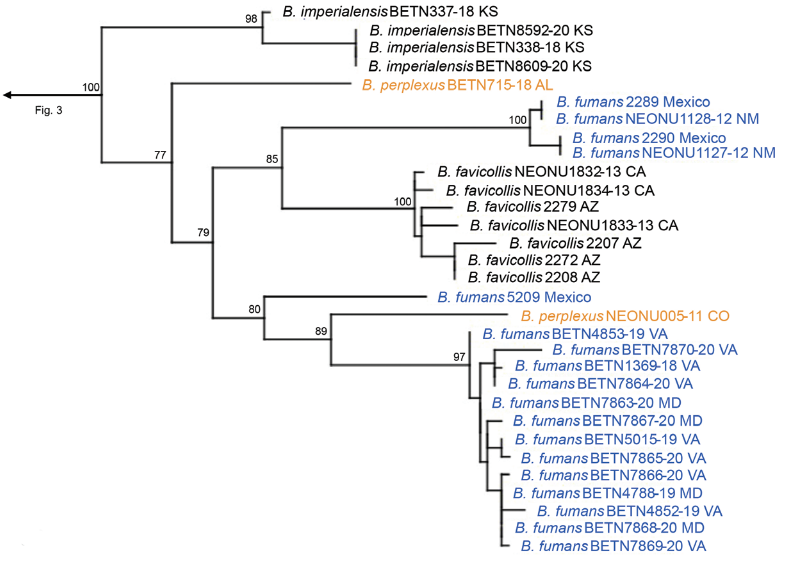

Figure 5. Phylogeny within the *fumans* species group, *B. fumans* colored blue and *B. perplexus* colored orange to highlight cryptic diversity and/or potential misidentifications of sequences on public databases.

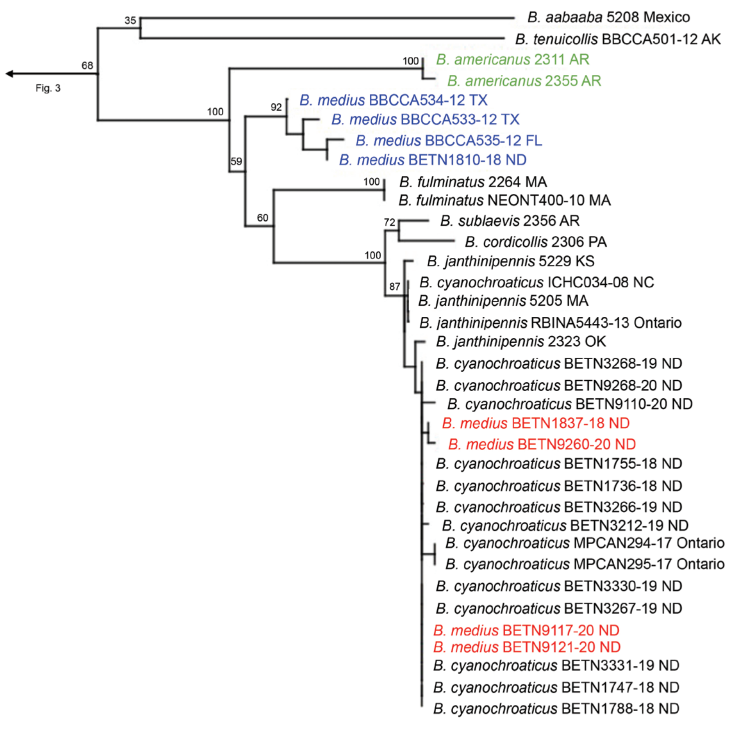

Figure 6. Phylogeny within the *tenuicollis*, *americanus*, *medius*, and *cordicollis* species groups. Novel additions to the *cordicollis* group are color-coded: *americanus* group (green) and *B. medius* (blue). Misidentifications of sequences on public databases are colored red.

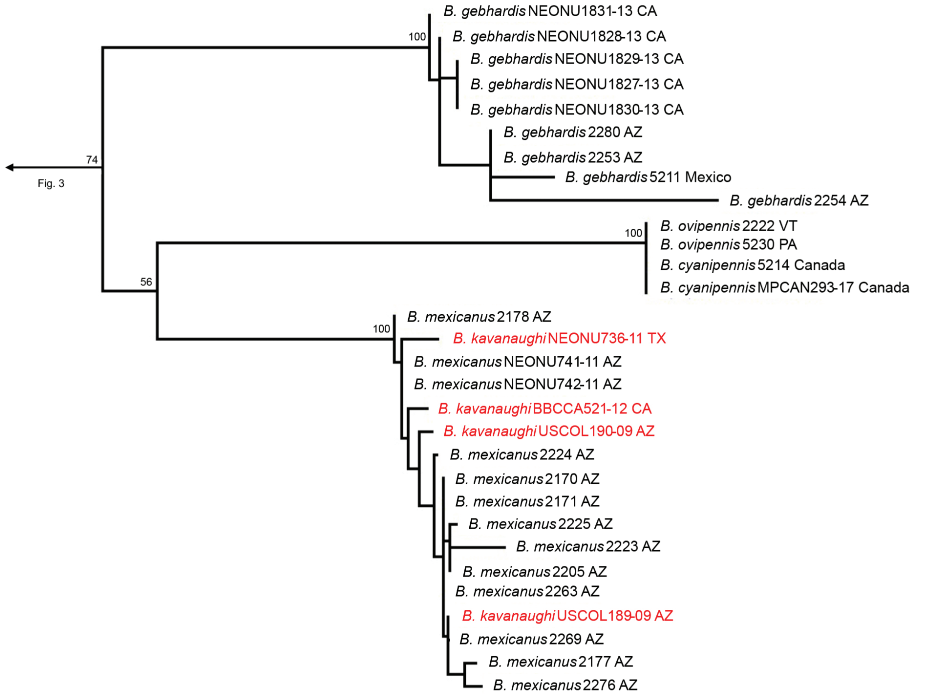

Figure 7. Phylogeny within the *mexicanus*, *cyanipennis*, and *gebhardis* species groups. *B. kavanaughi* colored red to highlight potential misidentifications of sequences or the need to synonymize this species with *B. mexicanus*.

	clade	3G	28S	CAD	COI
1	Subgenus *Neobrachinus*	99, -1	83, -9	98, -1	5, -69
2	*cinctipennis*	100, -0	-	-	100, -0
3	*cordicollis*	100, -0	98, -1	94, -1	99, -1
4	*costipennis*	100, -0	-	100, -0	100, -0
5	*cyanipennis*	100, -0	-	-	100, -0
6	*fumans*	100, -0	96, -1	99, -1	96 -3
7	*galactoderus*	100, -0	-	-	100, -0
8	*gebhardis*	100, -0	100, -0	-	98, -1
9	*hirsutus*	100, -0	31, -60	91, -5	99, -0
10	*lateralis*	90, -9	65, -34	70, -24	89, -6
11	*mexicanus*	100, -0	100, -0	77, -10	100, -0
12	*phaeocerus*	98, -1	100, -0	82, -15	89, -9
13	*quadripennis*	100, -0	100, -0	100, -0	99, -1
14	*texanus*	100, -0	97, -3	91, -5	99, -0

Figure 8. Bootstrap support for and against clades of *Neobrachinus*. Each column has maximum likelihood bootstrap values as percentages for or against each clade recovered in each dataset: the three-gene concatenated matrix (3G), and the single-gene datasets, 28S, CAD, and COI. Positive values indicate support while negative numbers indicate support for the contradictory clade with the highest support. Cells with bootstrap values ≥ 90 are in black, values between 75 and 89 in dark grey, and values between 50 and 74 in light grey. Cells in red have bootstrap values for the contradictory clade ≥ 50.

Table 1. Revised classification of Nearctic *Brachinus*. New species groups indicated with a triangle. Species groups and species not present in molecular phylogeny are indicated with an asterisk. Species present in South America are indicated with (SA). *Incertae sedis* taxa not considered in Erwin (1970) are indicated with a circle.

***aabaaba* species group**	***fumans* species group△**	***incertae sedis***
B. aabaaba Erwin	*B. fumans* (Fabricius)	*B. conformis* Dejean*
B. sonorous Erwin*	*B. favicollis* Erwin	*B. cyanipennis* Say
***alternans* species group**	*B. imperialensis* Erwin	*B. gebhardis* Erwin
B. alternans Dejean	*B. perplexus* Dejean	*B. kavanaughi* Erwin
B. rugipennis Chaudoir*	*B. puberulus* Chaudoir*	*B. mexicanus* Dejean
B. viridipennis Dejean*	*B. velutinus* Erwin*	*B. neglectus* LeConte
brunneus* species group	***galactoderus* species group△**	*B. oaxacensis* Erwin*
B. brunneus Laporte*	*B. galactoderus* Erwin	*B. ovipennis* LeConte
B. melanarthrus Chaudoir*	***grandis* species group***	*B. patruelis* LeConte*
***cinctipennis* species group△**	*B. grandis* Brullé ^{SA}	*B. quadripennis* Dejean
B. cinctipennis Chevrolat	***hirsutus* species group**	*B. tenuicollis* LeConte
B. cibolensis Erwin	*B. hirsutus* Bates	*Brachinus sp. C* ^{SA}
***cordicollis* species group**	*B. pallidus* Erwin	*Brachinus sp. E* ^{SA}
B. cordicollis Dejean	***kansanus* species group***	*B. atramentarius* Mannerheim○ ^{SA}*
B. americanus (LeConte)	*B. kansanus* LeConte*	*B. bilineatus* Laporte○ ^{SA}*
B. alexiguus Erwin*	***lateralis* species group**	*B. bruchi* Liebke○ ^{SA}*
B. capnicus Erwin*	*B. lateralis* Dejean	*B. fulvipennis* Chaudoir○ ^{SA}*
B. cyanochroaticus Erwin	*B. adustipennis* Erwin	*B. fuscicornis* Dejean○ ^{SA}*
B. fulminatus Erwin	*B. aeger* Chaudoir ^{SA}	*B. genicularis* Mannerheim○ ^{SA}*
B. ichabodopsis Erwin*	*B. arboreus* Chevrolat* ^{SA}	*B. hylaenus* Reichardt○ ^{SA}*
B. janthinipennis (Dejean)	*B. bilineatus* Castelnau*	*B. immarginatus* Brullé○ ^{SA}*
B. medius T.W. Harris	*B. chalchihuitlicue* Erwin*	*B. intermedius* Brullé○ ^{SA}*
B. microamericanus Erwin*	*B. chirriador* Erwin*	*B. limbiger* Chaudoir○ ^{SA}*
B. mobilis Erwin	***phaeocerus* species group△**	*B. marginellus* Dejean○ ^{SA}*
B. oxygonus Chaudoir*	*B. phaeocerus* Chaudoir	*B. marginiventris* Brullé○ ^{SA}*
B. sublaevis Chaudoir	*B. azureipennis* Chaudoir	*B. niger* Chaudoir○ ^{SA}*
B. vulcanoides Erwin*	*B. consanguineus* Chaudoir*	*B. nigricans* Chaudoir○ ^{SA}*
***costipennis* species group**	*B. imporcitis* Erwin	*B. nigripes* G.R. Waterhouse○ ^{SA}*
B. costipennis Motschulsky	*B. javalinopsis* Erwin	*B. olidus* Reiche○ ^{SA}*
explosus* species group	***texanus* species group**	*B. pachygaster* Perty○ ^{SA}*
B. explosus Erwin*	*B. texanus* Chaudoir*	*B. pallipes* Dejean○ ^{SA}*
	B. elongatulus Chaudoir	*B. vicinus* Dejean○ ^{SA}*
	B. geniculatus Dejean ^{SA}	*B. xanthophryus* Chaudoir○ ^{SA}*
	sallei* species group	*B. xanthopleurus* Chaudoir○ ^{SA}*
	B. sallei Chaudoir*	

Discussion

Neobrachinus species groups

This study used molecular data to test previous hypotheses of species group membership and phylogenetic relationships in the subgenus *Neobrachinus* that were proposed based on morphological data (Erwin 1970). The majority of Erwin's species groups were recovered as monophyletic and were supported with high bootstrap values in all analyses (Figs 3–7). However, both molecular and morphological evidence support splitting the *fumans* species group into new species groups. Furthermore, relationships between species groups, for the most part, remain unclear.

The shape of the virga was not found to be phylogenetically informative as envisioned by Erwin (1970). For example, the revised *cordicollis* group now encompasses members of the former *americanus* group, as well as *B. medius* which was previously placed in the *fumans* group (Fig. 5). The virga of the *americanus* group was considered plesiomorphic among *Neobrachinus*, while the "H-shaped" virga of the *cordicollis* group was considered highly derived. Erwin (1970) also hypothesized that speciation within the subgenus *Neobrachinus* was largely connected to the evolution of the virga. Although molecular data largely corroborated species groups that were diagnosed by morphological characters, including the form of the virga, the polyphyly of Erwin's *fumans* group indicates that molecular data is necessary to confirm the monophyly of species groups within *Neobrachinus*.

Polyphyly of the *fumans* species group

Erwin's *fumans* group contained 26 morphologically diverse species and was defined by a troughed virga. Considering the molecular evidence that supports splitting the *fumans* group, the troughed virga could be an ancestral or convergent form among *Neobrachinus*.

Species subgroups of the *fumans* group were also polyphyletic in the molecular phylogeny, highlighting potential convergent character states of the male genitalia. Members of Erwin's *quadripennis* subgroup of the *fumans* group were recovered throughout the *Neobrachinus* tree: in the *phaeocerus* species group (Fig. 4), the *quadripennis* species group (Fig. 3), and the *mexicanus* species group (Fig. 7). This group was characterized by a ridge on the ventral surface of the male genitalia. The two members of Erwin's *gebhardis* subgroup, *B. gebhardis* and *B. galactoderus*, were recovered in separate clades (Figs 3, 7); this group was characterized by the form of the median lobe of the male genitalia and the restriction of elytral pubescence to outer edge in the eighth depression.

Erwin's *fumans* species group also contained seven monotypic species subgroups, of which four were included in this study. Two of these, *B. cyanipennis* and *B. ovipennis*, formed a clade and are now placed together in the *cyanipennis* species group (Fig. 7). As previously mentioned, *B. medius* had strong molecular support for its new placement in the revised *cordicollis* species group. Finally, *B. tenuicollis* remains a monotypic species group, as proposed by Erwin, with the support of molecular and morphological data (Fig. 6). All species of the *fumans* group that were in monotypic species groups not included in the molecular study, and all taxa not included in Erwin (1970) are considered *incertae sedis* (Table 1).

Biogeographic implications

Erwin postulated all 84 species of *Neobrachinus* evolved from a single most recent common ancestor that crossed the Bering Land Bridge. The molecular phylogeny supports a Nearctic origin of the *Neobrachinus*, as predicted by Erwin (1970). Two clades, the *lateralis* and *texanus* species groups, have members that are present in South America (Figs 3–7). All other clades of *Neobrachinus* are only present in the Nearctic (Figs 3–7). He also hypothesized that the South American *Neobrachinus* species diversified from a single colonization event by an ancestral *Neobrachinus* lineage, giving rise to a monophyletic group containing the *brunneus*, *grandis*, *lateralis*, and *texanus* species groups (1970). However, the molecular phylogeny inferred in this study indicates otherwise. The two clades represented in this study with membership in South America, the *lateralis* and *texanus* species groups, are not sister taxa (Figs 3–7), indicating that multiple colonization events to South America must have occurred. Inclusion of additional South American taxa in a molecular phylogeny (Table 1) would illuminate their biogeographic history.

Species identifications

Among the previously published sequences downloaded from public databases, molecular phylogenetic analysis revealed several cases where specimens were likely misidentified. Some specimens from North Dakota were identified as *B. medius* (BETN1837-18, BETN9260-20, BETN9117-20, BETN9121-20), however the sequences were in a well-supported clade, separate from *B. medius* from the same region (Fig. 6, Suppl. material 1: fig. S1).

Other potential misidentifications exist yet are difficult to confirm. For example, within the new *fumans* species group, there are several clades of the species *B. fumans* and *B. perplexus* (Fig. 5). Given the lack of molecular sequence data from other members of the species group, it is impossible to determine whether these clades represent cryptic diversity or whether the specimens are misidentified members of other species of the *fumans* group.

Another example is the clade containing *B. kavanaughi* and *B. mexicanus* (Fig. 7). Representatives of the species *B. kavanaughi* do not form a separate clade from *B. mexicanus*. Without examining the voucher specimens it is impossible to determine whether these specimens represent misidentified members of *B. mexicanus*, or whether *B. kavanaughi* should be synonymized with *B. mexicanus*.

Conclusions

This research presents a molecular test of Erwin's (1970) morphology-based hypothesis of *Neobrachinus* phylogeny, and our analyses largely support the monophyly of species groups posited in his enormous study. Utilizing multiple approaches and datasets for phylogenetic inference illuminates the power of integrative methods. Our finding that Erwin's *fumans* species group was polyphyletic highlights the benefit of using molecular sequence data to infer phylogeny, especially in taxonomically and morphologically difficult groups like *Neobrachinus*.

Considering the challenges of morphological identification to the species level among *Neobrachinus*, molecular sequence data offer an accurate, alternative path to identification. Continued contribution of sequences from expertly identified specimens to libraries within databases such as BOLD and GenBank, will facilitate rapid, accessible, and accurate species identification. As sequencing technologies become cheaper and more readily available, acquiring sequence data for comparison in such databases is increasingly cost- and time-effective.

The present study elucidates the species group classification of more than half of the species of *Neobrachinus* detailed in Erwin (1970). We were able to place some species into molecularly defined species groups based on the presence of apomorphic morphological characters largely codified by Terry Erwin during the past 55 years (Erwin 1965, 1967, 1970). Many other species remain *incertae sedis*. Of those, most species are rarely collected and are known from few specimens collected long ago. Targeted efforts to acquire fresh material for molecular phylogenetic analysis, particularly of rare species, and the 22 species known only from Central and South America, will help provide a clearer picture of the evolutionary and biogeographic histories within *Neobrachinus*.

This systematic study of *Neobrachinus* emphasizes the importance of continued taxonomic and phylogenetic work to better understand their species boundaries, biogeography, and evolutionary history, and will enable future efforts to better understand these remarkable beetles.

Acknowledgements

It is our pleasure to dedicate this work to Dr. Terry L. Erwin [1940–2020], virtuoso coleopterist, biodiversity explorer, scholar, and gentleman. As a former colleague, mentor, and friend his enthusiasm for carabid systematics was contagious and his inspiration timeless. This work is in partial fulfilment of RI's Master's degree in the Graduate Interdisciplinary Program in Entomology and Insect Science (GIDP-EIS) at the University of Arizona (UA) and is a product of the Arizona Sky Island Arthropod Project based in W.M.'s laboratory. We thank those who helped collect specimens in the field including Davide Bergamaschi and Carlos Martinez. A special thanks to Jacob Simon, who contributed to collecting specimens in the field and molecular data acquisition. We also thank Jason Schaller for early advice on how to collect and identify *Neobrachinus*. We thank Daniel Shpeley (University of Alberta) and Evan Waite (Arizona State University) for loans of *Brachinus* specimens included in our molecular phylogeny. We thank Drs. David Kavanaugh and David Maddison for their insightful comments that improved the quality of the manuscript. Funding for this project came from the UA's GIDP-EIS, as well as from T&E, Inc. and is gratefully acknowledged.

References

Akhil SV, Divya M, Sabu KT (2020) Bombardier beetles of genus *Brachinus* Weber, 1801 (Carabidae: Brachininae: Brachinini) from India. Zootaxa 4816(4): 576–600. https://doi.org/10.11646/zootaxa.4816.4.7

Aneshansley DJ, Eisner T, Widom JM, Widom B (1969) Biochemistry at 100 degrees C - explosive secretory discharge of bombardier beetles (*Brachinus*). Science 165(3888): 61–63. https://doi.org/10.1126/science.165.3888.61

Arndt EM, Moore W, Lee WK, Ortiz C (2015) Mechanistic origins of the bombardier beetle (Brachinini) explosion-induced defensive spray pulsation. Science 348: 563-567. https://doi.org/10.1126/science.1261166

Ball GE (1960) Carabidae, Fascicle 4. The Beetles of the United States (A Manual for Identification). The Catholic University of America Press, Washington, DC 58: 55–210.

Brandmayr TZ, Bonacci T, Massolo A, Brandmayr P (2006) What is going on between aposematic carabid beetles? The case of *Anchomenus dorsalis* (Pontoppidan, 1763) and *Brachinus sclopeta* (Fabricius, 1792) (Coleoptera Carabidae). Ethology Ecology and Evolution 18(4): 335–348. https://doi.org/10.1080/08927014.2006.9522700

Dean J, Aneshansley DJ, Edgerton HE, Eisner T (1990) Defensive spray of the bombardier beetle: A biological pulse jet. Science 248(4960): 1219–1221. https://doi.org/10.1126/science.2349480

Eisner T (1958) The protective role of the spray mechanism of the bombardier beetle, *Brachynus ballistarius* Lec. Journal of Insect Physiology 2(3): 215–220. https://doi.org/10.1016/0022-1910(58)90006-4

Erwin TL (1965) A Revision of *Brachinus* of North America: Part I. The California Species (Coleoptera: Carabidae). Coleopterists Bulletin 19: 1–19.

Erwin TL (1967) Bombardier Beetles (Coleoptera, Carabidae) of North America: Part II. Biology and Behavior of *Brachinus pallidus* Erwin in California. Coleopterists Bulletin 21: 41–55.

Erwin TL (1970) A reclassification of bombardier beetles and a taxonomic revision of the north and middle American species (Carabidae: Brachinida). Quaestiones Entomologicae 6: 4–215.

Erwin TL (1973) A supplement to the bombardier beetles of north and middle America: new records for middle America (Coleoptera: Carabidae). Coleopterists Bulletin 27: 79–82.

Green P (1999) Phrap, version 0.990329. http://phrap.org

Green P, Ewing B (2002) Phred, version 0.020425c. http://phrap.org

Juliano SA (1984) Multiple feeding and aggression among larvae of *Brachinus lateralis* Dejean (Coleoptera: Carabidae). The Coleopterists' Bulletin 358–360.

Juliano SA (1985) The effects of body size on mating and reproduction in *Brachinus lateralis* (Coleoptera: Carabidae). Ecological Entomology 10(3): 271–280. https://doi.org/10.1111/j.1365-2311.1985.tb00724.x

Kalyaanamoorthy S, Minh BQ, Wong TKF, von Haeseler A, Jermiin LS (2017) ModelFinder: Fast model selection for accurate phylogenetic estimates. Nature Methods 14(6): 587–589. https://doi.org/10.1038/nmeth.4285

Katoh K, Standley DM (2013) MAFFT Multiple Sequence Alignment Software Version 7: Improvements in Performance and Usability. Molecular Biology and Evolution 30(4): 772–780. https://doi.org/10.1093/molbev/mst010

Kavanaugh DH, Maddison DR, Simison WB, Schoville SD, Schmidt J, Faille A, Moore W, Pflug JM, Archambeault SL, Hoang T, Chen J-Y (2021) Phylogeny of the supertribe Nebriitae (Coleoptera, Carabidae) based on analyses of DNA sequence data. ZooKeys 1044: 41–152. https://doi.org/10.3897/zookeys.1044.62245

Maddison WP, Maddison DR (2019) Mesquite: a modular system for evolutionary analysis. Version 3.61. http://www.mesquiteproject.org

Maddison DR, Maddison WP (2020) Chromaseq: a Mesquite package for analyzing sequence chromatograms. Version 1.52. http://chromaseq.mesquiteproject.org

Maddison DR, Kanda K, Boyd OF, Faille A, Porch N, Erwin TL, Roig-Juñent S (2019) Phylogeny of the beetle supertribe Trechitae (Coleoptera: Carabidae): unexpected clades, isolated lineages, and morphological convergence. Molecular Phylogenetics and Evolution 132: 151–176. https://doi.org/10.1016/j.ympev.2018.11.006

McManus R, Ravenscraft A, Moore W (2018) Bacterial associates of a gregarious riparian beetle with explosive defensive chemistry. Frontiers in Microbiology 9: 2361. https://doi.org/10.3389/fmicb.2018.02361

Miller MA, Pfeiffer W, Schwartz T (2010) Creating the CIPRES Science Gateway for inference of large phylogenetic trees. In: Proceedings of the Gateway Computing Environments Workshop (GCE), New Orleans (United States), November 2010, 1–8. https://doi.org/10.1109/GCE.2010.5676129

Moody EK, Sabo JL (2017) Dissimilarity in the riparian arthropod communities along surface water permanence gradients in aridland streams. Ecohydrology 10(4): 1819. https://doi.org/10.1002/eco.1819

Nguyen L-T, Schmidt HA, von Haeseler A, Minh BQ (2015) IQ-TREE: A fast and effective stochastic algorithm for estimating maximum-likelihood phylogenies. Molecular Biology and Evolution 32: 268–274. https://doi.org/10.1093/molbev/msu300

Ober KA (2002) Phylogenetic relationships of the carabid subfamily Harpalinae (Coleoptera) based on molecular sequence data. Molecular Phylogenetics and Evolution 24(2): 228–248. https://doi.org/10.1016/S1055-7903(02)00251-8

Saska P, Honek A (2004) Development of the beetle parasitoids, *Brachinus explodens* and *B. crepitans* (Coleoptera: Carabidae). Journal of Zoology 262: 29–36. https://doi.org/10.1017/S0952836903004412

Saska P, Honek A (2012) Efficiency of host utilisation by coleopteran parasitoid. Journal of Insect Physiology 58(1): 35–40. https://doi.org/10.1016/j.jinsphys.2011.09.011

Scaccini D, Panini M, Chiesa O, Nicoli Aldini R, Tabaglio V, Mazzoni E (2020) Slug monitoring and impacts on the ground beetle community in the frame of sustainable pest control in conventional and conservation agroecosystems. Insects 11: 380. https://doi.org/10.3390/insects11060380

Schaller JC, Davidowitz G, Papaj DR, Smith RL, Carriere Y, Moore W (2018) Molecular phylogeny, ecology and multispecies aggregation behaviour of bombardier beetles in Arizona. PLoS ONE 13(10): e0205192. https://doi.org/10.1371/journal.pone.0205192

Schildknecht H, Holoubek K, Weis KH, Krämer H (1964) Defensive substances of the arthropods, their isolation and identification. Angewandte Chemie International Edition in English 3(2): 73–82. https://doi.org/10.1002/anie.196400731

Silver A, Perez S, Gee M, Xu B, Garg S, Will K, Gill A (2021) Persistence of the ground beetle (Coleoptera: Carabidae) microbiome to diet manipulation. PLoS ONE 16(3): e0241529. https://doi.org/10.1371/journal.pone.0241529

Sproul JS, Maddison DR (2017) Sequencing historical specimens: Successful preparation of small specimens with low amounts of degraded DNA. Molecular Ecology Resources 17(6): 1183–1201. https://doi.org/10.1111/1755-0998.12660

Supplementary material 1

Supplementary data

Authors: Raine M. Ikagawa, Wendy Moore

Data type: occurences, morphological, phylogenetic

Explanation note: IQ-Tree maximum-likelihood phylogeny on concatenated dataset containing 282 specimens of *Neobrachinus* and outgroups with bootstrap values. IQ-Tree maximum-likelihood phylogeny on 28S dataset containing 54 specimens of *Neobrachinus* and outgroups with bootstrap values. IQ-Tree maximum-likelihood phylogeny on CAD dataset containing 70 specimens of *Neobrachinus* and outgroups with bootstrap values. IQ-Tree maximum-likelihood phylogeny on COI dataset containing 270 specimens of *Neobrachinus* and outgroups with bootstrap values. Voucher specimens. Voucher number, collection information, and GenBank or BOLD accession numbers are provided for each specimen.

Link: https://doi.org/10.3897/zookeys.1131.85218.suppl1

ZooKeys 1131: 173–195 (2022)
doi: 10.3897/zookeys.1131.91235
https://zookeys.pensoft.net

RESEARCH ARTICLE

A peer-reviewed open-access journal
ZooKeys
Launched to accelerate biodiversity research

Five new troglobitic species of *Tyrannochthonius* (Arachnida, Pseudoscorpiones, Chthoniidae) from the Yunnan, Guizhou and Sichuan Provinces, China

Yun-Chun Li[1]

1 *College of Life Science, China West Normal University, Nanchong, Sichuan 637009, China*

Corresponding author: Yun-Chun Li (liyc2260@cwnu.edu.cn)

Academic editor: Jason Dunlop | Received 4 August 2022 | Accepted 8 November 2022 | Published 23 November 2022

https://zoobank.org/E6519ACB-2945-462D-BA95-BB1B14404D62

Citation: Li Y-C (2022) Five new troglobitic species of *Tyrannochthonius* (Arachnida, Pseudoscorpiones, Chthoniidae) from the Yunnan, Guizhou and Sichuan Provinces, China. ZooKeys 1131: 173–195. https://doi.org/10.3897/zookeys.1131.91235

Abstract
Five new species of the genus *Tyrannochthonius* Chamberlin, 1929 are described from caves in the provinces of Yunnan (*T. huilongshanensis* **sp. nov.**, *T. xinzhaiensis* **sp. nov.**, and *T. yamuhensis* **sp. nov.**), Guizhou (*T. dongjiensis* **sp. nov.**), and Sichuan (*T. huaerensis* **sp. nov.**). An identification key is provided for all known representatives of the genus *Tyrannochthonius* from China.

Keywords
Cave-inhabiting, identification key, pseudoscorpion, soil-dwelling, taxonomy

Introduction

The pseudoscorpion tribe Tyrannochthoniini Chamberlin, 1962 belongs to the subfamily Chthoniinae Daday, 1889 and the family Chthoniidae Daday, 1889. It is distributed on all continents except Antarctica and contains six genera: *Lagynochthonius* Beier, 1951; *Maorichthonius* Chamberlin, 1925; *Paraliochthonius* Beier, 1956; *Troglochthonius* Beier, 1939; *Tyrannochthonius* Chamberlin, 1929; and *Vulcanochthonius* Muchmore, 2001 (World Pseudoscorpiones Catalog 2022). The tribe Tyrannochthoniini is characterized by one or two rows of chemosensory setae extending along the dorsum of the chelal hand; coxal spines are present only on coxae II; interior basal and interior sub-basal trichobothria situated slightly proximal of the middle of chelal hand; male sternite III elongated medially, with a very long notch (Judson 2007). Two of the genera, *Lagynochthonius* Beier, 1951 and *Tyrannochthonius* Chamberlin, 1929, have been reported in China.

The pseudoscorpion genus *Tyrannochthonius* was erected by Chamberlin for the Thai type species *Chthonius terribilis* With, 1906 (by original designation) (Chamberlin 1929). The genus *Tyrannochthonius* is characterized by tergites V–IX each with eight setae at most; long coxal spines; apodeme of movable finger normal, not complex or strongly sclerotized; the sub-basal trichobothrium is positioned midway between sub-terminal and basal, or nearer to sub-terminal; chelal fingers usually straight in dorsal view; the hand of chela normal, not narrowed at base of fingers; chelal hand usually with a single large, medial acuminate spine-like seta near the base of the fixed finger, but this can be reduced or absent (Muchmore and Chamberlin 1995; Edward and Harvey 2008). During the identification of pseudoscorpion specimens collected from the Yunnan–Guizhou Plateau from 2017 to 2019, five new cave-inhabiting species of *Tyrannochthonius* were found, which are described in this article.

Materials and methods

The specimens were preserved in 75% ethanol. They were cleared in lactic acid for 12–24 h at room temperature and, after the study, washed in distilled water and returned to alcohol. The specimens were examined with a Leica M205FA stereomicroscope and an Olympus CX31 compound microscope. Photographs were taken using a Canon 6D Mark II camera fitted with Laowa 25 mm f/2.8 2.5–5X and 100 mm F2.8 2.0X Ultra Macro lenses. The final high depth-of-field (DoF) images were stacked from 30 to 80 single photos using Helicon Focus 7.6.1., and CorelDRAW 2018 and SAI 2 softwares were used to draw the figures. The type specimens of the new species are deposited in the collection of the Museum of China West Normal University (**MCWNU**; Sichuan, China).

Pseudoscorpion terminology and measurements mostly follow Chamberlin (1931), with some minor modifications to the terminology of the trichobothria (Harvey 1992) and chelicera (Judson 2007).

Systematic account

Family Chthoniidae Daday, 1889
Subfamily Chthoniinae Daday, 1889
Tribe Tyrannochthoniini Chamberlin, 1962
Genus *Tyrannochthonius* Chamberlin, 1929

***Tyrannochthonius dongjiensis* sp. nov.**
https://zoobank.org/B395357D-20CA-4B95-8423-9BC09EF468B4
Figs 1, 6A, B

Type material. ***Holotype*** male: China, Guizhou Province, Luodian County, Dongjia Town, Dongjia Village, Nameless Cave, 25°38.53'N, 106°54.67'E, 869 m a.s.l., 7 October 2019, Yun-Chun Li leg., in MCWNU (Ar-Ps-GZ-0055). ***Paratypes*:** 2 males, 4 females, collected with the holotype, in MCWNU (Ar-Ps-GZ-0008); 5 males, 2 females, Guizhou Province, Pingtang County, Tangbian Town, Baima Cave, 25°40'6.13"N, 106°45'53.89"E, 870 m a.s.l., 6 October 2019, Yun-Chun Li leg., in MCWNU (Ar-Ps-GZ-0010).

Diagnosis. Troglobiont habitus. This new species is distinguished from other members of the genus *Tyrannochthonius* by the following combination of characters: carapace without eyes or eyespots, anterior margin with six setae; epistome absent; rallum composed of six blades; tergites I–IV with two setae; apex of coxa I with long and rounded anteromedial process, near the apex with a seta; chelal hand dorsal surface with chemosensory setae; fixed chelal finger with 24 or 25 teeth, movable chelal finger with 27–29 retrorse teeth. Pedipalpal femur (♂) 7.58–7.63×, (♀) 7.36–7.42× longer than broad, length (♂) 0.91–0.95 mm, (♀) 1.03–1.07 mm; chela (♂) 7.88–7.90×, (♀) 7.06–7.10 longer than deep, length (♂) 1.25–1.28 mm, (♀) 1.20–1.24 mm; ratio movable chelal finger/chelal hand (♂) 1.86–1.90×, (♀) 1.88–1.93×.

Etymology. Latinized adjective, derived from the village of Dongjia, located near the type locality.

Description. Adult male (Fig. 6A).

Pale yellow-orange, chelicera slightly darker, soft parts pale (Fig. 6A).

Carapace (Fig. 1A): 1.26–1.30× longer than broad, no eyes or eyespots; epistome absent; carapace surface smooth, lateral margins distinctly constricted posteriorly. With 18 setae arranged 6: 4: 4: 2: 2, anterolateral setae much shorter than others. ***Coxae*:** manducatory process pointed, with two distal setae, one long and the other slightly shorter. Pedipalpal coxa with three setae, coxa I 3, II 4, III 5, IV 5; intercoxal tubercle absent. Apex of coxa I with long and rounded anteromedial process, near the apex with a seta (Fig. 1E); coxae II with nine terminally indented coxal spines on each side, set as an oblique row, longer spines present in the middle of the row, becoming shorter distally and proximally and incised for ~ ½ their length (Fig. 1D). ***Chelicera*** (Fig. 1B): 1.82–1.85× longer than broad, hand with five setae and one lyrifissure dorsally, movable finger with one submedial seta. Cheliceral hand with moderate hispid granulation dorsally. Fixed finger with eight or nine teeth, distal one largest, decreasing in size proximally; movable finger with 12 or 13 teeth; galea absent. Serrula exterior with 22–25 blades. Rallum composed of six blades (Fig. 1C), distal blade weakly recumbent basally, with fine barbules and set apart from the other blades, the latter tightly grouped and with long pinnae. ***Pedipalp*** (Fig. 1H–J): all setae acuminate. Trochanter 1.56–1.61×, femur 7.58–7.63×, patella 2.73–2.76× longer than broad and with three lyrifissures (Fig. 1H). Femur 2.22–2.31× longer than patella. Chela 7.88–7.90×, hand 2.63–2.66× longer than deep; movable chelal finger 1.86–1.90× longer than hand. Chelal hand dorsal surface with a single row of five chemosensory setae between *esb* and *ib*/*isb* trichobothria; distal paraxial seta of hand not enlarged. Fingers straight in dorsal view (Fig. 1J). Fixed finger with 24 or 25 teeth, middle ones larger than those at both ends; movable finger with 27–29 retrorse teeth (Fig. 1I). Venom apparatus absent. Fixed chelal finger with eight trichobothria and movable finger with four, *ib* and *isb* situated close together, submedially on dorsum of chelal hand; *eb*, *esb*, and *ist* forming a straight oblique row at base of fixed chelal finger; *it* slightly distal to *est*, situated subdistally; *et* slightly nearer to tip of fixed finger; *dx* situated distal to *et*; *sb* half-way between *st* and *b*; *b* and *t* situated subdistally, *t* situated at same level as *est*. ***Opisthosoma*:** tergites and sternites undivided; setae uniseriate and acuminate. Tergal chaetotaxy (I–XII): 2: 2: 2: 2: 3–4: 4: 4: 4: 4: 2: 0; sternal chaetotaxy (IV–XII): 12: 7: 7: 7: 7: 7: 7: 0: 2. Anterior genital operculum with ten setae, genital opening slit-like, with 14 or 15 setae on the right side and 18 on the left (Fig. 1K). ***Legs*** (Fig. 1F, G): leg I: trochanter 1.00–1.03×, femur 7.63–7.66× longer than deep and 1.91–1.97× longer than patella; patella 4.57–4.59×, tibia 4.33–4.37×, tarsus 13.40–13.44× longer than deep. Leg IV: trochanter 0.88–0.96×, femoropatella 3.83–3.87×, tibia 6.89–6.92× longer than deep, basitarsus 3.75–3.80×longer than deep, with a basal tactile seta (TS = 0.24–0.25), telotarsus 15.2–15.5×longer than deep and 2.53–2.55× longer than basitarsus, with a tactile seta near base (TS = 0.23–0.24). Arolia on legs I and IV shorter than claws.

Adult female (Fig. 6B).

Mostly the same as the holotype with the differences listed below.

***Carapace*:** slightly longer than broad (1.13–1.15×). ***Chelicera*:** 2.30–2.33× longer than broad. ***Pedipalp*:** trochanter 1.80–1.86× longer than broad, femur 7.36–7.42× longer than broad, patella 2.63–2.70× longer than broad, femur 2.45–2.49× longer than patella. Chela 7.06–7.10× longer than deep, hand 2.41–2.46× longer than deep; movable finger 1.88–1.93× longer than hand. ***Opisthosoma*:** tergal chaetotaxy (I–XII): 2: 2: 2: 2: 4: 4: 4: 4: 4: 2: 2: 0; sternal chaetotaxy (IV–XII): 14: 12: 8: 7: 7: 9: 7: 0: 2. Anterior genital operculum with 9 + 14 setae on posterior margin (Fig. 1L).

Dimensions (mm, length/width or, in the case of the legs, chela, and chelal hand, length/depth).

Males (females in parentheses): body length 2.24–2.30 (2.49–2.56). Carapace 0.54–0.57/0.43–0.45 (0.53–0.55/0.47–0.48). Pedipalp: trochanter 0.25–0.28/0.16–0.18 (0.27–0.29/0.15–0.17), femur 0.91–0.95/0.12–0.14 (1.03–1.07/0.14–0.16), patella 0.41–0.44/0.15–0.17 (0.42–0.44/0.16–0.18), hand 0.42–0.45/0.16–0.17 (0.41–0.44/0.17–0.18), length of movable chelal finger 0.78–0.80 (0.77–0.79), chela 1.25–1.28/0.16–0.17 (1.20–1.24/0.17–0.18). Chelicera: 0.51–0.53/0.28–0.29 (0.53–0.55/0.23–0.24). Leg I: trochanter 0.15–0.17/0.15–0.16 (0.15–0.17/0.14–0.16), femur 0.61–0.64/0.08–0.09 (0.62–0.65/0.08–0.09), patella 0.32–0.35/0.07–0.08 (0.31–0.34/0.07–0.08), tibia 0.26–0.27/0.06–0.07 (0.27–0.29/0.06–0.07), tarsus 0.67–0.69/0.05–0.06 (0.66–0.68/0.05–0.06). Leg IV: trochanter 0.15–0.17/0.17–0.18 (0.17–0.19/0.14–0.16), femoropatella 0.88–0.92/0.23–0.25 (0.90–0.93/0.22–0.24), tibia 0.62–0.65/0.09–0.10 (0.63–0.65/0.09–0.10), basitarsus

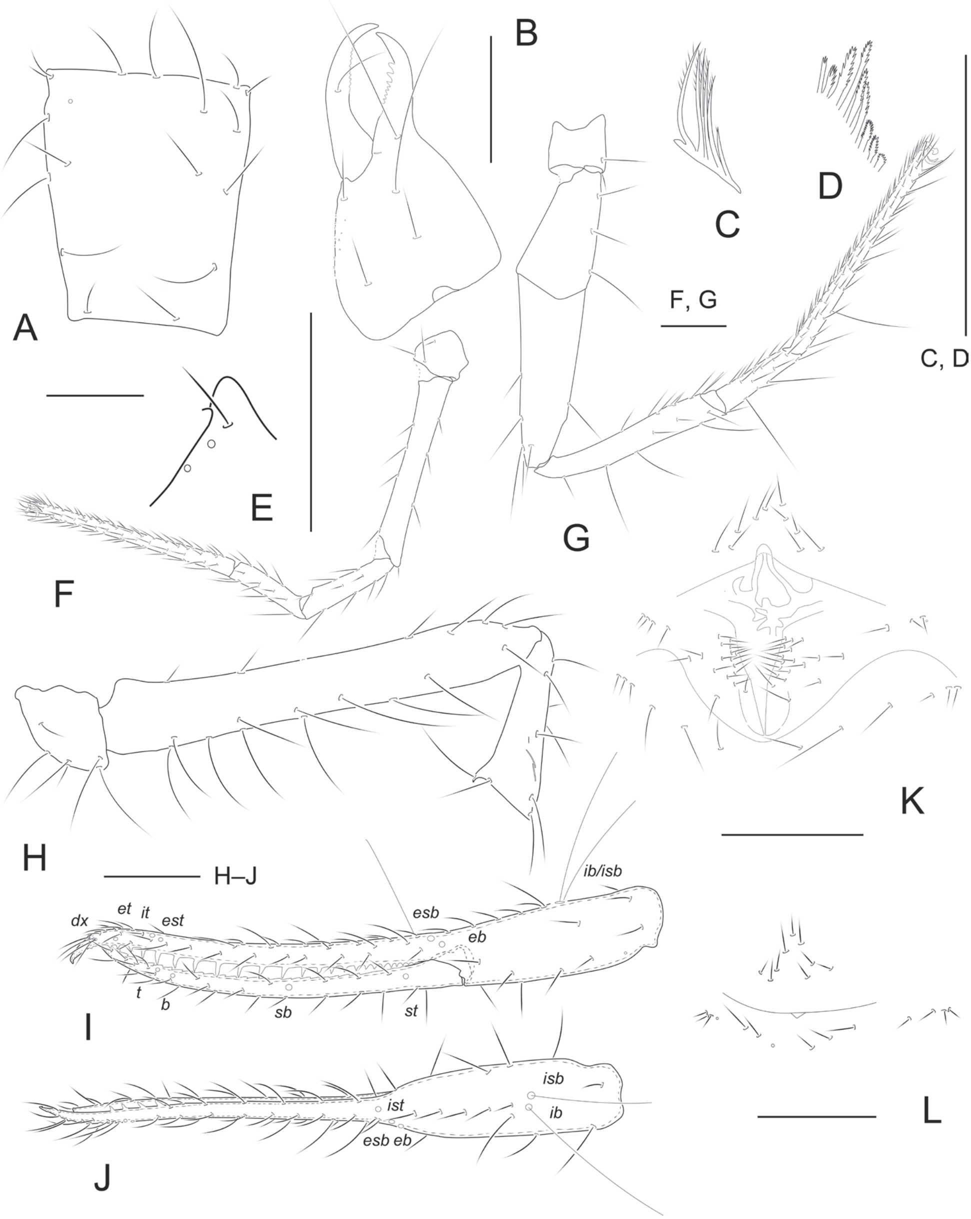

Figure 1. *Tyrannochthonius dongjiensis* sp. nov., holotype male (**A–K**) and paratype female (**L**) **A** carapace **B** left chelicera **C** rallum of left chelicera **D** coxal spines **E** process of left coxa I, ventral view **F** left leg I, lateral view **G** left leg IV, lateral view **H** palp (minus chela) **I** chela, retrolateral view **J** chela, dorsal view **K** male genital area **L** female genital area. Scale bars: 0.20 mm

0.30–0.32/0.08–0.09 (0.29–0.31/0.08–0.09), telotarsus 0.76–0.79/0.05–0.06 (0.79–0.82/0.06–0.07).

Distribution. China (Guizhou).

Tyrannochthonius huaerensis **sp. nov.**
https://zoobank.org/E7DE51E4-4C4D-41E5-A949-9095DB01128E
Figs 2, 6C, D

Type material. ***Holotype*** male: China, Sichuan Province, Luzhou City, Gulin County, Shipping Town, Xiangding Village, Huaer Cave, 28°02.22'N, 106°01.43'E, 760 m a.s.l., 3 November 2019, Yun-Chun Li leg., in MCWNU (Ar-Ps-SC-0052). ***Paratypes*****:** 4 males, 2 females, collected with the holotype, in MCWNU (Ar-Ps-SC-0001).

Diagnosis. Troglobiont habitus. This new species is distinguished from other members of the genus *Tyrannochthonius* by the following combination of characters: carapace without eyes or eyespots, anterior margin with four setae; epistome very small; rallum composed of eight blades; tergites I–VI with four setae; chelal finger without intercalary teeth; coxae II with 12 terminally indented coxal spines on each side; chelal hand dorsal surface with chemosensory setae; apex of coxa I with long and rounded anteromedial process, near the apex without setae; movable finger retrolateral margins weakly curved between *st* and *sb* trichobothria; fixed chelal finger with 23 or 24 teeth, movable chelal finger with 14 or 15 macrodenticles and 7–9 vestigial teeth. Pedipalpal femur (♂) 8.92–8.95×, (♀) 8.54–8.59× longer than broad, length (♂) 1.16–1.19 mm, (♀) 1.11–1.17 mm; chela (♂) 7.00–7.07×, (♀) 8.67–8.69× longer than deep, length (♂) 1.61–1.64 mm, (♀) 1.56–1.58 mm; ratio movable chelal finger/chelal hand (♂) 1.56–1.59×, (♀) 1.52–1.55×.

Etymology. Latinized adjective, derived from the type locality, namely Huaer Cave.

Description. Adult male (Fig. 6C).

Carapace, chelicera, pedipalps, and tergites I–VI reddish brown, remaining parts yellowish brown (Fig. 6C).

Carapace (Fig. 2A): 1.11–1.13× longer than broad, no eyes or eyespots; epistome very small, triangular; carapace surface smooth, lateral margins distinctly constricted posteriorly. With 18 setae arranged 4: 6: 4: 2: 2, anterolateral setae much shorter than others. ***Coxae*****:** manducatory process pointed, with two distal setae, one long and the other slightly shorter. Pedipalpal coxa with three setae, coxa I 3, II 4, III 5, IV 5; intercoxal tubercle absent. Apex of coxa I with long and rounded anteromedial process, near the apex without setae (Fig. 2D); coxae II with 12 terminally indented coxal spines on each side, set as an oblique row, longer spines present in the middle of the row, becoming shorter distally and proximally and incised for ~ ½ their length. ***Chelicera*** (Fig. 2B): 2.31–2.33× longer than broad, hand with five setae and one lyrifissure dorsally, movable finger with one submedial seta. Cheliceral hand with moderate hispid granulation dorsally. Fixed finger with 12 or 13 teeth, distal one largest, decreasing in size proximally; movable finger with 13 or 14 teeth; galea absent. Serrula exterior with 20–22 blades. Rallum composed of eight blades (Fig. 2C), distal blade weakly recumbent basally, with fine barbules and set apart from the other blades, the latter tightly grouped and with long pinnae. ***Pedipalp*** (Fig. 2E–G): all setae acuminate.

Trochanter 1.25–1.30×, femur 8.92–8.95×, patella 2.75–2.78× longer than broad and with one lyrifissure. Femur 2.64–2.70× longer than patella. Chela 7.00–7.07×, hand 2.74–2.76× longer than deep; movable chelal finger 1.56–1.59× longer than hand. Chelal hand dorsal surface with a single row of seven chemosensory setae between *esb* and *ib*/*isb* trichobothria; distal paraxial seta of hand not enlarged. Fingers straight in dorsal view (Fig. 2G). Fixed finger with 23 or 24 teeth, middle ones larger than those at both ends; movable finger with 14 or 15 macrodenticles, base of finger with 7–9 very low, vestigial teeth (Fig. 2F). Venom apparatus absent. Movable finger retrolateral margins weakly curved between *st* and *sb* trichobothria. Fixed chelal finger with eight trichobothria and movable finger with four, *ib* and *isb* situated close together, submedially on dorsum of chelal hand; *eb*, *esb*, and *ist* forming a straight oblique row at base of fixed chelal finger; *it* slightly distal to *est*, situated subdistally; *et* slightly nearer to tip of fixed finger; *dx* situated distal to *et*; *sb* near to *st*; *b* and *t* situated subdistally, *t* situated at same level as *it*. ***Opisthosoma*:** tergites and sternites undivided; setae uniseriate and acuminate. Tergal chaetotaxy (I–XII): 4: 4: 4: 4: 4: 4: 3: 3: 4: 4: 2: 0; sternal chaetotaxy (IV–XII): 10: 10: 9: 9: 9: 11: 8: 0: 2. Anterior genital operculum with ten setae, genital opening slit-like, with 14 or 15 marginal setae on each side (Fig. 2H). ***Legs*:** leg I: trochanter 1.58–1.59×, femur 8.25–8.30× longer than deep and 2.00–2.04× longer than patella; patella 4.71–4.75×, tibia 4.14–4.18×, tarsus 11.17–11.20× longer than deep. Leg IV: trochanter 1.15–1.18×, femoropatella 3.33–3.39×, tibia 6.70–6.72× longer than deep, basitarsus 3.75–3.79× longer than deep, with a basal tactile seta (TS = 0.21–0.22), telotarsus 12.67–12.70× longer than deep and 2.53–2.55× longer than basitarsus, with a tactile seta near base (TS = 0.19–0.20). Arolia on legs I and IV shorter than claws.

Adult female (Fig. 6D).

Mostly the same as the holotype with the differences listed below.

***Carapace*:** slightly longer than broad (1.08–1.10×). ***Chelicera*:** 2.27–2.29× longer than broad. ***Pedipalp*:** trochanter 1.81–1.84× longer than broad, femur 8.54–8.59× longer than broad, patella 2.87–2.89× longer than broad, femur 2.58–2.60× longer than patella. Chela 8.67–8.69× longer than deep, hand 3.44–3.47× longer than deep; movable finger 1.52–1.55× longer than hand. ***Opisthosoma*:** tergal chaetotaxy (I–XII): 4: 4: 4: 4: 4: 4: 4: 4: 5: 4: 2: 0; sternal chaetotaxy (IV–XII): 10: 9: 9: 8: 10: 10: 8: 0: 2. Anterior genital operculum with 10 + 6 setae on posterior margin (Fig. 2I).

Dimensions (mm, length/width or, in the case of the legs, chela, and chelal hand, length/depth).

Males (females in parentheses): body length 1.89–1.95 (1.87–1.99). Carapace 0.59–0.60/0.53–0.54 (0.53–0.55/0.49–0.51). Pedipalp: trochanter 0.20–0.22/0.16–0.18 (0.29–0.30/0.16–0.17), femur 1.16–1.19/0.13–0.15 (1.11–1.17/0.13–0.15), patella 0.44–0.45/0.16–0.17 (0.43–0.44/0.15–0.16), hand 0.63–0.65/0.23–0.25 (0.62–0.65/0.18–0.20), length of movable chelal finger 0.98–0.99 (0.94–0.97), chela 1.61–1.64/0.23–0.25 (1.56–1.58/0.18–0.20). Chelicera: 0.60–0.61/0.26–0.28 (0.59–0.60/0.26–0.27). Leg I: trochanter 0.19–0.20/0.12–0.14 (0.19–0.21/0.12–

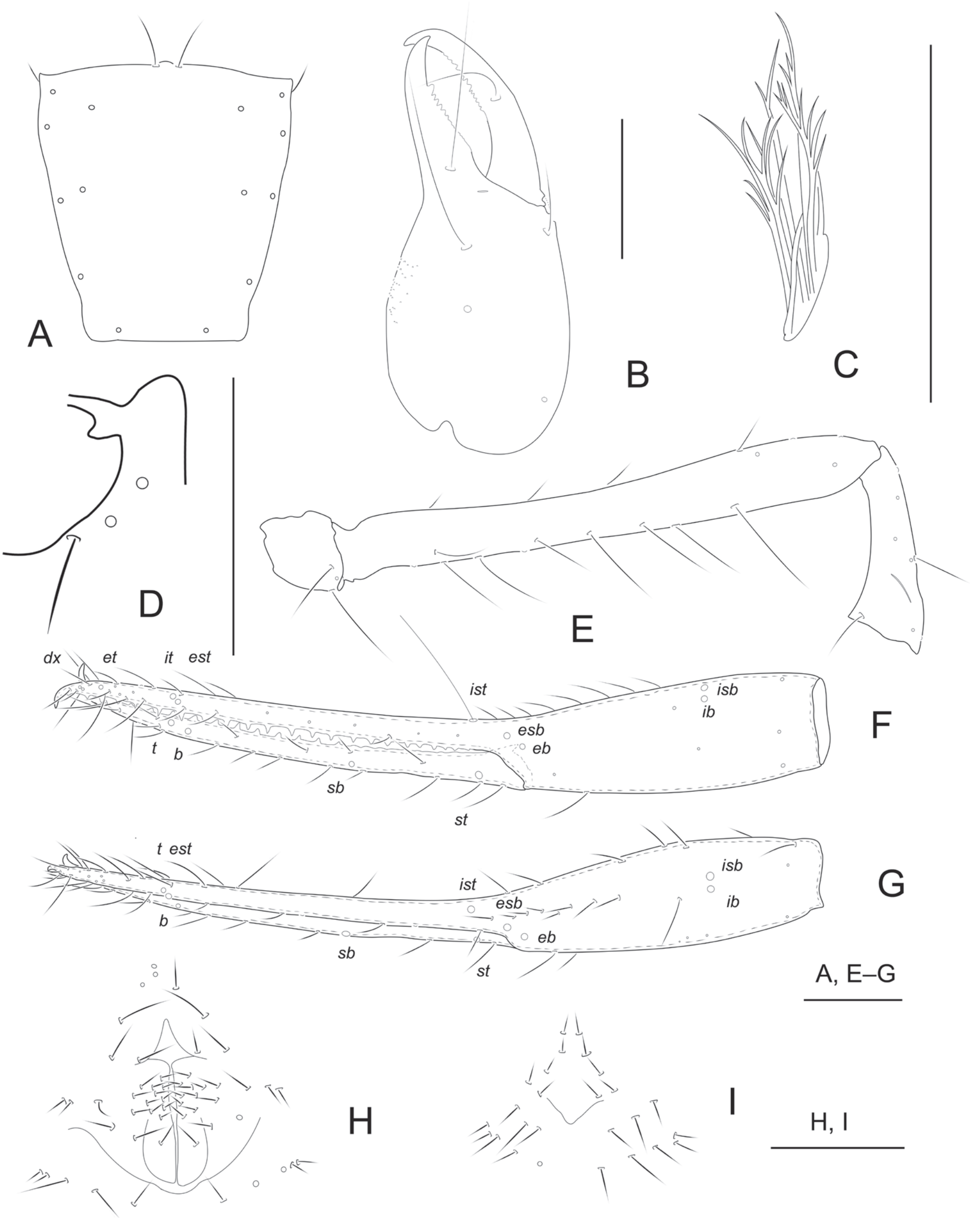

Figure 2. *Tyrannochthonius huaerensis* sp. nov., holotype male (**A–H**) and paratype female (**I**) **A** carapace **B** right chelicera **C** rallum of left chelicera **D** process of left coxa I, ventral view **E** palp (minus chela) **F** chela, retrolateral view **G** chela, dorsal view **H** male genital area **I** female genital area. Scale bars: 0.20 mm.

0.14), femur 0.66–0.69/0.08–0.09 (0.57–0.59/0.08–0.09), patella 0.33–0.35/0.07–0.08 (0.30–0.32/0.07–0.08), tibia 0.29–0.30/0.07–0.08 (0.29–0.30/0.06–0.07), tarsus 0.67–0.69/0.06–0.07 (0.65–0.67/0.05–0.06). Leg IV: trochanter 0.23–

0.25/0.20–0.21 (0.17–0.19/0.14–0.16), femoropatella 0.90–0.92/0.27–0.29 (0.83–0.86/0.25–0.27), tibia 0.67–0.69/0.10–0.11 (0.62–0.64/0.10–0.11), basitarsus 0.30–0.32/0.08–0.09 (0.27–0.29/0.08–0.09), telotarsus 0.76–0.79/0.06–0.07 (0.70–0.74/0.05–0.06).

Distribution. China (Sichuan).

Tyrannochthonius huilongshanensis sp. nov.

https://zoobank.org/E1FC5D11-2ACA-4ED1-9750-A71BA3248737

Figs 3, 7A, B

Type material. ***Holotype*** male: China, Yunnan Province, Dali City, Nanjian County, Xiaowan Town, Huilongshan Village, Banpoyan Cave, 24°56.01'N, 100°18.87'E, 1990 m a.s.l., 23 August 2018, Yun-Chun Li leg., in MCWNU (Ar-Ps-YN-0079). ***Paratypes*:** 2 males, 7 females, collected with the holotype, in MCWNU (Ar-Ps-YN-0012).

Diagnosis. Troglobiont habitus. This new species is distinguished from other members of the genus *Tyrannochthonius* by the following combination of characters: carapace without eyes or eyespots, anterior margin with four- setae; epistome present; tergites I–V with four setae; coxae II with eight terminally indented coxal spines on each side; apex of coxa I with long and rounded anteromedial process, near the apex with a seta; chelal hand dorsal surface with chemosensory setae; fixed chelal finger with 28 teeth and 16 or 17 intercalary teeth, movable chelal finger with 15 or 16 macrodenticles, 12 or 13 intercalary teeth and 5–7 vestigial teeth. Pedipalpal femur (♂) 4.87–4.90×, (♀) 5.33–5.37× longer than broad, length (♂) 0.73–0.76 mm, (♀) 0.80–0.83 mm; chela (♂) 5.61–5.66×, (♀) 6.37–6.40× longer than deep, length (♂) 1.01–1.09 mm, (♀) 1.21–1.25 mm; ratio movable chelal finger/chelal hand (♂) 1.75–1.80×, (♀) 1.80–1.83×.

Etymology. Latinized adjective, derived from the village of Huilongshan, which is near the type locality.

Description. Adult male (Fig. 7A).

Chelicera reddish brown, remaining parts yellowish brown (Fig. 7A).

Carapace (Fig. 3A): 1.02–1.06× longer than broad, no eyes or eyespots; epistome small, triangular, with two setae flanking base; carapace surface smooth, lateral margins distinctly constricted posteriorly. With 18 setae arranged 4: 6: 4: 2: 2, anterolateral setae much shorter than others. ***Coxae*:** manducatory process pointed, with two distal setae, one long and the other slightly shorter. Pedipalpal coxa with three setae, coxa I 3, II 4, III 5, IV 5; intercoxal tubercle absent. Apex of coxa I with long and rounded anteromedial process, near the apex with a seta; coxae II with eight terminally indented coxal spines on each side, set as an oblique row, longer spines present in the middle of the row, becoming shorter distally and proximally and incised for ~ ½ their length. ***Chelicera*** (Fig. 3B): 2.25–2.29× longer than broad, hand with five setae and one lyrifissure dorsally, movable finger with one submedial seta. Cheliceral hand with moderate hispid granulation dorsally. Fixed finger with eight or nine teeth, distal one largest, decreasing in size proximally; movable finger with 7–9 teeth; galea absent. Serrula exterior with 19–21 blades. Rallum composed of eight blades (Fig. 3C), distal blade weakly recumbent basally, with fine barbules and set apart from the other blades, the latter tightly grouped and with long pinnae. ***Pedipalp*** (Fig. 3D–F): all setae acuminate. Trochanter 1.60–1.61×, femur 4.87–4.90×, patella 1.61–1.64× longer than broad and with one lyrifissure. Femur 2.52–2.55× longer than patella. Chela 5.61–5.66×, hand 2.00–2.10× longer than deep; movable chelal finger 1.75–1.80× longer than hand. Chelal hand dorsal surface with a single row of five chemosensory setae between *esb* and *ib*/*isb* trichobothria; distal paraxial seta of hand not enlarged. Fingers straight in dorsal view (Fig. 3F). Fixed finger with 28 teeth and 16 or 17 intercalary teeth, middle ones larger than those at both ends; movable finger with 15 or 16 macrodenticles and 12 or 13 intercalary teeth, base of finger with 5–7 very low, vestigial teeth (Fig. 3E). Venom apparatus absent. Fixed chelal finger with eight trichobothria and movable finger with four, *ib* and *isb* situated close together, submedially on dorsum of chelal hand; *eb*, *esb*, and *ist* forming a straight oblique row at base of fixed chelal finger; *it* slightly distal to *est*, situated subdistally; *et* slightly nearer to tip of fixed finger; *dx* situated distal to *et*; *sb* near to *st*; *b* and *t* situated subdistally, *t* situated at same level as *it*. ***Opisthosoma*:** tergites and sternites undivided; setae uniseriate and acuminate. Tergal chaetotaxy (I–XII): 4: 4: 4: 4: 4: 6: 6: 6: 6: 4: 2: 0; sternal chaetotaxy (IV–XII): 8: 10: 6: 6: 6: 7: 7: 0: 2. Anterior genital operculum with ten setae, genital opening slit-like, with 11 or 12 marginal setae on each side (Fig. 3G). ***Legs*:** leg I: trochanter 1.68–1.70×, femur 6.50–6.58× longer than deep and 1.56–1.59× longer than patella; patella 4.17–4.20×, tibia 4.00–4.06×, tarsus 8.40–8.47× longer than deep. Leg IV: trochanter 1.00–1.07×, femoropatella 2.59–2.63×, tibia 4.40–4.47× longer than deep, basitarsus 2.71–2.74× longer than deep, with a basal tactile seta (TS = 0.15–0.17), telotarsus 9.60–9.66× longer than deep and 2.53–2.55× longer than basitarsus, with a tactile seta near base (TS = 0.15–0.16). Arolia on legs I and IV shorter than claws.

Adult female (Fig. 7B).

Mostly the same as the holotype with the differences listed below.

***Carapace*:** slightly longer than broad (0.90–0.99×). ***Chelicera*:** 2.13–2.17× longer than broad. ***Pedipalp*:** trochanter 1.86–1.88× longer than broad, femur 5.33–5.37× longer than broad, patella 1.94–1.98× longer than broad, femur 2.58–2.59× longer than patella. Chela 6.37–6.40× longer than deep, hand 2.11–2.15× longer than deep; movable finger 1.80–1.83× longer than hand. ***Opisthosoma*:** tergal chaetotaxy (I–XII): 4: 4: 4: 4: 5: 6: 6: 6: 5: 4: 2: 0; sternal chaetotaxy (IV–XII): 12: 10: 7: 8: 7: 7: 6: 0: 2. Anterior genital operculum with 10 + 17 setae on posterior margin (Fig. 3H).

Dimensions (mm, length/width or, in the case of the legs, chela, and chelal hand, length/depth).

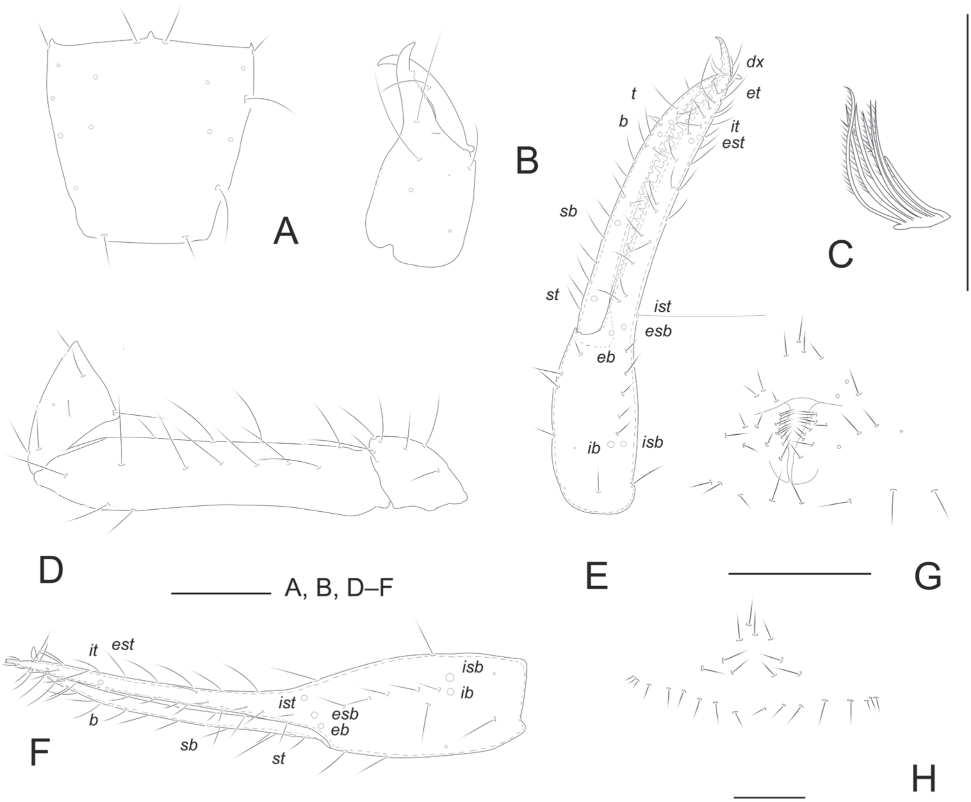

Figure 3. *Tyrannochthonius huilongshanensis* sp. nov., holotype male (**A–G**) and paratype female (**H**) **A** carapace **B** right chelicera **C** rallum of left chelicera **D** palp (minus chela) **E** chela, retrolateral view **F** chela, dorsal view **G** male genital area **H** female genital area. Scale bars: 0.20 mm.

Males (females in parentheses): body length 1.68–1.75 (1.89–1.95). Carapace 0.44–0.46/0.43–0.44 (0.45–0.49/0.50–0.51). Pedipalp: trochanter 0.24–0.26/0.15–0.17 (0.26–0.28/0.14–0.16), femur 0.73–0.76/0.15–0.17 (0.80–0.83/0.15–0.17), patella 0.29–0.31/0.18–0.19 (0.31–0.33/0.16–0.17), hand 0.36–0.40/0.18–0.20 (0.40–0.44/0.19–0.20), length of movable chelal finger 0.63–0.67 (0.72–0.76), chela 1.01–1.09/0.18–0.20 (1.21–1.25/0.19–0.20). Chelicera: 0.45–0.47/0.20–0.22 (0.51–0.54/0.24–0.26). Leg I: trochanter 0.17–0.19/0.10–0.11 (0.16–0.18/0.14–0.15), femur 0.39–0.42/0.06–0.07 (0.45–0.46/0.08–0.09), patella 0.25–0.27/0.06–0.07 (0.28–0.30/0.07–0.08), tibia 0.20–0.22/0.05–0.06 (0.22–0.25/0.06–0.07), tarsus 0.42–0.45/0.05–0.06 (0.49–0.53/0.05–0.06). Leg IV: trochanter 0.16–0.17/0.16–0.17 (0.21–0.22/0.15–0.17), femoropatella 0.57–0.59/0.22–0.24 (0.54–0.57/0.20–0.22), tibia 0.44–0.46/0.10–0.11 (0.43–0.46/0.11–0.12), basitarsus 0.19–0.21/0.07–0.08 (0.21–0.23/0.08–0.09), telotarsus 0.48–0.50/0.05–0.06 (0.50–0.54/0.05–0.06).

Distribution. China (Sichuan).

Tyrannochthonius xinzhaiensis **sp. nov.**
https://zoobank.org/3DFBBE98-7B37-4AB6-851E-6256660A4F9F
Figs 4, 7C, D

Type material. ***Holotype*** male: China, Yunnan Province, Zhaotong City, Zhenxiong County, Wude Town, Xinzhai Village, Daguoquan Cave, 27°35.90'N, 104°46.25'E, 1301 m a.s.l., 8 April 2017, Yun-Chun Li leg., in MCWNU (Ar-Ps-YN-0080). ***Paratypes*****:** 1 male, 6 females, 6 tritonymphs, collected with the holotype, in MCWNU (Ar-Ps-YN-0007).

Diagnosis. Troglobiont habitus. This new species is distinguished from other members of the genus *Tyrannochthonius* by the following combination of characters: carapace without eyes or eyespots, anterior margin with five or six setae; epistome present; tergites V–X with four setae; coxae II with 12 terminally indented coxal spines on each side; apex of coxa I with long and rounded anteromedial process, near the apex without setae; chelal hand dorsal surface with chemosensory setae; fixed chelal finger with 26 teeth, movable chelal finger with 34 or 35 teeth. Pedipalpal femur (♂) 6.94–6.97×, (♀) 6.71–6.77× longer than broad, length (♂) 1.18–1.21 mm, (♀) 1.14–1.18 mm; chela (♂) 7.90–7.91×, (♀) 6.44–6.42× longer than deep, length (♂) 1.66–1.68 mm, (♀) 1.61–1.64 mm; ratio movable chelal finger/chelal hand (♂) 1.61–1.64×, (♀) 1.76–1.80×.

Etymology. Latinized adjective, derived from the village of Xinzhai, located near the type locality.

Description. Adult male (Fig. 7C).

Carapace and chelicera reddish brown, remaining parts yellowish brown (Fig. 7C).

Carapace (Fig. 4A): 0.98–1.01× longer than broad, no eyes or eyespots; epistome very pointed and small, triangular; carapace surface smooth, lateral margins weakly constricted posteriorly. With 17 or 18 setae arranged 5–6: 4: 4: 2: 2, anterolateral setae much shorter than others. ***Coxae*****:** manducatory process pointed, with two distal setae, one long and the other slightly shorter. Pedipalpal coxa with three setae, coxa I 3, II 4, III 5, IV 5; intercoxal tubercle absent. Apex of coxa I with long and rounded anteromedial process, near the apex without setae; coxae II with 12 terminally indented coxal spines on each side, set as an oblique row, longer spines present in the middle of the row, becoming shorter distally and proximally and incised for ~ ½ their length. ***Chelicera*** (Fig. 4B): 2.59–2.61× longer than broad, hand with five setae and one lyrifissure dorsally, movable finger with one submedial seta. Cheliceral hand with moderate hispid granulation dorsally. Fixed finger with 16 teeth, distal one largest, decreasing in size proximally; movable finger with 14 or 15 teeth; galea absent. Serrula exterior with 23 or 24 blades. Rallum composed of eight blades (Fig. 4C), distal blade weakly recumbent basally, with fine barbules and set apart from the other blades, the latter tightly grouped and with long pinnae. ***Pedipalp*** (Fig. 4E–G): all setae acuminate. Trochanter 1.56–1.59×, femur 6.94–6.97×, patella 1.83–1.86× longer than broad and with four lyrifissures. Femur 2.68–2.70× longer than patella. Chela 7.90–7.91×, hand 2.90–2.93× longer than deep; movable chelal finger 1.61–1.64× longer than hand. Chelal hand dorsal surface with a single row of five chem-

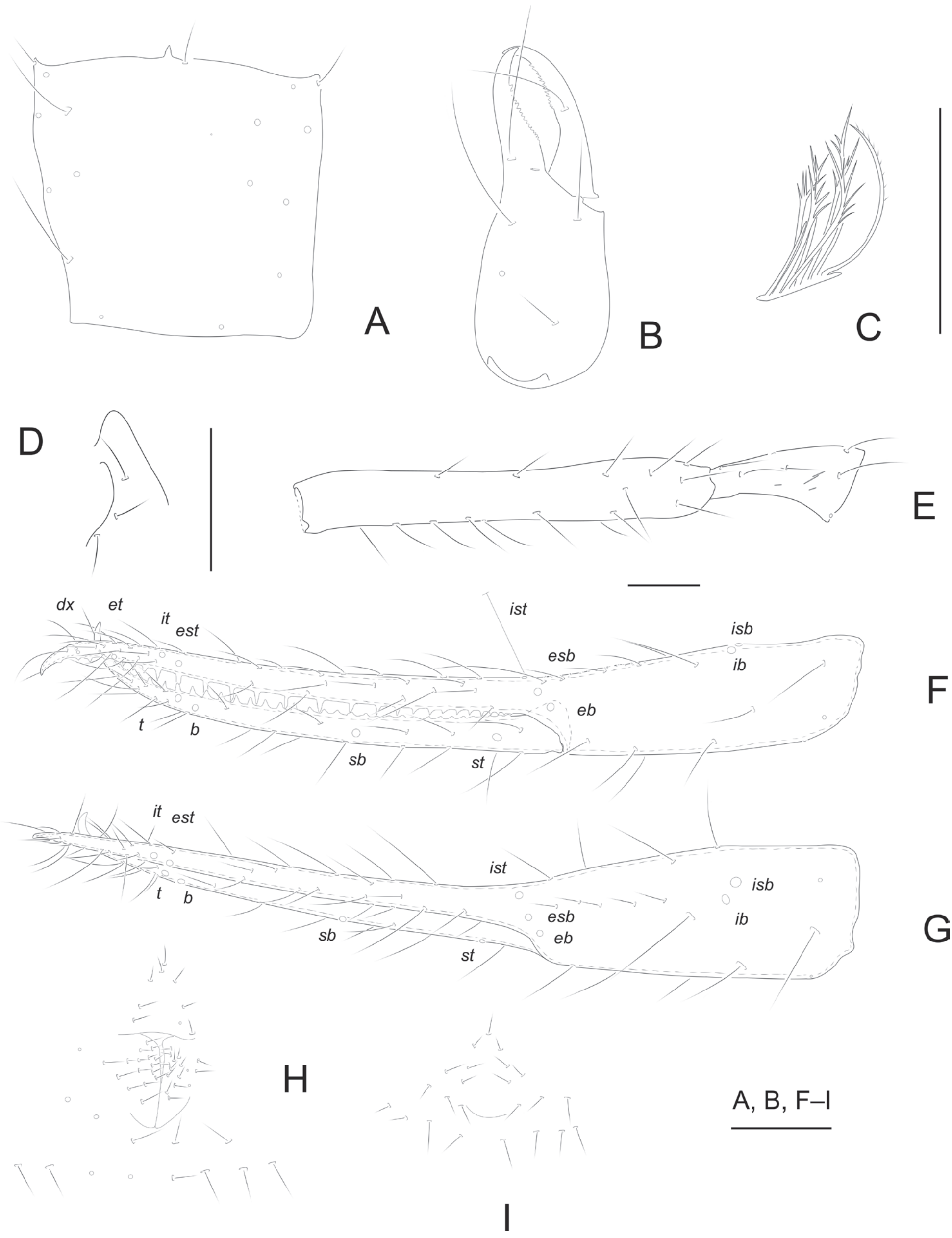

Figure 4. *Tyrannochthonius xinzhaiensis* sp. nov., holotype male (**A–H**) and paratype female (**I**) **A** carapace **B** right chelicera **C** rallum of left chelicera **D** process of left coxa I, ventral view **E** palp (minus chela) **F** chela, retrolateral view **G** chela, dorsal view **H** male genital area **I** female genital area. Scale bars: 0.20 mm.

osensory setae between *esb* and *ib*/*isb* trichobothria; distal paraxial seta of hand not enlarged. Fingers straight in dorsal view (Fig. 4G). Fixed finger with 26 teeth, middle ones larger than those at both ends; movable finger with 34 or 35 teeth (Fig. 4F).

Venom apparatus absent. Fixed chelal finger with eight trichobothria and movable finger with four, *ib* and *isb* situated close together, submedially on dorsum of chelal hand; *eb*, *esb*, and *ist* forming a straight oblique row at base of fixed chelal finger; *it* slightly distal to *est*, situated subdistally; *et* slightly nearer to tip of fixed finger; *dx* situated distal to *et*; *sb* near to *st*; *b* and *t* situated subdistally, *t* situated at same level as *est*. ***Opisthosoma*:** tergites and sternites undivided; setae uniseriate and acuminate. Tergal chaetotaxy (I–XII): 4: 4: 4: 4: 4: 4: 4: 4: 4: 4: 2: 0; sternal chaetotaxy (IV–XII): 12: 10: 10: 9: 9: 9: 7: 0: 2. Anterior genital operculum with nine setae, genital opening slit-like, with 15 or 16 marginal setae on each side (Fig. 4H). ***Legs*:** leg I: trochanter 1.43–1.44×, femur 6.60–6.62× longer than deep and 1.78–1.79× longer than patella; patella 4.11–4.14×, tibia 3.88–3.92×, tarsus 9.57–9.60× longer than deep. Leg IV: trochanter 1.05–1.07×, femoropatella 3.83–3.85×, tibia 5.91–5.93× longer than deep, basitarsus 3.75–3.76× longer than deep, with a basal tactile seta (TS = 0.20–0.21), telotarsus 12.17–12.20× longer than deep and 2.43–2.45× longer than basitarsus, with a tactile seta near base (TS = 0.18–0.19). Arolia on legs I and IV shorter than claws.

Adult female (Fig. 7D).

Mostly the same as the holotype with the differences listed below.

***Carapace*:** slightly longer than broad (1.00–1.02×). With 18 setae, including six on the anterior margin and two on the posterior margin. ***Chelicera*:** 2.26–2.27× longer than broad. ***Pedipalp*:** trochanter 1.82–1.86× longer than broad, femur 6.71–6.77× longer than broad, patella 1.76–1.79× longer than broad, femur 3.08–3.12× longer than patella. Chela 6.44–6.42× longer than deep, hand 2.20–2.22× longer than deep; movable finger 1.76–1.80× longer than hand. ***Opisthosoma*:** tergal chaetotaxy (I–XII): 4: 4: 3: 3: 4: 4: 4: 4: 4: 4: 2: 0; sternal chaetotaxy (IV–XII): 14: 10: 9: 9: 9: 9: 7: 0: 2. Anterior genital operculum with 9 + 6 setae on posterior margin (Fig. 4I).

Dimensions (mm, length/width or, in the case of the legs, chela, and chelal hand, length/depth).

Males (females in parentheses): body length 2.76–2.85 (2.69–2.88). Carapace 0.59–0.61/0.60–0.61 (0.58–0.60/0.58–0.59). Pedipalp: trochanter 0.25–0.26/0.16–0.17 (0.31–0.34/0.17–0.19), femur 1.18–1.21/0.17–0.19 (1.14–1.18/0.17–0.19), patella 0.44–0.46/0.24–0.26 (0.37–0.40/0.21–0.23), hand 0.61–0.63/0.21–0.22 (0.55–0.58/0.25–0.26), length of movable chelal finger 0.98–1.00 (0.97–1.01), chela 1.66–1.68/0.21–0.22 (1.61–1.64/0.25–0.26). Chelicera: 0.70–0.73/0.27–0.29 (0.61–0.64/0.27–0.29). Leg I: trochanter 0.20–0.22/0.14–0.15 (0.16–0.18/0.14–0.15), femur 0.66–0.68/0.10–0.11 (0.62–0.65/0.08–0.09), patella 0.37–0.39/0.09–0.10 (0.31–0.34/0.06–0.07), tibia 0.31–0.32/0.08–0.09 (0.31–0.33/0.06–0.07), tarsus 0.67–0.69/0.07–0.08 (0.64–0.67/0.06–0.07). Leg IV: trochanter 0.21–0.23/0.20–0.21 (0.19–0.21/0.17–0.19), femoropatella 0.92–0.95/0.24–0.26 (0.83–0.86/0.22–0.24), tibia 0.65–0.67/0.11–0.12 (0.57–0.60/0.09–0.10), basitarsus 0.30–0.31/0.08–0.09 (0.27–0.29/0.07–0.08), telotarsus 0.73–0.75/0.06–0.07 (0.68–0.70/0.05–0.06).

Distribution. China (Yunnan).

Tyrannochthonius yamuhensis sp. nov.

https://zoobank.org/0DBC3106-021A-4D81-BC44-92B6D00E600C

Figs 5, 8A

Type material. ***Holotype*** male: China, Yunnan Province, Lushui City, Fugong County, Shiyueliang Town, Lishadi Village, Yamu River, Nameless Cave, 27°07.69'N, 98°51.61'E, 1500 m a.s.l., 18 August 2018, Yun-Chun Li leg., in MCWNU (Ar-Ps-YN-0078). ***Paratypes*:** 1 male, collected with the holotype, in MCWNU (Ar-Ps-YN-0014).

Diagnosis (male, female unknown). Troglobiont habitus. This new species is distinguished from other members of the genus *Tyrannochthonius* by the following combination of characters: carapace without eyes or eyespots, anterior margin with four setae; epistome present; tergites II–VI with four setae; coxae II with ten terminally indented coxal spines on each side; apex of coxa I with long and rounded anteromedial process, near the apex with a seta; chelal hand dorsal surface with chemosensory setae. Fixed chelal finger with 25 teeth and 20 intercalary teeth, movable chelal finger with 22–24 teeth and three or four intercalary teeth. Pedipalpal femur 6.06–6.07× longer than broad, length 0.97–0.99 mm; chela 7.63–7.66× longer than deep, length 1.45–1.46 mm; ratio movable chelal finger/chelal hand 1.91–1.92×.

Etymology. Latinized adjective, derived from the river of Yamuhe, which is near the type locality.

Description. Adult male (Fig. 8).

Chelicera reddish brown, carapace and opisthosoma brown, remaining parts yellowish brown (Fig. 8).

Carapace (Fig. 5A): 1.06–1.08× longer than broad, no eyes or eyespots; epistome very pointed and small, triangular; carapace surface smooth, lateral margins weakly constricted posteriorly. With 18 setae, including four on anterior margin and two on posterior margin, anterolateral setae much shorter than others. ***Coxae*:** manducatory process pointed, with two distal setae, one long and the other slightly shorter. Pedipalpal coxa with three setae, coxa I 3, II 4, III 5, IV 5; intercoxal tubercle absent. Apex of coxa I with long and rounded anteromedial process, near the apex with a seta; coxae II with ten terminally indented coxal spines on each side, set as an oblique row, longer spines present in the middle of the row, becoming shorter distally and proximally and incised for ~ ½ their length (Fig. 5D). ***Chelicera*** (Fig. 5B): 2.31–2.33× longer than broad, hand with five setae and two lyrifissures dorsally, movable finger with one submedial seta. Cheliceral hand with moderate hispid granulation dorsally. Fixed finger with eight or nine teeth, distal one largest, decreasing in size proximally; movable finger with 12 or 13 teeth; galea absent. Serrula exterior with 20 or 21 blades. Rallum composed of eight blades (Fig. 5C), distal blade weakly recumbent basally, with fine barbules and set apart from the other blades, the latter tightly grouped and with long pinnae. ***Pedipalp*** (Fig. 5F–H): all setae acuminate. Trochanter 1.01–1.04×, femur 6.06–6.07×, patella 2.38–2.40× longer than broad. Femur 2.55–2.56× longer than patella. Chela 7.63–7.66×, hand 2.47–2.50× longer than deep; movable chelal finger 1.91–1.92× longer than hand. Chelal hand dorsal surface with a single row of five

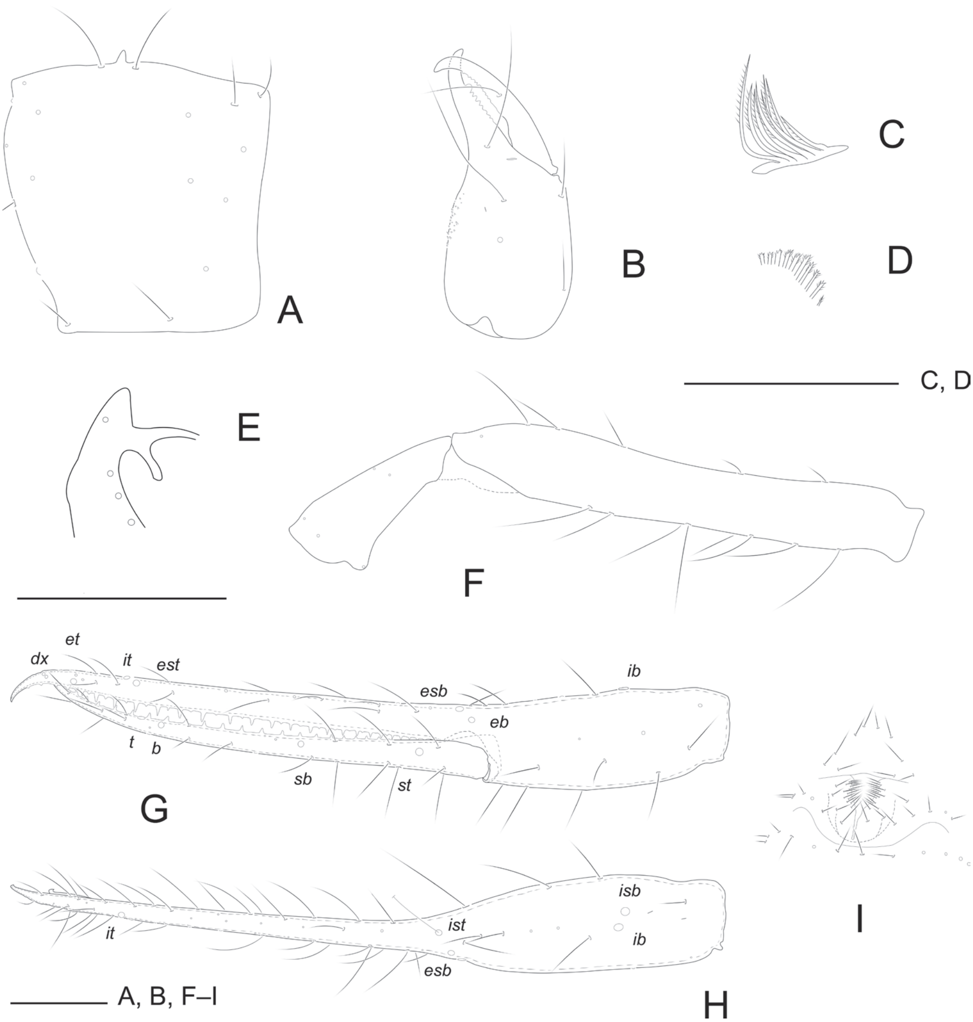

Figure 5. *Tyrannochthonius yamuhensis* sp. nov., holotype male (**A–I**) **A** carapace **B** right chelicera **C** rallum of left chelicera **D** coxal spines **E** process of right coxa I, ventral view **F** palp (minus chela) **G** chela, retrolateral view **H** chela, dorsal view **I** male genital area. Scale bars: 0.20 mm.

chemosensory setae between *esb* and *ib*/*isb* trichobothria; distal paraxial seta of hand not enlarged. Fingers straight in dorsal view (Fig. 5H). Fixed finger with 25 teeth and 20 intercalary teeth, middle ones larger than those at both ends; movable finger with 22–24 teeth and three or four intercalary teeth (Fig. 5G). Venom apparatus absent. Fixed chelal finger with eight trichobothria and movable finger with four, *ib* and *isb* situated close together, submedially on dorsum of chelal hand; *eb*, *esb*, and *ist* forming a straight oblique row at base of fixed chelal finger; *it* slightly distal to *est*, situated subdistally; *et* slightly nearer to tip of fixed finger; *dx* situated distal to *et*; *sb* near to *st*; *b* and *t* situated subdistally, *t* situated at same level as *est*. ***Opisthosoma*:** tergites and sternites undivided; setae uniseriate and acuminate. Tergal chaetotaxy (I–XII): 3: 4: 4:

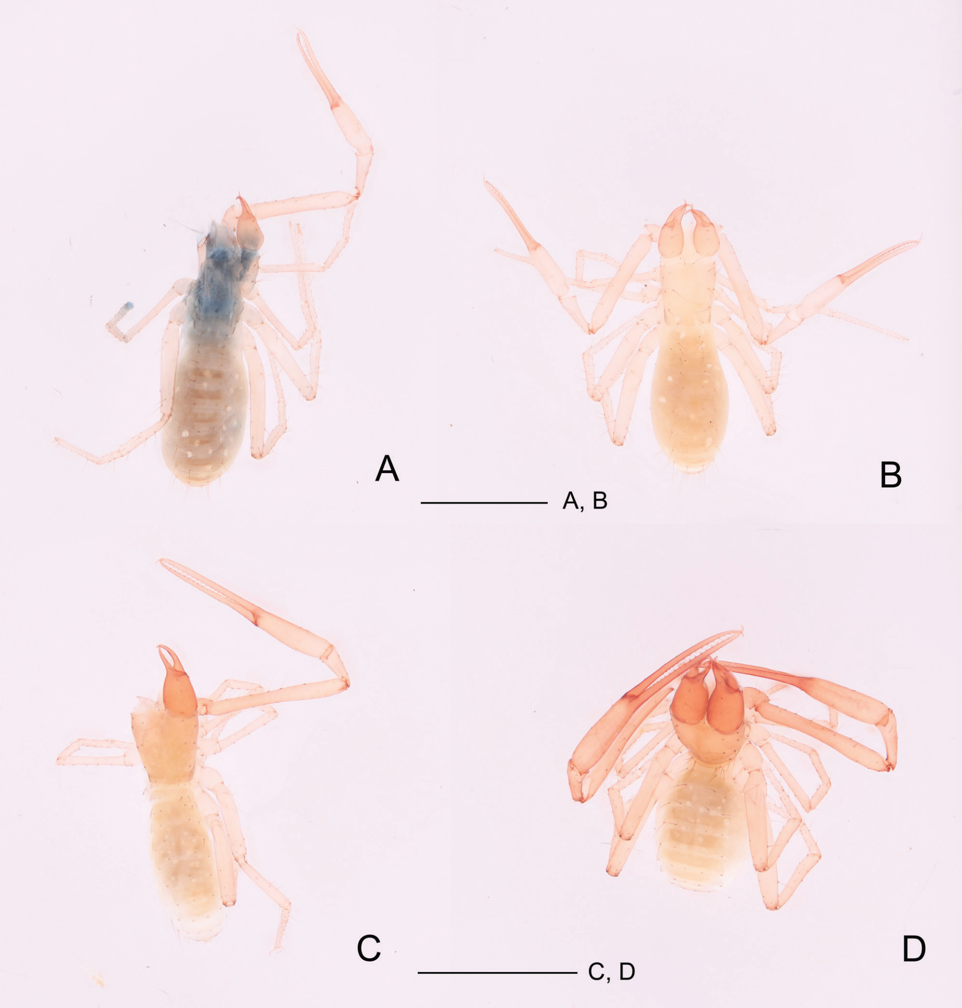

Figure 6. A, B *Tyrannochthonius dongjiensis* sp. nov., dorsal views **A** holotype male **B** paratype female **C, D** *T. huaerensis* sp. nov., dorsal views **C** holotype male **D** paratype female. Scale bar: 1.00 mm (**A–D**).

4: 4: 4: 6: 5: 5: 5: 2: 0; sternal chaetotaxy (IV–XII): 12: 10: 7: 7: 7: 7: 6: 0: 2. Anterior genital operculum with ten, genital opening slit-like, with 15 or 16 marginal setae on each side (Fig. 5I). ***Legs*:** leg I: trochanter 1.38–1.40×, femur 6.63–6.65× longer than deep and 1.77–1.79× longer than patella; patella 4.29–4.30×, tibia 5.20–5.22×, tarsus 11.80–11.81× longer than deep. Leg IV: trochanter 1.06–1.07×, femoropatella 3.00–3.02×, tibia 5.70–5.71× longer than deep, basitarsus 3.00–3.01× longer than deep, with a basal tactile seta (TS = 0.20–0.21), telotarsus 12.80–12.81× longer than deep and 2.67–2.69× longer than basitarsus, with a tactile seta near base (TS = 0.19–0.20). Arolia on legs I and IV shorter than claws.

Dimensions (mm, length/width or, in the case of the legs, chela, and chelal hand, length/depth).

Figure 7. A, B *Tyrannochthonius huilongshanensis* sp. nov., dorsal views **A** holotype male **B** paratype female **C, D** *T. xinzhaiensis* sp. nov., dorsal views **C** holotype male **D** paratype female. Scale bar: 1.00 mm (**A–D**).

Males: body length 2.25–2.30. Carapace 0.56–0.57/0.53–0.54. Pedipalp: trochanter 0.14–0.15/0.14–0.15, femur 0.97–0.99/0.16–0.18, patella 0.38–0.39/0.16–0.17, hand 0.47–0.49/0.19–0.20, length of movable chelal finger 0.90–0.92, chela 1.45–1.46/0.19–0.20. Leg I: trochanter 0.18–0.19/0.13–0.15, femur 0.53–0.55/0.08–0.09, patella 0.30–0.31/0.07–0.08, tibia 0.26–0.28/0.05–0.06, tarsus

Figure 8. *Tyrannochthonius yamuhensis* sp. nov., dorsal view, holotype male. Scale bar: 1.00 mm.

0.59–0.60/0.05–0.06. Leg IV: trochanter 0.18–0.20/0.17–0.18, femoropatella 0.75–0.77/0.25–0.26, tibia 0.57–0.59/0.10–0.11, metatarsus 0.24–0.25/0.08–0.09, tarsus 0.64–0.66/0.05–0.06.

Distribution. China (Yunnan).

Key to the species of *Tyrannochthonius* known from China (subspecies not included)

1 Carapace with eyes **2**

– Carapace without eyes or eyespots **4**

2 Chelal finger without intercalary teeth **3**

– Chelal finger with intercalary teeth .... ***T. robustus* Beier, 1951**

3 Carapace with 18 setae; tergites VIII–IX each with 8 setae .... ***T. japonicus* (Ellingsen, 1907)**

– Carapace with 16 setae; tergites VIII–IX each with 6 setae .... ***T. pachythorax* Redikorzev, 1938**

4 Chelal finger with intercalary teeth **5**
– Chelal finger without intercalary teeth **11**
5 Intercalary teeth only present on chelal finger **6**
– Intercalary teeth present on both chelal fingers.. **7**
6 Rallum with 6 pinnate blades; coxae II with 5 or 6 terminally indented coxal spines on each side; epistome present....................... ***T. zhai*** **Gao, Zhang & Chen, 2020**
– Rallum with 7 or 8 pinnate blades; coxae II with 7 terminally indented coxal spines on each side; epistome absent................ ***T. chixingi*** **Gao, Wynne & Zhang, 2018**
7 Carapace anterior margin with 6 setae; chemosensory setae absent.................... **8**
– Carapace anterior margin with 4 setae; chemosensory setae present **10**
8 Tergites I–II each with 2 setae **9**
– Tergites I–II each with 4 setae .... ***T. antridraconis*** **Mahnert, 2009**
9 Palpal femur 6.60× as long as broad (length 0.90 mm), chela 7.70× longer than deep .... ***T. akaleus*** **Mahnert, 2009**
– Palpal femur 5.90–6.70× as long as broad (length 0.95–0.97 mm), chela 6.90–7.30× longer than deep .... ***T. ganshuanensis*** **Mahnert, 2009**
10 Coxae II with 8 terminally indented coxal spines on each side ; chela 5.61–5.66× longer than deep .... ***huilongshanensis*** **sp. nov.**
– Coxae II with 10 terminally indented coxal spines on each side; chela 7.63–7.66× longer than deep .... ***T. yamuhensis*** **sp. nov.**
11 Chelal fingers straight in dorsal view **12**
– Chelal fingers gently curved in dorsal view .... ***T. pandus*** **Hou, Gao & Zhang, 2022**
12 Chelal movable fingers without retrorse teeth; epistome present...................... **13**
– Chelal movable fingers with retrorse teeth; epistome absent...................................... .... ***T. dongjiensis*** **sp. nov.**
13 Carapace anterior margin with 4 setae... **14**
– Carapace anterior margin with 5 or 6 setae .... ***T. xinzhaiensis*** **sp. nov.**
14 Coxae II with 8 terminally indented coxal spines on each side; rallum with 6 pinnate blades .... ***T. harveyi*** **Gao, Zhang & Chen, 2020**
– Coxae II with 12 terminally indented coxal spines on each side; rallum with 8 pinnate blades .... ***T. huaerensis*** **sp. nov.**

Discussion

There are 146 known species of *Tyrannochthonius*, including four subspecies, of which 52 species live in caves. Other than China, these cave species are distributed in Africa, Oceania, and North America. Among them, there are 31 species in the United States, five species in Australia, four species in Mexico, one species in Kenya, one species in New Caledonia, one species in Guatemala, one species in Peru, and one species in Jamaica (Hou et al. 2022; World Pseudoscorpiones Catalog 2022).

In China, ten species and one subspecies have been recorded (Fig. 9), including seven cave-dwelling species, three species and one subspecies that are soil-dwelling: *T. akaleus*

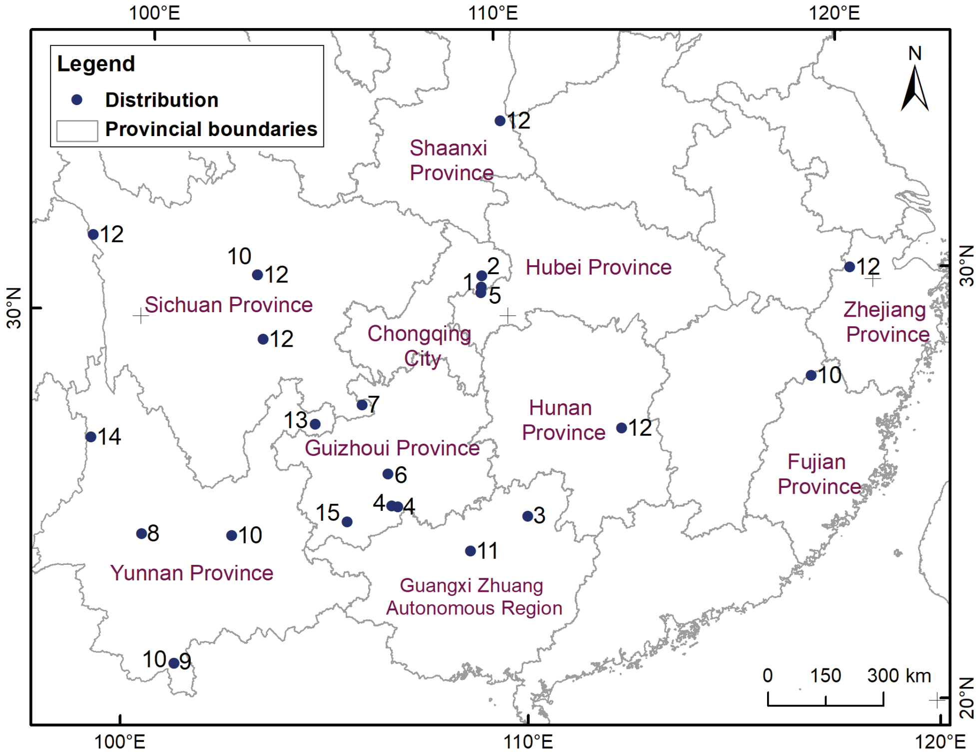

Figure 9. Known distribution of genus *Tyrannochthonius* from China. 1 *T. akaleus*; 2 *T. antridraconis*; 3 *T. chixingi*; 4 *T. dongjiensis* sp. nov.; 5 *T. ganshuanensis*; 6 *T. harveyi*; 7 *T. huaerensis* sp. nov.; 8 *T. huilongshanensis* sp. nov.; 9 *T. japonicus*; 10 *T. pachythorax*; 11 *T. pandus*; 12 *T. robustus*; 13 *T. xinzhaiensis* sp. nov.; 14 *T. yamuhensis* sp. nov.; 15 *T. zhai*.

Mahnert, 2009 (Chuandongzi Cave) and *T. antridraconis* Mahnert, 2009 (Perte du Dragon Cave) from Chongqing; *T. ganshuanensis* Mahnert, 2009 (Changcao Cave) from Hubei; *T. chixingi* Gao, Wynne & Zhang, 2018 (Maomaotou Cave) from Guangxi; *T. dongjiensis* sp. nov. (Nameless Cave and Baima Cave), *T. harveyi* Gao, Zhang & Chen, 2020 (Yutang Cave) and *T. zhai* Gao, Zhang & Chen, 2020 (Jiangjia Cave) from Guizhou; *T. huaerensis* sp. nov. (Huaer Cave) from Sichuan; *T. huilongshanensis* sp. nov. (Banpoyan Cave), *T. pandus* Hou, Gao & Zhang, 2022 (Biyun Cave), *T. xinzhaiensis* sp. nov. (Daguoquan Cave) and *T. yamuhensis* sp. nov. (Nameless Cave) from Yunnan; *T. japonicus* (Ellingsen, 1907) and *T. japonicus japonicus* (Ellingsen, 1907), soil-dwelling species from Yunnan and Taiwan; *T. pachythorax* Redikorzev, 1938, a soil-dwelling species from Yunnan, Sichuan, and Fujian; and *T. robustus* Beier, 1951 a soil-dwelling species from Sichuan, Zhejiang, Hunan, and Shaanxi (Schawaller 1995; Mahnert 2009; Gao et al. 2018, 2020; Hou et al. 2022). The eyes of these cave-dwelling species are completely degraded.

The five new cave-dwelling species are easily distinguished from the seven known species: the chelal fingers of all new species are straight in dorsal view, while in *T. pandus* they are slightly curved. The movable finger of *T. dongjiensis* sp. nov. has retrorse teeth, which is similar to that of *T. zhai*, but the new species have a carapace with 18 setae and tergites I–IV each with two setae; the latter carapace only with 16 setae, and tergites I–IV each with four setae. There are only 16 setae on the carapace of *T. chixingi*, the other species have 17 or 18 setae. *T. huaerensis* sp. nov., *T. huilongshanensis* sp. nov., *T. xinzhaiensis* sp. nov., and *T. yamuhensis* sp. nov. are different from the remaining species (except *T. antridraconis*) in that the new species have tergites I-II each with three or four setae, while the latter only has two setae. In the new species, the chelal hand presents chemosensory setae on the dorsum, while in *T. antridraconis* they are absent. *T. huilongshanensis* sp. nov. and *T. yamuhensis* sp. nov. have intercalary teeth, the former with ten coxal spines and chela 7.63–7.66× longer than broad; in the latter, with eight coxal spines and chela 5.61–5.66× longer than broad. In *T. huaerensis* sp. nov., the anterior margin of the carapace with four setae, a slender and pointed epistome, palpal femur 8.92–8.95× as long as broad, and movable finger retrolateral margins weakly curved between *st* and *sb* trichobothria; in contrast, in *T. xinzhaiensis* sp. nov. the anterior margin of the carapace with five or six setae, epistome very small, palpal femur 6.94–6.97× as long as broad, movable finger retrolateral margins straight between *st* and *sb* trichobothria. In the known species, the chemosensory setae on the dorsal surface of the chelal hand are absent, while in the new species, there is a row of five to seven setae on the dorsal surface of the chelal hand.

Acknowledgements

Many thanks to Prof. Mark Harvey (Western Australian Museum, Perth, Australia) and an anonymous reviewer for comments that improved the manuscript. This study was supported by the Doctoral Scientific Research Foundation of China West Normal University (18Q043).

References

Chamberlin JC (1929) A synoptic classification of the false scorpions or chela-spinners, with a report on a cosmopolitan collection of the same. Part 1. The Heterosphyronida (Chthoniidae) (Arachnida-Chelonethida). Annals & Magazine of Natural History 4(10): 50–80. https://doi.org/10.1080/00222932908673028

Chamberlin JC (1931) The arachnid order Chelonethida. Stanford University Publications, University Series (Biological Sciences) 7(1): 1–284.

Edward KL, Harvey MS (2008) Short-range endemism in hypogean environments: the pseudoscorpion genera *Tyrannochthonius* and *Lagynochthonius* (Pseudoscorpiones: Chthoniidae) in the semiarid zone of Western Australia. Invertebrate Systematics 22(2): 259–293. https://doi.org/10.1071/IS07025

Gao ZZ, Wynne JJ, Zhang F (2018) Two new species of cave-adapted pseudoscorpions (Pseudoscorpiones: Neobisiidae, Chthoniidae) from Guangxi, China. The Journal of Arachnology 46(2): 345–354. https://doi.org/10.1636/JoA-S-17-063.1

Gao ZZ, Zhang F, Chen HM (2020) Two new cave-dwelling species of *Tyrannochthonius* Chamberlin, 1929 (Pseudoscorpiones: Chthoniidae) from the Guizhou karst, China. Zootaxa 4853(4): 572–580. https://doi.org/10.11646/zootaxa.4853.4.6

Harvey MS (1992) The phylogeny and classification of the Pseudoscorpionida (Chelicerata: Arachnida). Invertebrate Taxonomy 6(6): 1373–1435. https://doi.org/10.1071/IT9921373

Hou YM, Gao ZZ, Zhang F (2022) Two new species of cave-adapted pseudoscorpions (Pseudoscorpiones, Chthoniidae) from Yunnan, China. ZooKeys 1097: 65–83. https://doi.org/10.3897/zookeys.1097.82527

Judson MLI (2007) A new and endangered species of the pseudoscorpion genus *Lagynochthonius* from a cave in Vietnam, with notes on chelal morphology and the composition of the Tyrannochthoniini (Arachnida, Chelonethi, Chthoniidae). Zootaxa 1627(1): 53–68. https://doi.org/10.11646/zootaxa.1627.1.4

Mahnert V (2009) New species of pseudoscorpions (Arachnida, Pseudoscorpiones: Chthoniidae, Chernetidae) from caves in China. Revue Suisse de Zoologie 116: 185–201. https://doi.org/10.5962/bhl.part.79492

Muchmore WB, Chamberlin JC (1995) The genus *Tyrannochthonius* in the eastern United States (Pseudoscorpionida: Chthoniidae). Part 1. The historical taxa. Insecta Mundi 9: 249–257.

Schawaller W (1995) Review of the pseudoscorpion fauna of China (Arachnida: Pseudoscorpionida). Revue Suisse de Zoologie 102(4): 1045–1064. https://doi.org/10.5962/bhl.part.80489

World Pseudoscorpiones Catalog (2022) World Pseudoscorpiones Catalog. Natural History Museum Bern. https://wac.nmbe.ch/order/pseudoscorpiones/3 [Accessed on 15 July 2022]

ZooKeys 1131: 197–215 (2022)
doi: 10.3897/zookeys.1131.90688
https://zookeys.pensoft.net

RESEARCH ARTICLE

A peer-reviewed open-access journal
ZooKeys
Launched to accelerate biodiversity research

A new species and three newly recorded species of Tetrastichinae (Hymenoptera, Eulophidae) from China

Wen-Jian Li[1,2], Cheng-De Li[3]

1 *Jiangsu Provincial Key Laboratory of Coastal Wetland Bioresources and Environmental Protection, School of Wetland, Yancheng Teachers University, Yancheng, 224007, China* **2** *Jiangsu Key Laboratory for Bioresources of Saline Soils, School of Wetland, Yancheng Teachers University, Yancheng, 224007, China* **3** *School of Forestry, Northeast Forestry University, Harbin, 150040, China*

Corresponding author: Cheng-De Li (lichengde0608@sina.com)

Academic editor: Zachary Lahey | Received 22 July 2022 | Accepted 28 October 2022 | Published 24 November 2022

https://zoobank.org/17D6DA06-6B46-426E-8363-5CB93EF4E207

Citation: Li W-J, Li C-D (2022) A new species and three newly recorded species of Tetrastichinae (Hymenoptera, Eulophidae) from China. ZooKeys 1131: 197–215. https://doi.org/10.3897/zookeys.1131.90688

Abstract

Five species of five genera in Tetrastichinae (Hymenoptera, Eulophidae) from China are reviewed, including one new species, *Mestocharella qingdaoensis* **sp. nov.**, and three new country record species: *Nesolynx thymus* (Girault, 1916), *Holcotetrastichus rhosaces* (Walker, 1839), and *Peckelachertus diprioni* Yoshimoto, 1970. New distributional data for *Ceratoneura indi* Girault, 1917 are provided.

Keywords

Chalcidoidea, genera, parasitoids, taxonomy

Introduction

The subfamily Tetrastichinae (Hymenoptera, Eulophidae) is one of the largest groups of Chalcidoidea (Graham 1987; LaSalle 1994). Species are distributed in almost all geographic realms and play a vital role in terrestrial ecosystems (Graham 1987; LaSalle 1994). Most species of Tetrastichinae are parasitic; they attack species from approximately 1000 families in 10 different orders of Insecta (Graham 1987; LaSalle 1994). Also, some species, such as *Leptocybe invasa* Fisher and LaSalle, 2004, are phytophagous and live in galls produced by their hosts.

Unfortunately, Chinese species of Tetrastichinae are poorly investigated compared to other countries and regions (Kostjukov 1978, 2000; Graham 1987, 1991; Bouček 1988; LaSalle 1994; Narendran 2007). In the early stage, foreign entomologists reported several Tetrastichinae from Guangdong, Macao, and Taiwan in China (Perkins 1912; Timberlake 1921; Miwa and Sonan 1935). With more research on parasitic wasps, Chinese entomologists realized the importance of this faunal group: Liao et al. (1984) reported 201 economically important insect species of China including eight species of Tetrastichinae; Yang (1996) systematically investigated parasitic wasps on bark beetles from China and reported 141 species including 16 species of Tetrastichinae; Zhu and Huang (2001) investigated Eulophidae from Zhejiang province and reported 12 species of Tetrastichinae; Zhu and Huang (2002) investigated Eulophidae from Guangxi province and reported 23 species of Tetrastichinae; Zhang et al. (2007) investigated Eulophidae from south Gansu and Qinlin Mountains and reported 14 species of Tetrastichinae; Yang et al. (2015) systematically investigated parasitic wasps on forest defoliators, reporting 115 species including 20 species belonging to four genera of Tetrastichinae. Subsequently, there are many more reports of new species and records of Tetrastichinae (Yang 1989; Sheng and Wang 1992, 1993; Sheng 1995; Sheng and Zhao 1995; Sheng and Zhu 1998; Yang and Wei 2003; Jiao et al. 2006; Zhang et al. 2009; Wu et al. 2009; Li et al. 2014; Yang et al. 2014; Feng et al. 2016; Li et al. 2016; Song et al. 2017; Li and Li 2020, 2021; Song et al. 2020; Guo et al. 2022; Ning et al. 2022). In terms of Tetrastichinae species richness, there is an obvious imbalance among provinces of China. Most southern provinces have more species than northern provinces, such as 27 species in Guangxi Province compared with just two species in Ningxia Province. Therefore, there is still much to study, and knowledge to be gained, about this group in China.

Materials and methods

Specimens were collected by sweep netting and yellow-pan trapping. They were preserved and were dissected and mounted in Canada balsam following the method of Noyes (1982), or fixed on triangular cards. Photographs were taken with a digital CCD camera attached to an Olympus BX51 compound microscope and a AOSVI HK-830 microscope. Most measurements were made from slide-mounted specimens using an eye-piece reticule with an Olympus CX21 microscope. Terminology follows Gibson et al. (1997) and the following abbreviations are used:

F1–4 (flagellomeres 1–4);
POL (minimum distance between lateral ocelli);
OOL (minimum distance between lateral ocellus and eye margin);
OD (longest diameter of a lateral ocellus);
MV (marginal vein);
STV (stigmal vein);
SMV (submarginal vein);
PMV (postmarginal vein).

All the specimens listed below are deposited in Northeast Forestry University (**NEFU**), Harbin, China.

Species accounts

The genus *Mestocharella* (Eulophidae, Tetrastichinae) was erected by Girault (1913) with *Mestocharella feralis* Girault, 1913 as the type species. It is a small genus with 12 valid species worldwide (Noyes 2019) and only one species occurring in China, *M. javensis* (Kamijo 1994). Because the propodeum is different from the propodeum of all the other species included in *Mestocharella*, *M. deltoids* Khan, Agnihotri & Sushil, 2005 and *M. indica* Jaikishan Singh & Khan, 1995 probably do not belong to the genus (Narendran 2007).

Mestocharella is a unique genus and can be distinguished from Tetrastichinae by the following characteristics: malar sulcus present; antenna slender, one anellus, funicle with four segments and clava bi-segmented in female; funicle 4-segmented and clava 3-segmented in male; pronotum long, collar with or without transverse carina; axillae not so advanced; dorsellum with a median carina; propodeum long, with a large subpentagonal area; spiracles small; gastral petiole conspicuous, strongly carinate; gaster usually shorter than mesosoma.

The species of *Mestocharella* can be divided into three species groups: the *kumatai*, *feralis*, and *javensis* groups (Kamijo 1994). The species of *Mestocharella* are parasitic on Lepidoptera (Bouček 1988; Kamijo 1994).

***Mestocharella qingdaoensis* sp. nov.**

https://zoobank.org/BA195019-145C-4A7E-838E-BAEB094AF9FB
Figs 1–4

Type material. ***Holotype***, female [on card], China, Shandong Province, Qingdao City, Mount Xiao Zhu, 18–20.V.2014, Guo-Hao Zu, Si-Zhu Liu, by yellow pan trapping (deposited in NEFU). ***Paratypes***,1 female [on slide], same data as holotype (deposited in NEFU).

Diagnosis. Female. Body mainly brownish, head and posterior half of mesoscutum and axillae yellow; propodeum median carina not forked anteriorly; plicae distinct but not connected with median carina; forewing SMV with three dorsal setae, MV 6.9–7.3× as long as STV. *Mestocharella qingdaoensis* belongs to the *kumatai* group (Kamijo 1994) in that the pronotal collar is without transverse carina, and it is similar to *M. kumatai* Kamijo, 1994. However, it can be separated from *M. kumatai* by the following characteristics: head yellow (vs blackish); mid-lobe of mesoscutum without median line (vs vague); median carina of propodeum not forked anteriorly (vs always forked); plicae distinct but not connected with median carina (connected by anterior oblique carinae); forewing SMV with three dorsal setae (vs five).

Description. Female. Body length 1.8–1.9 mm, mainly yellow (Figs 1, 2). Head yellow, eyes deep reddish brown, ocellus yellowish white; antenna scape yellowish, pedi-

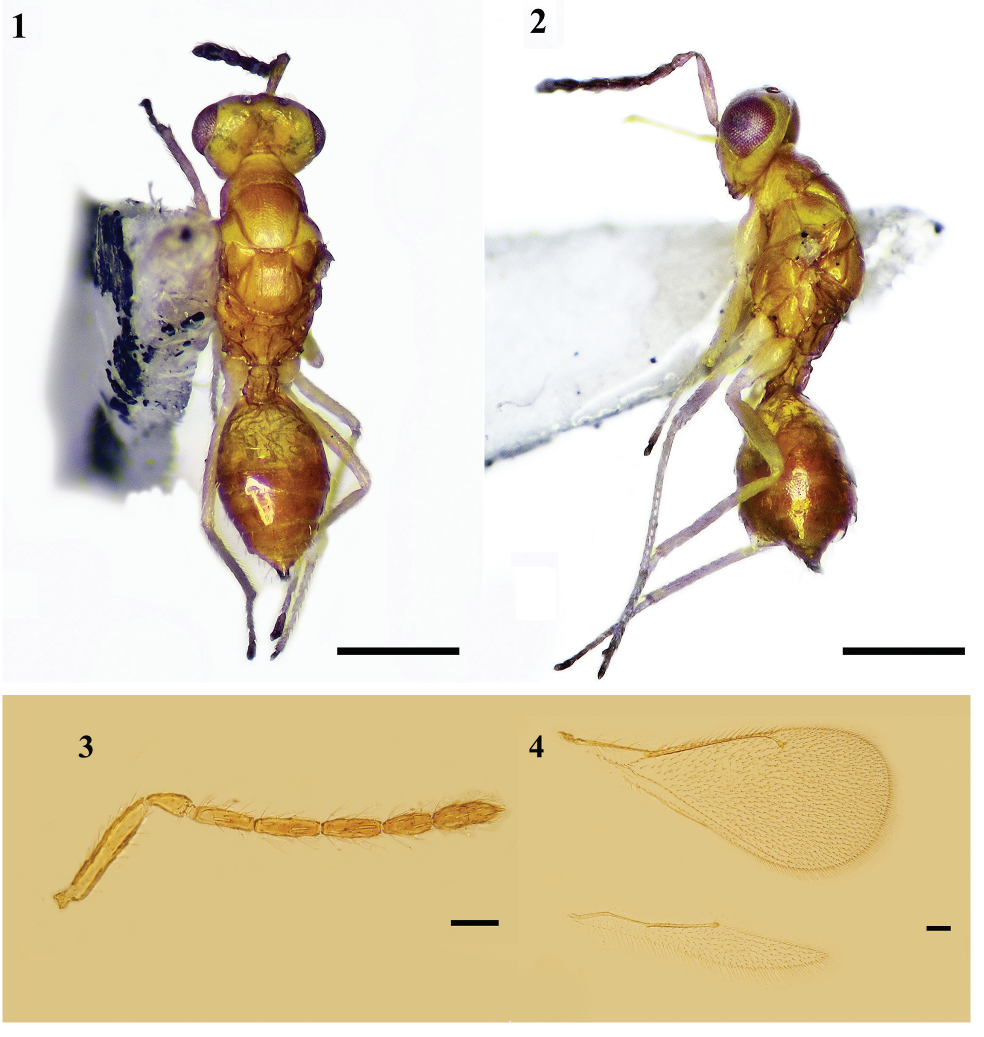

Figures 1–4. *Mestocharella qingdaoensis* sp. nov., holotype, female **1** habitus, dorsal view **2** habitus, lateral view. Scale bars: 500 μm **3** antenna, lateral view **4** fore and hind wings, dorsal view. Scale bars: 100 μm.

cel and flagellum yellowish brown. Metasoma mainly brownish with posterior half of mesoscutum and axillae yellow; wings hyaline, venation yellowish brown; legs yellow, tarsomere IV of all legs dark brown. Mesosoma brownish with basal 1/3 yellowish brown.

Head in dorsal view, nearly as broad as mesosoma, 2.5–2.6× (2.5×) as broad as long; vertex with setae shorter than OD, POL 1.3× OOL, OOL 2. × OD. Face depressed slightly, without median line; torulus with lower edge above the ventral edge of eyes; eyes separated by 1.45× their height. Malar sulcus present; malar space 0.6× as long as eye height. Mouth cavity 1.4× as wide as malar space; clypeus with anterior margin bidentate; mandible tridentate. Antenna (Fig. 3) scape 5× as long as broad with shorter setae on dorsal and ventral side; two anelli, first anellus slightly transverse, second anellus lamellar; pedicel 2.2–2.3× as long as broad, shorter than F1; F1–F4: 3.0×, 3.4×, 3.2×, 2.3× as long as broad respectively; clava 3.2× as long as broad, ca as broad as F3, bi-segmented; flagellum with long whorled setae.

Metasoma relatively long, 1.7–1.8× (1.8×) as long as broad. Pronotum subconical, 3.15× as broad as long, ~0.6× as long as mid-lobe of mesoscutum; collar rounded anteriorly and without transverse carina. Mid-lobe of mesoscutum with extremely fine reticulation; without median line; 3 adnotaular setae in one row on each side. Scutellum ca. as long as broad; submedian grooves shallow but distinct enclosing a space ~2.9× as long as broad, sublateral grooves distinct without weak costulae; anterior setae situated before middle distinctly. Dorsellum ~3× as broad as long, with a weak median carina. Propodeum subpentagonal area broad, smooth, without reticulation, median carina distinct and thin, not forked anteriorly; plicae distinct but not connecting with median carina; spiracle small, circular; callus with 2 setae. Forewing (Fig. 4) 2.2× as long as broad, SMV with 3 dorsal setae; costal cell shorter than MV, MV 6.9–7.3× (7.3×) as long as STV with front edge 12–15 setae; STV short with a long uncus; speculum small, nearly closed posteriorly, subcubital line of setae not reaching to distal edge of speculum. Legs slender, spur of metatibia 0.5× as long as length of metabasitarsus.

Gastral petiole long with several transverse weak carinae anteriorly and 3 or 4 longitudinal strong carinae. Gaster 1.2–1.4× as long as broad, shorter than mesosoma; ovipositor 0.5× as long as gaster and slightly exserted at apex of gaster, tip of hypopygium situated at basal 4/5 of gaster.

Male. Unknown.

Host. Unknown.

Distribution. China (Shandong).

Etymology. The epithetic *qingdao* refers to the place where the species collected.

Nesolynx Ashmead, 1905

Note. The genus *Nesolynx* was erected by Ashmead (1905) with *Nesolynx flavipes* Ashmead, 1905 as the type species. Bouček (1988) proposed *Aceratoneurella* Girault, 1917, *Ceratotrastichus* Girault & Dodd, 1913, and *Omphalomomyia* Girault, 1913 as synonyms of *Nesolynx*. It is a characteristic genus with 17 species recorded worldwide (Noyes 2019), but only one species, *Nesolynx thymus* (Girault, 1916), is found in China. It is distributed in tropical and subtropical countries, in the warmer parts of the temperate zones of Europe, Africa, Asia, Australia, and the Pacific islands (Bouček 1988). It can be distinguished from Tetrastichinae particularly by the mid-lobe of mesoscutum bearing dense setae and without a median line (Bouček 1988). The species are parasitoids of various groups of Diptera and Lepidoptera (Bouček 1988).

Nesolynx thymus (Girault, 1916), new record from China

Figs 5–10

Omphalomomyia thymus Girault, 1916: 485.

Omphalomomyia thymus javae Girault, 1917: 7 (subspecies). [Synonymized by Bouček 1977: 404].
Buonapartea aeniceps Girault, 1924: 5. Syntypes. [Synonymized by Bouček 1988: 697].
Syntomosphyrum obscuriceps Ferrière, 1940: 138. [Synonymized by Bouček 1977: 404].
Omphalomonyia [sic] *thymus*: Thompson 1955: 292.
Nesolynx thymus: Bouček 1977: 404.

Material examined. 7 females: [1 female on slide], Henan Province, Xinyang City, Mount Yan, Temple Xianyin, 6–7.VIII.2015, Hui Geng, Zhi-Guang Wu, Yan Gao, by yellow pan trapping; [1 female on slide], Hainan Province, Changjiang County, Mount Bawanglin, 15–17.V.2019, Wen-Jian Li, Jun Wu, by yellow pan trapping; [1 female on slide], Hainan Province, Haikou City, Hainan University, 27–29.VI.2019, Yu-Ting Jiang, by yellow pan trapping; [2 females on cards], Yunnan Province, Yuanjiang County, 26–28.XI.2020, Jun Wu, Jun-Jie Fan; Ming-Rui Li, Gang Fu, by yellow pan trapping; [2 females on cards], Yunnan Province, Shuangjiang County, 21.IV.2013, Xiang-Xiang Jin, Guo-Hao Zu, Chao Zhang, by sweeping. (All deposited in NEFU).

Diagnosis. Female. Body mainly yellow (Figs 5, 6); upper face, vertex, gena, and occiput dark green with metallic reflections, lower face yellow (Fig. 7); gaster yellow with black sides. Mesosoma with dense setae on mid-lobe of mesoscutum, especially a pair of long black setae posteriorly similar to setae on scutellum; propodeum with median carina distinct, cup-shaped. Gaster 1.6–1.8× as long as broad.

Male. Unknown.

Hosts. Not known from China. Non-Chinese records include *Musca domestica* Linnaeus, 1758, *Exorista bombycis* (Louis, 1880), *Bombyx mori* Linnaeus, 1758 (Bansude et al. 2010), *Argyrophylax leefmansi* Baranov, 1933, *Bessa remota* (Aldrich, 1925), *Chaetogena bezziana* Baranov, 1934, *Nephantis serinopa* Meyrick, 1905, *Artona catoxantha* Hampson, 1892 (Herting 1978), *Exorista sorbillans* (Wiedemann, 1830) (Kumar et al. 1991), *Ptychomyia remota* Aldrich, 1925, *Cadurcia leefmansi* Baranov, 1933 (Lever 1964), *Zaratha* sp. (Bouček 1988), *Sturmiopsis inferens* Townsend, 1916,

Figures 5–7. *Nesolynx thymus* (Girault), female **5** habitus, dorsal view **6** habitus, lateral view. Scale bars: 500 μm **7** head, frontal view. Scale bar: 200 μm.

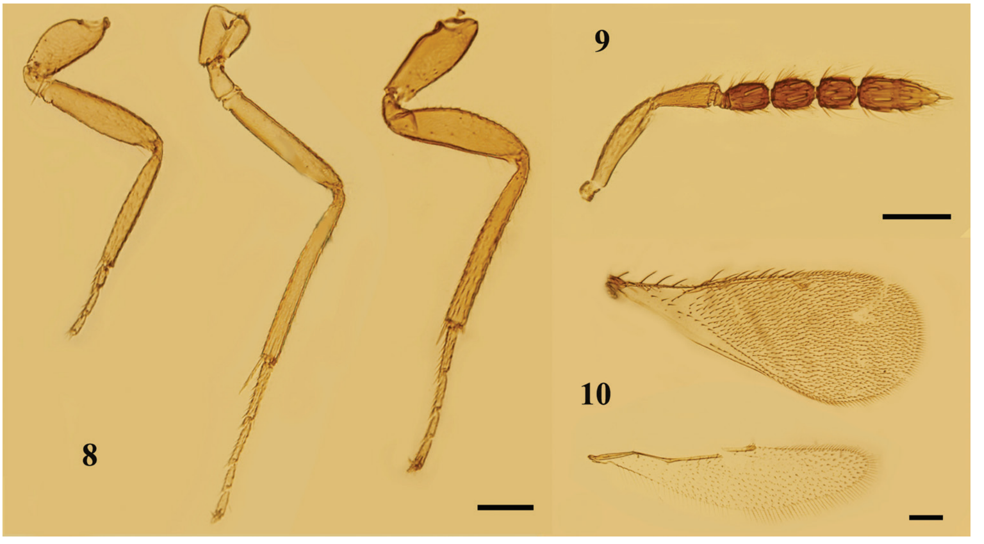

Figures 8–10. *Nesolynx thymus* (Girault), female **8** legs, lateral view, from left to right: fore, mid, and hind legs **9** antenna, lateral view **10** fore and hind wings, dorsal view. Scale bars: 100 μm.

Chilo auricilius Dudgeon, 1905 (Varma 1989), *Cnaphalocrocis medinalis* (Guenée, 1854) (Talgeri and Dalaya 1971), *Maruca testulalis* (Geyer, 1832), Tachinidae unspecified sp. (Narendran 2007), *Apanteles artonae* (Rehwer, 1926) (Herting 1977).

Distribution. China (Henan, Yunnan, Hainan); Bangladesh (Rahman 1989), Myanmar (Husain and Khan 1986), Indonesia (Bouček 1988), Malaysia (Lever 1964), India, and Sri Lanka (Narendran 2007).

Comments. The species can be easily identified by the unique color of head.

Holcotetrastichus Graham, 1987

Note. This is a small genus erected by Graham (1987), with *Cirrospilus rhosaces* Walker, 1839 as the type species. Only two species have been described: *Holcotetrastichus manaliensis* Graham, 1991 and *Holcotetrastichus rhosaces* (Walker, 1839). It can be distinguished from other Tetrastichinae especially by the strong transverse costulae in deep broad sublateral grooves and the hypopygium reaching nearly the tip of the gaster (Graham 1987). The species are parasitoids of some species of *Cassida* (Coleoptera, Chrysomelidae) (Graham 1991).

Holcotetrastichus rhosaces (Walker, 1839), new record from China

Figs 11–20

Cirrospilus rhosaces Walker, 1839: 293.

Cirrospilus racilla Walker, 1839: 312. [Synonymised by Graham 1961: 37].
Tetrastichus racilla: Walker 1848: 149.
Tetrastichus rhosaces: Walker 1848: 147.
Aprostocetus rhosaces: Graham 1961: 37.
Holcotetrastichus rhosaces: Graham 1991: 272; Narendran 2007: 120.
Holcotetrastichus rhosaceus [sic]: Boyadzhiev 2000: 27.

Material examined. 9 females and 2 males: [2 females on slides], Liaoning Province, Anshan City, Mount Qianshan, 23.VI.2013, Hui Geng, Zhi-Guang Wu, Yan Gao, Si-Zhu Liu, by sweeping; [1 female on slide], Jiangxi Province, Yichun City, Mount Guanshan, 22–24.VIII.2018, Xiang-Xiang Jin, Wang-Ming Li, by yellow- pan trapping; [1 female and 1 male on slides, 1 female and 1 male on cards], Qinghai Province, Prefecture Huangnan, Forestry Station Maixiu, 26–29.VIII.2019, Ming-Rui Li, by yellow pan trapping; [2 females on cards], Jinlin Province, County Wangqing, Forestry

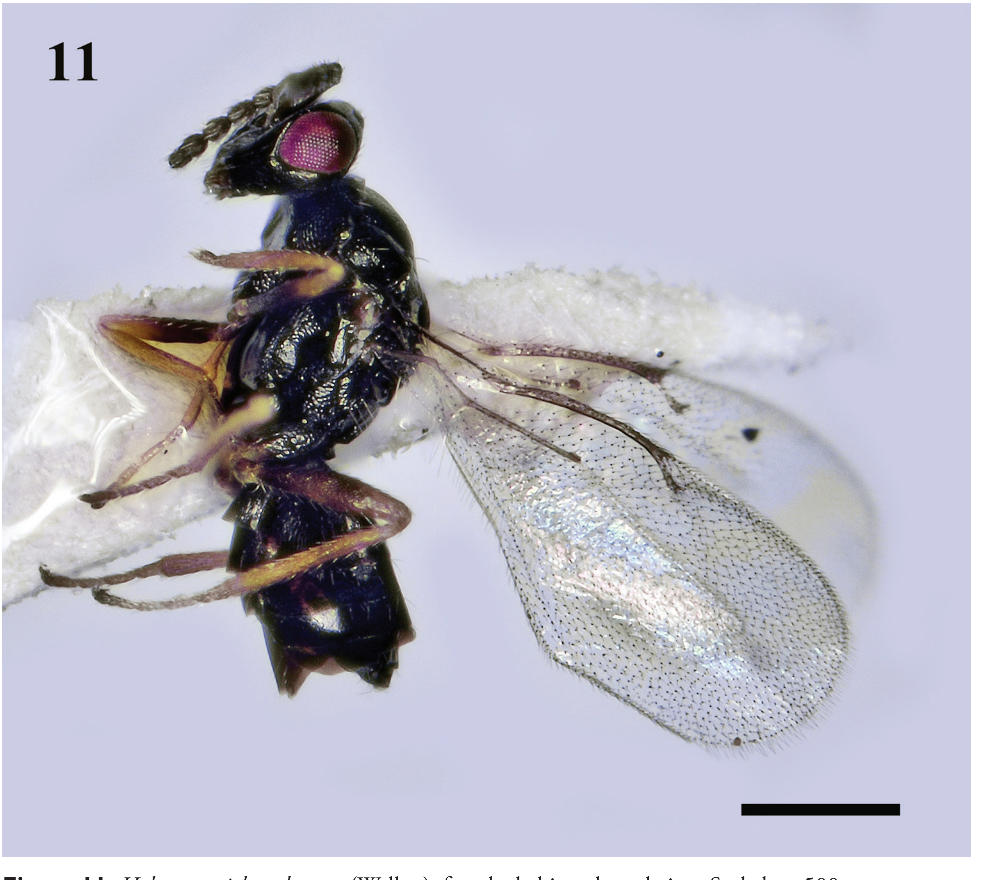

Figure 11. *Holcotetrastichus rhosaces* (Walker), female, habitus, lateral view. Scale bar: 500 µm.

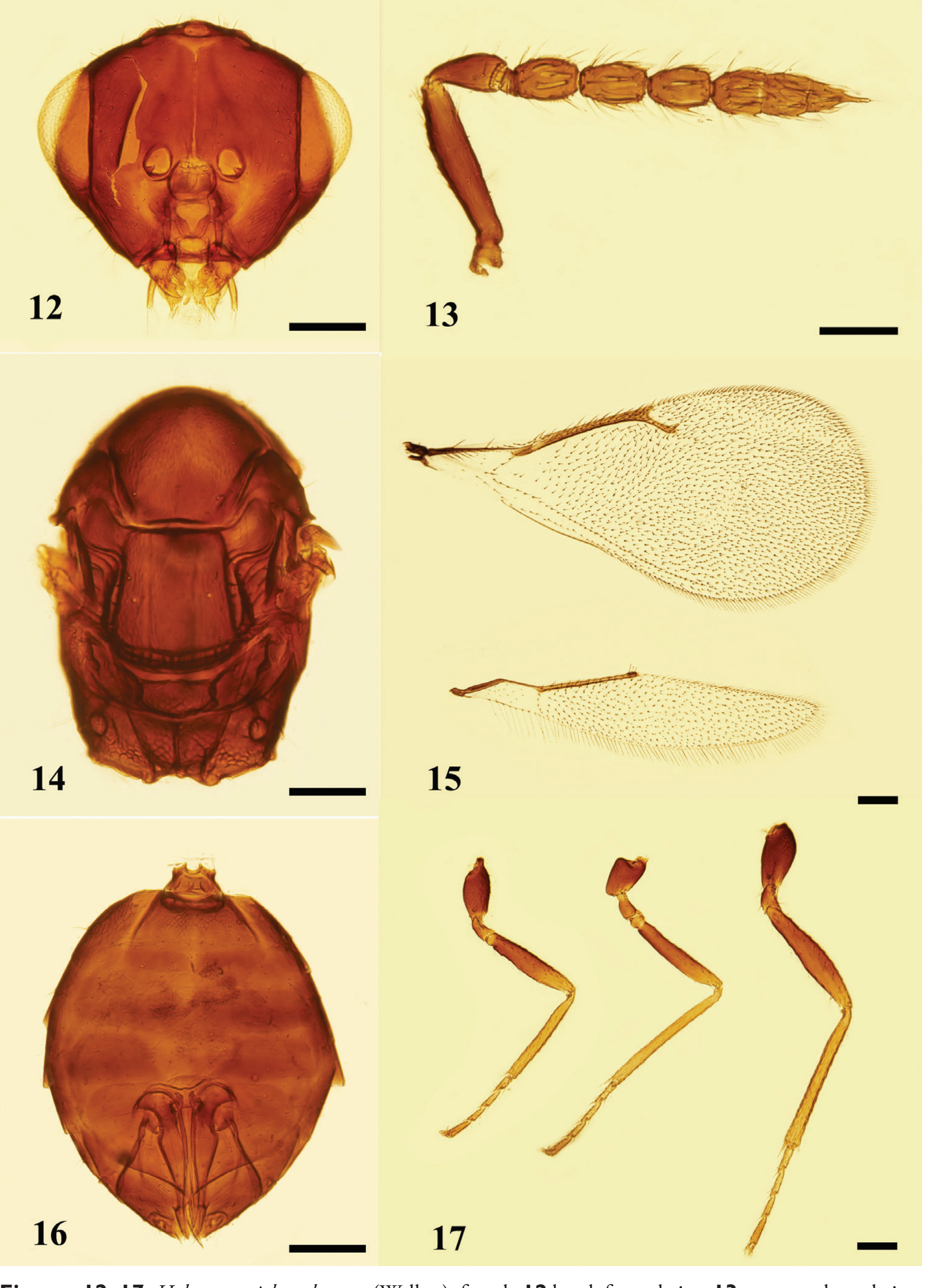

Figures 12–17. *Holcotetrastichus rhosaces* (Walker), female **12** head, frontal view **13** antenna, lateral view **14** mesosoma, dorsal view **15** fore and hind wings, dorsal view **16** metasoma, ventral view **17** legs, lateral view, from left to right: fore, mid, and hind legs. Scale bars: 100 µm.

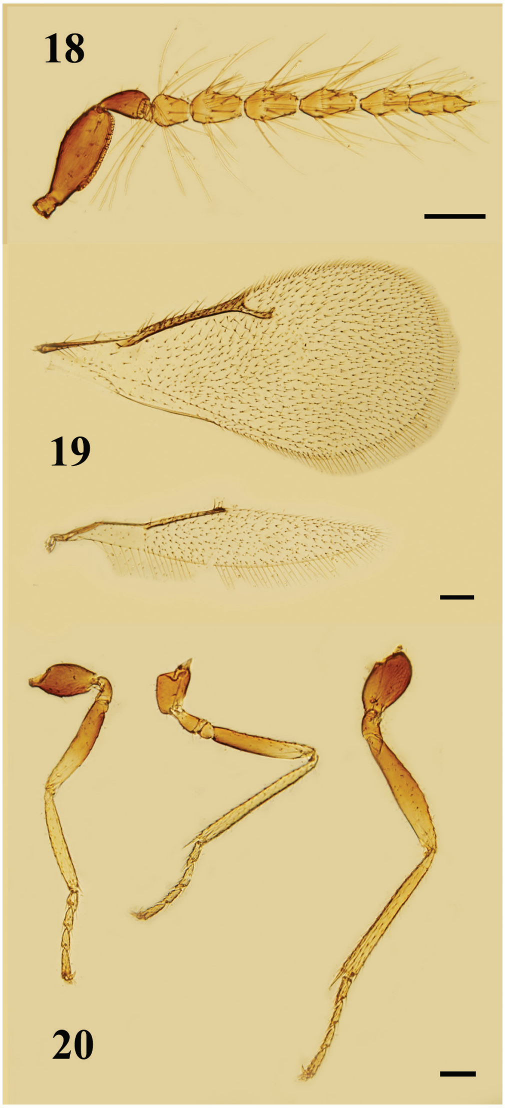

Figures 18–20. *Holcotetrastichus rhosaces* (Walker), male **18** antenna, lateral view **19** fore and hind wings, dorsal view **20** legs, lateral view, from left to right: fore, mid, and hind legs. Scale bars: 100 µm.

Station Qinhe, 8.VII.2013, Ye Chen, Zhi-Guang Wu, by sweeping; [2 females on cards], Heilongjiang Province, City Heihe, Park Beishang, 22.VII.2020, Ming-Rui Li, by sweeping. (All deposited in NEFU).

Diagnosis. Female. Body black, with weak metallic reflections (Fig. 11). Mesosoma (Fig. 14) with mid-lobe of mesoscutum weakly reticulate, 2 adnotaular setae in single row on each side, median line indicated only posteriorly; sublateral grooves of scutellum deep and broad with strong transverse costulae, submedian grooves rather weak. Forewing (Fig. 15) broad, 2.0× as long as broad, SMV with 2 dorsal setae, MV

2.8–3.2 times length of STV, PMV distinctly short. Gaster (Fig. 16) with hypopygium almost reaching tip of gaster.

Male. Antenna (Fig. 18) with scape broad, ventral plaque 0.7 length of scape; F1 shorter than F2; each segment of funicle with whorl setae reaching well beyond the tip of the segment.

Hosts. Unknown from China. Non-Chinese records include *Cassida deflorate* Suffrian, 1844, *Cassida murraea* Linnaeus, 1767, *Cassida nebulosa* Linnaeus, 1758, *Cassida nobilis* Linnaeus, 1758, *Cassida rubiginosa* Mueller, 1776, *Cassida viridis* Linnaeus, 1758, *Cassida vittate* Villers, 1789 (Graham 1991), *Cassida piperata* Hope, 1842 (Nagasawa et al. 2003).

Distribution. China (Heilongjiang, Liaoning, Jilin, Qinghai, Jiangxi); Austria, Czech Republic, Czechoslovakia, France, Germany, Hungary, Ireland, Italy, Moldova, Romania, Switzerland, United Kingdom (Graham 1991), Bulgaria (Boyadzhiev 2000), Netherlands (Gijswijt 2003), Poland (Domenichini 1966), Russia (Yegorenkova et al. 2007), Sweden (Hansson 1991), Japan (Ikeda 1997), and United States of America (Boyadzhiev 2000).

Comments. Most species we collected had weak metallic reflections compared to the species reported by Graham (1991).

Peckelachertus Yoshimoto, 1970

Note. This is a small genus with only two known species worldwide (Noyes 2019): *P. diprioni* Yoshimoto, 1970 and *P. anglicus* Graham, 1977. Both of these were transferred from the subfamily Elachertinae to Tetrastichinae by Graham (1977). The genus can be distinguished from other Tetrastichinae especially by having the PMV equally or nearly as long as STV and scutellum without submedian grooves (Graham 1977).

Peckelachertus diprioni Yoshimoto, 1970, new record from China

Figs 21–26

Peckelachertus diprioni Yoshimoto, 1970: 909.
Peckelachertus diprioni: Graham 1977: 47.

Material examined. 2 females. [2 females on slides], China, Heilongjiang Province, Shangzhi City, Mount Laoyeling, 9.VII.2015, Ye Chen, Chao Zhang, by sweeping.

Diagnosis. Female. Body dark brown, without metallic reflections. Head with anterior margin of clypeus truncate, without any teeth, malar sulcus present and distinct. Antenna with pedicel 1.8–1.9× as long as broad, F11.6× as long as broad. Mesosoma (Fig. 14) 1.5× as long as broad, mid-lobe of mesoscutum with 2 adnotaular setae in single row on each side, median line absent; scutellum submedian grooves absent or indicated at posterior half, anterior pair of setae situated near anterior margin of scutel-

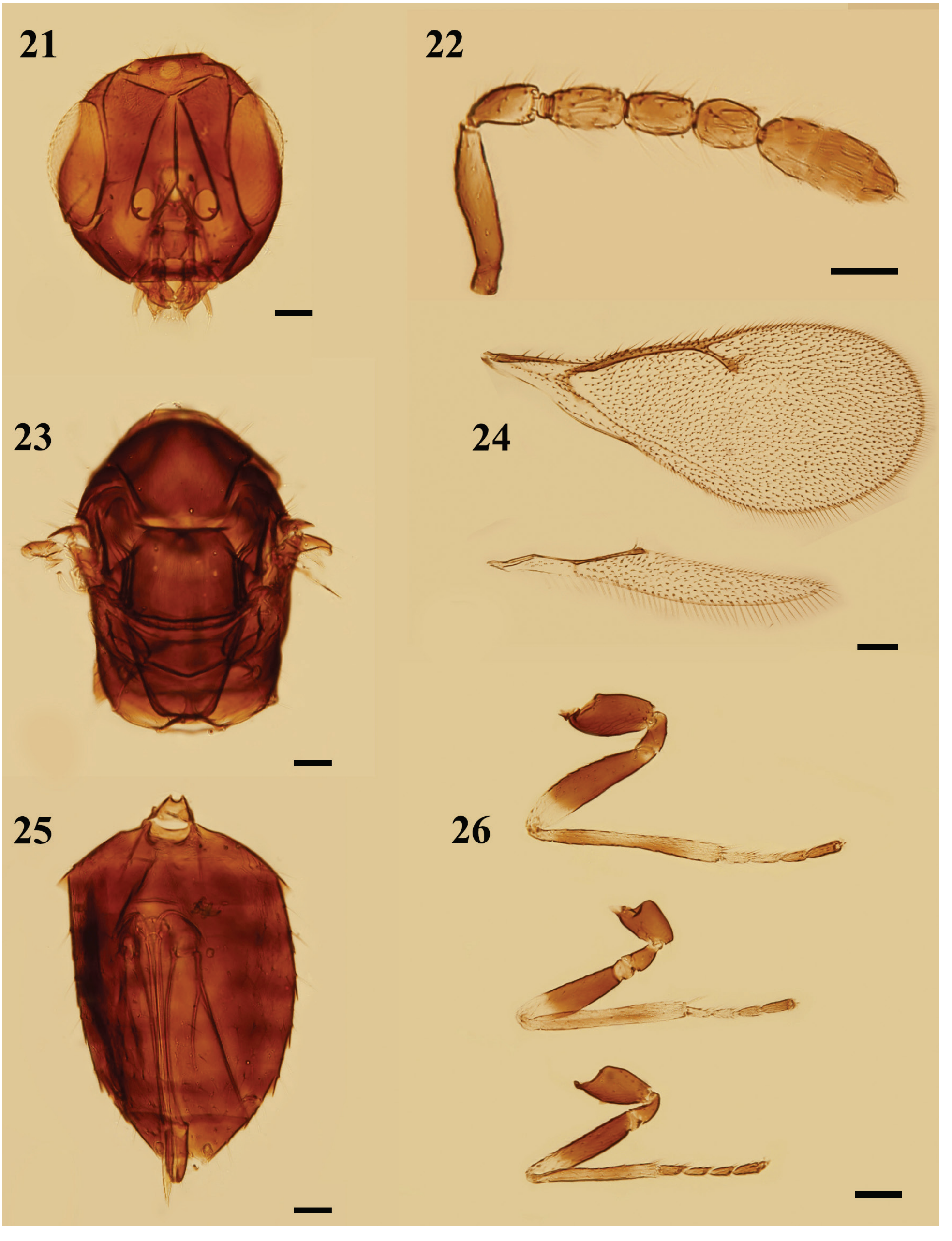

Figures 21–26. *Peckelachertus diprioni* Yoshimoto, female **21** head, frontal view **22** antenna, lateral view **23** mesosoma, dorsal view **24** fore and hind wings, dorsal view **25** metasoma, ventral view **26** legs, lateral view, from bottom to top: fore, mid, and hind legs. Scale bars: 100 µm.

lum. Forewing (Fig. 15), 2.2× as long as broad, SMV with 4 dorsal setae, the length of PMV as long as STV.

Male. Unknown from Chinese material.

Hosts. Unknown from China. Non-Chinese records include *Gilpinia frutetorum* (Fabricius, 1793) (LaSalle 1994), *Gilpinia pallida* (Klug, 1812) (Graham 1977).

Distribution. China (Heilongjiang); Finland, Canada (Graham 1977).

Comments. Graham (1977) pointed out that Yoshimoto's description of genus *Peckelachertus* and of its type species *P. diprioni* are not correct in some respects and proposed some remarks after examining material. Our specimens agree well with the remarks by Graham (1977).

Ceratoneura Ashmead, 1849

Note. The genus *Ceratoneura* was erected with *Ceratoneura petiolata* Ashmead, 1894 as the type species by subsequent designation of Ashmead (1904). Ikeda (2001) revised of the world species of *Ceratoneura* in detail, describing five new species and redescribing six known species. It is a small genus with 12 species recorded worldwide (Noyes 2019), but only one species *Ceratoneura indi* Girault, 1917 has been reported from China (Ikeda 2001). This genus can be distinguished from other Tetrastichinae especially by the strongly sclerotized body and the face with conspicuous striae radiating from the mouth. The species are parasitoids of various groups of Diptera and Lepidoptera (Bouček 1988).

Ceratoneura indi Girault, 1917
Figs 27–31

Ceratoneura indi Girault, 1917: 10.
Ceratoneura indica Rohwer, 1921: 127. [Synonymized by Bouček 1988: 670].

Material examined. 7 females: [1 female on slide and 2 females on cards], China, Zhejiang Province, County Panan, Mount Dapan, 30.VI. –2.VII.2019, Jun Wu, Jun-Jie Fan, by yellow pan trapping; [4 femles on cards], China, City Chongqin, Mount

Figures 27, 28. *Ceratoneura indi* Girault, female **27** habitus, lateral view. Scale bar: 500 μm **28** head, frontal view. Scale bar: 100 μm.

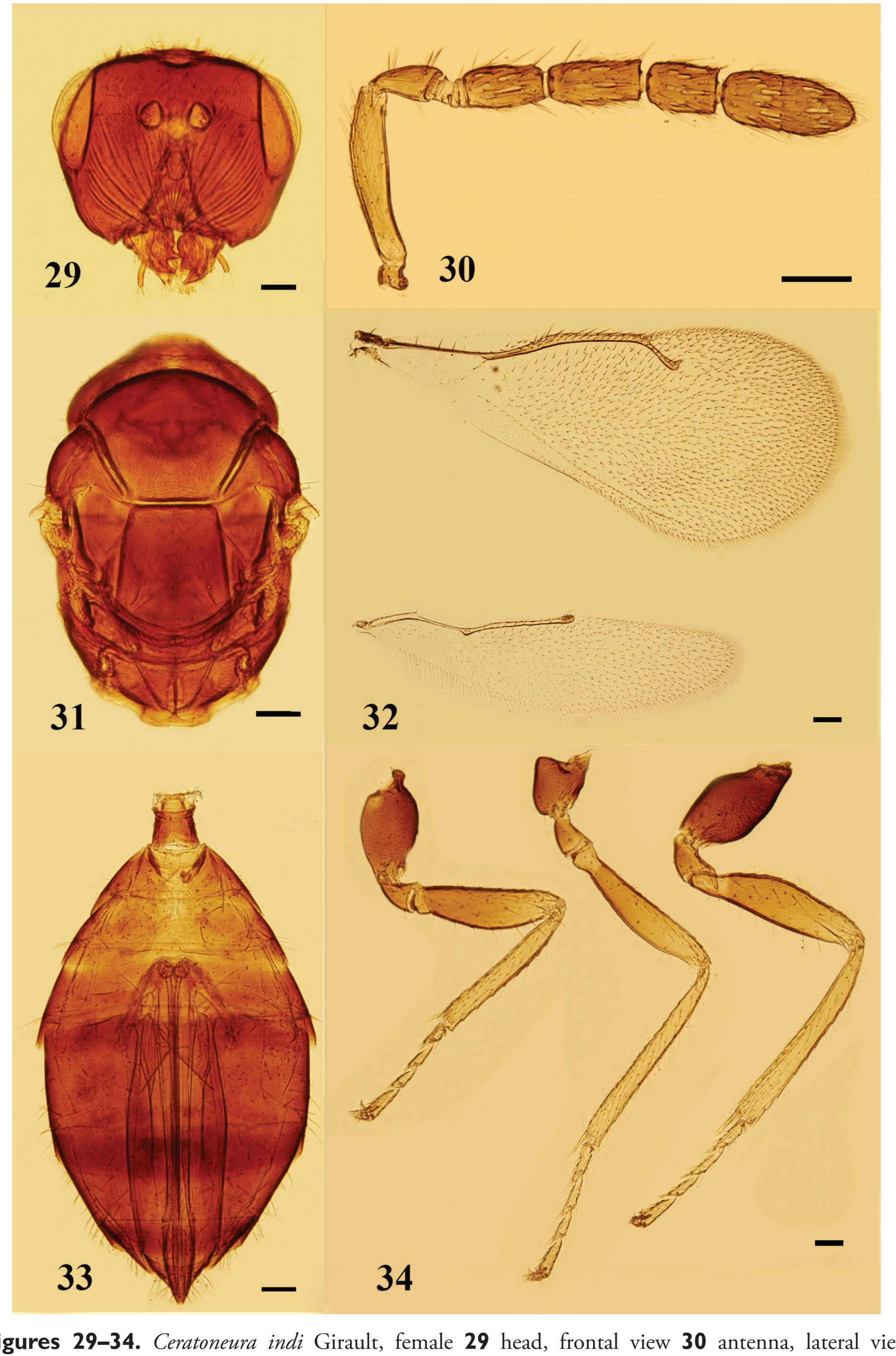

Figures 29–34. *Ceratoneura indi* Girault, female **29** head, frontal view **30** antenna, lateral view **31** mesosoma, dorsal view **32** fore and hind wings, dorsal view **33** metasoma, ventral view **34** legs, lateral view, from left to right: fore, mid, and hind legs. Scale bars: 100 µm.

Simianshan, Village Hongdong, 26.VII.2019, Ting-Ting Zhao, Shu-Cheng Deng, by sweeping. (All deposited in NEFU).

Diagnosis. Female. Body black, strongly sclerotized. Face with conspicuous striae radiating from mouth, torulus with lower margin distinctly above the level of ventral margin of eyes. Mesosoma with mid-lobe of mesoscutum weakly reticulate, 4 or 5 adnotaular setae in single row on each side, median line absent. Forewing 2.2–2.3× as long as broad, SMV with 3 dorsal setae, speculum large. Petiole distinct, 0.4–0.5× as long as propodeum. Gaster 1.7–2.0× as long as broad.

Male. Unknown for Chinese material.

Hosts. Unknown from China. Non-Chinese records include *Asphondylia sphaera* Monzen, 1937 (Ikeda 2001).

Distribution. China (Zhejiang, Chongqing, Hong Kong), Japan, India, Malaysia, New Caledonia, Papua New Guinea, Sri Lanka.

Comments. Ikeda (2001) reported only one specimen from Hong Kong, and we add seven additional specimens from Zhejiang and Chongqing, which are new locality records for China.

Acknowledgements

We are grateful to Dr Xiang-Xiang Jin, Dr Si-Zhu Liu, Dr Hui Geng, Dr Guo-Hao Zu, Dr Ye Chen, Dr Ming-Rui Li, Miss Ting-Ting Zhao, Miss Shu-Cheng Deng, Miss Yan Gao, Mr Jun Wu, Mr Jun-Jie Fan, Mr Gang Fu, and Mr Chao Zhang for specimen collections.

References

Ashmead WH (1904) Classification of the chalcid flies of the superfamily Chalcidoidea, with descriptions of new species in the Carnegie Museum, collected in South America by Herbert H. Smith. Memoirs of the Carnegie Museum 1(4): i–xi, 225–551. [39 pls] https://doi.org/10.5962/p.234821

Ashmead WH (1905) Additions to the recorded hymenopterous fauna of the Philippine Islands, with decriptions of new species. Proceedings of the United States National Museum 28(1413): 957–971. https://doi.org/10.5479/si.00963801.28-1413.957

Bansude V, Berde V, Chaphalkar S (2010) Emergence potential of *Nesolynx thymus* Girault and environmental impact. Karnataka Journal of Agricultural Sciences 23(1): 115–117.

Bouček Z (1977) Taxonomic studies on some Eulophidae (Hym.) of economic interest mainly from Africa. Entomophaga 21(4): 401–414. https://doi.org/10.1007/BF02371639

Bouček Z (1988) Australasian Chalcidoidea (Hymenoptera). A Biosystematic Revision of Genera of Fourteen Families, with a Reclassification of Species. CAB International, Wallingford /Cambrian News, Aberystwyth, 832 pp.

Boyadzhiev P (2000) Unknown species of family Eulophidae to the fauna of Bulgaria from the Rhodopes (Hymenoptera: Chalcidoidea). Acta Zoologica Bulgarica 52(2): 25–29.

Domenichini G (1966) Hym. Eulophidae. Palaearctic Tetrastichinae. Index of Entomophagous Insects, Vol. 1 (Eds: Delucchi V, Remaudière G) Le François, Paris, 101 pp.

Feng MX, Cao HX, Hao HH, Wang W, Cheng LS (2016) A new record species of *Quadrastichus* (Hymenoptera: Eulophidae) from China. Redai Zuowu Xuebao 37(3): 582–585.

Ferrière C (1940) On some parasites and hyperparasites of *Artona catoxantha*, Hmps. Bulletin of Entomological Research 31(2): 131–139. https://doi.org/10.1017/S0007485300004910

Gibson GAP, Huber JT, Woolley JB (1997) Annotated keys to the genera of Nearctic Chalcidoidea (Hymenoptera). National Research Council Research Press, Ottawa, 794 pp.

Gijswijt MJ (2003) Naamlijst van de Nederlandse bronswespen (Hymenoptera: Chalcidoidea). Nederlandse Faunistische Mededelingen 18: 17–79.

Girault AA (1913) Australian Hymenoptera Chalcidoidea – IV. Memoirs of the Queensland Museum 2: 140–296. https://doi.org/10.5962/bhl.title.9562

Girault AA (1916) New Javanese chalcidoid Hymenoptera. Proceedings of the United States National Museum 51(2161): 479–485. https://doi.org/10.5479/si.00963801.2161.479

Girault AA (1917) New Javanese Hymenoptera. Private publication, Washington, 12 pp.

Graham MWR de V (1961) The genus *Aprostocetus* Westwood *sensu lato* (Hym., Eulophidae) notes on the synonymy of European species. Entomologist's Monthly Magazine 97: 34–64.

Graham MWR de V (1977) Systematic position of *Peckelachertus* Yoshimoto (Hym., Eulophidae) and description of a new species from Britain. Systematic Entomology 2(1): 45–47. https://doi.org/10.1111/j.1365-3113.1977.tb00356.x

Graham MWR de V (1987) A reclassification of the European Tetrastichinae (Hymenoptera: Eulophidae), with a revision of certain genera. Bulletin of the British Museum (Natural History) [Entomology] 55(1): 1–392.

Graham MWR de V (1991) A reclassification of the European Tetrastichinae (Hymenoptera: Eulophidae): revision of the remaining genera. Memoirs of the American Entomological Institute 49: 1–322.

Guo SH, Kang N, Li Q, Hu HY (2022) Species and identification of *Dzhanokmenia* in China (Hymenoptera: Eulophidae). Sichuan Journal of Zoology 41(1): 63–73.

Hansson C (1991) A catalogue of Chalcidoidea described by C.G. Thomson, with a checklist of Swedish species. Entomologica Scandinavica (Supplement No 38): 1–70.

Herting B (1977) A Catalogue of Parasites and Predators of Terrestrial Arthropods. Section A. Host or Prey/Enemy. Volume IV. Hymenoptera. Commonwealth Agricultural Bureaux, Institute of Biological Control, Farnham Royal, iii + 206 pp.

Herting B (1978) A Catalogue of Parasites and Predators of Terrestrial Arthropods. Section A. Host or Prey/Enemy. Volume V. Neuroptera, Diptera, Siphonaptera. Commonwealth Agricultural Bureaux, Commonwealth Institute of Biological Control, Farnham Royal, 1–156.

Husain T, Khan MY (1986) Family Eulophidae. In: Subba Rao BR, Hayat M (Eds) The Chalcidoidea (Insecta: Hymenoptera) of India and the adjacent countries. Oriental Insects 20: 211–245. https://doi.org/10.1080/00305316.1986.10433730

Ikeda E (1997) Three species of Tetrastichinae (Hymenoptera, Eulophidae), newly recorded from Japan. Japanese Journal of Entomology 65(1): 186–192.

Ikeda E (2001) A revision of the world species of *Ceratoneura* Ashmead (Hymenoptera, Eulophidae). Insecta Matsumurana 58: 27–50.

Jiao Y, Chen ZL, Yu DJ, Kang L, Yang WD (2006) A new record genus and new record species of Eulophidae (Hymenoptera) in continental China. Entomotaxonomia 28(1): 69–74.

Kamijo K (1994) A revision of *Mestocharella* (Hymenoptera, Eulophidae), with descriptions of six new species. Japanese Journal of Entomology 62(4): 747–762.

Kostjukov VV (1978) Hymenoptera II. Chalcidoidea 13. Eulophidae (Tetrastichinae). Opredeliteli Nasekomykh Evropeyskoy Chasti SSR 3: 430–467.

Kostjukov VV (2000) Nadsem. Chalcidoidea 46. Sem. Eulophidae. Opredeliteli Nasekomikh Dalinego Vostoka Rossii 4(4): 582–601.

Kumar P, Kishore R, Jayaprakas CA, Sengupta K (1991) Parasitoids of uzi fly, *Exorista sorbillans* Wiedermann (Diptera: Tachinidae), XII: studies on the efficiency of *Nesolynx thymus* (Girault) at the field level. Indian Journal of Sericulture 30(2): 161–163.

LaSalle J (1994) North American genera of Tetrastichinae (Hymenoptera: Eulophidae). Journal of Natural History 28(1): 109–236. https://doi.org/10.1080/00222939400770091

Lever RJAW (1964) Notes on some parasites, hyperparasites and predators of coconut pests in Malaya. FAO Plant Protection Bulletin 12(2): 42–43.

Li WJ, Li CD (2020) A new species of *Oomyzus* Rondani (Hymenoptera, Eulophidae) and first record of *O. gallerucae* (Fonscolombe) from China, with a key to Chinese species. ZooKeys 950: 41–49. https://doi.org/10.3897/zookeys.950.48795

Li WJ, Li CD (2021) Two new species of *Neotrichoporoides* Girault (Hymenoptera, Eulophidae) from China and a key to Chinese species. ZooKeys 1023: 61–79. https://doi.org/10.3897/zookeys.1023.61580

Li XX, Xu ZJ, Zhu CD, Zhao JN, He YY (2014) A new phytophagous eulophid wasp (Hymenoptera: Chalcidoidea: Eulophidae) that feeds within leaf buds and cones of *Pinus massoniana*. Zootaxa 3753(4): 391–397. https://doi.org/10.11646/zootaxa.3753.4.8

Li Q, Wang C, Hu HY, Kostjukov VV, LaSalle J, Zhu CD (2016) Descriptions of three new species of *Dzhanokmenia* (Hymenoptera: Eulophidae) from China. Zootaxa 4121(4): 447–457. https://doi.org/10.11646/zootaxa.4121.4.5

Liao DX, Li XL, Pang XF, Cheng TL (1984) Economic Insect Fauna of China. Fasc. 34. Hymenoptera: Chalcidoide (1). Science Press, Beijing, 241 pp.

Miwa Y, Sonan J (1935) Description of a new egg parasite of *Melanauster chinensis* Först. from Formosa. Transactions of the Natural History Society of Formosa 25(146): 406–407.

Nagasawa A, Konno Y, Matsuda K (2003) New record of *Holcotetrastichus rhosaces* (Walker) (Hymenoptera: Eulophidae), a hymenopterous parasitoid of *Cassida nebulosa* L. and *C. piperata* Hope (Coleoptera: Chrysomelidae), from Japan. Japanese Journal of Entomology 6(3): 117–118. [New Series]

Narendran TC (2007) Indian chalcidoid parasitoids of the Tetrastichinae (Hymenoptera: Eulophidae). Records of the Zoological Survey of India, Occasional Paper 272: 1–390.

Ning HF, Cao HX, Zhu CD (2022) Notes on the genus *Aceratoneuromyia* Girault (Hymenoptera: Eulophidae). Insects 13(5): 450. https://doi.org/10.3390/insects13050450

Noyes JS (1982) Collecting and preserving chalcid wasps (Hymenoptera: Chalcidoidea). Journal of Natural History 16(3): 315–334. https://doi.org/10.1080/00222938200770261

Noyes JS (2019) Universal Chalcidoidea Database. http://www.nhm.ac.uk/chalcidoids [Accessed on 2022-7-1]

Perkins RCL (1912) Parasites of insects attacking sugar cane. Bulletin of the Hawaiian Sugar Planters'. Association Experiment Station 10: 1–27. [Entomology Series]

Rahman SM (1989) Some observations on *Nesolynx thymus* Girault (Hymenoptera: Eulophidae), and endoparasite of *Tricholyga bomycis* Beck (Diptera: Tachinidae). Annals of Entomology, Dehra Dun 7(1): 27–30.

Sheng JK (1995) Two new species of Tetrastichinae from China. Acta Agriculturae Universitatis Jiangxiensis 17(1): 21–24.

Sheng JK, Wang GH (1992) Four species of Tetrastichinae including a new record to China. Jiangxi Plant Protection 2(15): 35.

Sheng JK, Wang GH (1993) One new species and two new records of parasitoids of *Phyllocnistis citrella* Stainton (Hymenoptera: Eulophidae) from Jiangxi. Acta Agriculturae Universitatis Jiangxiensis 15(1): 36–39.

Sheng JK, Zhao FX (1995) A new species of *Aprostocetus* from China (Hymenoptera: Eulophidae: Tetrastichinae). Entomologia Sinica 2(4): 308–310. https://doi.org/10.1111/j.1744-7917.1995.tb00052.x

Sheng JK, Zhu XF (1998) Two new species of the genus *Oomyzus* Rondani (Hymenoptera: Eulophidae: Tetrastichinae). Acta Zootaxonomica Sinica 23(3): 313–315.

Song LW, Cao LM, Li XP, Yang ZQ, Chen YQ (2017) A new species of *Baryscapus* (Hymenoptera: Eulophidae) parasitizing pupae and larvae of two *Dioryctria* species (Lepidoptera: Pyralidae). Annals of the Entomological Society of America 110(3): 288–292. https://doi.org/10.1093/aesa/saw099

Song HT, Fei MH, Li BP, Zhu CD, Cao HX (2020) A new species of *Oomyzus* Rondani (Hymenoptera, Eulophidae) reared from the pupae of *Coccinella septempunctata* (Coleoptera, Coccinellidae) in China. ZooKeys 953: 49–60. https://doi.org/10.3897/zookeys.953.53175

Talgeri GM, Dalaya VP (1971) New record of parasites of paddy leaf roller. Research Journal of Mahatma Phule Agricultural University 2(2): 156–158.

Timberlake PH (1921) Description of a new species of *Ootetrastichus* from Formosa. Proceedings of the Hawaiian Entomological Society 4: 557–564.

Varma A (1989) Record of a hyperparasitoid *Nesolynx thymus* (Girault) on *Sturmiopsis inferens* Townsend in Jagadhari area of Haryana State. Indian Journal of Plant Protection 17(1): 103.

Walker F (1839) Monographia Chalciditum. (Continued.). Entomological Magazine 3(5): 465–496. https://doi.org/10.5962/bhl.title.67725

Walker F (1848) List of the Specimens of Hymenopterous Insects in the Collection of the British Museum, Part 2. E. Newman, London, [i–iv +] 99–237.

Wu YJ, Jiang XJ, Li DW, Luo JT, Zhou GF, Chang MS, Yang ZQ (2009) *Leptocybe invasa*, a new invasive forest pest making galls on twigs and leaves of eucalyptus trees in China (Hymenoptera: Eulophidae). Linye Kexue 45(7): 161–163.

Yang ZQ (1989) A new genus and species of Eulophidae (Hymenoptera: Chalcidoidea) parasitizing *Hyphantria cunea* (Drury) (Lepidoptera: Arctiidae) in China. Entomotaxonomia 11(1–2): 117–130.

Yang ZQ (1996) Parasitic wasps on bark beetles in China (Hymenoptera). Science Press, Beijing, 363 pp.

Yang ZQ, Wei JR (2003) Two new species of *howardi* species group in the genus *Tetrastichus* (Hymenoptera: Eulophidae) parasitizing fall webworm from China. Linye Kexue 39(5): 67–73.

Yang MM, Lin YC, Wu YJ, Fisher N, Saimanee T, Sangtongpraow B, Zhu CD, Chiu WCH, LaSalle J (2014) Two new *Aprostocetus* species (Hymenoptera: Eulophidae: Tetrastichinae), fortuitous parasitoids of invasive eulophid gall inducers (Tetrastichinae) on *Eucalyptus* and *Erythrina*. Zootaxa 3846(2): 261–272. https://doi.org/10.11646/zootaxa.3846.2.6

Yang ZQ, Yao YX, Cao LM (2015) Chalcidoidea parasitizing forest defoliators (Hymenoptera). Science Press, Beijing, 296 pp.

Yegorenkova EN, Yefremova ZA, Kostjukov VV (2007) Contributions to the knowledge of tetrastichine wasps (Hymenoptera, Eulophidae, Tetrastichinae) of the middle Volga region. Entomologicheskoe Obozrenie 86(4): 781–796. https://doi.org/10.1134/S0013873807090084

Yoshimoto CM (1970) A new eulophid parasite (Hym., Chalcidoidea) from eggs of the nursery pine sawfly *Diprion frutetorum* (Hym., Diprionidae). Canadian Entomologist 102(7): 908–910. https://doi.org/10.4039/Ent102908-7

Zhang YZ, Ding L, Huang HR, Zhu CD (2007) Eulophidae fauna (Hymenoptera, Chalcidoidea) from south Gansu and Qinling mountain areas, China. Acta Zootaxonomica Sinica 32(1): 6–16.

Zhang YP, Li DS, Zhao YC, Huang SH, Zhang BX (2009) *Aceratoneuromyia indica* (Silvestri), a new recorded species of parasitoid for *Bactrocera dorsalis* (Hendel) in China and its parasitic efficiency. Chinese Journal of Biological Control 25(2): 106–111.

Zhu CD, Huang DW (2001) A taxonomic study on Eulophidae from Zhejiang, China (Hymenoptera: Chalcidoidea). Acta Zootaxonomica Sinica 26(4): 533–547.

Zhu CD, Huang DW (2002) A taxonomic study on Eulophidae from Guangxi, China (Hymenoptera: Chalcidoidea). Acta Zootaxonomica Sinica 27(3): 583–607.